CRANFIELD UNIVERSITY

NITTAYA BOONTIAN

USING THE ACTIVATED SLUDGE MODEL 2D (ASM2D) TO UNDERSTAND AND PREDICT THE PHOSPHORUS ACCUMULATING ORGANISMS MECHANISM IN ENHANCED BIOLOGICAL PHOSPHORUS REMOVAL IN RELATION TO DISINTEGRATED SLUDGE AS A CARBON SOURCE

SCHOOL OF APPLIED SCIENCES

Cranfield Water Science Institute

Ph.D. THESIS

2012

CRANFIELD UNIVERSITY

School of Applied Sciences

Cranfield Water Science Institute

Ph.D. Thesis

2012

NITTAYA BOONTIAN

USING THE ACTIVATED SLUDGE MODEL 2D (ASM2D) TO UNDERSTAND AND PREDICT THE PHOSPHORUS ACCUMULATING ORGANISMS MECHANISM IN ENHANCED BIOLOGICAL PHOSPHORUS REMOVAL IN RELATION TO DISINTEGRATED SLUDGE AS A CARBON SOURCE

Supervisors: Professor Dr. Elise Cartmell and Dr. Ana Soares

September 2012

This thesis is submitted in partial fulfillment of the requirements
for the Degree of Doctor of Philosophy

ABSTRACT

Carbon sources are considered as one of the most important factors in the performance of enhanced biological phosphorus removal (EBPR). Disintegrated sludge (DS) can act as carbon source to increase the efficiency of EBPR. This research explores the influence of DS upon phosphorus removal efficiency using mathematical simulation modeling. Activated Sludge Model No. 2d (ASM2d) is one of the most useful of activated sludge (AS) models. This is because ASM2d can express the integrated mechanisms of phosphorus accumulating organisms (PAOs) under aerobic, anaerobic and anoxic conditions.

A novel calibration approach is presented. It can reduce ASM2d parameter subsets and decrease model complexity. This approach does not require high computational demand and reduces the number of modeling parameters required to achieve ASM's calibration. It does so by employing a sensitivity and iteration methodology. Calibrated parameters of PAOs and autotrophs include: Y_{PAO}, Y_{PO4}, Y_{PHA}, q_{PHA}, q_{PP}, μ_{PAO}, b_{PAO}, b_{PP}, b_{PHA}, K_{PS}, Y_A, μ_{AUT}, b_{AUT}, $K_{O2\ AUT}$, and $K_{NH4\ AUT}$. Use of disintegrated sludge (DS) resulted in an influent phosphorus to acetate (P/HAc) ratio (0.26 g P g^{-1} COD) that was higher than without DS (0.21 g P g^{-1} COD). Influent phosphorus contents with and without DS were 0.83 % and 0.73 % of TSS, respectively. Y_{PAO} and Y_{PHA} values were different when utilizing DS and then when not doing so. Y_{PAO} with and without DS were 0.64 and 0.61 g COD g^{-1} COD, respectively. Y_{PHA} with and without DS were 0.26 and 0.24 g COD g^{-1} P, respectively. These results were based on phosphorus, volatile fatty acids, fermentable biodegradable products and slowly biodegradable products in DS. Effects of these components were studied using paired-t tests resulting in p-value < 0.00001 in all cases. An effect of temperature with use of DS was seen by observation of Arrhenius equation constants (θ). It was found that only Y_{PAO} and q_{PHA} were changed. The values of both coefficients increased when temperature increased from 17°C to 23°C. However, higher phosphorus removal efficiency occurred at the lower temperature (17°C).

ACKNOWLEDGMENTS

I would like to thank my supervisors, Professor Dr. Elise Cartmell and Dr. Ana Soares, for their guidance, tireless support and encouragement throughout this project. Their comments and advice have always been helpful.

I am grateful for the fellowship awarded to me by the Thai Government and Suranaree University of Technology.

I would like to acknowledge Dr. Sutthipong Meeyai, Professor Dr. Jeffrey Nash, Dr. Nantiya Nash, and Dr. Buratin Khampirat who have always made available their help on mathematical simulation modeling and statistical analysis.

I would like to thank Dr. Davide Minervini and Dr. Pantelis Kampas who advised on operating ultrasound equipment and pilot-scale operation. They also supported me by providing information on mechanically disintegrated sludge.

I would like to thank Dr. Wut Dankittikul, Dr. Chareeya Yimrattanabovorn, Dr. Sanan Tangsathit, Dr. Boonchai Wichitsathian, Dr. Chatpet Yossapol, Dr. Apichon Watcharenwong, Dr. Patcharin Racho and Dr. Sudjit Karuchit who are my friends working in the School of Environmental Engineering at Suranaree University of Technology. They always supported me during the time I was writing last year in Thailand.

I would also thank to all the great people I have met at Cranfield University during these 4 years.

Finally, I owe my deepest gratitude to my family, my mother and father who always encouraged and supported me in the difficult moments.

TABLE OF CONTENTS

LIST OF FIGURES

CHAPTER 2

CHAPTER 3

CHAPTER 4

CHAPTER 5

LIST OF TABLES

CHAPTER 1

CHAPTER 2

CHAPTER 3

CHAPTER 4

CHAPTER 5

CHAPTER 6

NOTATION AND ABBREVIATION

$<$	Less than
$\leq$	Less than or equal
$>$	Greater than
%	Percent
$=$	Equals
$\pm$	Plus or minus
°C	Degree Celsius
ε	Phosphate transport coefficient
ε_O	Phosphate transport coefficient under aerobic conditions
ε_N	Phosphate transport coefficient under anoxic conditions
δ	Efficient oxidative phosphorylation coefficient
δ_O	Efficient oxidative phosphorylation coefficient under aerobic conditions
δ_N	Efficient oxidative phosphorylation coefficient under anoxic conditions
α	Confidence level at 95%
$\sigma_{mea,\ i}$	Standard deviation of real list variables
θ	Arrhenius equation constants
$\partial y_i / \partial \theta_j$	The absolute sensitivity of the model output y to the parameter θ_j
$\Delta\theta_j$	The uncertainty range of the parameter θ_j
$f_{p,UPT1}$	Stoichiometric parameters of aerobic growth
$f_{p,UPT2}$	Stoichiometric parameters anoxic growth
η_{NO3}	Reduction factor of the rates of anoxic poly-P formation and anoxic PAOs growth
η_P	The reducing fraction in denitrification
$\eta_{NO,\ resp,\ PAO}$	Reduction respiration under anoxic conditions
$\eta_{NO,\ lys,\ PAO}$	Reduction lysis under anoxic conditions
η_{NO3}	Reduction factor for anoxic activity
μ_{PAO}	Maximum growth rate of PAOs
μ_{AUT}	The maximum growth rate for autotrophs

$\Delta\psi$	Electrical potential difference
A_2	Anaerobic/anoxic
A/O	Anaerobic/aerobic
AOB	Ammonium oxidizing biomass
Aquasim	Aquasim programme
ASMs	Activated sludge models
ASM1	Activated Sludge Model No. 1
ASM2	Activated Sludge Model No. 2
ASM2d	Activated Sludge Model No. 2d
ASM3 with Bio-P model	Activated Sludge Model No. 3 with biological phosphorus removal
ASP	The activated sludge process
ATP	Internal glycogen energy for anaerobic VFAs conversion to PHA
ANOs	Autotrophic nitrifying organisms
b_{AUT}	Rate for Lysis of X_{AUT}
b_{PAO}	Rate for Lysis of X_{PAO}
b_{PHA}	Rate for Lysis of X_{PHA}
b_{PP}	Rate for Lysis of X_{PP}
BEPR	Biological enhanced phosphorus removal
BNR	Biological nutrient removal
BNRAS	Biological nutrient removal activated sludge
EBPR	Enhanced biological phosphorus removal
ENBNRAS	External nitrification biological nutrient removal activated sludge
COD	Chemical oxygen demand
C_{TCOD}	The total organic content
C_{TN}	The total nitrogen
C_{TP}	The total phosphorus
DNPAOs	Denitrifying PAOs
DS	Disintegrated sludge
f	Arbitrary parameter value calculated by Aquasim
FIM	Fisher information matrix
$f_{meas,\ i}$	Values of real list variables

FSA	Free and saline ammonium
f_{XI}	Fraction of inert COD generated in biomass Lysis
GAOs	Glycogen accumulating organisms
GPS-X	GPS-X programme
H_0	The null hypothesis
Ha	The alternate hypothesis
i_{ci}	Conversion factor to convert the units of component i to the units of the material c
i_{NXI}	Mass of N per mass of COD in inerts
i_{NXS}	Mass of N per mass of COD in biomass
k_1	Reaction rates at temperatures T_1
k_2	Reaction rates at temperatures T_2
K_A	Saturation coefficient for acetate, S_A
K_{ALK}	Saturation coefficient for alkalinity (HCO_3)
K_F	Saturation coefficient for growth on S_F
K_h	Hydrolysis rate constant
K_{IPP}	Inhibition coefficient for PP storage
K_{max}	Maximum ratio of X_{PP}/X_{PAO}
K_{NH4}	Saturation coefficient for ammonium (nutrient)
$K_{NH4\ AUT}$	Saturation coefficient for ammonium (substrate)
K_{NO3}	Saturation coefficient for nitrate, S_{NO3}
K_{O2}	Saturation/inhibition coefficient for oxygen
$K_{O2\ AUT}$	Saturation coefficient for oxygen
K_P	Saturation coefficient for phosphate (nutrient)
K_{PHA}	Saturation coefficient for PHA
K_{PS}	Saturation coefficient for phosphorus in storage of polyphosphate
K_{PP}	Saturation coefficient for polyphosphate
K_X	Saturation coefficient for particulate COD
MLSS	Mixed liquor suspended solid
MUCT	The Modified University of Cape Town
$NADH_2$	Intracellular PHB storage for reduction equivalents

NDBEPR	Nitrification and denitrification biological excess phosphorus removal systems
NO_3	Nitrate
OHOs	Ordinary heterotrophic organisms
p_i	Model parameter
P	Phosphorus
P/C	Phosphorus/Carbon
P/COD	Phosphorus/Chemical oxygen demand
P/HAc	Phosphorus/Acetate
PAOs	Phosphorus accumulating organisms
PHA	Poly-hydroxy-alkanoates
PHB	Poly-hydroxy-butyrate
p_j	Processes rate equations
poly-P	Polyphosphate
p-value	Probability value
PO_4	Orthophosphate
q_{ac}^{max}	Maximum specific acetate uptake rate
q_{fe}	Maximum rate for fermentation
q_{PHA}	Rate constant for storage of X_{PHA}
q_{PP}	Rate constant for storage of X_{PP}
Q_1	Anoxic recirculation flow rate
Q_2	Aerobic recirculation flow rate
Q_{IN}	Influent wastewater flow rate
Q_R	Return activated sludge flow rate
RBCOD	Readily biodegradable chemical oxygen demand
ReH	Reject H_0
r_j	The rate of parallel processes
S and $\tilde{S}$	Matrices,
S_A	Fermentation products (acetate)
S_{Ain}	Influent fermentation products (acetate)
S_{ALK}	Alkalinity of the wastewater
SBR	Sequential batch reactors

SBCOD	Slowly biodegradable chemical oxygen demand
sc_i	Characteristic scale of the variable y_i
SCFAs	Short-chain fatty acids
SCOD	Soluble chemical oxygen demand
S_F	Fermentable, readily bio-degradable organic substrates
S_{Fin}	Influent fermentable, readily bio-degradable organic substrates
S_I	Inert soluble organic material
$S_{i,j}$	Normalized sensitivity coefficient
S_{Iin}	Influent inert soluble organic material
S_{N2}	Dinitrogen (N_2), 0.78 atm at 20 ºC
S_{N2in}	Influent dinitrogen (N_2), 0.78 atm at 20 ºC
S_{NH4}	Ammonium plus ammonia nitrogen
S_{NH4in}	Influent ammonium plus ammonia nitrogen
S_{NO3}	Nitrate plus nitrite nitrogen
S_{NO3in}	Influent nitrate plus nitrite nitrogen
S_{O2}	Dissolved oxygen
S_{O2in}	Influent dissolved oxygen
S_{PO4}	Inorganic soluble phosphorus, primarily ortho-phosphate
S_{PO4in}	Influent inorganic soluble phosphorus, primarily ortho-phosphate
SRT	Solid retention time
S_S	Readily biodegradable substrate
S_{TKN}	Soluble Kjeldahl nitrogen
S_{TP}	Soluble phosphorus
TOC	Total organic carbon
TN	Total nitrogen
TP	Total phosphate
UCT	Activated sludge University of Cape Town systems
UCTOLD	The University of Cape Town (UCT) old model
UCTPHO	The University of Cape Town (UCT) model of phosphate accumulating organisms (PAOs)
UNSIM	UNSIM programme
VFAs	Volatile fatty acids

v_{ji}	Stoichiometric coefficient for component i in process j
WWTPs	Wastewater treatment plants
X_{AUT}	Nitrifying organisms
X_H	Heterotrophic organisms
X_I	Inert particulate organic substrates
X_{Iin}	Influent inert particulate organic substrates
X_{PAO}	Phosphorus accumulating organisms (PAOs)
X_{PAOin}	Influent phosphorus accumulating organisms (PAOs)
X_{PHA}	A cell internal storage product of PAOs
X_{PHAin}	Influent a cell internal storage product of PAOs
X_{PP}	Poly-phosphate
X_{PPin}	Influent poly-phosphate
X_S	Slowly biodegradable substrate
X_{Sin}	Influent slowly biodegradable substrate
X_{TKN}	Particulate Kjeldahl nitrogen
X_{TSS}	Total suspended solids
X_{TP}	Particulate phosphorus
yi	Model output
Y_A	Yield coefficient (Biomass/Nitrate)
Y_H	Yield coefficient
$Y_{H,ANA}$	Yield of ordinary heterotrophic organisms (OHOs)
Y_{PAO}	Growth yield coefficient
Y_{PHA}	PHA requirement for poly-P storage
Y_{PHB}	Yield of poly-hydroxy-butyrate (PHB)
Y_{PO4}	Poly-phosphate requirement (PO_4 release) per PHA

CHAPTER 1:

INTRODUCTION

CHAPTER 1. INTRODUCTION

1.1 PROJECT BACKGROUND

Eutrophication is the excessive enrichment of waters with nutrients and associated adverse biological effects. It is still one of the major environmental problems across Europe (EEA, 2005). The whole range of European waters is affected from inland water bodies such as groundwater, rivers and lakes, to transitional and coastal waters and ecosystems in open seas. Phosphorous (P) loads that enrich rivers as nutrients from point and diffuse (nonpoint) sources provide critical information to catchment manager. This information allows them to select the most suitable nutrient mitigation options to reduced P concentration and eutrophication risks (Withers and Sharpley, 2008). China is one of the largest producers and consumers of chemical fertilizers in the world. Excessive nutrient loading from agricultural watersheds is considered the principal component of nonpoint source (NPS) pollution in China (Yan et al., 1999). These pollutants come mainly from fertilizers, pesticides, rural dwellers, and distributed livestock farms. Eutrophication due to NPS P has become a serious pollution problem in many Chinese rivers. Phosphorus from excessive use of fertilizers can be discharged into receiving water with rainfall and irrigation. This can induce eutrophication in the receiving water and loss of biodiversity in the aquatic ecosystem.

Regarding phosphorus, point sources such as households and industry still tend to be the most significant sources. However, as point source discharges in many countries have been markedly reduced during the last 15 years, agriculture has sometimes become the main source (EEA, 2005). Examining phosphorus load in selected countries and catchments, the total area-specific load of phosphorus is highest in countries and catchments with high population density and large areas of agricultural land. In countries/catchments having high population density and without nutrient removal at the majority of wastewater treatment plants, point sources generally account for more than two thirds of the load. The percentage breakdown of point source discharge into the Baltic Sea in year 2000 from municipal wastewater, industry and fish farms are 85%, 14% and 1%, respectively. In addition, the percentage breakdown of point source

discharges into the North Sea in the year 2000 from sewage treatment works, households not connected to sewage treatment works, industry, and aquaculture are 68%, 15%, 16%, and 1%, respectively. Moreover, the percentage breakdown of point source discharges into the Danube River basin in the years 1996/1997 from municipal point sources, industrial point sources and agriculture point sources are 78%, 15% and 7%, respectively. Bowes et al. (2005) used the recently developed Load Apportionment Model to study the changes in the relationship between soluble reaction phosphorus (SRP) concentration and the flow of the River Frome, UK, between 1966 and 2005 (Table 1.1) . It was shown that the point contribution to the total river load increased from 46% to 62% between 1970 and 1985. The predicted mean SRP load was 30 ton/year between 1996 and 2000, with 49% coming from point sources. However during 2001 to 2005, the model predicted a reduced load of 18.1 ton/year. This was equivalent to 34% of the total load. This decrease occurred because of major improvements in sewage treatment made within the catchment in 2002.

Table 1.1 Load apportionment modelling of the five-year data subsets

Date	Point source load (ton/year)	Diffuse source load (ton/year)	Estimated total load (ton/year)	Proportion of load from point soures (%)
1966-1970	10.6	12.5	23.1	46
1971-1975	10.4	12.3	22.7	46
1976-1980	12.4	12.4	24.8	50
1981-1985	14.6	8.9	23.5	62
1986-1990	12.5	9.2	21.7	58
1991-1995	-	-	-	-
1996-2000	14.6	15.4	30.0	49
2001-2005	6.1	12.0	18.1	34

Neal et al. (2005) proposed that the reduction of point sources may help to minimize the size of nutrient fluxes at the catchment scale. Reduction of diffuse sources may help restore good water quality in individual tributaries. Pieterse et al. (2003) studied the River Dommel. It was shown that point sources were the overall main contributor to nutrient fluxes, although they actually impacted a few tributaries. Additionally, Edwards and Withers (2008) proposed the individual sources of phosphorus in the temporal aspects of their strength, mobility/transport pathway and their subsequent delivery to receiving waters having variable degreees of dependency upon rainfall events. Ranges in composition and loading are shown in Table 1.2.

Table 1.2 Total P (TP) concentrations of various sources

Source type	TP, mg L^{-}	Range of TP, mg L^{-1}	Source type	TP, mg L^{-1}	Range of TP, mg L^{-1}
Farmyard runoff	30.80	0.02-247	Septic effluent	10.20	1-22
Pig slurry	41.10	39.4-43.6	STW effluent	2.90	<DL-13.10
Road runoff	0.26	0.18-0.34	Track runoff	2.69	0.24-7.30

STW: sewage treatment works, <DL – less than detection limit. Source of data: Farmyard runoff – Dunne et al. (2005), Chadwick and Chen (2002), Tanner et al. (1995), Cumby et al. (1999), Newman et al. (2000), Kern and Idler (1999) and Mantovi et al. (2003), Pig slurry – Lee et al. (2004), Road runoff – Mitchell (2001), Septic effluent – Greenway and Woolley (1999), Kern and Idler (1999), Luederitz et al. (2001), Gschlossl et al. (1998), STW effluent –Edwards and Withers (2008), Track runoff – Edwards and Withers (2008)

Discharges of phosphorus from point sources have decreased significantly during the past 30 years (EEA, 2005), whereas the number of diffuse sources has generally remained at a constant level. The changes have been largest for phosphorus. The largest reduction the total load was due to previously reduction in the very high number of point source discharges. The contribution from diffuse sources has become relatively more significant as a consequence of the reduction in point source discharges. The changes are mainly due to improved purification of urban wastewater.

In recent decades eutrophication has become a serious water pollution problem in many Chinese rivers. It is the result of human activities that caused a cumulative increase in nitrogen (N) and P in bodies of water (Ma et al., 2008). With effective abatement of point source pollution, contributions from NPS, such as agriculture, street runoff, deposition of atmospheric pollutants, mine sites, transportation corridors such as road and railways, etc., have become a major cause of water quality degradation in China (State Environment Protection Administration of China, 2000). Also, NPS pollution, especially that which results from agricultural activities, has been identified as a significant source of water quality pollution in the United States (USEPA, 2003) and other western countries (Bowes et al., 2005). For water pollution, two types of NPS are of particular concern — agricultural/rural NPS and urban NPS (Ongley et al., 2010). The export coefficient model (ECM) was used to assess the influence of NPS on P loading in the Three Gorges Reservoir Area (TGRA) of Hubei Province, People's Republic of China (Xiao Ma et al., 2011). The potential P loading from NPS originated from a variety of sources from 1995 to 2007 were estimated and analyzed using the ECM. These included runoff from rural domestic waste, livestock farms, land use, and

atmospheric deposition. The calculated TP load was 2.14×10^3 tonnes in 2007. The major source of TP was land use (729 tonnes), the live stock was also significant part (689 tonnes). It was followed by atmospheric deposition (452 tonnes) and rural domestic waste (270 tonnes).

Enhanced biological phosphorus removal (EBPR) systems have been widely used to avoid eutrophication problems (Cao et al., 2006). EBPR operations can reduce the phosphorus content. The presence of readily biodegradable substrates as carbon sources is important to EBPR (Barker, et al., 1996 & 1997). A metabolic model of EBPR processes is important for the study of phosphorus accumulating organisms (PAOs) (López-Vázquez et al., 2007; Oehmen et al., 2007).

In an anaerobic phase, the PAOs can take up volatile fatty acids (VFAs) through cell membranes and convert them to intracellular poly-hydroxy-alkanoates (PHA), mainly poly-hydroxy-butyrate (PHB), as an energy and carbon sources (Smolders et al., 1994a & 1994b). VFAs uptake is based on transport energy in relation to pH (energy requirement) and polyphosphate (poly-P, energy production). The energy requirement for transport of VFAs is affected by a pH gradient and an electrical potential difference ($\Delta\psi$) (Smolders et al., 1994a & 1994b; Smolders et al., 1995a & 1995b). The transformation of internal poly-P to external orthophosphate (PO_4) provides the energy which is required for uptake of VFAs. Meanwhile, internal glycogen in glycolysis supplies the reducing equivalents (ATP) for anaerobic VFAs conversion to PHA (Pijuan et al., 2008; Zhou et al., 2009). The utilisation of VFAs for PHA synthesis accomplishes synthesis of poly-P, biomass, and glycogen under anoxic and aerobic conditions (Kuba et al., 1996; Mino et al., 1998; Hu et al., 2003). In subsequent reactors (aerobic and/or anoxic phase), the PHA are oxidized by oxygen or nitrate, as an electron acceptor in aerobic and anoxic conditions, respectively. It provides energy for orthophosphate uptake and then produces intracellular poly-P. The PHA is used as energy and carbon sources in both aerobic and anoxic conditions (1) for glycogen synthesis, (2) for biomass synthesis, and (3) for poly-P synthesis (Mino et al., 1998; Yagci et al., 2003; Cao et al., 2006; Whang et al., 2006; Oehmen et al., 2007). Therefore, the efficiency of phosphorus removal in the EBPR systems depends on the metabolism of the PAOs.

With regard internally stored phosphate as poly-P in PAOs, the phosphorus can be removed from the system as excess sludge.

The use of VFAs as a carbon source significantly enhances biological phosphorus removal processes (Llabres et al., 1999; Chen et al., 2004; Elefsiniotis et al., 2004; Tong and Chen, 2007; Feng et al., 2009; Zheng et al., 2009). An improvement in the efficiency of biological nitrogen and phosphorus removal was evident when using VFAs in an alkaline fermentation of municipal waste activated sludge (Ji and Chen, 2010; Zhang et al., 2010; Zheng et al., 2010; Gao et al., 2011; Li et al., 2011). Also, the study of Carucci et al. (1999) concluded that increasing phosphorus release is due to VFAs and fermentable organics. A number of researches have been showed that mechanically disintegrated sludge (DS) can generate carbon sources which are useful for the EBPR systems (Schmitz et al., 2000; Tiehm et al., 2001; Onyeche et al., 2002; Bougrier et al., 2005; Dewil et al., 2006; Wang et al., 2006; Kampas et al., 2006; Kampas, 2007; Zhang et al., 2007a & 2007b; Minervini, 2008). DS can act as an EBPR carbon source to increase the efficiency of EBPR (Onyeche et al., 2002; Dewil et al., 2006). DS is comprised in part of soluble chemical oxygen demand (SCOD) including acetic acid and other volatile fatty acids (VFAs), total phosphate (TP), protein, DNA, polysaccharide and carbohydrate (Schmitz et al., 2000; Kampas et al., 2007). Protein is the predominant component among the various carbon compounds (Wang et al., 2006). This is because microbial cell walls were disrupted (Tiehm et al., 2001; Kampas, 2006; Minervini, 2008). VFAs in DS can accelerate the anaerobic digestion process (Bougrier et al., 2005; Zhang et al., 2007a & 2007b). Phosphate (PO_4) release was enhanced by this treatment (Kampas et al., 2009; Soares et al., 2010). In a pilot scale experiment, Kampas (2006) showed that influent DS can result in removal of phosphorus between 44 to 89% more than without DS. In experimental results, the SCOD and VFAs increased from 50 to 1300 mg L^{-1} and from 236 to 852 mg L^{-1}, respectively. Minervini (2008) reported that using ultrasound treatment for floc breakage, sludge solubilisation was observed. Floc size was reduced by 88% at 42 kJ L^{-1} while the degree of SCOD release increased almost linearly from 11 to 36% between 42 to 168 kJ L^{-1}. In addition, total phosphorus removal was increased from 0.1 to 1 mg-P/ L at 168 kJ L^{-1} and 6,048 kJ L^{-1} energy input. Zhang et al. (2007b) reported that an advantage of sludge

disintegration in aerobic sequential batch reactors (SBR) is seen by an observed improvement in chemical oxygen demand (COD) and total nitrogen (TN) removal. The magnitudes of increase in these values were reported as 81% and 17-66%, respectively. The result is that internal carbon sources from sludge disintegration are likely to be relevant substances for improvement of enhanced phosphorus removal efficiency. Therefore, understanding the microbiological mechanisms is a desirable for investigating the effects of DS on the efficiency of phosphorus removal. These methods of investigation were implemented with mathematical modeling and statistical analysis (Deo et al., 2009; Chi et al., 2010).

The use of a mathematical model for understanding the PAOs mechanism is relevant to the EBPR processes. A useful biological nutrient model can simulate metabolic processes of microorganisms under anaerobic, aerobic and anoxic conditions. Activated Sludge Model No. 2d (ASM2d) (Henze et al., 1999) was chosen for use in this study because it can model organic, nitrogen and phosphorus substrates under the above conditions. The ASM2d model was developed on the basis of Activated Sludge Model No. 2 (ASM2) (Henze et al., 1995) and Activated Sludge Model No. 1 (ASM1) (Henze et al., 1987). ASM1 is an excellent tool for modeling nitrification-denitrification processes. Additionally, ASM2 simulates phosphorus utilization by PAOs under aerobic conditions only. In contrast, ASM2d models phosphorus up take under anoxic and aerobic conditions (Kerrn-Jespersen and Henze, 1993; Mino et al., 1998; Meinholt et al., 1999). ASM2d was further extended to model the kinetics of nitrate and phosphate metabolism under anoxic conditions (Henze et al., 1999). PAOs can utilise VFAs and store poly-hydroxy-butyrate (PHB) intracellularly for (1) an anoxic polyphosphate (poly-P) formation process and (2) an anoxic PAOs growth process. Simulation of these processes is modified from PAOs growth and poly-P formation under aerobic conditions in ASM2. Under anoxic conditions, PAOs use nitrate as a terminal electron acceptor instead of oxygen to metabolize phosphorus. The rates of anoxic poly-P formation and anoxic PAOs growth are given by the aerobic poly-P storage rate and the aerobic growth rate multiplied by a reduction factor η_{NO3}, respectively. This is because some PAOs can grow and/or utilize orthophosphate (PO_4) under anoxic conditions. This

takes into account that the metabolism of PAOs growth and the poly-P storage is reduced under anoxic conditions (Hu et al., 2003).

1.2 PROJECT DEVELOPMENT

The work presented in this research was sponsored by a fellowship of the Thai Government and Suranaree University of Technology to investigate influence of disintegrated sludge (DS) on phosphorus removal efficiency.

1.3 AIMS AND OBJECTIVES

It was hypothesized that the use of DS as carbon sources could enhance phosphorus removal efficiency at a higher rate when compared with just acetate. The goal of this thesis was therefore to investigate effects of DS on PAOs mechanisms in activated sludge EBPR systems. Accordingly a series of objectives were identified:

1. To propose a novel calibration approach for reducing parameter subset sizes in ASM2d modeling.
2. To investigate stoichiometric and kinetic coefficients of the ASM2d model for evaluation of the effects of DS on EBPR processes using a novel calibration approach.
3. To identify the significant DS sludge components that impact phosphorus removal efficiency using statistical analysis.
4. To verify the above calibration approach to determine if the resulting model can achieve specified performance requirements.

1.4 THESIS PLAN

The calibration of the mathematical simulation modeling was completely by Nittaya Boontian. All chapters were written by the primary author and edited by thesis supervisors: Dr. Ana Soares and Professor Dr. Elise Cartmell. This thesis is presented as a series of chapters which have been formatted for journal papers as follows:

Initially, a literature review was conducted investigating the biological nutrient removal (BNR) and enhanced biological phosphorus removal (EBPR) models. Mathematical simulation modelling is a tool to aid the design and operation of activated sludge wastewater treatment systems. Six models were examined: (1) UCTPHO, (2) ASM2, (3) ASM2d, (4) the Barker and Dold model, (5) the Delft model and (6) ASM3 with Bio-P.

In Chapter 3, literature data obtained in Chapter 2 was employed to assess the most accurate EBPR system kinetic models. This chapter describes the selected mathematical simulation modeling with information and explains operation of simulations. The steps of calibrate the model for biological nutrient removal were shown. In addition, a verification method to determine model acceptability was described.

In Chapter 4, a novel calibration approach is presented to reduce ASM2d parameter subsets and decrease the model complexity. This approach does not require high computational demand and reduces the number of modeling parameters required to achieve the ASM's calibration. This is done by employing a sensitivity and iteration methodology.

In Chapter 5, the evaluation of disintegrated sludge (DS) upon enhanced biological phosphorus removal (EBPR) processes was completed using Activated Sludge Model No. 2d (ASM2d) modeling. Successful calibration of phosphorus accumulating organisms (PAOs) and autotrophic mechanisms was achieved.

In Chapter 6, a biological phosphorus removal pilot plant was used to study the effects temperature and use of disintegrated sludge (DS) as a carbon source upon phosphorus accumulating organisms (PAOs). Experiments were carried out at 17°C and 23°C.

In Chapter 7, the overall impact of the research was discussed. The evaluation of influence of influent DS on PAOs obtained from calibration model is discussed.

In Chapter 8, conclusions of this research concerning the impact of influent DS on PAOs in relation to the EBPR systems is presented.

CHAPTER 2:

BIOLOGICAL NUTRIENT REMOVAL MODELS: A REVIEW

CHAPTER 2. BIOLOGICAL NUTRIENT REMOVAL MODELS: A REVIEW

ABSTRACT

The evaluation of biological nutrient removal (BNR) and enhanced biological phosphorus removal (EBPR) models is presented. Mathematical simulation modeling is a tool to aid the design and operation of activated sludge wastewater treatment systems. Six models are examined: (1) UCTPHO, (2) ASM2, (3) ASM2d, (4) the Barker and Dold model, (5) the Delft model and (6) ASM3 with Bio-P. UCTPHO and ASM2 models predict chemical oxygen demand (COD), nitrogen (N) and phosphorus (P) removal. ASM2d, the Barker and Dold model, the Delft model and ASM3 with Bio-P can be used to describe reduced uptake of P and associated phosphorus accumulating organisms (PAOs) denitrification. In fact, all of them have limiting conditions. ASM2d can only model the amount of denitrifying PAOs, but it is unable to simulate reduced uptake of P under anoxic conditions. The Barker and Dold model has the limitation of reduced yields under anoxic conditions. The Delft model cannot demonstrate the interaction between PAOs and ordinary heterotrophic organisms (OHOs). Fermentation processes convert readily biodegradable chemical oxygen demand (RBCOD) to short-chain volatile fatty acids (VFAs) by OHOs. ASM3 with Bio-P cannot model the intermediate nitrite reactions in a single-step process. Hence, modification of ASM2d, the Barker and Dold model, the Delft model and ASM3 with Bio-P is the best approach to avoid the limiting conditions of each of these models.

Keywords: ASM2; ASM2d; ASM3 with Bio-P; Barker and Dold; Delft; UCTPHO

2.1 INTRODUCTION

Successful biological nutrient removal processes (BNR) use carbon sources for growth resulting in internal carbon storage (Thomas et al., 2003). Short-chain volatile fatty acids (VFAs) are a suitable carbon source for BNR (Elefsiniotis et al., 2004; Tong and Chen, 2007). In addition, use of VFAs as a carbon source significantly enhance biological phosphorus removal (EBPR) processes (Llabres et al., 1999; Chen et al., 2004; Feng et al., 2009). Different approaches can increase VFAs in wastewater. Mechanical disintegration of thickened surplus activated sludge by a deflaker technology was shown to increase soluble chemical oxygen demand (SCOD) as well as VFAs (Kampas et al., 2007). Phosphate (PO_4) release was enhanced by this treatment (Kampas et al., 2009; Soares et al., 2010). VFAs in ultrasonicated disintegrated sludge can accelerate the anaerobic digestion process (Bougrier et al., 2005; Zhang et al., 2007). Furthermore VFAs in an alkaline fermentation of municipal waste activated sludge can enhance the efficiency of biological nitrogen and phosphorus removal (Ji and Chen, 2010; Zhang et al., 2010; Zheng et al., 2010; Gao et al., 2011; Li et al., 2011). To achieve successful operation of BNR as well as EBPR processes it is important to investigate the effects of carbon sources as well as VFAs upon the behavior of organisms by using mathematical modeling. It helps in design, operation and optimization of activated sludge wastewater treatment plants (WWTPs) (Hu et al., 2003).

The most widely used BNR system kinetic models were evaluated in this current study. These models are: (1) The University of Cape Town (UCT) model (UCTPHO); (2) Activated Sludge Model No. 2 (ASM2); (3) Activated Sludge Model No. 2d (ASM2d); (4) the Barker and Dold model; (5) the Delft model and (6) Activated Sludge Model No. 3 with biological phosphorus (P) (ASM3 with Bio-P). Evaluation of models mainly focused on P uptake under anoxic conditions and associated denitrification by phosphate accumulating organisms (PAOs). These are important considerations. In model evaluation, it is not possible to present all aspects of each of the models. The primary focus is on biological nitrogen and phosphorus removal.

2.2 SLUDGE DISINTEGRATION

A large number of activated sludge in biological wastewater treatment processes are currently used (Yu et al., 2010). Many operational problems arise from treatment and disposal. These sludge treatment methods are costly. The disposal of waste activated sludge presents the most important and complex problems in operation of sludge reduction in municipal wastewater treatment plants (Ahn et al., 2009; Park et al., 2009). Mechanical pre-treatment is used to enhance substrate solubilizing microbial cells. It is rather complicated and expensive (Carballa et al., 2007). Disintegration techniques for sludge minimization have been developed to accelerate the sludge digestion processes. Sludge disintegration is used as a mechanical pre-treatment to disrupt microbial cells. In the sludge disintegration process, bacteria release extracellular enzymes breaking down and then solubilizing organic matter (Ahn et al., 2009). Breakdown products are used as substrates in subsequent reactions. Solubilization of sludge converts slowly biodegradable, particulate organic materials into readily biodegradable products.

Sonication of sludge can disrupt microbial cells up to 100%. However, energy consumption is high. Chemical and thermochemical pre-treatments are efficient technologies in enhancing sludge digestion. These methods are often used when there are special material requirements requiring aggressive reaction conditions. Sludge disintegration with thermal pre-treatment prior to anaerobic digestion has been examined (Ahn et al., 2009). Conventional low-temperature thermal treatment requires a longer contact time than high temperature treatments. Among the oxidation processes, sludge ozonation is of special interest. This is because the process leaves no oxidant residues and does not increase salt concentration (Erden et al., 2010). Wet sludge disintegration causes corrosion problems and there is limited knowledge of the process. Therefore, an effective and economical pre-treatment method is essential.

Other researchers proposed microwave irradiation as a possible approach (Park et al., 2009). The advantages of microwaves include rapid heating, pathogen destruction, compactness, and low overall costs. Ultrasonic treatment is one of the most effective recent technologies in sludge disintegration. It has positive aspects, i.e., reliability of

operation, no odour generation, no clogging problems, ease of implementation in WWTPs (Wang et al., 2005; Khanal et al., 2007).

In order to reduce sludge volume, many physical and chemical techniques have been used including thermal hydrolysis (Wilson and Novak, 2009), ultrasonic treatment (Feng et al., 2009), hydrolysis and acidification (Liu et al., 2008), microwave irradiation (Park et al., 2009), ozonation (Cheng et al., 2012), and mechanical disintegration (Kampas et al., 2007; Kampas et al., 2009). Mechanical sludge disintegration uses a pulp deflaker. It is a technology employed in paper processing industries. It used to generate extra carbon for surplus activated sludge in order to improve BNR.

2.2.1 Ultrasonic pre-treatment of sludge

Extensive research has been done to determine the best economically feasible pre-treatment technology to enhance the digestibility of sludge. Ultrasonication techniques are a promising means for mechanical disruption in sludge disintegration. This is true for several reasons, i.e., efficiency of sludge disintegration, improvement in biodegradability, improved biosolids quality, increased methane concentration in biogas, no chemical additions required, less retention time and greater sludge reduction (Barber, 2005; Khanal et al., 2007). In ultrasonic techniques, sound waves are applied at frequencies greater than 20 kHz. Intracellular materials can be recovered after ultrasonic biological cell disruption (Pilli et al., 2011).

2.2.1.1 Cavitation phenomena induced by ultrasound

The principle of ultrasound techniques is to destroy bacterial cell walls, subsequently making intracellular matter available for degradation to CH_4 and CO_2 in anaerobic digestion. Ultrasound waves generate compressions and rarefactions when they propagate through a sludge medium. The compression cycles provide a positive pressure on the liquid by pushing the molecules. The rarefaction cycles provide a negative pressure pulling the molecules from one another. An excessively large negative pressure results produces microbubbles (cavitation bubbles) in the rarefaction regions.

These microbubbles develop to an unstable diameter. Large shock waves are produced due to their violent collapse. Local temperatures of 5,000 ºC and pressures of 500 atmospheres can exist for several microseconds (Pilli et al., 2011). This phenomenon is known as cavitation.

2.2.1.2 Ultrasound generation and disintegration mechanisms

Ultrasonic conditions can be developed using magnetostrictive and piezoelectric techniques. The magnetostrictive techniques involve vibration of materials such as nickel and Terfenol-D in a magnetic field. Electrical energy is converted to mechanical energy with a magnetic coil (Pilli et al., 2011). Piezoelectric techniques involve vibration of specialized materials (sonotrode, probe and horn) generated by electrical energy. High frequency electrical energy is applied to piezoelectric crystals. Subsequently, a transducer (converter) converts electrical or mechanical energy to sound waves. A booster mechanically amplifies the resulting vibration, increasing its amplitude. Finally a horn delivers ultrasonic waves to liquid.

2.2.1.2.1 Sludge disintegration

The energy for ultrasonic sludge disintegration is characterized in several ways. These include (a) specific energy input, (b) ultrasonic dose, (c) ultrasonic density and (d) ultrasonic intensity. The disintegration mechanisms during use of ultrasonication on sludge are shown below (Wang et al., 2005; Khanal et al., 2007):

(a) Hydro-mechanical shear forces
(b) Oxidising effects of $^{\cdot}OH$, $^{\cdot}H$, $^{\cdot}N$, and $^{\cdot}O$ produced during ultrasonic conditions
(c) Thermal decomposition of volatile hydrophobic substances in the sludge
(d) Temperature increase during ultrasonic activated sludge disintegration

Powerful hydro-mechanical shear forces in the bulk liquid surrounding the bubbles occur as a result of the violent collapse of huge numbers of microbubbles (Wang et al., 2005; Khanal et al., 2007).

2.2.1.3 Evaluation of ultrasound disintegration

Ultrasound de-agglomerates biological flocs and disrupts large organic particles breaking them into smaller sizes. Bacterial cell walls are broken down by shear forces generated by high pressure waves. Subsequently, intracellular substances releases into the aqueous phase occur. Physical, chemical and biological properties of sludge change during ultrasonic disintegration. Therefore, evaluation of degree of sludge disintegration is based upon the changes these properties. Physical changes include particle size distribution, turbidity, settleability, mass composition and microscopic appearance. Chemical modifications include increase in soluble chemical oxygen demand (SCOD), protein concentration, polysaccharide content of the supernatant, nitrate nitrogen and release of NH_3. Biological changes are also observed including heterotrophic counts and specific oxygen uptake rates.

2.2.1.3.1 Physical changes

Sludge disintegration by ultrasonication influences its physical properties. It enhances anaerobic digestion (AD). Qualitative measures of sludge disintegration are used to evaluate physical parameters. There are many techniques to measure the degree of ultrasonic disintegration, i.e., particle size analysis, sludge settleability, mass composition, microscopic image, turbidity, and sludge dewaterability. The specific technique used in a particular case for particle size analysis depends upon sizes of the particles. Available methods include use of sieves, sedimentation, electrozone sensing, microscopy, and laser diffraction. Laser diffraction is usually used for particle size analysis of ultrasonic disintegration products. This is due to the very small sizes of disintegrated sludge particles. Sonication parameters can be changed by varying ultrasound density, ultrasound intensity, and sonication time. Varying these parameters can change the turbidity of sludge. Analysis of turbidity is done using a turbidity meter with NTU units. Dewaterability of sludge is measured using capillary suction time (CST) and specific resistance to filtration (SRF) (Pilli et al., 2011).

Particle size. Particle size solubilization is done on the influent for methane production in mature digesters (Akin et al., 2006 & 2008). Ultrasound pre-treatment is essential for reducing the particle sizes in sludge. The efficiency of particle size reduction depends upon sonication duration (Guangming et al., 2006), ultrasonic density (Show et al., 2007; El-Hadj et al., 2007; Mao and Show, 2006 & 2007; Laurent et al., 2009), sonication power (Mao and Show, 2006; Wang et al., 2006; Show et al., 2007), sludge volume and sludge characteristics (Bougrier et al., 2005; Akin et al., 2006; Mao and Show, 2006). Increasing the sonication time gradually reduces particle sizes.

Dewaterability of sludge. Influences of ultrasonication on sludge dewaterability are both positive and negative. Lower power is needed with less sonication time increasing dewaterability. However, the degree of sludge disintegration is low due to decreased cell lysis (Pilli et al., 2011). The dewaterabililty of sludge decreases with increasing ultrasonication intensity. Dewaterability develops after disintegration of anaerobically digested sludge. Thus, the dewaterability of digested sludge increases after sonication. This is because flocs are not broken into smaller particles at lower power levels and there is less sonication time.

Settleability of sludge. Increasing specific energy applied to influent sludge changes its settleability. Improvement in the settleability of wastewater activated sludge (WAS) occurs when the applied specific energy is less than 1000 kJ/kg TS. This is because disruption of flocs is less with lower specific energy (Feng et al., 2009). Deterioration of WAS settleability takes place when specific energy is greater than 5000kJ/kg TS. At these power levels, flocs are completely broken down.

Microscopic examination of sludge. Evaluation of the degree of disintegration can be seen by comparing microscopic images of microbes before and after sludge disintegration. Sludge disintegration disrupts flocs and lyses cell walls (Khanal et al., 2007). Microscopic evaluations reveal cellular aspects of disintegrated sludge. After different sonication times, changes in the structural integrity of flocs and microbial cell walls can be observed. Even though ultrasonication has significant effects on microbial disruption, the efficiency of the disruption is not clear. It is still required to evaluate the

effects of ultrasonication on microbial disruption at different specific energy input levels and sonication times.

Change in turbidity. The turbidity of disintegrated sludge is increased by greater degrees of particle size reduction (Laurent et al., 2009). Higher sludge disintegration efficiency occurs at a lower ultrasonic frequency (20 kHz) (El-Hadj et al., 2007; Na et al., 2007; Feng et al., 2009; Laurent et al., 2009). The turbidity of disintegrated sludge increases drastically when specific energy input is greater than 5000 kJ/kg TS. The turbidity of supernatant sludge decreases when the specific energy input is less than 5000 kJ/kg TS (Feng et al., 2009). When the specific energy input is less than 1000 kJ/kg, flocs are not disrupted. Thus, the minimum specific energy input requirement for disintegration sludge is 1000 kJ/kg TS (Bougrier et al., 2005; Feng et al., 2009). The efficiency of disintegrating sludge can be evaluated by measuring physical parameters. Extensive studies are still needed to understand the relation between sonication parameters and physical parameters.

2.2.1.3.2 Chemical evaluation

Various types of micro-organisms exist in the complex substrate sludge. The strength of cell walls of various micro-organisms is different. Efficiency of sludge disintegration is evaluated using chemical parameters (Khanal et al., 2007). The degree of disintegration (DD) is used to evaluate efficiency of sludge disintegration (Pilli et al., 2011).

Soluble COD assessment. Both cellular and extracellular matter are disrupted by ultrasonication. This generates organic debris and extracellular polymer substrates (EPS). Solubilisation of solid materials and EPS in the aqueous phase indicates a change in SCOD. Therefore, SCOD is used to evaluate efficiency of sludge disintegration. There are also other important parameters for chemical evaluation after disintegrating sludge, i.e., ammonium nitrogen, nitrate nitrogen and EPS concentrations (Bougrier et al., 2005).

Protein assessment. Extracellular organic carbon is mostly in the form of proteins and saccharides (Pilli et al., 2011). Proteins are important in bacteria. They are responsible for many different functions of living cells. Protein is used in quantification of sludge disintegration in WAS (Akin et al., 2006; Wang et al., 2006).

NH_3 assessment. Organic nitrogen and ammonia are released by sludge disintegration (Bougrier et al., 2005; Khanal et al., 2007; Akin et al., 2008; Feng et al., 2009). Therefore, evaluation of NH_3 can also be used to determine the degree of sludge disintegration. Organic nitrogen solubilisation is 40% at a specific energy of 15,000 kJ/kg TS and the maximum solubilisation of organic nitrogen occurs at a specific energy input of 10,000kJ/kg (Bougrier et al., 2005). Other research found that as specific energy input is increased, release of ammonia nitrogen is also increased (Khanal et al., 2007). As specific energy is increased above 3600 kJ/kg TS, the total nitrogen solubilisation increases linearly (Salsabil et al., 2009). At a specific energy input of 108,000 kJ/kg TS, solubilisation was reported as 19.6% (Salsabil et al., 2009). Increase in NH_3 concentration during sludge disintegration it is due to disruption of bacterial cell walls and release intracellular organic nitrogen, which is subsequently hydrolyzed to ammonia (Akin et al., 2008).

Biological evaluation. Sludge disintegration breaks down bacterial cell walls. This was observed in biological utilization tests. WAS contains aerobic and facultative bacteria. Here, the oxygen utilization rate (OUR) is used to evaluate microorganisms' kinetics. When bacterial cells are completely disrupted, the degree of disintegration is 100%. Thus, OUR can be used to evaluate the efficiency of sludge disintegration (Pilli et al., 2011).

2.2.2 Microwave irradiation

Microwave technology is used in different applications, e.g., organic decomposition, the sterilization of medical waste, and the inactivation of microorganisms in foods, animal manure and soil (Eskicioglu et al., 2006). The advantages of microwave treatment include rapid heating, pathogen destruction, ease of control, compactness, and low overall cost. Generally, the thermal effects of microwave exposure destroy microorganisms.

Several researchers are still investigating whether microwave irradiation also has a non-thermal effect. The microwave fields cause polarized side-chains of macromolecules to move in the direction of the electric field. Breakage of hydrogen bonds and alteration of hydration zones are possible. Several variables associated with microwave irradiation affect dielectric materials including strength (frequency), irradiation time, concentration, and penetration depth (Eskicioglu et al., 2006). After World War II, many applications using microwave irradiation were developed for industrial processes including those in environmental engineering field. Waste processing also attracted much interest (Tang et al., 2010). The use of microwave technology can be used for the processing of excess sewage sludge (ESS).

The treatment of ESS with microwave irradiation normally uses a shorter wavelength (12.24 cm at 2450 MHz). The thermal effect is the main effect of microwave irradiation when pre-treating ESS. Rotation of dipole molecules under an oscillating electromagnetic field generates the thermal energy. Energy-efficient heating of intracellular water causes the cells of microorganisms to be broken down releasing bound water. Eskicioglu et al. (2007) hypothesized that there is no thermal effect on COD solubilization of ESS. However, they found that it had positive impact on mesophilic anaerobic biodegradability of sludge. It was realized that the thermal effect of microwave irradiation is caused by polarized molecules. Microwave heating causes breakage of hydrogen bonds leading to death of microorganisms at lower temperatures. Synergistic pre-treatment with microwave irradiation and use of strong oxidizers has been investigated as methods to enhance sludge reduction (Eskicioglu et al., 2008; Yin

et al., 2008; Yin et al., 2007). Increasing microwave irradiation temperature enhances the decomposition of H_2O_2 into OH^- radicals. Both oxidation of COD and solubilization of particulate COD are thereby increased. Other researchers investigated the effectiveness of microwave irradiation in combination with alkaline pre-treatments and found improvement of COD solubilization and biogas production (Doğan and Sanin, 2009).

2.2.3 Ozone

Among different physical and chemical pre-treatments, sludge ozonation is a promising technology (Yasui et al., 2005; Bougrier et al., 2007; Dogruel et al., 2007; Cheng et al., 2012). Ozonation dosage and contact time are the primary factors affecting enhanced solubilisation. Sludge ozonation-cryptic growth (i.e., the recycling of nutrients derived from disrupted cells for the maintenance of surviving cells) is accomplished by partial or complete sludge treatment in an activated sludge wastewater treatment system with ozone. Subsequently, sludge is recycled to other WAS processes. A large number of microorganisms can be linked by extracellular polymeric substances (EPS), positive ions and some granules. Small flocs are formed as solid granules of sludge become a core. This material adsorbs a great number of bacteria. Microorganisms release compounds such as saccharides, organic acids, nucleic acids, proteins, and fats, forming loose three-dimensional structures. Ozone is a strong oxidizing agent and disinfectant. It is toxic to bacteria. Ozone damages cell walls of microorganisms and destroys the zoogloea structures (Zhang et al., 2009). As a result, transformed soluble substances can be further degraded biologically in wastewater treatment processes. The production of excess sludge is reduced using ozonation-cryptic growth technology. In this process, waste water under pressure is supersaturated with an ozone/air mixture. Pressure is released forming microbubbles. The expanding bubbles have diameters ranging in size from nanometers and micrometers to centimeters. Microbubbles containing ozone are very effective for removing organic contaminants from sediment and water (Hong et al., 2008b; Cha et al., 2010). The expanding microbubbles accumulate aqueous contaminants in the gas-liquid phase (Chu et al., 2008; Hong et al., 2008a; Hong and Nakra, 2009). As a result, the contaminants of sewage sludge are more efficiently

removed. Microbubbles uniformly form with depressurization in the reactor. Their formation is not dependent upon the location of an injector. Implementation of this new sludge treatment process is done by placing the treatment equipment between the secondary clarifier and the digestion reactor in the wastewater treatment plant. Ozonation is done to a sludge fraction. Treated sludge is then recycled in the activated sludge treatment plant system. This is a method of minimizing sludge production (Dytczak and Oleszkiewicz, 2008). An application of sludge ozonation to pre-anoxic zones helps to improve denitrification. This is because addition carbon is generated from solubilization of sludge by ozonation. For economic reasons, an application of sludge ozonation at low ozone doses is used to inhibit filamentous bulking (Chu et al., 2009). At an ozone dose of 18 mg O_3 g^{-1} volatile suspended solids (VSS), the respiratory activity of whole flocs was inhibited by 54–60%, and by 87% for filamentous bacteria (Caravelli et al., 2006). These ozonation conditions were optimal to control filamentous bulking. The critical ozone dose causing a decrease in the maximum oxygen uptake rate ranged between 1 and 16 mg O_3 g^{-1} TSS, depending on the sludge tested (Dziurla et al., 2005).

2.3 MICROBIAL METABOLISM IN ACTIVATED SLUDGE PROCESSES

2.3.1 The anaerobes metabolism

Anaerobic zone phosphorus accumulating organisms (PAOs) utilize volatile fatty acids (VFAs), mainly acetate (HAc), as a carbon source to produce polyhydroxybutyrate (PHB). Subsequently, they release organic phosphate (poly-P) and produce adenosine-5-triphosphate (ATP) which is an energy storage molecule. The energy to transport poly-P and for storage of PHB are obtained from the hydrolysis of intracellular polyphosphate to phosphate. The uptake of acetate, storage of PHB and the transformation of poly-P are limited by metabolic constraints. Consequently, the consistency of the ratio between phosphate release and acetate uptake should be estimated. Data of other researchers provides a range of these values which vary from 0.25 to 0.75 P-mol/c-mol as presented in Table 2.1. These results suggest that this ratio is not constant (Jenkins and Tandoi, 1991). It is obviously essential to clarify the metabolism by measuring degradation. This is because anaerobic phase acetate used by PAOs can be measured.

Table 2.1 Phosphate/acetate ratios reported in scientific literature

Author	Year	Ratio (P-mol/C-mol)
Arvin	1985	0.62-0.74
Wentzel	1986	0.24
Mino	1987	0.39
Comeau	1987	0.70-0.75
Arun	1988	0.21-0.39
Wentzel	1988	0.52-0.57

Stoichiometry of microbial anaerobic metabolism has been expressed using two models. They are based on the anaerobic production of reduction equivalents after acetate uptake and PHA storage. The first model proposes that the reduction equivalents are produced by nicotinamide adenine dinucleotide (NADH) generated by the TCA cycle during degradation of acetate in anaerobic conditions (Eikelboom et al., 1983; Comeau et al., 1986). The other model suggests that NADH production is related to the degradation of internally stored glycogen in the Embden-Meyerhof (EM) pathway. In earlier studies of EM model, the glycogen degradation process was able to reduce energy and produce ATP required to lower the energy contribution of hydrolysis from poly-P. This results in a decreased in the ratio of phosphate released to acetate taken up. As a result, the ratio between acetate and phosphate was adjusted in the Entner-Doudoroff (ED) pathway to account for degradation of glycogen. Neither model explains experimentally observed variations of this ratio, although these models have been used to find a constant value for the phosphate to acetate ratio. Alternate sources of reduction equivalents for modeling microbial anaerobic conversion are possible with either TCA cycle or EM pathway in degradation of glycogen (Figure 2.1). For both models, the acetate uptake process is divided into transport and energy processes in which energy used for the transport process is dependent upon pH. At low pH values, only ATP from poly-P degradation is supplied for the transport of acetate and it is used for the conversion of acetate to acetyl CoA. The amount of phosphate release in the glycogen model is half of the TCA model at low pH, due to the ATP reactions in acetate degradation glycogen conversion being diverted to PHB.

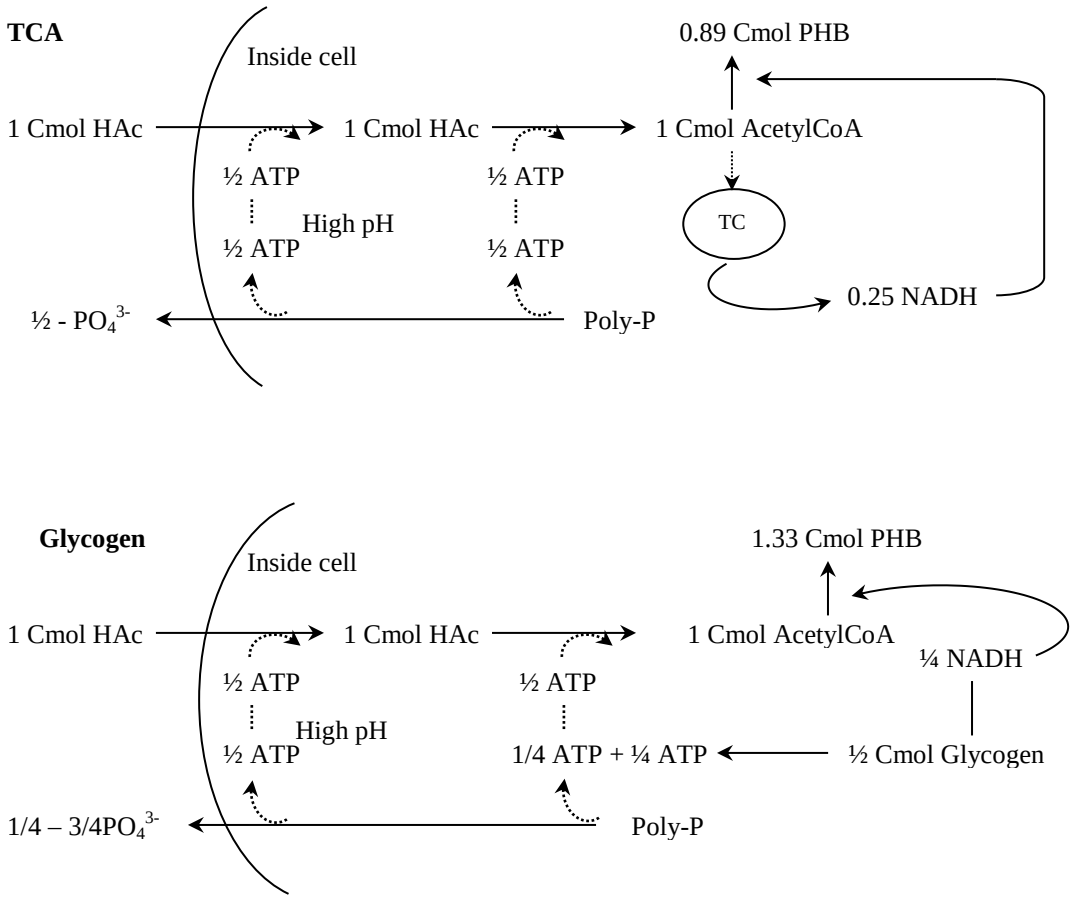

Figure 2.1 Schematic diagram of the microbial anaerobic models: the TCA cycle and glycogen degradation as source of the reduction equivalents, and the energy requirements of the pH contributing to acetate transport.

At high pH values, more phosphate release is generated to liquid phase. This is due to the ATP required for acetate uptake (α_1) mol ATP/C-mol acetate is contributed in the acetate uptake into the cell (with $\alpha_1 \approx 0.5$). This phenomenon can be demonstrated using three principle reactions. Reaction one is the transport and storage of PHB from acetate conversion. Reaction two is the released phosphate from poly-P degradation. Reaction three is the reduction equivalents phenomenon which shown by Equation 2.1. The last reaction is different from the TCA and the glycogen models.

2.3.1.1 Acetate uptake and PHB storage

The metabolic uptake and conversion of 1 C-mol acetic acid to PHB involves in three inputs: α_1 mol ATP of acetate uptake depends on the pH (α_1= 0-0.5), acetyl CoA conversion needs 0.5 mol ATP (Gottschalk, 1979), and the conversion to PHB requires 0.25 mol NADH per C-mol acetic acid (Dawer et al., 1973):

$$CH_2COOH + \left(\frac{1}{2} + \alpha_1\right) ATP + \frac{1}{4} NADH \rightarrow CH_{1.5}O_{0.5} + \frac{1}{2} H_2O \quad (2.1)$$

2.3.1.2 Polyphosphate degradation for ATP production

ATP is produced by the degradation of poly-P for the uptake and storage of acetate. Poly-P is represented as HPO_3. The composition of poly-P in bulk liquid phase depends on the release of phosphorus, magnesium, and potassium, expressed as $Mg_{1/3}K_{1/3}PO_3$. Effects of magnesium and potassium were not examined, just phosphorus which provides a proton for the electroneutral process. The number of ATP molecules produced from poly-P degradation is represented by α_2. When no energy is generated by the conversion of phosphate (α_2 = 1) then 1 P-mol polyphosphate is transformed to 1 mol ATP and 1 mol phosphate (van Groenestijn et al., 1987):

$$HPO_3 + H_2O \rightarrow \alpha_2 ATP + H_3PO_4 \quad (2.2)$$

2.3.1.3 NADH production in the TCA cycle

In Equation 2.1, reduction equivalents are in the form of NADH and are generated from acetate conversion in the TCA cycle (Wentzel et al., 1986). In the TCA cycle, ATP is assumed to be used for the conversion of FADH to NADH:

$$CH_2O + \left(\frac{1}{2} + \alpha_1\right) ATP + H_2O \rightarrow 2NADH + CO_2 \quad (2.3)$$

2.3.1.4 NADH production from degradation of glycogen

The conversion of a 0.5 C-mol glycogen through EM pathway to acetyl CoA process produces NADH which is subsequently converted to PHB and generates 0.25 mol ATP (Mino et al., 1987):

$$CH_{10/6}O_{5.6} + \frac{1}{6}H_2O \rightarrow \frac{2}{3}CH_{1.5}O_{0.5} + \frac{1}{3}CO_2 + \frac{1}{2}NADH + \frac{1}{2}ATP \quad (2.4)$$

The internal reactions occurring in the cell are represented by Equations 2.1 to 2.3 which cannot be examined directly. They are based on biochemical knowledge and stoichiometry. However, these reactions can be determined in observable reaction rates outside the cell which are related to internal reaction rates.

TCA cycle as source of NADH

$$r_s = -r_1 - r_{3a} \quad (2.5)$$

$$r_{phb} = r_1 \quad (2.6)$$

$$r_{pp} = -r_2 \quad (2.7)$$

$$r_p = r_2 \quad (2.8)$$

$$r_c = \frac{1}{3}r_{3a} \quad (2.9)$$

$$r_w = \frac{1}{2}r_1 - r_2 - r_{3a} \quad (2.10)$$

$$r_{ATP} = -(0.5 + \alpha_1)r_1 + \alpha_2 r_2 - (0.5 + \alpha_1)\alpha_3 \quad (2.11)$$

$$r_{NADH} = -\frac{1}{4}r_1 + 2r_{3a} \quad (2.12)$$

Glycogen as source of NADH

$$r_s = -r_1 \tag{2.13}$$

$$r_{phb} = r_1 + \frac{2}{3} r_{3b} \tag{2.14}$$

$$r_{gl} = -r_{3b} \tag{2.15}$$

$$r_{pp} = -r_2 \tag{2.16}$$

$$r_p = r_2 \tag{2.17}$$

$$r_c = \frac{1}{3} rb \tag{2.18}$$

$$r_w = \frac{1}{2} r_1 - r_2 - \frac{1}{6} r_{3b} \tag{2.19}$$

$$r_{ATP} = -(0.5 + \alpha_1) r_1 + \alpha_2 r_2 + 0.5 r_{3b} \tag{2.20}$$

$$r_{NADH} = -\frac{1}{4} r_1 + \frac{1}{2} r_{3b} \tag{2.21}$$

The internal reaction rates can be described by linear equations with parameters including the stoichiometry coefficients shown above. The value, $r_{ATP} = 0$, occurs under the condition of no net accumulation of NADH and ATP taking place. The TCA model contains nine unknown variables and eight linear rates. The glycogen model involves ten unknown variables and nine linear rates. Therefore, both models have one degree of freedom, and subsequently, the anaerobic metabolism can be expressed with one overall reaction rate according to the following alternatives of TCA and glycogen models.

2.3.1.5 Overall reaction TCA cycle as source of NADH

$$-CH_2O - \frac{0.5 + \alpha_1}{\alpha_2} HPO_3 - \left(\frac{1}{3} - \frac{0.5 + \alpha_1}{\alpha_2}\right) H_2O + 0.89 CH_{1.5}O_{0.5} + 0.11 CO_2 + \frac{0.5 + \alpha_1}{\alpha_2} H_3PO_4 = 0 \tag{2.22}$$

2.3.1.6 Overall reaction glycogen as source of NADH

$$r_5 : -CH_2O - \frac{1}{2}CH_{10/6}O_{5/6} - \frac{0.25+\alpha_1}{\alpha_2}HPO_3 + 1.33CH_{1.5}O_{0.5} + 0.17CO_2 + \frac{0.25+\alpha_1}{\alpha_2}H_{3PO_4} + \frac{5}{12} - \frac{0.25+\alpha_1}{\alpha_2}H_2O = 0 \quad (2.23)$$

For the overall equations, stoichiometric coupling of acetate conversion to the conversion of all other reactants occurs during anaerobic metabolism. According to both overall equations, PHB/acetate, glycogen/acetate, and CO_2/acetate ratios are independent of α_1 and thus are pH independent. However, this is different for the TCA cycle and glycogen model. The phosphorus/acetate ratio is dependent on the ATP requirement for transport of acetate (α_1) and on ATP production during poly-P conversion (α_2). The phosphorus/acetate ratios in the TCA and glycogen model are found to be between 0.5 and 1 P-mol/C-mol acetate, and between 0.25 and 0.75 P-mol/C-mol acetate, respectively, when α_1 varies between 0 and 0.5 mol ATP/C-mol acetate. This depends on the pH, and (α_2) = 1 mol ATP per released phosphate. Establishing these ratios was done by a set of experiments to conclude the validity of the TCA (Equation 2.22) and glycogen model (Equation 2.23).

2.3.2 The aerobic metabolism

Under aerobic conditions poly-P, is generated and serves as an energy source for the organisms in anaerobic conditions. This enables these organisms to take up and store substrate in the absence of an electron acceptor (Comeau et al., 1986; Mino et al., 1987; Wentzel et al. 1989a; Jenkins et al., 1991). There are fewer metabolic aerobic studies, although effective phosphate removal takes place in this phase. In the steady state process, anaerobically consumed poly-P and glycogen must be replenished in the aerobic phase, although anaerobically produced PHB is consumed in the aerobic phase. In the phosphorus removal process of the aerobic process, PHB is produced under anaerobic conditions and is utilized for cell growth, polyphosphate synthesis, and glycogen formation. A model describing this process in the aerobic phase was

developed by Wentzel et al. (1989a). Under aerobic conditions, energy is used for the synthesis of poly-P and for the transport of phosphate into the cell, which is transformed from the poly-P as energy source. Moreover, the ATP energy is used for growth and glycogen synthesis from PHB. All conversions (growth, poly-P and glycogen synthesis) are related to oxygen consumption, due to production of ATP from oxidative phosphorylation. Stoichiometry of the aerobic phase was established and used to describe the kinetics of biological phosphorus removal process (Dawes et al., 1973).

In the aerobic phase, metabolic reactions are classified into two groups. These are energy generating reactions and the energy consuming reactions. The energy producing reactions can be described using two equations, PHB catabolism (Equation 2.24) and oxidative phosphorylation (Equation 2.25). The energy consuming reactions are described by three reactions. These are production of biomass (Equation 2.26), poly-P synthesis (Equations 2.27 and 2.28); and glycogen synthesis (Equation 2.29).

2.3.2.1 Reaction 1: PHB catabolism

PHB is degraded to acetyl CoA in the tricarboxylic acid cycle (TCA) (Dawes et al., 1973). Flavin adenine dinucleotide ($FADH_2$), produced in this cycle, is assumed to be equivalent to nicotinamide adenine dinucleotide oxidase ($NADH_2$):

$$\underset{PHB}{CH_{1.5}O_{0.5}} + 1.5H_2O \rightarrow 2.25NADH_2 + 0.5ATP + CO_2 \qquad (2.24)$$

2.3.2.2 Reaction 2: oxidative phosphorylation

In oxidative phosphorylation ATP is generated from $NADH_2$. The ATP level produced per electron pair is represented by δ. This is demonstrated by the P/O ratio denoting the efficiency of oxidative phosphorylation. The stoichiometry of this process can be illustrated by:

$$NADH_2 + 0.5O_2 \rightarrow H_2O + \delta ATP \qquad (2.25)$$

2.3.2.3 Reaction 3: biomass synthesis from PHB

An amount equal to 0.27 mol CO_2 product is generated per C-mol biomass in biomass synthesis (Gommers et al., 1988). The requirement of ATP for the formation of biomass precursors from acetyl-CoA and polymerization of these precursors to 1 C-mol is represented by the parameter, K. Previous experimental biochemical analysis results show that the expected value of K is 1.5 mol ATP per C-mol biomass (Stouthamer et al. 1979). Regarding the maintenance process in biomass synthesis, the maintenance term, m_{ATP}, is the specific ATP consumption. The biomass composition was corrected for poly-P, PHB, and glycogen content, and analyzed using CHON determination. It was found that 1 C-mol active biomass is equal to 26 g. For definition of symbols, see Nomenclature.

$$1.27CH_{1.5}O_{0.5} + 0.20NH_3 + 0.015H_3PO_4 + \left(K + m_{ATP}/\mu\right)ATP + 0.385H_2O \rightarrow CH_{2.09}O_{0.54}N_{0.20}P_{0.015} + 0.615NADH_2 + 0.27CO_2 \quad (2.26)$$

2.3.2.4 Reaction 4a: phosphate transport

The process of phosphate transport through the cell membrane requires energy. Phosphate is a negatively charged ion that has to be taken up against an electric potential difference over cell membranes. Positive ions (Mg^{2+} and K^+) required for poly-P synthesis are consumed without supporting energy (Mitchell, 1986; Harold, 1991). The import protons generates the energy for transport of phosphate are subsequently exported through cell membranes in the oxidation of $NADH_2$. Subsequently, each consumed $NADH_2$ can be predicted to require a certain amount of phosphate, ε. The oxidation Gibbs energy of $NADH_2$ by O_2 per two electrons is -220 kJ/mol (Harold, 1991). The utilization of 1 mol of negatively charged ion will produce 14.7 kJ/mol of energy (Smolders et al., 1994a). Results of Westerhoff et al. (1987) experimentally show that membrane-coupled processes have thermodynamic efficiencies of 30% to 60%. Utilisation of phosphate requires at least 14.7/(0.6 x 220) = 0.11 mol $NADH_2$ per mol phosphate at 60% thermodynamic

efficiency and 0.22 mol $NADH_2$ per mol phosphate if the reaction proceeds with a thermodynamic efficiency of 30%. Therefore, $1/\varepsilon$ will vary from 0.11 to 0.22:

$$H_3PO_4^{OUT} + 1/\varepsilon\, NADH_2 \rightarrow 1/2\varepsilon\, O_2 + H_3PO_4^{in} + 1/\varepsilon\, H_2O \tag{2.27}$$

2.3.2.5 Reaction 4b: polyphosphate synthesis

$Mg_{1/3}K_{1/3}PO_3$, is a principle polyphosphate component. The formula is based upon the measured release of phosphorus, magnesium, and potassium. In the aerobic model, phosphate is represented as HPO_3 only. Magnesium and potassium are not involved in this model. The magnitude of ATP concentration is represented as α_3. ATP is required for synthesis for poly-P. A typical concentration of ATP is 1, and therefore $\alpha_3 = 1$, which is necessary for poly-P synthesis (Kulaev, 1979):

$$H_3PO_4^{in} \rightarrow \alpha_3 ATP + HPO_3 + H_2O \tag{2.28}$$

2.3.2.6 Reaction 5: glycogen production

Glycogen is produced from oxaloacetate in glyconeogenesis (Stryer, 1981). Oxaloacetate is derived from PHB through the glyoxylate cycle:

$$\underset{\text{PHB}}{4/3\, CH_{1.5}O_{0.5}} + 5/6\, ATP \rightarrow 5/6\, H_2O + \underset{\text{Glycogen}}{CH_{10/6}O_{5/6}} + 1/3\, CO_2 + NADH_2 \tag{2.29}$$

Internal aerobic reactions (2.24) - (2.29) are based on stoichiometry and biochemical knowledge. These reactions occur intracellularly and cannot be examined directly. However, conversion rates are observed extracellularly and are represented by $NADH_2$ and ATP concentrations. These concentrations reflect internal reaction rates.

2.3.2.7 PHB conversion rate

The conversion reaction rates are modeled as a function of the internal reaction rates with a set of linear equations having parameters consisting of stoichiometric coefficients of the internal reactions (Roels, 1983). The reaction rates (1)-(5) are ν_1 to ν_5, and can be demonstrated using the transposed reaction rate vector r^T:

$$v_T = \left(v_1, v_2, v_3, v_{4a}, v_{4b}, v_5\right) \tag{2.30}$$

If the transposed conversion rate vector for the 12 compounds is:

$$r^T = \left(r_{phb}, r_x, r_{gl}, r_{pp}, r_n, r_{p_{out}}, r_{p_{in}}, r_o, r_c, r_w, r_{ATP}, r_{NADH_2}\right) \tag{2.31}$$

and α the metabolic reaction matrix is:

$$\alpha = \begin{bmatrix} -1 & 0 & -1.27 & 0 & 0 & -4/3 \\ 0 & 0 & 1 & 0 & 0 & 0 \\ 0 & 0 & 0 & 0 & 0 & 1 \\ 0 & 0 & 0 & 0 & 1 & 0 \\ 0 & 0 & -0.20 & 0 & 0 & 0 \\ 0 & 0 & 0 & -1 & 0 & 0 \\ 0 & 0 & -0.015 & 1 & -1 & 0 \\ 0 & -1/2 & 0 & -1/2\varepsilon & 0 & 0 \\ 1 & 0 & 0.27 & 0 & 0 & 1/3 \\ -1.5 & 1 & -0.385 & 1/\varepsilon & 1 & -5/6 \\ ½ & \delta & (K+m_{ATP}/\mu) & 0 & -\alpha_3 & -5/6 \\ 2.25 & -1 & 0.615 & -1/\varepsilon & 0 & 1 \end{bmatrix}$$

Then a set of 12 linear relations is obtained, by writing out the compound balances for each of the 12 compounds (PHB……$NADH_2$):

$$r = \alpha \bullet v \tag{2.32}$$

Roels (1983) worked under assumption that no net accumulation of $NADH_2$ and ATP takes place, i.e., $r_{ATP} = 0$ and $r_{NADH2} = 0$. Moreover, an assumption is made that the internal ortho-phosphate concentration is constant and, therefore, $r_{pin} = 0$. Using these equations, there are 15 unknown rates ($\nu_1 \ldots \nu_5$ and $r_{phb} \ldots r_{w)}$ and 12 linear equations. Then, by measurement of 3 unknown rates, all remaining conversion rates in the process can be expressed. The following unknown rates were chosen: r_x, r_{pp}, and r_{gl}. The overall equation for the conversion of PHB in the aerobic phase then becomes:

$$-r_{phb} = \frac{1}{Y_{sx}^{\max}} r_x + \frac{1}{Y_{spp}^{\max}} r_{pp} + \frac{1}{Y_{sgl}^{\max}} r_{gl} + m_s C_x \tag{2.33}$$

The following relations for the defined maximal yields and maintenance with metabolic model parameters (δ, K, ε, α_3, m_{ATP}) are found:

$$\frac{1}{Y_{sx}^{\max}} = \frac{0.635 + 2.243\delta + K}{2.25\delta + 0.5} \tag{2.34}$$

$$\frac{1}{Y_{spp}^{\max}} = \frac{\delta/\varepsilon + \alpha_3}{2.25\delta + 0.5} \tag{2.35}$$

$$\frac{1}{Y_{sgl}^{\max}} = \frac{2\delta + 1.5}{2.25\delta + 0.5} \tag{2.36}$$

$$m_s = \frac{m_{ATP}}{2.25\delta + 0.5} \tag{2.37}$$

Equation 2.33 describes the amount of PHB required for the production of biomass, polyphosphate and glycogen synthesis, and maintenance.

2.3.2.8 Oxygen conversion rate

In similar manner, the total consumption of oxygen in the aerobic phase as a function of cell growth (r_x), polyphosphate (r_{pp}), and glycogen (r_{gl}) rates can be expressed from the set of 12 linear equations with 15 unknown rates [Equation 2.32].

$$-r_0 = \frac{1}{Y_{ox}^{\max}} r_x + \frac{1}{Y_{opp}^{\max}} r_{pp} + \frac{1}{Y_{ogl}^{\max}} r_{gl} + m_o C_x \tag{2.38}$$

The following equations express the defined maximal oxygen based yields and maintenance coefficient as a function of the metabolic model parameters (δ, K, ε_3, m_{ATP}):

$$\frac{1}{Y_{ox}^{\max}} = \frac{0.714 + 2.523\delta + 1.125K}{2.25\delta + 0.5} - 1.121 \tag{2.39}$$

$$\frac{1}{Y_{opp}^{\max}} = \frac{1.125\left(\delta/\varepsilon + \alpha_3\right)}{2.25\delta + 0.5} \tag{2.40}$$

$$\frac{1}{Y_{ogl}^{\max}} = \frac{1.125\left(2\delta + 1.5\right)}{2.25\delta + 0.5} - 1 \tag{2.41}$$

$$m_o = \frac{1.125 m_{atp}}{2.25\delta + 0.5} \tag{2.42}$$

Moreover, combining Equations 2.34 – 2.37 with (2.39)-(2.42), the following direct relations are found between the substrate and maximal oxygen based yields and maintenance coefficient:

$$\frac{1}{Y_{ox}^{\max}} = 1.125 \frac{1}{Y_{sx}^{\max}} - 1.121 \tag{2.43}$$

$$\frac{1}{Y_{opp}^{\max}} = 1.125 \frac{1}{Y_{spp}^{\max}} \tag{2.44}$$

$$\frac{1}{Y_{ogl}^{\max}} = 1.125 \frac{1}{Y_{sgl}^{\max}} - 1 \tag{2.45}$$

$$m_0 = 1.125 m_s \tag{2.46}$$

2.3.2.9 Determination of the stoichiometric coefficients of the metabolic model

The maximal yield for biomass formation ($1/Y_{ox}^{\max}$), poly-P synthesis ($1/Y_{opp}^{\max}$), and glycogen formation ($1/Y_{ogl}^{\max}$) on oxygen as a function of the P/O ratio (δ), the coefficient for the transport of phosphate (ε), the polymerization constant (K), and the maintenance energy (m_{ATP}) are shown. Procedures to find coefficients used in these relations, Equations (2.33) - (2.42), are shown as the following.

2.3.2.10 Determination of the P/O Ratio (δ) and transport coefficient (ε)

Measurement of phosphate and oxygen establishes the oxygen/phosphate ratio, ($1/Y_{opp}^{\max}$), for various amounts of accumulated phosphate. Both cell growth and glycogen production were assumed to be not influenced by the degree of phosphate accumulation. The oxygen/phosphate ratio in Equation 2.38 could be demonstrated from the difference in oxygen consumption rate ($r_0^{+P} - r_0^{-P}$) in both absence and presence of phosphate as depicted in the following equation:

$$r_0^{+P} r_0^{-P} = \frac{1}{Y_{opp}^{\max}} r_{pp} \tag{2.47}$$

In a batch experiments, the cumulative concentration of oxygen consumption, M_O, and mass of polyphosphate accumulation, M_{pp}, are based on Equation 22.40 and 2.47, related as:

$$M_O^{+P} - M_O^{-P} = 1\frac{1}{Y_{opp}^{\max}} M_{pp} = 1.125\frac{\delta/\varepsilon + \alpha_3}{2.25\delta + 0.5} M_{pp} \tag{2.48}$$

The ATP concentration coefficient, α_3, is assumed to be equal to 1 (Kulaev, 1979), and ε is represented a value between 5 and 9. The value of $1/Y_{opp}^{\max}$ is based on the P/O ratio (δ) and the transport coefficient of phosphate, ε. The P/O ratio calculated from the measured value of $Y_{opp}^{\max}$ is based on the assumed ε value, although, this value does not appreciably affect the oxygen based yields. The average value of the coefficient for the transport of phosphate, ε, is equal to 7 and is an appropriately estimated value. The ATP concentration coefficient value, α_3, and the transport coefficient of phosphate, ε, are used to achieve an accurate value for the oxygen/phosphate ratio. These are directly derived from the P/O ratio (δ) of Equation 2.48.

2.3.2.11 Determination of the maintenance coefficient (m_{ATP})

In the experiment to determine the achievement of the maintenance coefficient, the oxygen consumption rate was observed for 25 hrs. Due to the utilization of PHB for poly-P uptake, growth, and glycogen formation, the oxygen consumption in the aerobic phase is initially high. During the aerobic phase the PHB fraction in the biomass and the oxygen consumption rate are decreased. The oxygen consumption rate decreased to a constant value. This consumption rate was measured at 25 hrs. Oxygen consumption is related to maintenance, m_O, as seen in Equation 2.42. Oxygen consumption is affected by m_{ATP} using the resulting value for δ.

2.3.2.12 Determination of the polymerization coefficient (K)

The polymerization constant, K, can be known after determination of δ, ε, and m_{ATP}, and using the value of $\alpha_3 = 1$. Combining Equations 2.39 - 2.42, and the oxygen balance [Equation 2.38], the value of K can be expressed as:

$$K = \frac{(2.25\delta + 0.5)r_0 + (0.154 + 1.125\, m_{atp}/\mu)r_x + 1.125(\delta/\varepsilon + \alpha_3)r_{pp} + 1.188 r_{gl}}{1.125 r_x} \qquad (2.49)$$

Hence, the polymerization coefficient, K, can be calculated using oxygen consumption (r_0), biomass production (r_x), poly-P accumulation (r_{pp}), and glycogen production (r_{gl}) parameters.

2.3.3 The anoxic metabolism

Denitrifying phosphorus-removing bacteria (DPB) have been found in anoxic zones as well as in laboratory cultures (Vlekke et al., 1988; Wanner et al., 1992; Kerrn-Jespersen and Henze, 1993; Kuba et al., 1993). In this phase nitrate is utilized for the oxidation of stored PHA and is removed as nitrogen gas from the wastewater treatment system. Not only phosphorus but also nitrogen, which induce eutrophication of reservoirs, are removed simultaneously by DPB. Early studies showed that DPB have similar potential for phosphorus removal (Kuba et al., 1993) and a similar biological metabolism based on intracellular PHA and glycogen (Kuba et al., 1994). Many mathematical models of phosphorus removal processes have been presented, but only a few studies have been done on denitrifying dephosphatation. For example, phosphorus-removing bacteria in the Activated Sludge Model No. 2 presented by the IAWQ task group did not investigate denitrifying dephosphatation (Gujer et al., 1995). Additionally, this model did not predict intracellular glycogen metabolism. The AO model can be modified for the denitrifying dephosphatation process, since the aerobic and anaerobic processes are obviously classified in their metabolisms. The difference between their metabolic reactions is only electron transport phosphorylation:

$$Aerobic: NADH_2 + 0.5O_2 \rightarrow \delta ATP + H_2O \quad (2.50)$$

$$Anoxic: NADH_2 + 0.4HNO_3 \rightarrow \delta_N ATP + 0.2N_2 + 1.2H_2O \quad (2.51)$$

For the determining a value for P/NADH, the P/O ratio (amount of ATP produced per NADH oxidized), δ, the difference of measured oxygen consumption rates in the absence and presence of phosphorus are used (Smolders et al., 1994b). In a similar manner, a value for the P/NADH ratio under anoxic condition, δ_N, can be determined. The metabolic model for the conventional aerobic process can be applied to denitrifying dephosphatation under anoxic conditions. The denitrifying model derived was using the metabolic model and the exact values of most of the reaction stoichiometry. This model was used in early work Smolders et al. (1994a; 1994b; 1995a; 1995b), representing a metabolic model for the conventional AO process. The modified denitrifying dephosphatation process was based on the conventional AO process.

2.3.3.1 Electron Transport Phosphorylation with Nitrate

Five basic reactions are applied in the denitrifying dephosphatation model in aerobic metabolism (Smolders et al., 1994b): (i) PHB catabolism, (ii) electron transport phosphorylation, (iii) production of biomass, (iv) phosphate transport and poly-P synthesis, and (v) glycogen synthesis. The typical characteristic for the anoxic metabolism is that it involves only electron transport phosphorylation with oxygen or nitrate [Equations 2.50 and 2.51]. This is different from aerobic metabolism. However, the P/$NADH_2$ ratio under anoxic conditions will be different than the aerobic value of δ = 1.85 mol ATP/mol $NADH_2$, (Smolders et al., 1994b).

2.3.3.2 Anoxic PHB and Nitrate Conversion Rates

The linear relations for PHB or nitrate conversion rates as a function of growth, poly-P formation, and glycogen synthesis are derived in a way similar to that presented for phosphorus removal under aerobic condition by Smolders et al. (1994b). The principle

assumption for NADH and ATP concentration is that there is no net accumulation of either. The overall stoichiometry of this assumption is related to the PHB conversion rate under anoxic conditions, r_{phb}. It can be derived as the following using three PHB yield coefficients $1/Y_{phb-x}, 1/Y_{phb-pp}, 1/Y_{phb-gl}$ and one maintenance coefficient m_{phb}:

$$r_{phb} = (1/Y_{phb-x})r_x + (1/Y_{phb-pp})r_{pp} + (1/Y_{phb-gl})r_{gl} + m_{phb}C_x \tag{2.52}$$

$$1/Y_{phb-x} = (0.635 + 2.2425\delta_N + K)/(2.25\delta_N + 0.5) \tag{2.53}$$

$$1/Y_{phb-pp} = (\delta_N/\varepsilon_N + \alpha_3)/(2.25\delta_N + 0.5) \tag{2.54}$$

$$1/Y_{phb-gl} = (2\delta_N + 1.5)/(2.25\delta_N + 0.5) \tag{2.55}$$

$$m_{phb} = m_{atp_N}/(2.25\delta_N + 0.5) \tag{2.56}$$

Equation (2.52) represented the amount of PHB required for biomass production (r_x), poly-P (r_{pp}), glycogen synthesis (r_{gl}), and maintenance (m_{phb}). Under aerobic conditions the coefficients of yield and maintenance for the metabolic parameters ($\delta_N, K, \varepsilon_N, \alpha_3, m_{atp_N}$) are defined by Smolders et al. (1994b). For anoxic conditions, these coefficients of yield and maintenance are represented as δ, ε and m_{atp}. Moreover, under anoxic condition the stoichiometric nitrate conversion rate (r_{no_3}) can be determined using three nitrate yield coefficients $(1/Y_{no_3-x}, 1/Y_{no_3-pp}, 1/Y_{no_3-gl})$ and one maintenance coefficient (m_{no_3}):

$$-r_{no_3} = (1/Y_{no_3-x})r_x + (1/Y_{no_3-pp})r_{pp} + (1/Y_{no_3-gl})r_{gl} + m_{no_3}C_x \tag{2.57}$$

$$1/Y_{no_3-x} = (0.123 + 0.9K)/(2.25\delta_N + 0.5) \tag{2.58}$$

$$1/Y_{no_3-pp} = (0.9\,\delta_N/\varepsilon_N + 0.9\alpha_3)/(2.25\delta_N + 0.5) \tag{2.59}$$

$$1/Y_{no_3-gl} = 0.95/(2.25\delta_N + 0.5) \tag{2.60}$$

$$m_{no_3} = 0.9m_{atp_N}/(2.25\delta_N + 0.5) \tag{2.61}$$

Under anoxic conditions these coefficients of yield and maintenance are similar to the coefficients under an aerobic condition. However, the aerobic coefficients are 1.25 times higher than the anoxic coefficients. This is due to the difference in available electrons per mole of electron acceptor for oxygen (four electrons) and nitrate (five electrons).

2.3.3.3 Kinetics

Under anoxic conditions, the conversion rates of HAc, phosphate, nitrate, PHB, and glycogen were expressed by the same kinetic equations as proposed by Smolders et al. (1995a; 1995b). These are summarized in Table 2.2. In an anoxic condition, the coefficients for biomass synthesis, phosphate uptake, and glycogen synthesis and a maintenance coefficient were defined. From the stoichiometric [Equations 2.52 and 2.57], the PHB and nitrate conversion rates under anoxic conditions can be calculated using these three kinetic equations.

Table 2.2 Kinetic equations for anoxic reactions of phosphorus-removing organisms.

Reaction	Equation	Parameter	Value	Units	[a]A/O value
Biomass synthesis	$k_x f_{phb} C_x C_{no_3} / \left(C_{no_3} + K_{no_3}\right)$	k_x	0.05	mol C/mol C.h	0.14
Phosphate uptake	$k_{pp} C_p / \left(C_p + K_p\right)\left(1 - \left(\frac{f_{pp}}{f_{pp}^{\max}}\right)\right)$ $f_{phb}^{1/3} C_x C_{no_3} / \left(C_{no_3} + K_{no_3}\right)$	k_{pp}	0.1	mol P/mol C.h	0.2
Glycogen formation		K_p	0.1	mmol P/L	0.1
	$K_{gl}\left(f_{gl}^{\max} - f_{gl}\right) C_x C_{no_3} / \left(C_{no_3} + K_{no_3}\right)$	$f_{pp}^{\max}$	0.3	mol P/mol C	0.3
Maintenance	$m_{no_3} C_x C_{no_3} / \left(C_{no_3} + K_{no_3}\right)$	k_{gl}	0.8	mol C/mol C.h	0.8
		$f_{gl}^{\max}$	0.3	mol C/mol C	0.27
		m_{no_3}	$3.6*10^{-3}$	mol C/mol C.h	$4*10^{-3}$

[a]Reported values for organisms enriched in an anaerobic-aerobic SBR (Smolders et al., 1994b; 1995b)

2.3.3.4 Determination of the Stoichiometric Coefficients of the Anoxic Metabolic

The yield coefficients for biomass synthesis $(1/Y_{phb-x}, 1/Y_{no_3-x})$, poly-P formation $(1/Y_{phb-pp}, 1/Y_{no_3-pp})$, and glycogen synthesis $(1/Y_{phb-gl}, 1/Y_{no_3-gl})$ are now expressed as a function of the NADH ratio (δ_N), the coefficient for the NADH requirement for phosphate transport (ε_N), the requirement ATP for poly-P synthesis (α_3), the polymerization constant in biomass synthesis (k), and the maintenance energy (m_{atp_N}). In this anoxic metabolic model, the parameters α_3 and k can be assumed to be equal in value to the aerobic parameters. Smolders et al. (1994b) reported α_3 = 1 mol ATP/mol P and k = 1.6 mol ATP/mol C (biomass). The other parameters $(\varepsilon_N, m_{atp_N}, \delta_N)$ are determined by the following procedure.

2.3.3.5 Determination of the Phosphate Transport Coefficient (ε_N)

Under anoxic conditions and during transport, phosphate is converted into poly-P through in cell walls by energy consuming processes. These processes are for the metabolism of phosphate removing organisms. In these phosphate energy-consuming energy processes, energy is generated by the imported protons which are subsequently exported through cell membranes for oxidation of NADH, [Equations 2.50 or 2.51] (Mitchell, 1986). The energy consumption ratio for phosphate transport under anoxic conditions to that under aerobic conditions will be identical to the ratio of the P/$NADH_2$ concentrations under both conditions:

$$\varepsilon_N = \varepsilon \delta_N / \delta \tag{2.62}$$

Smolders et al. (1994b) obtained values of δ = 1.85 mol ATP/mol $NADH_2$, and ε = 7 mol P/mol $NADH_2$, leading to:

$$\varepsilon_N = 7 \delta_N / 1.85 \tag{2.63}$$

2.3.3.6 Determination of the Maintenance Coefficient under the Anoxic Condition (m_{atp_N})

The ATP maintenance coefficient (m_{atp_N}) from the endogenous oxygen consumption rate was 0.019 mol ATP/C-mole.h. (Smolders et al., 1994b). In the anaerobic-anoxic process, the maintenance coefficient of ATP $(m_{atp_N}$, 0.01 mol ATP/C-mole.h$)$ was involved for the mathematical of this experimental maintenance (m_{atp_N}).

2.3.3.7 Determination of the P/NADH$_2$ Ratio under the Anoxic Condition (δ_N)

Determination of the P/NADH$_2$ ratio under anoxic conditions (δ_N) can be achieved by combining measured conversion rates of nitrate (r_{no_3}), biomass (r_x), PHB (r_{phb}), and poly-P (r_{pp}) in batch tests of the enriched denitrifying dephosphatation sludge using the equation below. It is obtained from Equations 2.52 and 2.57 by elimination of the glycogen conversion rate (r_{pp}):

$$0 = r_{no_3} + (1/Y_{no_3-x})r_x + (1/Y_{no_3-pp})r_{pp} - \left\{ \begin{matrix} r_{phb} + (1/Y_{phb-x})r_x + (1/Y_{phb-pp})r_{pp} + \\ m_{phb}C_x \end{matrix} \right\} * \\ (Y_{phb-gl}/Y_{no_3-gl}) + m_{no_3}C_x \qquad (2.64)$$

Since all conversion yield (Y) and ε_N values are linked to δ_N [Equation 2.14, and Equations 2.53 – 2.56 and 2.58 – 2.61 and] and that k, α, and m_{atp_N} are known, Equation 2.64 only contains δ_N and measured conversion rates (r). This equation then allows us to find the best estimate of δ_N.

2.4 BIOLOGICAL PHOSPHORUS REMOVAL MODELS

2.4.1 The UCTPHO model

The UCTPHO model (Wentzel et al., 1992) was extended from the UCTOLD model (Dold et al., 1991) and Activated Sludge Model No. 1 (ASM1) (Henze et al., 1987). This model extension dealt with an implementation of biological excess phosphorus removal (BEPR). BEPR was taken into account in order to gain an understanding of the kinetic processes in biological nutrient removal activated sludge (BNRAS). A basis of the BEPR model investigates and predicts to PAOs metabolisms. PAOs have a unique ability to store polyphosphate (poly-P) internally (Hu et al., 2007). Biochemical behaviors consist of the anaerobic phosphorus release and aerobic (or anoxic) phosphorus uptake (Moodley et al., 2000). PAOs biochemical pathways can be evaluated using biochemical models developed from the studies of different BEPR systems, i.e. anoxic/aerobic, and anaerobic/anoxic/aerobic as elucidated in previous work (Comeau et al., 1986; Wentzel et al., 1986; Mino et al., 1987; Wentzel et al., 1991; Wentzel et al., 1992).

The UCTPHO model was developed from the experimental results of Wentzel et al. (1988). That study was carried out through the use of continuous-flow activated sludge UCT systems with PAOs enhanced culture. The medium for culture of PAOs is significant. The substrate used will determine the dominate organisms and their effect upon the system response. VFAs are the substrates that favor PAOs. Conversely, slowly biodegradable substrates are not useful for growth of PAOs. Continuous-flow activated sludge systems as well as batch tests were investigated to develop the UCTPHO model (Wentzel et al., 1989a & 1989b). PAOs mechanisms in UCTPHO for aerobic P uptake were considered according to the distribution of the general kinetic model pattern in BNRAS systems. The relevant organisms consist of three groups: (1) PAOs, (2) autotrophic nitrifying organisms (ANOs) and (3) ordinary heterotrophic organisms (OHOs). It is significant that among these three organisms PAOs are able to take up P. Short-chain fatty acids (SCFAs) under anaerobic conditions are transported internally by PAOs. Following their uptake, SCFAs are stored intracellularly as poly-

hydroxy-alkanoates (PHA) with simultaneous P release into bulk liquid. Under aerobic conditions internally stored PHA are degraded and phosphorus simultaneously taken up following polyphosphate (poly-P) formation (Wentzel et al., 1991). In addition, PAOs, ANOs, and OHOs were investigated in regard to COD removal, nitrification, denitrification and BEPR (Wentzel et al., 1992). UCTPHO is an integrated general kinetic model of nitrification and denitrification biological excess phosphorus removal (NDBEPR) systems (Wentzel et al., (1992). The individual behavior of microorganism in a variety of processes has been investigated. The conceptual behaviors of OHOs and ANOs, and PAOs are discussed in the following two sections.

2.4.1.1 OHOs and ANOs behavior

The rate formulations and stoichiometric values of rate processes of both OHOs and ANOs remained the same as in UCTOLD. Additionally, P was included in these processes. Optimization of P level is a critical function to control the growth processes of both OHOs and ANOs (Hu et al., 2003). Also, P level is important in death/decay rates of OHOs and ANOs. SCFAs result from fermentation processes of readily biodegradable chemical oxygen demand (RBCOD) by OHOs under anaerobic conditions. Then SCFAs are utilized by PAOs under the same conditions. Hydrolysis rate of utilization of slowly biodegradable chemical oxygen demand (SBCOD) of OHOs under anoxic and aerobic condition was observed to increase from 0.33 to 0.6 mg NO_3-N/(mg OHO.d) (Clayton et al., 1991; Wentzel et al., 1992; Moodley et al., 2000).

2.4.1.2 PAOs behavior

Growth and decay/death processes of PAOs in UCTPHO are the same as described in the study of Wentzel et al. (1989b). PAOs were investigated in batch culture. It was shown that PAOs utilize SCFAs and then store PHA intracellulary under anaerobic, anoxic and aerobic conditions (Wentzel et al., 1989b). In contrast, PAOs BNRAS systems were able to utilize SCFAs under anaerobic conditions only. Additionally, PAOs were not able to utilize nitrate as an electron acceptor. These behaviors were observed by Wentzel et al. (1989a) and Clayton et al. (1991). As a result, it was

concluded that PAOs are only able to grow under aerobic conditions. PAOs death kinetics was investigated using a modified endogenous respiration method (Wentzel et al., 1989a). The study was conducted in separate experiments under aerobic, anaerobic and anoxic trials. The conclusions of this work were that PHA and poly-P are stored internally in PAOs and then released followed by the release of SBCOD and P to bulk liquid phase. Break down of poly-P during maintenance processes generates energy and releases phosphate to liquid phase. This is done to meet energy requirements under anaerobic and anoxic conditions.

UCTPHO has two limitations (Wentzel et al., 1992). First, anoxic P uptake by denitrifying PAOs cannot be described fully. This limiting aspect was already theoretically demonstrated (Wentzel et al., 1986). However, this limitation is supported by experimental observation. Second, the UCTPHO model validation results in minimal anoxic P uptake by denitrifying PAOs and associated PAO denitrification behavior in enhanced culture systems (Wentzel et al., 1989a & 1989b; Hu et al., 2003). As a result, the UCTPHO model does not provide any support for anoxic PAOs growth with anoxic P uptake by denitrifying PAOs (Hu et al., 2003). The modified UCTPHO model predicts external nitrification biological nutrient removal activated sludge (ENBNRAS) as a PAOs behavior. Furthermore, it demonstrates carbonaceous material removal, nitrification and denitrification (Hu et al., 2007). The modification of anoxic processes with associated anoxic phosphorus uptake and denitrification of PAOs was expressed. A separate reduced growth yield coefficient (Y_{PAO2}) for anoxic conditions and a separate reduced ratio of phosphorus uptake per unit PHA substrate utilized (Y_{PP2}) were observed in these PAOs anoxic growth processes. The processes of anoxic death/maintenance of PAOs were included in the modified UCTPHO model. Nitrifying PAOs can utilize biodegradable products from decay processes. Biodegradable products were not released into liquid phase. In addition, a separate reduced anoxic growth yield of OHOs (Y_{H2}) was observed. Also, organic nitrogen and phosphorus corresponding to COD fractions were included. However, this modified UCTPHO mode is still limited because anaerobic SBCOD hydrolysis and COD loss mechanisms are not included (Hu et al., 2007). Also, this model has not been validated in either conventional nitrification BNRAS systems or ENBNRAS systems.

2.4.2 The Activated Sludge Model no. 2 (ASM2)

ASM2 was developed from ASM1 (Henze et al., 1987) and UCTPHO models (Wentzel et al., 1992). The resulting metabolic model for considering biological phosphorus removal is similar to UCTPHO (Gujer et al., 1995; Henze et al., 1995). However growth and decay processes of PAOs are improved. For example, growth and biological phosphorus removal under phosphorus-limited conditions cannot be predicted using UCTPHO if influent phosphorus is equal to zero (Hu et al., 2003). ASM2 relieves that limitation by including poly-P accumulation processes. Additionally, PAOs growth in ASM2 uses only free and saline ammonium (FSA). In contrast, UCPHO uses both FSA and nitrate. Furthermore, ASM2 does not include PAOs maintenance processes to model the phenomenon of secondary phosphorus release under anaerobic/anoxic conditions. Details of using ASM2 model to predict growth and decay/death processes is presented in the following two sections.

2.4.2.1 OHOs and ANOs behavior

The growth processes of OHOs and ANOs incorporate poly-P. These are similar to the UCTPHO model. Also under anaerobic conditions RBCOD degradation to SCFAs by OHOs, as well as utilization of SCFAs by PAOs, is included in both ASM2 and UCTPHO models. SCFAs and RBCOD in ASM2 are utilized by OHOs in growth processes under aerobic and anoxic conditions. In contrast, only RBCOD is utilized by OHOs. SBCODs hydrolysis in the ASM2 model is done under anaerobic, aerobic and anoxic conditions. In contrast, the UCTPHO model considers hydrolysis only under aerobic and anoxic conditions. The decay processes of OHOs and ANOs are the same as in the UCTPHO model (Gujer et al., 1995).

2.4.2.2 PAOs behavior

The processes of PAOs growth and associated BEPR in the UCTPHO model are based upon phosphorus-limited conditions. In contrast, PAOs growth processes in the ASM2 mode are based upon a poly-P accumulation process. This is through the half saturation

constants of poly-P storage. PAOs in UCTPHO can utilize FSA as well as nitrate for aerobic growth. In contrast, PAOs in the ASM2 model utilize only FSA as their N source. As a result, aerobic PAOs growth rate is based on only FSA concentration. In the UCTPHO model, both aerobic PAOs growth and phosphorus uptake for poly-P formation are modeled as a single process. In contrast to ASM2, these PAOs processes are treated as separate processes. The endogenous mass lost and biodegradable portion of PAOs during decay are predicted in the UCTPHO model. Oxygen utilization under aerobic conditions and portions of PAOs in SBCOD under anaerobic and anoxic conditions are included in PAOs decay. PAOs decay in the ASM2 model can be predicted under aerobic, anaerobic and anoxic conditions. In addition, the maintenance portion of PAOs energy requirements is not included in the ASM2 model. That process is presented as a second phosphorus release in the UCTPHO model.

2.4.3 The Activated Sludge Model no. 2d (ASM2d)

ASM2d is an extended ASM2 model. ASM2d describes an extra biological phosphorus removal with denitrification (Henze et al., 1999). It incorporates a relationship between nitrate (NO_3) and phosphorus in PAOs under anoxic conditions (Henze et al., 1999). PAOs under anaerobic conditions are able to utilise SCFAs and consequently store intracellular PHA. PHA are used for (1) anoxic poly-P formation and (2) anoxic PAOs growth processes (Henze et al., 1999). Modeling of these processes was modified from the ASM2 model for PAOs growth and poly-P formation under aerobic conditions. PAOs use nitrate instead of oxygen as a terminal electron acceptor to take up phosphorus under anoxic conditions. The reduction factor (η_{NO3}) is multiplied by aerobic poly-P storage and by the aerobic growth rate was to yield anoxic poly-P formation and anoxic PAOs growth, respectively. Under this assumption not all PAOs are able to grow or utilize P under anoxic conditions. Furthermore, they may not show reduction of poly-P storage under anoxic conditions (Hu et al., 2003). From the available information in the literature, a η_{NO3} value is difficult to determine because of variability in anoxic PAOs growth and associated denitrification, as well as anoxic phosphorus uptake (Šorm et al., 1996; Artan et al., 1997; Barker and Dold, 1997; Kuba et al., 1997; Ekama and Wentzel, 1999; Hu et al., 2003). However, η_{NO3} is significant

for growth and poly-P storage under anoxic conditions (Wentzel et al., 1992). The ASM2d model approaches evaluation of denitrifying PAOs by multiplying the aerobic PAOs growth rate by a reduction factor η_{NO3}. This result represents the fraction PAOs capable of denitrification. Obtaining η_{NO3} is a limiting condition of the ASM2d model for this particular process (Hu et al., 2003). The reduction factor for OHO anaerobic hydrolysis (η_{Fe}) of SBCOD to RBCOD increased significantly from 0.1 in ASM2 to 0.4 in ASM2d. As a result, SCFAs fermentation products of RBCOD were utilized more by PAOs, and consequently BEPR increased significantly, as discussed above.

Many applications of the ASM2d model and additional processes included have been proposed for prediction and simulation. Several studies using this model have been done. The effects of dissolved oxygen (DO) on the behavior of biological nutrient removal organisms in a sequencing batch reactor (SBR) system were determined based upon the simulation of the ASM2d model (Gao et al., 2009). The time arrangement of every phase adapted to the SBR conditions was used to predict the changes in COD, nitrogen and phosphorus concentrations. The growth and activity of nitrifying organisms and phosphorus accumulating organisms (PAOs) were inhibited when DO was lower than 1 mg/L. Therefore, maintaining DO above 1.5 mg/L is optimal for nutrient removal performance. Daigger et al. (2010) used the ASM2d model to calibrate the MBR process. The simulation followed guidelines including: (1) direct membrane recirculation flow to the aerobic zone, (2) provide intense mixing at the inlets of the anaerobic and anoxic zones, (3) maintain internal recirculation flow rates to maintain the desired mixed liquor suspended solids distribution, and (4) carefully control supplemental metal salt addition in proportion to the phosphorus remaining after biological removal is complete. The model results were used to enhance full-scale configurations, in particular nutrient removal.

Zhou et al. (2010) used the ASM2d model to simulate data collected from a pilot-scale study and to optimize WWTPs. Their mathematical model simulation was based upon experimental results. It showed that a combination of anaerobic/anoxic/aerobic districts accomplished design optimization. The effluent quality could be further improved after achieving optimization. Dymaczewski (2007) used the ASM2d model to simulate the

best complex C, N and P removal. The model calibration was conducted using a pilot study. The applied calibration methodology was obtained by combining simulations of the steady state pilot plant and kinetic experiments conducted in batch reactors. The model parameters were adjusted on the basis of simulation accuracies using experimental data. The ASM2d model was verified using a full-scale WWTP. Its result was used for defining initial operational guidelines. The optimization of process design for nitrogen and phosphorus removal in urban sewage plants was based upon the simulation of the ASM2d model (Zhou et al., 2009b). The model was calibrated using the operational conditions of the A_2/O process. The optimization of the model was compared to traditional activated sludge process design and trial calculation methods. In comparison of two methods, the optimization results obtained enabled a high reduction in sewage plant capital construction expenses and running costs. As a result, the ASM2d model was useful in achieving optimal design and control of sewage plants. It helped reduce plant expenses and provided a theoretical guide for future process design.

Guisasola et al. (2006) used the ASM2d to simulate the EBPR. The objective of this study was to improve the startup of an EBPR system in a sequencing batch reactor. A reduction in the length of the aerobic phase, and depletion of orthophosphate from the medium was investigated to improve the system. A good online orthophosphate sensor was needed to generate accurate experimental data providing a successful simulation. A link between oxygen uptake rate and orthophosphate was used instead to avoid the technical limitation of the online sensor.

Chai et al. (2006) used the ASM2d model to simulate experimental results from a biological wastewater treatment plant at Duvbacken in Gvle, Sweden. A systematic approach for parameter identifiability analysis was presented. The combination of a standard least squares criterion and a direct optimization method was used to calculate improved parameter estimates. Then, the adjusted model was validated against collected data from an industrial plant.

The ASM2d model was calibrated for determination of optimal recycle rate and basin retention time for Modified Bardenpho (MB), the MUCT and anaerobic-anoxic-oxic

(A2O) biological nutrient removal processes (Kennedy and McHarg, 2007). Two temperatures and three primary effluent concentrations were used in the simulations. All BNR processes were successful keeping soluble phosphorus below 1 mg/L at all conditions without considering nitrogen. However, these BNR processes produced an effluent N above 5 mg/L at high primary effluent concentration. The MB and MUCT process both achieved phosphorus and nitrogen concentrations below 1 mg/L and 5 mg/L, respectively for low primary effluent (PE) concentrations at 10 and 20 ºC. Dynamic tests at an Ottawa wastewater treatment plant indicated that the MB process was more robust than the MUCT process.

Bixio et al. (2001) used the ASM2d model to determine the fractionation of raw sewage, the primary effluent and the fermentation characteristics. In this study, cold weather, dilute sewage, a critical COD and an excessive N concentration made it a challenge to attain full biological nutrient removal. The fermentation products could be optimized in available reactors by achieving high-rate denitrification and enhanced biological phosphorus removal. The results clearly showed that fermentation played an important role and temperature was the driving parameter determining the characteristics of dissolved COD.

Simulation of the Tielt wastewater treatment plant (WWTP) was based upon the ASM2d model (Carrette et al., 2001). It shown that calibration based upon an expert-approach was obtained by changing only four parameters (the anaerobic hydrolysis reduction factor η_{fe}, the reduction factor for denitrification η_{NO3}, the decay rate of autotrophs b_{AUT} and the decay rate of the bio-P organism building blocks b_{PAO}, b_{PHA}, b_{PP}).

Influent fractionation is a critical step in model calibration. The validation result of the ASM2d model used data based upon a pilot scale plant treating municipal wastewater from the city of Valencia (Spain) (Penya-Roja et al., 2002). The ASM2d was first calibrated using experimental data from anaerobic, anoxic and aerobic batches. It provided a set of stoichiometric and kinetic parameters. The presence of glycogen accumulating organisms (GAOs) resulted in differences between the values obtained

and default values proposed in ASM2d. Then, calibration of the ASM2d model was based up on the experimental data from a pilot plant. Its result showed the same stoichiometric and kinetic values for heterotrophic, autotrophic and polyphosphate accumulating bacteria.

A new systematic approach was proposed based on parameter identifiability analysis of a parameter subset (Brun et al., 2002). This was done because the ASM2d model (and other ASMs) was over-parameterized with respect to the available data. It was often a calibration approach addressed by ad hoc selecting and tuning procedures. The new approach consisted of a preliminary prior parameter analysis and a subsequent iterative parameter subset selection with a tuning procedure. It also demonstrated the identified method and analyzed interdependencies.

The simulation and optimization of a full-scale Carrousel oxidation ditch wastewater treatment plant (WWTP) used an integration of ASM2d, support vector regression (SVR) and accelerating genetic algorithm (AGA) (Xie et al., 2011). SVR was employed to correlate the operating factors and the effluent quality. Then, the AGA approach was used to obtain the optimal operating conditions. It has an advantage in achieve simultaneous nutrient removal using multiple-objective optimization with different weighted indexes. In this case study, a better effluent quality could be achieved by increasing hydraulic retention time (HRT) in the aerobic tank and reducing the HRT in the anoxic tank, internal recirculation ratio and the solid retention time (SRT). The application of a WWTP Online Simulation using the ASM2d model was used to explain the reduction of total emission into receiving water (Seggelke and Rosenwinkel, 2002). More influent storm water than usual and different control strategies affected effluent wastewater quality. The ASM2d simulation gave accurate predictions when comparing predicted results and experimental data in the aeration tank (NH_4-N, NO_3-N) over a period of several months. The significant prerequisites for good simulations are accurate knowledge of the WWTP plant and having alternative methods for the measuring values in the event of sensor failure.

The prediction capability of ASM2d was evaluated from experimental data of enhanced biological phosphorus removal (EBPR) performance of a sequencing batch reactor (SBR) (Yagci et al., 2006). To approach this objective, a laboratory-scale SBR was operated with a synthetic feed containing acetate as the sole carbon source. Four different runs over a range of influent phosphate/acetate ratios were conducted. Concentration profiles of a representative cycle at steady state were used for model evaluations. Sensitivity analysis was used for an iterative calibration methodology using four different data sets. The change in coefficients was interpreted in the SBR system. At low P/Ac ratios glycogen accumulating microorganisms, GAOs, can store substrate under anaerobic conditions without using polyphosphate energy. Instead, GAOs utilize energy from the degradation of glycogen. This indicates that the ASM2d model needs glycogen and GAOs at low P/Ac ratios, in order to obtain better prediction of X_{PHA} and oxygen uptake rate (OUR) profiles in the system.

Filali-Meknassi et al. (2005) use the ASM2d model to develop a dynamic SBR simulation model for biological nitrogen removal of slaughterhouse wastewater. The SBR treatment process achieved simultaneous organic matter removal of 95-96% and nitrogen removal of 95-97%. The calibration and validation of the model used a laboratory scale nitrification/denitrification SBR. The model provides a powerful tool in reducing the experimental costs and time to find the optimum strategy.

The characteristics of a biological nutrient removal in a six-stage membrane bioreactor (MBR) pilot plant were based on the ASM2d model (Fleischer et al., 2005). This model also was used to simulate the experimental results from MBR pilot plant providing that the stoichiometry of chemical phosphorus removal was known. This MBR process produced a low-nutrient effluent. The effluent total nitrogen was less than 3 mg/L as nitrogen. The characteristics of the solids produced in the MBR and a full-scale conventional biological nitrogen removal process were similar. As a result, a valuable insight to the design and operating characteristics of MBRs was gained to produce effluents with very low nutrient concentrations. The disadvantages of developed biological nutrient removal (BNR) processes were improved by reconfiguring the process into (1) an anaerobic zone followed by multiple stages of aerobic-anoxic zones

(TNCU3 process) or (2) anaerobic, oxic, anoxic, oxic zones in sequence (TNCU2 process) (Pai et al., 2004). A recycling ratio of 0.5 without internal recycle of nitrified supernatant was operated for these two pilot plants. The sludge retention time was 10 d. The ASM2d was used to simulate and analyze the kinetics of different microorganism in these two processes and the A2O process. The efficiencies of effective removal of carbon, total phosphorus and total nitrogen were 87-98%, 92-100% and 63-80%, respectively. The results of model simulation showed that the microbial kinetics in the TNCU3 and TNCU2 processes were affected by different operations.

Expansion of the ASM2d was used to model the consumption of readily biodegradable substrates by PAOs under only anoxic and aerobic conditions (Swinarski et al., 2012). Under these conditions, a model change was included for a new substrate component and process terms for PAOs and other heterotrophs. The ASM2d was calibrated using experimental data from batch tests with settled wastewater and mixed liquor from a MUCT wastewater treatment plant. Validation was done using data collected from a full-scale MUCT process. The calibration results of an expanded ASM2d were similar to ASM2d. The expanded ASM2d was developed based upon batch tests with ethanol and fusel oil as the external carbon sources. Comparing the ASM2d and the expanded ASM2d, the new model better predicted the anoxic behaviors of carbonaceous oxygen demand, nitrate-nitrogen (NO_3-N), and phosphorous (PO_4-P) in batch experiments with ethanol and fusel oil. Evaluation of a nitrogen removal (WWTP1) and a combined nitrogen and phosphorus removal (WWTP2) benchmark wastewater treatment plant was examined for a series of ASM 1, 2d & 3 model assumptions (Flores-Alsina et al., 2012). In these studies, ASM1 & 3 model implementations were used to simulate WWTPs. ASM2d was calibrated based upon experimental data of WWTP2. The modified model included a reactive settler. It described a non-reactive TSS sedimentation and transportation in a reference case with the full set of ASM processes. In addition, an electron acceptor dependency of biomass decay rate model was included into ASM2 & 2d. The incorporation of reactive settling affected process in the following ways: (1) hydrolysis of particulates was increased; (2) increases were seen in the overall plant's denitrification efficiency by reducing the S_{NOx} concentration at the bottom of the clarifier; (3) increases were seen in the oxidation of COD compounds; (4) increases in X

$_{OHO}$ and X_{ANO} decay were observed; and, finally, (5) increases the growth of X_{PAO} and formation of $X_{PHA,Stor}$ were noted for ASM2d. At the bottom of the clarifier, a substantial increase of the concentration of X_{ANO}, X_{OHO} and X_{PAO} occurred due to the introduction of electron acceptor dependent decay.

Expansion of the ASM2d model was used to simulate experimental investigations both lab scale and full scale wastewater treatment processes (Makinia et al., 2012). The objective of this study was to investigate the effects of chemical precipitation and addition of external carbon sources on denitrification capability and the EBPR process. Different batch experiments were carried out using settled wastewater (without pre-treatment and after coagulation-flocculation) and external carbon sources (ethanol and fusel oil). Denitrification and EBPR processes significantly relied on the precipitation of colloidal and particulate organic fractions. The phosphorus and nitrogen removal by coagulation-flocculation was reduced 30-70%. The model results accurately predicted the effects of precipitation and external carbon addition in batch tests. It revealed that addition of external carbon sources can compensate for the effects of precipitation resulting in a similar NO_3-N concentration in comparison to trials without precipitation and external carbon addition. Furthermore, the model result showed that the addition of external carbon sources and precipitation significantly affected the PO_4-P concentration.

Reduction of high calcium concentration combined with enhanced biological phosphorus removal achieved an understanding of calcium phosphate precipitation and its inclusion in the Activated Sludge Model No 2d (ASM2d) (Barat et al., 2011). In aqueous phase, reaction chemical equilibrium and aqueous-solid phase change takes place. The proposed precipitation model can reproduce the dynamics of amorphous calcium phosphate (ACP) formation and later crystallization to hydroxyapatite (HAP).

A novel anoxic/anaerobic/aerobic (Reversed AAO, RAAO) process is a modified configuration of the conventional anaerobic/anoxic/aerobic (AAO) process (Zhou, 2011). The ASM2d model and a secondary clarifier model were calibrated in order to evaluate a pilot-scale RAAO test and the operational performance of the RAAO process. Only four kinetic parameters in the ASM2d model were adjusted to accurately

simulate in-process variation of ammonium, nitrate and phosphate. It showed that PAOs in the RAAO process contained less poly-phosphate (0.243 gP/gCOD) than the AAO process (0.266 gP/gCOD). The increased mixed liquor recirculation ratio in the RAAO process caused increases in both heterotrophic and autotrophic biomass. However, PAOs concentration decreased due to adverse effects of electron acceptors on phosphorus release and poly-hydroxy-alkanoate (PHAs) synthesis.

A combination of a new conceptual model of organic conversions and the ASM2d model was used to predict organic N conversions under conditions of separation process and constant contents of organic fractions (Makinia et al., 2011). A combined model included a new insight into the processes of ammonification, biomass decay and hydrolysis of particulate and colloidal organic nitrogen. Three incorporated organic nitrogen (ON) fractions were defined as dissolved (DON) (<0.1 μm), colloid ON (0.1-1.2 μm) and particulate ON (>1.2 μm). The accuracy of steady state predictions of DON and colloid ON profiles were based upon varying ammonification and hydrolysis rates using different electron acceptors.

Integration of mathematical modeling of fixed-film activated sludge (IFAS) and moving-bed biofilm reactor wastewater processes into the ASM2d was developed (Boltz et al., 2009). The integrated model assumed identical reaction kinetics for bacteria within suspended biomass and biofilm. The model was based on theoretical considerations. It includes simultaneous diffusion and Monod-type reaction kinetics inside the biofilm. The competition between autotrophs and heterotrophs was modeled inside the biofilm. Suspended biomass compartments existed for both the electron donor and electron acceptors.

Integration of the biological phosphorus metabolism model and the ASM2d model was used to simulate microorganisms' behavior in the membrane (MSBR) system for biological nutrient removal (Wang et al., 2010). Different specific substrate conversion rates for PAOs were observed under aerobic and anoxic conditions. This simulation model accurately predicted experimental results.

A novel modified A2/O process was proposed for nitrogen and phosphorus removal in municipal sewage (Zhang et al., 2008). Performance evaluation of the MMAO process treating municipal sewage at normal temperature was based upon a bench-scale study. The ASM2d was used to predict biological kinetics of the MMAO process and to optimize its design and operation. The calibration and validation ASM2d model results simulated the biological reactions of these systems very well.

Mechanical activated sludge modeling accomplished optimal design and operational parameters. The model was also used to evaluate process performance under peak load and low temperature. In addition, the ASM2d could be used to develop unit combination and operational control.

ASM2d with soluble microbial products (ASM2dSMP) was an extension of ASM2d. ASM2dSMP was used to predict MBR biochemical conditions using only 4 additional SMP-related parameters (Jiang et al., 2008). The SMP parameter estimation led to reasonable parameter confidence based on batch experimental results. The impacts of operational parameters on SMP concentration was predicted using the ASM2dSMP model. This model indicated that solids retention time (SRT) was the key parameter controlling the SMP concentration. A lower SRT improved the utilization associated products (UAP) concentration, but reduced the biomass associated products (BAP) concentration. A minimum SMP concentration can be predicted from an optimum SRT. The dynamic conditions and biological nutrient removal with variation of SRT conditions were used to control the MBRs. The modified ASM2d model was used to accurately indicate nitrite inhibition by incorporating the assumed intracellular reaction product of nitrite (Yoshida et al., 2009).

The modified model also included tolerance mechanisms to nitrite inhibition by the denitrifying activity of PAOs. The modified model was based on previous findings, namely 1) nitrite inhibits phosphate uptake and growth of PAOs, 2) nitrite inhibition persists even after nitrite disappearance, 3) PAOs with the higher relative anoxic activity are less sensitive to nitrite exposure. The incorporation of only nitrite inhibition into the modified model was matched the measured phosphate concentration while

nitrite exists. However, the model could not explain the persistence of inhibition after nitrite disappeared. In contrast, the incorporation of nitrite and reaction complex inhibition accurately modeled measured phosphate concentration and predicted values both before and after nitrite disappeared. The results shown that the predicted valued correspond well to the order of the anoxic activity of PAOs. This is due to resistance to nitrite inhibition or the rate of inhibitor removal. Therefore, the assumption of secondary inhibition by the reaction complex produced inside of PAOs supported the Nitrite-Complex model proposed in this study. In addition, there are two mechanisms that describe inhibition of denitrifying activity by nitrite. These are 1) less sensitivity (high tolerability) of PAOs with the higher relative anoxic activity to nitrite in solution, and, 2) high decomposition (denitrification) ability of inhibitors, i.e., nitrite and the reaction complexes.

The ASM2d and the Biological Nutrient Removal Model No. 1 (BNRM1) were used to evaluate the effect of pH on enhanced biological phosphorus removal in an anaerobic/aerobic (A/O) laboratory scale sequencing batch reactor (SBR) (Serralta et al., 2006). Under an anaerobic phase, pH varied slightly. However, the pH rose significantly in the aerobic phase during observations made of seven steady states. Increasing pH was due to phosphorus uptake and carbon dioxide stripping. BNRM1 modeled the pH variations and the decrease in phosphorus uptake rate. This model integrated a switch function in the kinetic expression to represent pH inhibition. The phosphorus concentrations in relation to the pH inhibition constant were represented by adjusting the polyphosphate storage process in the model. Therefore, for accurate prediction of phosphorus evolution in an A/O SBR, a pH inhibition term should be included in the ASM2d model. The combination of Anaerobic Digestion Model No. 1 (ADM) and ASM2d model with FORTRAN ODE software was used to simulate a sequencing batch reactor (Kauder et al., 2007). It showed that alternative treatment characteristics were based upon the sequence of anaerobic and aerobic steps. The Jacobian matrix method was used for describing the error handling of negative gas-rates and negative concentrations.

A modified ASM2d model for SBR was developed (Marsili Libelli et al., 2001). According to the well known Nitrosomonas-Nitrobacter oxidation sequence, the equations split the nitrification stage in a two-step process. It described the improvement of X_{PAO} dynamics seen in the anaerobic/aerobic phosphorus removal process. For description of the effluent qualities of the enhanced biological phosphate removal (EBPR) system, A_2O used a modified mathematical model based upon ASM2d (Pai et al., 2001). Three mathematical modifications were incorporated into the ASM2d model. These were (1) the biosorption effect of soluble COD, (2) the hydrolysis of organic nitrogen in influent wastewater, and, (3) the growth of heterotrophic organisms in the anaerobic tank. Simultaneous nitrification-denitrification taking place in the A_2O process consists of an anaerobic/anoxic/oxide processes. It removed biological phosphorus. The return sludge ratios and sludge retention time were 0.25 and 12 days, respectively. Three different mixed liquid recycling ratios (MLRR) used in the model plant and were set at 0.5, 1.25 and 2. Comparison between measured and predicted values at steady state was made for each test. Its result showed strong consistency. This is due to the biosorption effect of the SCOD, the hydrolysis of organic nitrogen and heterotrophic organism growth in the anaerobic phase of activated sludge systems.

The ASM2d model was extended by including a chemical model to calculate the pH value in biological processes (Serralta et al., 2004). The chemical model affects the values of ASM2d describing non-equilibrium biochemical processes. Every component of the ASM2d model affects the pH value as well as the ion-balance for pH calculation and dissociation species. SBR operation for enhanced biological phosphorus removal was done for verification of the extended pH model to predict the dynamics of pH changes. It showed that a pH can inhibit PAOs. Incorporation of both predation and viral infection processes was integrated to the ASM2d model (Hao et al., 2011). The evaluation of predation contributions and viral infection upon sludge minimization in a SBR system enriching PAOs was based on this extended model. Three individual decay processes were included in the extended model. The evaluation of predation and viral infection on sludge minimization was based upon the calibration and validation of different experimental results. It indicated that predation contributes approximately twice as much to sludge minimization as viral infection.

2.4.4 The Barker and Dold model

Barker and Dold (1997) presented a general model for biological nutrient removal in activated sludge. It considers carbonaceous energy removal, nitrification, and denitrification processes as in the ASM1 model (Henze et al., 1987). In addition Barker and Dold built upon previous results (Wentzel et al., 1989a & 1989b) to elucidate biological phosphorus removal. Also, readily biodegradable chemical oxygen demand (RBCOD) is converted to volatile fatty acids (VFAs) by fermentation processes (Barker and Dold, 1997). Furthermore, a degradation of slowly biodegradable chemical oxygen demand (SBCOD) to RBCOD in hydrolysis process can occur under anaerobic, anoxic and aerobic conditions. In contrast, hydrolysis in the ASM1 model occurs under aerobic conditions only (Henze et al., 1987). The Barker and Dold (1887) model was developed to model mechanisms of autotrophic nitrifying organisms (ANOs), ordinary heterotrophic organisms (OHOs) and PAOs. In particular, nitrification, denitrification, biological excess phosphorus removal processes (NDBEPR) are important in all three of these organism groups (Barker and Dold, 1996). The ASM2 model also included NDBEPR processes. However, select aspects of these models differ. The details of the Barker and Dold model are discussed below.

2.4.4.1 Anoxic growth of PAOs

PAOs behavior was investigated in activated sludge University of Cape Town (UCT) systems (Figure 2.2). Release of poly-P and up take of phosphorus under anaerobic, anoxic, and aerobic conditions were investigated. The importance of anoxic recirculation flow is its enhancement of phosphorus removal. It prevents NO_3 from occurring in the anaerobic phase. As a result, biological enhanced phosphorus removal (BEPR) can occur. If NO_3 is available in the anaerobic phase, PAOs cannot utilize VFAs. Under these conditions, phosphate uptake is reduced. NO_3 does not appear to directly affect behavior of PAOs. However, EBPR in batch and continuous experiments demonstrated that PAOs are able to utilize phosphorus in anoxic phase (Barker and Dold, 1996). Four specific PAOs behaviors are seen during denitrification:

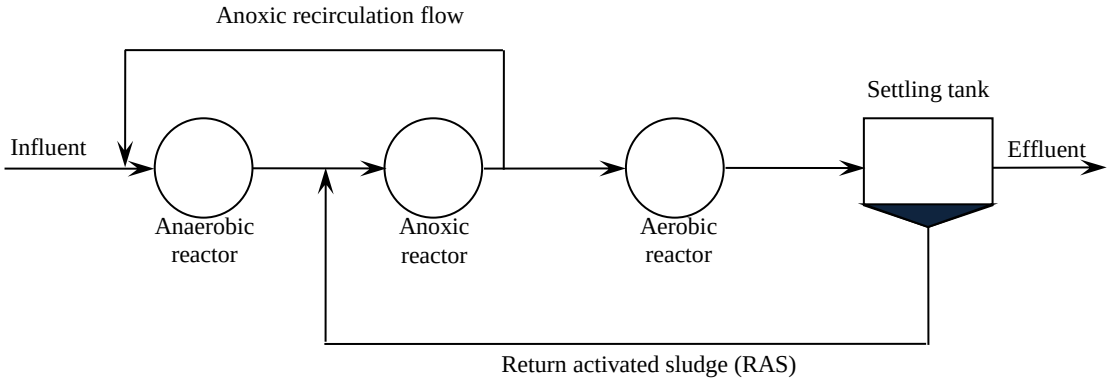

Figure 2.2 Schematic diagram of activated sludge UCT processes

1. Not all PAOs can take up phosphorus under denitrification.

Not all PAOs can utilize NO_3 as electron acceptor to store poly-hydroxy-butyrate (PHB).

2. The efficiency of phosphorus uptake using NO_3 as electron acceptor may be less than when using oxygen as electron acceptor. Experiments in batch culture have shown that under anoxic conditions more stored carbon is used for phosphorus utilization.

3. Phosphorus uptake/PHB oxidation and phosphorus release/PHB storage can occur simultaneously under anoxic and anaerobic conditions, respectively. These processes will only occur when SCFAs are available as a substrate under anaerobic conditions.

The reducing fraction (η_P = 0.4) in denitrification was represented. Not all PAOs can take up NO_3. An anoxic growth process in the Barker and Dold model duplicates one of aerobic growth process of a previous study (Wentzel et al. 1989a). In this study, four PAOs aerobic growth processes were included. PAOs used NH_3 and NO_3 as nitrogen sources for growth under anoxic conditions. It occurs with sufficient ammonia and with no phosphorus limitation under anoxic conditions. The stoichiometric coefficient for phosphorus uptake obtained from the batch experiments has values between 0.9 and 1.1 g P g^{-1}COD (Wentzel et al., 1989a). Two stoichiometric parameters of aerobic growth ($f_{p,UPT1}$) and anoxic growth ($f_{p,UPT2}$) were 0.95 g P g^{-1}COD and 0.55 g P g^{-1}COD respectively. These values were obtained from simulation (Barker and Dold, 1997).

2.4.4.2 COD loss

Prediction of oxygen consumption and volatile suspended solids production are based upon a COD loss assumption (Barker and Dold, 1996). It is used to investigate biological excess phosphorus removal (BEPR) activated sludge systems. COD loss is based on three mechanisms of COD balance for different activated sludge systems (Barker and Dold, 1996 & 1997):

1. The first mechanism is hydrolysis of slowly biodegradable COD (SBCOD) to readily biodegradable COD (RBCOD). Under anoxic and anaerobic conditions, SBCOD is hydrolyzed to RBCOD by ordinary heterotrophic organisms (OHOs). E_{ANOX} and E_{ANA} are hydrolysis efficiency factors under anoxic and anaerobic conditions, respectively. One COD unit of SBCOD produces E units of RBCOD production, thus COD lost is (1 - E) (Barker and Dold, 1997). This was observed to be correct under anoxic-aerobic and anoxic-only systems.
2. Furthermore, Barker and Dold (1997) proposed an empirical factor for modeling loss of COD. It is used in fermentation process to describe conversion of RBCOD to SCFAs. Modeling fermentation using Monod growth expression explains growth processes under anaerobic conditions. Yield of fermentation products is $(1\text{-}Y_{H,ANA})$, where $Y_{H,ANA}$ is a yield of OHOs. Additionally, Barker and Dold (1997) assumed that a portion of fermentation (Y_{AC} = 0.4) represents SCFAs (S_{BSA}), and the remainder ($1\text{-}Y_{AC}$ = 0.6) is COD lost from process.
3. The final mechanism describes uptake of SCFAs by PAOs. Under anaerobic condition PAOs utilize SCFAs converting them to PHB with simultaneous phosphorus release. It is assumed that the yield of PHB (Y_{PHB}) is 0.89 g COD g^{-1} COD (Wentzel et al., 1986). Therefore, the COD lost is ($1 - Y_{PHB}$ = 0.11).

This model can simulate the fraction of reduced PAOs under anoxic conditions. It also quantifies reduced uptake of phosphorus by denitrifying PAOs. However, it has not been adequately validated (Hu et al., 2003; Hu et al., 2007). Especially under anaerobic conditions, COD loss is taking place in fermentation processes for RBCOD conversion to SCFAs by OHOs. Subsequently a fraction of SCFAs is utilized by PAOs after

utilizing energy from poly-P degradation. Additionally, reduced uptake of phosphorus and associated denitrification were investigated under anoxic conditions. PAOs are responsible for denitrification in this case. However, it is possible to modify this model to predict behavior in BNRAS systems. Thereby adaptation of metabolic models of COD loss is included (Hu et al., 2003). Anoxic PAOs growth process is also modified to explain observation of anoxic PAOs behavior (Hu et al., 2003). Barker and Dold (1997) did not include a reduced biomass yield for anoxic PAO growth.

2.4.5 The Delft model

The Delft model (van Veldhuizen et al., 1999; Brdjanovic et al., 2000) is based on an integration of the PAOs metabolic model for biological phosphorus removal in anaerobic/aerobic (A/O) and anaerobic/anoxic (A_2) systems. The PAOs metabolic model under anaerobic conditions is based on A/O systems (Smolders et al., 1994a, 1994b, 1995a, 1995b). The Delft model combines PAOs behavior in denitrifying and non-denitrifying bio-P processes (van Veldhuizen et al., 1999; Brdjanovic et al., 2000). In addition the Delft model includes autotrophic and heterotrophic processes as presented in ASM1 (Murnleitner et al., 1997; van Veldhuizen et al., 1999; Brdjanovic et al., 2000; Gernaey et al., 2004). Delft considers all organic storage components (PHA, glycogen). In contrast ASM2 and ASM2d models investigate only PHA (Gernaey et al., (2004). The PAOs metabolic model under aerobic and anoxic conditions is based on A/O and A_2 systems (Kuba et al., 1996). Denitrifying PAOs modelling was modified using the metabolic model in A/O systems. The Delft model can describe two biological phosphorus removal processes. Both processes used the same set of biological reactions under aerobic and anoxic condition. An exception is the use of nitrate instead of oxygen and differences in ATP/NADH ratios (Murnleitner et al., 1997). Variable PAOs metabolisms under anaerobic, aerobic and anoxic conditions discussed as follows.

2.4.5.1 PAO metabolic model under anaerobic conditions

The anaerobic PAOs metabolic model of Delft is similar to anaerobic PAOs metabolic models in both A/O systems and A_2 systems (Kuba et al., 1996). However, the maximum specific acetate uptake rate (q_{ac}^{max} = 0.3 mmol/mmol h) is different from that in A/O systems (q_{ac}^{max} = 0.4 mmol/mmol h) and A_2 system (q_{ac}^{max} = 0.2 mmol/mmol h) (Hu et al., 2003). The anaerobic PAO metabolism (Smolders et al., 1994a; Smolders et al., 1995b; Kuba et al., 1996; Murnleitner et al., 1997; Yagci et al., 2003) yields two reactions: (1) acetate uptake and (2) maintenance. The acetate uptake reaction is directly linked to intracellular PHB storage and glycogen degradation for reduction equivalents ($NADH_2$) and ATP production. ATP from poly-P degradation is used to convert VFAs to PHB storage.

2.4.5.2 PAO metabolic model under aerobic and anoxic conditions

Five PAOs metabolism reactions of biological phosphorus removal under aerobic and anoxic conditions are simulated in the Delft model (Smolders et al., 1995b; Oehmen et al., 2007). They include: (1) PHB catabolism, (2) oxidative phosphorylation, (3) biomass synthesis, (4) phosphate transport and poly-P synthesis, and (5) glycogen synthesis. PAOs metabolic models under both aerobic and anoxic conditions are the same. An exception is that two kinetic parameters are included: the efficient oxidative phosphorylation coefficient (δ) and the phosphate transport coefficient (ε). Only the electron acceptor is different in aerobic and anoxic PAOs metabolisms. δ represented ATP production to $NADH_2$ utilization. δ_O under aerobic conditions and δ_N denitrifying conditions are 1.85 mol ATP/$NADH_2$ (Smolders et al., 1995b) and 1.0 mol ATP/$NADH_2$ (Kuba et al., 1996), respectively. As a result, conversion of $NADH_2$ to ATP by PAOs under anoxic conditions is reduced in comparison to aerobic conditions.

ε represents the ratio of orthophosphate (PO_4) utilized to $NADH_2$ oxidized. ε_O under aerobic conditions and ε_N under denitrifying conditions are 7 P-mol/mol $NADH_2$ (Smolder et al., 1994b) and 3.5 P-mol/mol $NADH_2$ (Kuba et al., 1996; Hu et al., 2003), respectively. As a result, efficiency of PO_4 uptake under anoxic conditions is less than

that under aerobic conditions. The Delft model predicts PAOs biological phosphorus removal under all conditions. However there are limiting conditions of this model:

1. It is valid in sequencing batch reactor (SBR) systems only (Smolders et al., 1995b; Kuba et al., 1996). Continuous systems and multi-reactors cannot employ the Delft model to investigate PAOs mechanisms (Hu et al., 2003).
2. In a previous study, enhanced culture SBR systems utilized acetate as a sole substrate (Kuba et al., 1996; Oehmen et al., 2007). Mixed culture biological nutrient removal (BNR) systems cannot be used by anoxic OHOs and anoxic PAOs due to limiting nitrate concentration (Hu et al., 2003). These disadvantages may not make the Delft model useful for predicting behavior of organisms in general systems.

2.4.6 The ASM3 with Bio-P Module

The Bio-P module is added to Activated Sludge Model No.3 (ASM3) to simulate biological phosphorus removal processes (Rieger et al., 2001; Siegrist et al., 2002). The biological phosphorus removal of ASM3 was developed from ASM2d phosphorus removal processes. Hydrolysis, autotrophic and heterotrophic processes in ASM3 were included in the ASM3 with Bio-P module. Conversion of readily biodegradable substrates (S_S) is used instead of fermentation products (S_A) to produce PHA storage. However S_S is not fermented by heterotrophic organisms. This is shown in the results of other researchers (Satoh et al., 1996; Mino et al., 1998). As a result, there is no phosphorus release limitation due to readily biodegradable substrate fermentation. Furthermore, anaerobic decay is neglected. The ASM3 with Bio-P module was used to obtain useful calibration results for batch experiments using pilot plant and full scale Swiss municipal wastewater treatment processes WWTP (Rieger et al., 2001; Siegrist et al., 2002). Biological inorganic calcium-phosphate precipitation under anaerobic conditions is neglected (Rieger et al., 2001; Siegrist et al., 2002). Other researchers (Maurer et al., 1999) also reported no significant biologically induced phosphorus precipitation at pH < 7.5 and temperatures less than 20°C. Chemical precipitation is also neglected. Modified endogenous respiration of heterotrophs in ASM3 was modified to PAOs decay in ASM3 with Bio-P. The modified phosphorus process did not consider

glycogen storage. The phosphorus process is controlled at low COD as described by earlier researchers (Brdjanovic et al., 1998; Carucci et al., 1999). Glycogen can significantly impact phosphorus removal (Liu et al., 1994; Liu et al., 1996; Liu et al., 1997). Four additional components presented in Bio-P (Rieger et al., 2001; Siegrist et al., 2002) were taken from ASM2d (Henze et al., 1999). They include: 1) inorganic soluble phosphorus (S_{PO4}), 2) phosphorus accumulating organism (X_{PAO}), 3) cell-internal storage product of PAOs (X_{PHA}) and 4) polyphosphate (X_{PP}). The modified Bio-P module includes 11 processes (Rieger et al., 2001; Siegrist et al., 2002). The poly-hydroxy-alkanoates storage (X_{PHA}) process (P1) is different from ASM2d. S_S is used for the PHA storage process of EAWAG Bio-P. In contrast S_A is used in ASM2d. X_{PHA} occurs primarily under anaerobic conditions. It can occur under aerobic and anoxic conditions. As a result, there is no inhibition factor included in the PHA storage process. Aerobic (P2) and anoxic (P3) storage of X_{PP} processes describe processes in which PAOs utilize energy of PHA respiration to take up orthophosphate phosphorus. Then phosphorus is stored internally as polyphosphate (poly-P). Energy from X_{PP} degradation to orthophosphate phosphorus is used for S_S utilization. The Bio-P module considers inhibition of poly-P storage by PAOs under aerobic conditions. Inhibition of poly-P storage can occur when the X_{PP}/X_{PAO} ratio approaches the K_{max} value (Rieger et al., 2001; Siegrist et al., 2002). K_{max} represents a maximum ratio of X_{PP}/X_{PAO}. Anoxic poly-P storage uses nitrate instead of oxygen as an electron acceptor. Not all PAOs can take up nitrate, thus a reduction factor ($\eta_{NO,\ PAO}$) is used as a multiplier to yield P2. As a result, P3 represents a reduction of aerobic poly-P storage (Rieger et al., 2001; Siegrist et al., 2002). Aerobic (P4) and anoxic (P5) growth of PAOs (X_{PAO}) describe how intracellular PHA storage is the energy source for PAOs growth. The same reduction factor ($\eta_{NO,\ PAO}$) represented in P3 was used to investigate PAOs anoxic growth. Aerobic (P6) and anoxic (P7) PAOs represent endogenous respiration processes. These endogenous respiration processes were included PAOs loss and energy requirement. However, they are not included PHA respiration for aerobic and anoxic PAOs growth. Anoxic endogenous processes are obtained by multiplying aerobic endogenous respiration by $\eta_{NO,\ end,\ PAO}$. Aerobic (P8, P10) and anoxic (P9, P11) processes are lysis of poly-P and respiration of internal storage product PHA. They represent decay of poly-P and PHA decay together in PAOs. These processes occur in a manner similar to

endogenous respiration of PAOs. The factors $\eta_{NO,\ resp,\ PAO}$ and $\eta_{NO,\ lys,\ PAO}$ are used to reduce respiration and lysis under anoxic conditions. A summary of the significant differences of processes in EAWAG Bio-P and ASM2d is presented in Table 2.3. ASM3 with Bio-P is used to predict the parameters of different WWTPs. An application of ASM3 with Bio-P is to simulate results of a five-stage step-feed enhanced biological phosphorus removal process. This was used as a comparison to ASM2d (Lee et al., 2006). It was reported that this simulation was better than that of ASM2d. ASM3 with Bio-P was validated by results of a long-term simulation of the activated sludge process at the Hanover-Gummerwald pilot WWTP (Makinia et al., 2005). Their results were observed in short-term hydraulic shock loading experiments. The three continuous influent wastewater components (COD, $N\text{-}NH_4$, $P\text{-}PO_4$) were monitored by online sensors. ASM3 with bio-P can be used to estimate the maximum allowable peak flow of wastewater to treatment plants during storm water conditions (Makinia et al., 2005). To study inhibition of biological phosphorus removal in a sequencing moving bed biofilm reactor using seawater, ASM3 with Bio-P was employed (Vallet et al., 2009).

Table 2.3 Summary of the significant differences of processes in ASM2d and ASM3 with Bio-P

Processes	**ASM2d**	**ASM3 with Bio-P**
Storage of PHA,X_{PHA}	Fermentation products	Readily biodegradable substrate
Aerobic storage of PP,X_{PP}	✓	✓
Anoxic storage of X_{PP}	✓	✓
Aerobic growth of PAOs, X_{PAO}	✓	✓
Anoxic growth of X_{PAO}	✓	✓
Aerobic endogenous respiration	-	✓
Anoxic endogenous respiration	-	✓
Aerobic lysis of X_{PP}	-	✓
Anoxic lysis of X_{PP}	-	✓
Aerobic respiration of X_{PHA}	-	✓
Anoxic respiration of X_{PHA}	-	✓

This model was used to investigate denitrifying biological phosphorus removal for conditions of high levels of nitrate and phosphate with a low level of organic matter. Two identical reactors were used. The first reactor was used to treat water from a marine mesocosm. The second reactor treated a synthetic freshwater influent. A systematic approach for model verification elucidated process errors of ASM3 with Bio-P (Hauduc et al., 2010).

It presented the collection of P9 and P11 processes (anoxic Lysis of X_{PP} and anoxic respiration of X_{PHA}) by substituting the term $S_{NO}/(K_{NO,PAO}+S_{NO})$ for $S_{NO}/K_{NO,PAO}$. In addition, saturation/inhibition constants for nitrate and nitrite (S_{NO}) of autotrophic organisms ($K_{NO,A}$) are missing for autotrophic processes (P12). ASM3 with Bio-P was used to investigate the enhanced biological phosphorus removal in anaerobic/aerobic activated sludge systems (Trutnau et al., 2010). Total organic carbon (TOC) was measured to investigate enhanced biological phosphorus removal (EBPR) in anaerobic/aerobic activated sludge systems (Trutnau et al., 2010). EBPR processes are based upon BOD and COD. ASM3 with Bio-P was used to simulate a modified EBPR on a TOC basis. An intermediate nitrite in biological nutrient removal (BNR) was studied using ASM3 with Bio-P. Its results were used to develop a mechanistic model for BNR activated sludge systems and application to full-scale WWTPs (Ni et al., 2010). However, ASM3 with Bio-P still has limiting conditions. The nitrification of this model is still treated as a single-step process (Iacopozzi et al., 2007). It does not consider nitrite as an intermediate product. A two-step model for the nitrification was presented to consider nitrites (Iacopozzi et al., 2007). It was an enhanced ASM3 model. This model was successful in predicting nitrite and nitrate concentrations in a study of the effects of endogenous decay of ammonium oxidizing biomass (AOB) (Munz et al., 2011). As a result, ASM3 with Bio-P is not satisfactory for describing overall behavior of organisms.

2.5 CONCLUSIONS

Mathematical modeling of biological nutrient removal (BNR) as well as EBPR processes is a useful tool to predict the mechanisms of ANOs, OHOs and PAOs. The denitrification biological nutrient removal activated sludge (DBNRAS) systems indicated that there are significant effects of wastewater treatment implementation. Mathematical simulation modeling is an invaluable tool for wastewater treatment implementation.

It is important to select the most suitable simulation model. Currently, no perfect model exists. In these studies, the six simulation models of BNR processes were considered and evaluated from observations reported in the literature. The differences between these modes occurred for anoxic growth of PAOs with associated PAOs denitrification, and enhancement of anoxic growth as a result of P uptake for poly-P formation.

The first two models (UCTPHO, ASM2) did not simulate the kinetics of PAOs under anoxic conditions. UCTPHO and ASM2 predict PAOs behavior under aerobic conditions only.

The kinetics of the last three models (ASM2d, the Barker and Dold model, the Delft model and ASM3 with Bio-P) can be used to describe reduced uptake of phosphorus and associated PAOs denitrification. These three models give useful information about the kinetics of PAOs under anoxic conditions. In addition, the anaerobic hydrolysis process of converting slowly biodegradable COD to readily biodegradable COD (RBCOD), and COD loss was included. This was done to completely predict biological phosphorus enhanced phosphorus removal (EBPR) performance. However, limitations still exist.

Existing models were further developed by including denitrifying PAOs and reduced P uptake by denitrifying PAOs thereby extending the models to consider EBPRAS systems. In the ASM2d model, denitrifying PAOs are found by multiplying the aerobic PAO growth rate by a reduction factor $\eta_{NO3;G;PAO}$.

The Barker and Dold as well as the Delf models also presented a reduction factor η_P to consider denitrifying PAOs under anoxic conditions. It modeled the proportion of PAOs capable of denitrification under anoxic conditions. The difficulty in the study of denitrifying, was determining the value of $\eta_{NO3;G;PAO}$ for a particular system. Differences PAO metabolism under both aerobic and anoxic conditions were not addressed. Thus, if a significant change in anoxic P uptake occurred, the model could not describe reduced EBPR.

In the ASM2d model, the η_{NO3} reduction factor allows P uptake to start earlier under anoxic conditions, but at a reduced rate. In contrast, the reduced anoxic P uptake of the Barker and Dold model, incorporate kinetic processes allowing a different P uptake to poly-P formation ratio in anoxic and aerobic metabolism.

Under anoxic conditions, reduced P uptake for poly-P formation by PAOs was predicted and occurred in agreement with observations. The Delf model also showed that there is difference between P uptake varying the ATP/$NADH_2$ ratio $\delta_{aerobic}$ under aerobic and anoxic conditions. The value of δ under anoxic conditions is lower than under aerobic conditions. A further effect is reduced anoxic PAOs biomass production.

In consideration of the above, the Barker and Dold and the Delf model both accurately simulate the kinetic processes of anoxic P uptake and associated denitrification by PAOs. There is still a need for further development since comparison of differences between experimental observations to predict values leave some uncertainties. Development of these types of kinetic process simulations always need to be evaluated against experimental observations.

CHAPTER 3:

METHODOLOGY

CHAPTER 3. METHODOLOGY

3.1 MATHEMATICAL MODELS

A useful biological nutrient model should simulate metabolic processes of microorganisms under anaerobic, aerobic and anoxic conditions. Activated Sludge Model No. 2d (ASM2d) (Henze et al., 1999) was chosen for use in this study because it can model organic, nitrogen and phosphorus substrates under the above conditions. The ASM2d model was developed based on Activated Sludge Model No. 2 (ASM2*)* (Henze et al., 1995) and Activated Sludge Model No. 1 (ASM1) (Henze et al., 1987). ASM1 is an excellent tool for modeling nitrification-denitrification processes. Additionally, ASM2 simulates phosphorus utilization by Phosphorus Accumulating Organisms (PAOs) under aerobic conditions only. In contrast, ASM2d models phosphorus up take under anoxic and aerobic conditions (Kerrn-Jespersen and Henze, 1993, Mino et al., 1998; Meinholt et al., 1999). Hence, ASM2d was developed to express phosphorus removal modeling with extension of the ASM2 model. ASM2d was further extended to model the kinetics of nitrate and phosphate metabolism under anoxic conditions (Henze et al., 1999). PAOs can utilize short-chain fatty acids (SCFA) and store poly-hydroxy-butyrate (PHB) intracellularly for (1) an anoxic polyphosphate (poly-P) formation process and (2) an anoxic PAOs growth process. Simulation of these processes is modified from PAOs growth and poly-P formation under aerobic conditions in ASM2. Under anoxic conditions, PAOs use nitrate as a terminal electron acceptor to metabolize phosphorus instead of oxygen. The rates of anoxic poly-P formation and anoxic PAOs growth are given by the aerobic poly-P storage rate and the aerobic growth rate multiplied by a reduction factor η_{NO3}, respectively. This is because some PAOs can grow and/or utilize P under anoxic conditions. This takes into account that the metabolism of PAOs growth and the poly-P storage is reduced under anoxic conditions (Hu et al., 2003). Values of η_{NO3} are difficult to determine due to the variety of anoxic PAOs growth, associated denitrification, and anoxic P uptake (Sorm et al., 1996; Artan et al., 1997; Barker and Dold, 1997; Kuba et al., 1997; Ekama and Wentzel, 1999; Hu et al., 2003).

However, there are 2 models, (1) the Barker and Dold model (Barker and Dold, 1997) and (2) the Delft model (Smolders et al., 1994a & 1994b & 1995a & 1995b), that can simulate denitrification by PAOs. Since both models have limitations, they were not used in this study.

3.2 THE ACTIVATED SLUDGE MODEL NO. 2D (ASM2D)

3.2.1 Conceptual approach in ASM2d

The purpose of ASM2d is to describe biological phosphorus removal processes in activated sludge. ASM2d is a minor extension of ASM2. There are two additional processes that need to be taken into account (1) poly-P storage and (2) growth under anoxic conditions. PAOs in ASM2 are able to store polyphosphate (poly-P) and to grow only under aerobic conditions. In contrast, ASM2d includes simulation of denitrifying PAOs metabolism for poly-P storage and growth. All limitations of ASM2 are valid for ASM2d. Further details of the ASM2d model are found in the literature (Henze et al., 1999). Kinetic and stoichiometric coefficients are used to describe metabolic processes based on Monod kinetics for all parameters and are presented in matrix format. The use of matrix notation makes accessing the stoichiometric coefficients straightforward. Thus, mass balances in the calculations are correctly maintained.

3.2.2 Parameters in the ASM2d model

Parameters in the ASM2d model were developed based on assumptions and correlations of the ASM2 model. Particulate material is represented by the symbol, X, subscripted with an abbreviation for the material that is present in particulate form. Similarly, soluble material is represented by the symbol, X, with an appropriate subscript identifying its composition. Particulate components are assumed to be associated with activated sludge. Soluble components are the components that can only be found dissolved in water.

The definition of soluble components in ASM2d

ASM2d model parameters for soluble components are defined as follows:

S_A [M(COD)L^{-3}]: Fermentation products that were assumed to be acetate. The calculations involving fermentation products are done separately from those for other soluble organic materials. Acetate is used as a carbon source for these biological processes.

S_{ALK} [mol (HCO3)L^{-3}]: The alkalinity of the wastewater was applied to evaluate the conservation of electrical charges in biological reactions. It was assumed that S_{ALK} was bicarbonate HCO_3^- only.

S_F [M(COD)L^{-3}]: Fermentable, readily bio-degradable organic substrates, which can be obtained directly from the transformation of the soluble COD fraction by heterotrophic organisms. These substrates were not included in the fermentation products because they were assumed to be substrates for fermentation.

S_I [M(COD)L^{-3}]: Inert soluble organic material. This material cannot be transformed any further. It was assumed that this material was presented in the influent and in the hydrolysis of X_S.

S_{N2} [M(N)L^{-3}]: Dinitrogen, N_2. This was represented as the only product of denitrification.

S_{NH4} [M(N)L^{-3}]: Ammonium plus ammonia nitrogen. To balance the electrical charges, S_{NH4} was assumed to be all S_{NH4}^+.

S_{NO3} [M(N)L^{-3}]: Nitrate plus nitrite nitrogen. S_{NO3} is represented a summation of nitrate and nitrite nitrogen. Nitrite was not separately calculated as a model component. In contrast to all stoichiometric computations (COD conservation), S_{NO3} was assumed to be NO_3^--N only.

S_{O2} [M(O2)L^{-3}]: Dissolved oxygen. It was assumed that S_{O2} may be subject to gas exchange.

S_{PO4} [M(P)L^{-3}]: Inorganic soluble phosphorus, primarily ortho-phosphate. To balance the electrical charges, it was assumed that S_{PO4} consisted of 50% H_2PO_4 and 50% HPO_4^{2-} at any pH.

S_S [M(COD)L^{-3}]: Readily biodegradable substrate. It was represented a summation of $S_F + S_A$.

Definition of particulate components in ASM2d

ASM2d model parameters for particulate components are defined as follows:

X_{AUT} [M(COD)L^{-3}]: Nitrifying organisms. These organisms participated in nitrification. It was assumed that autotrophs oxidize ammonium (S_{NH4}) directly to nitrate (S_{NO3}).
X_H [M(COD)L^{-3}]: Heterotrophic organisms. It was assumed that these heterotrophs can grow aerobically and anoxically (during denitrification) and transform substrates anoxically by fermentation. They are responsible for hydrolysis and can utilize all degradable organic substrates under all environmental conditions of this study.
X_I[M(COD)L^{-3}]: Inert particulate organic substrates. This flocculation was not degradable in these systems. They may be produced from decay processes or from a fraction of the influent.
X_{PAO} [M(COD)L^{-3}]: Phosphorus accumulating organisms (PAOs). It was assumed that these organisms are capable of forming internal cell storage products. X_{PP} and X_{PHA} are not found in PAOs. These organisms can grow under anoxic and aerobic conditions as per the assumption of the ASM2d model.
X_{PHA} [M(COD)L^{-3}]: A cell internal storage product of phosphorus-accumulating organisms. Poly-hydroxy-alkanoates (PHA) refers to the primary product of X_{PHA}, which can be generated only by PAOs.
X_{PP} [M(P)L^{-3}]: Poly-phosphate. This product is stored internally by PAOs, but it is not included as a fraction of PAOs mass.
X_S [M(P)L^{-3}]: Slowly biodegradable substrate. These particulate organic substrates must be hydrolysed and then may be fermented by heterotrophic organisms.
X_{TSS} [M(TSS)L^{-3}]: Total suspended solids. For stoichiometric biokinetic model computations, total suspended solid materials need to be taken in to account. Prediction of TSS is affected by phosphorus removal. Higher phosphorus removal efficiency increases the fraction of phosphorus in activated sludge.

3.3 ASSUMPTIONS AND CORRELATIONS IN ASM2D

The methods for characterizing municipal wastewater components in activated sludge systems of ASM2d are based on ASM1 and ASM2 models.

3.3.1 Organic fractions in municipal wastewater

The total organic content of wastewater can be characterized as COD (C_{TCOD}). COD can be subdivided, based on complexity and the model assumption. The chemical, dichromate, was used in COD determination instead of permanganate. This was done in order to prevent an error in calculation of mass balance. Total chemical oxygen demand (TCOD) is characterized in the following components:

$$C_{TCOD}= S_A+S_F+S_I+X_I+X_S+X_H+X_{PAO}+X_{PHA}+X_{AUT} \quad (3.1)$$

Biomass fractions in influent needs to be concentrated in order for the bloom to wash-out certain groups of microorganisms. For model assumptions, the concentration of heterotrophs in influent has influence on the TCOD. In contrast, PAOs and autotrophs show no effects on TCOD. This is because their concentration in influent is very small. Note that X_{PAO} does not include internal PHA storage product, X_{PHA}. Its concentration is equal to zero in municipal wastewater. Thus, the general fraction of COD in raw wastewater can be simplified to:

$$C_{TCOD}= S_A+S_F+S_I+X_I+X_S+X_H \quad (3.2)$$

In some cases, the concentration of heterotrophs is negligible or presented in slowly degradable suspended organics, X_S. The relationship can be further simplified to:

$$C_{TCOD}= S_A+S_F+S_I+X_I+X_S \quad (3.3)$$

3.3.2 Nitrogen fractions in municipal wastewater

Most of the nitrogen component is present as ammonia. The remaining portion of nitrogen is mostly found in other organic components. The total nitrogen concentration in municipal wastewater, C_{TN}, is expressed as the following fractions:

$$C_{TN}= C_{TKN}+S_{NO3}=X_{TKN}+S_{TKN}+S_{NO3`} \quad (3.4)$$

where: C_{TN} is total Kjeldahl nitrogen
X_{TKN} is particulate Kjeldahl nitrogen
S_{TKN} is soluble Kjeldahl nitrogen

All organic particulate fractions include nitrogen except for X_{PHA}. X_{TKN} is a summation of nitrogen fractions in all organic particulate matter:

$$X_{TKN}= X_I*i_{NXI}+X_S*i_{NXS}+(X_H+X_{PAO}+X_A)*i_{NBM} \quad (3.5)$$

The soluble Kjeldahl nitrogen contains ammonia, and nitrogen fractions in readily biodegradable organic substrates, S_F, and inert soluble organic material, i.e., S_I.

$$S_{TKN}= S_{NH4}+S_F*i_{NSF}+S_I*i_{NSI} \quad (3.6)$$

3.3.3 Phosphorus fractions in municipal wastewater

The total phosphorus concentration in municipal wastewater can be expressed as the following:

$$C_{TP}=X_{TP}+S_{TP} \quad (3.7)$$

where: X_{TP} is particulate phosphorus

S_{TP} is soluble phosphorus

The particulate phosphorus, X_{TP}, consists of inorganic and organic phosphorus:

$$X_{TP}= 0.205*X_{MeP}+X_{PP}+X_{S*}i_{PXS}+X_I*i_{PXI}+(X_H+X_{PAO}+X_{AUT})*i_{PBM} \quad (3.8)$$

Stored polyphosphate, X_{PP}, is close to zero in municipal wastewater, as is metalphosphate concentration, X_{MeP}.. Generally the particulate phosphorus concentration of autotrophs and PAOs is negligible.

$$X_{TP}= X_{S*}i_{PXS}+X_I*i_{PXI} \quad (3.9)$$

The soluble phosphorus includes:

$$S_{TP}= S_{PO4}+S_F*i_{PSF}+S_I*i_{PSI} \quad (3.10)$$

3.4 METHOD FOR MODEL PRESENTATION

The method of employing ASM2d using matrix notation was introduced by Henze et al. (1999). The matrix notation pattern includes the components and the transformation processes. The rate of parallel processes (r_j) can be calculated as the sum of the rate of production of component i ($r_j[M_j\ L^{-3}\ T^{-1}]$). The indices i and j are indicated in the transformation processes using the following notation:

$$r_j= \sum \nu_{ji.}\ p_j \quad (3.11)$$

The stoichiometric matrix v_{ji} and a vector p_j represent the stoichiometric coefficients and the processes rate equations, respectively. The values of +1 or -1 are dimensionless in the stoichiometric matrix on the stoichiometric coefficient, v_{ji}, of each process j. For other stoichiometric coefficients, algebraic equations may be dimensionless in order to introduce the conservation principle into the determination of the stoichiometric coefficients. Hence, v_{ji} can be represented in the form of its absolute value with the dimension $M_i M_k^{-1}$. M_k is the unit of the component k upon which the stoichiometry is based.

3.5 BASIS FOR INTRODUCING ASM2D

The ASM2d model consists of a conservation equation coupled with stoichiometry and biological processes. Conservation equations are the mathematical equivalent of presenting the chemical reactions, elements, electrons and net electrical charges (Henze et al., 1999). The stoichiometry of ASM2d is based on four conservations: COD, electrical charges, nitrogen and phosphorus. The biological processes in activated sludge systems refer to the relevant metabolic mechanisms of ordinary heterotrophic organisms (X_H), phosphorus accumulating organisms (X_{PAO}) and nitrifying organisms (X_{AUT}).

3.5.1 The conservation equation

The conservation equation is valid for all processes, j, and all materials, c. It may be written in equation form as:

$$\sum v_{ji} * i_{ci} = overall\ components \qquad (3.12)$$

where: v_{ji} = stoichiometric coefficient for component i in process j [$M_i\ M_k^{-1}$]

i_{ci} = factor to convert the units of component i to the units of the material c, to which conservation is to be applied [$M_c\ M_i^{-1}$]. The conservation factors (i_{ci}), for COD, electrical charges, nitrogen and phosphorus is presented in Table 3.1.

Table 3.1 Conversion factors, i_{ci}, to be applied in conservation equations of ASM2d. Missing values are equal to 0.

Index:	**Conservation**	**Units**	**COD**	**N**	**P**	**Charge**	**Mass**
Factor	**Component**		$\mathbf{i_{COD,i}}$	$\mathbf{i_{N,i}}$	$\mathbf{i_{P,i}}$	$\mathbf{i_{Charge,i}}$	$\mathbf{i_{TSS,i}}$
Index i:			**g COD**	**g N**	**g P**	**mole$^+$**	**g TSS**
1	S_{O2}	g O_2	-1	i_{NSF}	i_{PSF}		
2	S_F	g COD	1				
3	S_A	g COD	1			-1/64	
4	S_{NH4}	g N		1		+1/14	
5	S_{NO3}	g N	-64/14	1		-1/14	
6	S_{PO4}	g P			1	-1.5/31	
7	S_I	g COD	1	i_{NSI}	i_{PSI}		
8	S_{ALK}	mole HCO_3				-1	
9	S_{N2}	g N	-24/14	1			
10	X_I	g COD	1	i_{NXI}	i_{PXI}		i_{TSSXI}
11	X_S	g COD	1	i_{NXS}	i_{PXS}		i_{TSSXS}
12	X_H	g COD	1	i_{NBM}	i_{PBM}		i_{TSSBM}
13	X_{PAO}	g COD	1	i_{NBM}	i_{PBM}		i_{TSSBM}
14	X_{PP}	g P			1	-1/31	3.23
15	X_{PHA}	g COD	1				0.60
16	X_{AUT}	g COD	1	i_{NBM}	i_{PBM}		i_{TSSBM}
17	X_{TSS}	g TSS					-1

3.5.2 Biological processes, stoichiometry and process rate equation

Three groups of microorganism are relevant to a variety of unknown parameters in each of the processes. These parameters are presented in matrix notation. Use of matrices in calculations makes it easy to apply stoichiometric, kinetic and process rate equations. Simplified processes for each of microorganisms are described as follows.

3.5.2.1 Hydrolysis processes

Particulate organic matter or high molecular weight matter cannot be taken up directly by microorganisms. The hydrolysis processes take place by extracellular enzymatic reactions to transform slowly biodegradable substrates to other substrates. These are characterized based on the available electron acceptors. Hydrolysis processes take place with heterotrophic organisms. The stoichiometric coefficients of hydrolysis processes are summarized in Table 3.2. There are three types of hydrolysis done by heterotrophic organisms. These are presented below as processes 1-3.

Process 1: Aerobic hydrolysis of slowly biodegradable substrates under aerobic conditions.

Process 2: Anoxic hydrolysis of slowly biodegradable substrates under anoxic conditions. This reaction is slower than aerobic hydrolysis.

Process 3: Anaerobic hydrolysis of slowly biodegradable substrates under anaerobic conditions. These reactions are also slower than aerobic hydrolysis.

Table 3.2 Stoichiometry of hydrolysis processes in ASM2d

Process	S_F	S_{NH4}	S_{PO4}	S_I	S_{ALK}	X_S	X_{TSS}
1 Aerobic hydrolysis	$1-f_{SI}$	$\nu_{1,NH4}$	$\nu_{1,PO4}$	f_{SI}	$\nu_{1,ALK}$	-1	$\nu_{1,TSS}$
2 Anoxic hydrolysis	$1-f_{SI}$	$\nu_{2,NH4}$	$\nu_{2,PO4}$	f_{SI}	$\nu_{2,ALK}$	-1	$\nu_{2,TSS}$
3 Anaerobic hydrolysis	$1-f_{SI}$	$\nu_{3,NH4}$	$\nu_{3,PO4}$	f_{SI}	$\nu_{3,ALK}$	-1	$\nu_{3,TSS}$

3.5.2.2 Processes of ordinary heterotrophic organisms

These ordinary heterotrophic organisms utilize fermentable organic substrates (S_F) and fermentation products (S_A) for growth under aerobic and anoxic conditions. This can be described by process rate equations (Table 3.6). These organisms also are related to the decay and lysis processes of heterotrophs. The stoichiometric coefficients of heterotrophic processes are summarized in Table 3.3. Processes 4-9 represent the

metabolism of heterotrophic organisms including growth rate, fermentation and lysis (Table 3.6).

Processes 4 and 5: These are aerobic growth processes of heterotrophic organisms metabolizing fermentable substrates S_F and producing fermentation products S_A. Both processes are modeled to occur as parallel processes. Heterotrophic organisms use S_F and S_A in process 4 and process 5, respectively. A maximum growth rate on substrate (μ_H) and yield coefficient (Y_H) are assumed for both processes. The highest values of the rate equations are at the maximum growth rate of the heterotrophic organism. This is not altered even if both S_F and S_A increase. Heterotrophic organisms utilize oxygen, O_2, nutrients, S_{NH4}, and S_{PO4}, and possibly alkalinity, S_{ALK}, to produce suspended solids, X_{TSS}.

Processes 6 and 7: These two processes model the anoxic growth rate of heterotrophic organisms on S_F and S_A. Both processes are similar to the aerobic growth processes, except they require nitrate, S_{NO3}, instead of oxygen as an electron acceptor. The assumption for calculating the stoichiometric coefficient of nitrate is that all nitrate, S_{NO3}, is converted to dinitrogen, N_2. The stoichiometry of denitrification, which produces alkalinity, can be calculated by the charge conversion. The factor η_{NO3} was used in modeling denitrification growth rate because it was assumed that O_2 can inhibit this process. Additionally, μ_H is reduced under anoxic conditions from its value under aerobic conditions. This accounts for the fact that some heterotrophic organisms are capable of denitrification or that a denitrification growth process may occur at a reduced rate.

Process 8: This is a fermentation process which happens only under anaerobic conditions. It is assumed that heterotrophic organisms are capable of conversion of S_F to S_A. For fermentations producing negative charge in the process of S_A production, alkalinity, S_{ALK}, is required in order to maintain conservation of charge balance. The requirement of S_{ALK} was predicted from charge balance.

Process 9: This is a lysis process which demonstrates the sum of all decay and loss processes of heterotrophic organisms. Examples of this include endogenous respiration, lysis and predation. The rate is modeled is independent of environmental conditions.

Table 3.3 Stoichiometry of the facultative heterotrophic organisms, X_H in ASM2d

Process	S_{O2}	S_F	S_A	S_{NO3}	S_{N2}	X_I	X_S	X_H
4 Aerobic growth on S_F	$1-\frac{1}{Y_H}$	$-\frac{1}{Y_H}$						1
5 Aerobic growth on S_A	$1-\frac{1}{Y_H}$		$-\frac{1}{Y_H}$					1
6 Anoxic growth on S_F		$-\frac{1}{Y_H}$		$-\frac{1-Y_H}{2.86*Y_H}$	$-\frac{1-Y_H}{2.86*Y_H}$			1
7 Anoxic growth on SA			$-\frac{1}{Y_H}$	$-\frac{1-Y_H}{2.86*Y_H}$	$-\frac{1-Y_H}{2.86*Y_H}$			1
8 Fermentation		-1	1					
9 Lysis						f_{XI}	$1-f_{XI}$	-1

3.5.2.3 Processes of phosphorus accumulating organism, X_{PAO}

It is assumed that in phosphorus accumulating organisms, X_{PAO}, metabolism in ASM2d is present. This is also seen from ASM2 and is attributed to denitrification in PAOs, X_{PAO}. Under anaerobic conditions, short-chain fatty acids (SCFAs) are utilized and transformed into poly-hydroxy-alkanoates (X_{PHA}). X_{PAO} can store poly-P, and simultaneously grow under aerobic and anoxic conditions by using glycogen and internal X_{PHA} storage. In addition, lysis of X_{PHA}, X_{PP} and X_{PHA} is taken into account by X_{PAO} metabolism. The stoichiometric coefficients, kinetics and process rate equations of PAOs are presented in Table 3.4. The process rate equations for X_{PAO} are modeled to characterize all relevant metabolism (Table 3.6). The processes shown in Table 3.4 are valid for ASM2d only. They are each discussed further.

Process 10: The process for storage of X_{PHA}, in which it is assumed that PAOs may release phosphate, PO_4, from poly-phosphate, X_{PP}, and take up energy form hydrolysis of X_{PP}, in order to utilize S_A for storage of internal poly-hydroxy-alkanoates, PHA. This process has been reported not only under anaerobic conditions but also aerobic and anoxic conditions. The inhibition in terms of S_{O2} and the rate of storage of organics are relatively constant, whereas the release of the phosphorus varies. The rate constants for storage of X_{PHA}, q_{PHA}, and phosphate

Table 3.4 Stoichiometry of the phosphorus accumulating organisms, X_{PAO} in ASM2d

Process	S_{O2}	S_A	S_{N2}	S_{NO3}	S_{PO4}	X_I	X_S	X_{PAO}	X_{PP}	X_{PHA}
10 Storage of X_{PHA}		-1			Y_{PO4}				$-Y_{PO4}$	
11 Aerobic storage of X_{PP}	$-Y_{PHA}$				-1				1	$-Y_{PHA}$
12 Anoxic storage of X_{PP}			$v_{12,NO3}$	$v_{12,NO3}$	-1				1	$-Y_{PHA}$
13 Aerobic growth of X_{PAO}	$V_{13,O2}$				$-i_{PBM}$			1		$-1/Y_H$
14 Anoxic growth of X_{PAO}			$v_{14,NO3}$	$v_{14,NO3}$	$-i_{PBM}$			1		$-1/Y_H$
15 Lysis of X_{PAO}					$V_{15,PO4}$	f_{XI}	$1- f_{XI}$	-1		
16 Lysis of X_{PP}					1				-1	
17 Lysis of X_{PHA}		1								-1

requirement (PO_4 release) per PHA stored, Y_{PO4}, are determined from S_A removal and S_P release. The value of Y_{PO4} has been shown to depend on pH.

Processes 11 and 12: These processes are aerobic and anoxic storage of poly-phosphate (poly-P). To take up PO_4, PAOs require energy, which may be derived from aerobic and anoxic respiration of X_{PHA}. Limited phosphate consumption happens if the phosphorus content in PAOs becomes too high. This leads to an inhibition term of X_{PP} storage, which is represented as the X_{PP}/X_{PAO} ratio and can be used as an approach for determining the maximum allowable value of K_{MAX}. The factor η_{NO3} is used to multiply the process of the aerobic storage of poly-P to model the process of anoxic storage of poly-P. This accounts for the observation that some PAOs are capable of denitrification or that denitrification may happen at the reduced rate.

Processes 13 and 14: These model aerobic and anoxic growth of PAOs. It is assumed that the growth of PAOs uses only X_{PHA}. For the production of biomass, it is assumed that PAOs consume S_{PO4}. The maximum growth rate of PAO, μ_{PAO} under anoxic conditions is reduced relative to its value under aerobic conditions, by the factor η_{NO3}. This accounts for the observation that some PAOs are capable of denitrification or that denitrification may happen at the reduced rate.

Processes 15, 16 and 17: These represent the lysis and storage products of PAOs. Concentrations of all fractions of PAOs are relative to rates of death, endogenous

respiration and maintenance resulting in a loss or decay. All three components (processes 15, 16 and 17) are modeled separately since X_{PP} and X_{PHA} are not accounted for as part of the biomass, X_{PAO}.

3.5.2.4 Nitrification process

It is assumed that no intermediates such as nitrite in the nitrification reaction are included in the transformation of ammonium, NH_4, to nitrate, NO_3. This was done in order to simplify consumption of nitrite in modeling. The stoichiometric coefficients, kinetics and process rate equations are given in Table 3.5.

Table 3.5 Stoichiometry of the nitrifying organisms, X_{AUT} in ASM2d

Process	**S_{O2}**	**S_{NH4}**	**S_{NO3}**	**S_{PO4}**	**X_I**	**X_S**	**X_{AUT}**
18 Aerobic growth of X_{AUT}	$-\frac{4.57-Y_A}{Y_A}$	$\nu_{18,NH4}$	$-\frac{1}{Y_A}$	$-i_{PBM}$			1
19 Lysis		$\nu_{19,NH4}$		$\nu_{19,PO4}$	f_{XI}	$1- f_{XI}$	-1

Process 18: This represents growth of nitrifying organisms. These organisms utilize NH_4 as a nutrient, then produce NO_3^-, simultaneously reducing alkalinity. This is similar to the ASM1 model. However, ASM1 does not model phosphorus uptake by PAOs.

Process 19: This represents lysis of nitrifying organisms. The lysis of nitrifies is modeled in a manner similar to ASM1 for the lysis of heterotrophs. The decay products (X_S and S_F) are available for heterotrophs only, so that the observation of endogenous respiration of nitrifies can be determined from the growth rate and oxygen consumption of heterotrophs.

Table 3.6 Process rate equations for ASM2d

Process rate equations	
Hydrolysis Processes: X_H	
1 Aerobic Hydrolysis	$K_h \frac{S_{O2}}{K_{O2}+S_{O2}} + \frac{X_S/X_H}{K_X+X_S/X_H} X_H$
2 Anoxic Hydrolysis	$K_h \eta_{NO3} \frac{K_{O2}}{K_{O2}+S_{O2}} + \frac{S_{NO3}}{K_{NO3}+S_{NO3}} \frac{X_S/X_H}{K_X+X_S/X_H} X_H$
3 Anaerobic Hydrolysis	$K_h \eta_{fe} \frac{K_{O2}}{K_{O2}+S_{O2}} + \frac{K_{NO3}}{K_{NO3}+S_{NO3}} \frac{X_S/X_H}{K_X+X_S/X_H} X_H$
Heterotrophic organisms: X_H	
4 Growth on S_F	$\mu_H \frac{S_{O2}}{K_{O2}+S_{O2}} \frac{S_F}{K_F+S_F} \frac{S_F}{S_F+S_A} \frac{S_{NH4}}{K_{NH4}+S_{NH4}} \frac{S_{PO4}}{K_{PS}+S_{PO4}} \frac{S_{ALK}}{K_{ALK}+S_{ALK}} X_H$
5 Growth on S_A	$\mu_H \frac{S_{O2}}{K_{O2}+S_{O2}} \frac{S_A}{K_F+S_F} \frac{S_A}{S_F+S_A} \frac{S_{NH4}}{K_{NH4}+S_{NH4}} \frac{S_{PO4}}{K_{PS}+S_{PO4}} \frac{S_{ALK}}{K_{ALK}+S_{ALK}} X_H$
6 Denitrification with S_F	$\mu_H \eta_{NO3} \frac{K_{O2}}{K_{O2}+S_{O2}} \frac{S_{NO3}}{K_{NO3}+S_{NO3}} \frac{S_F}{K_F+S_F} \frac{S_F}{S_F+S_A} \frac{S_{NH4}}{K_{NH4}+S_{NH4}} \frac{S_{PO4}}{K_{PS}+S_{PO4}} \frac{S_{ALK}}{K_{ALK}+S_{ALK}} X_H$
7 Denitrification with S_A	$\mu_H \eta_{NO3} \frac{K_{O2}}{K_{O2}+S_{O2}} \frac{S_{NO3}}{K_{NO3}+S_{NO3}} \frac{S_A}{K_F+S_F} \frac{S_A}{S_F+S_A} \frac{S_{NH4}}{K_{NH4}+S_{NH4}} \frac{S_{PO4}}{K_{PS}+S_{PO4}} \frac{S_{ALK}}{K_{ALK}+S_{ALK}} X_H$
8 Fermentation	$q_{fe} \frac{K_{O2}}{K_{O2}+S_{O2}} + \frac{K_{NO3}}{K_{NO3}+S_{NO3}} \frac{S_F}{K_F+S_F} \frac{S_{ALK}}{K_{ALK}+S_{ALK}} X_H$
9 Lysis	$b_H X_H$
Phosphorus accumulating organisms (PAOs): X_{PAO}	
10 Storage of X_{PHA}	$q_{PHA} \frac{S_A}{K_{A+S_A}} \frac{X_{PP}/X_{PAO}}{K_{PP}+X_{PP}/X_{PAO}} \frac{S_{ALK}}{K_{ALK}+S_{ALK}} X_{PAO}$
11 Aerobic storage X_{PP}	$q_{PP} \frac{S_{O2}}{K_{O2}+S_{O2}} \frac{S_{PO4}}{K_{PS}+S_{PO4}} \frac{X_{PHA}/X_{PAO}}{K_{PHA}+X_{PHA}/X_{PAO}} \frac{K_{MAX}-X_{PP}/X_{PAO}}{K_{PP}+K_{MAX}-X_{PP}/X_{PAO}} \frac{S_{ALK}}{K_{ALK}+S_{ALK}} X_{PAO}$
12 Anoxic storage of X_{PP}	$\rho_{12=}\rho_{11} \frac{K_{O2}}{S_{O2}} \frac{S_{NO3}}{K_{NO3}+S_{NO3}}$
13 Aerobic growth on X_{PHA}	$\mu_{PAO} \frac{S_{O2}}{K_{O2}+S_{O2}} \frac{S_{PO4}}{K_{PS}+S_{PO4}} \frac{X_{PHA}/X_{PAO}}{K_{PHA}+X_{PHA}/X_{PAO}} \frac{S_{ALK}}{K_{ALK}+S_{ALK}} X_{PAO}$
14 Anoxic growth on X_{PHA}	$\rho_{14=}\rho_{13} \frac{K_{O2}}{S_{O2}} \frac{S_{NO3}}{K_{NO3}+S_{NO3}}$
15 Lysis of X_{PAO}	$b_{PAO} X_{PAO} \frac{S_{ALK}}{K_{ALK}+S_{ALK}}$
16 Lysis of X_{PP}	$b_{PP} X_{PP} \frac{S_{ALK}}{K_{ALK}+S_{ALK}}$
17 Lysis of X_{PHA}	$b_{PHA} X_{PHA} \frac{S_{ALK}}{K_{ALK}+S_{ALK}}$

Table 3.6 (cont.) Process rate equations for ASM2d

Process rate equations	
Nitrifying organisms (autotrophic organisms): X_{AUT}	
18 Aerobic growth of X_{AUT}	$\mu_{AUT}\frac{S_{O2}}{K_{O2}+S_{O2}}\frac{S_{NH4}}{K_{NH4}+S_{NH4}}\frac{S_{PO4}}{K_{PS}+S_{PO4}}\frac{S_{ALK}}{K_{ALK}+S_{ALK}}X_{AUT}$
19 Lysis of X_{AUT}	$b_{AUT}X_{AUT}$

3.6 THE MODIFIED UNIVERSITY OF CAPE TOWN (MUCT)

The modified University of Cape Town (MUCT) process is quite similar to the Virginia Initiative Plant (VIP) process. Typically the MUCT process is designed for a SRT of 13-25 days while VIP process is designed for 5-10 days (Reitsma et al., 2001a). However, when it comes to the membrane bioreactor (MBR) process, the differences between the two processes do not exist. The MUCT process comprises four cells within the bioreactor, two internal recycles and return activated sludge. It modifies the University of Cape Town (UCT) process with the first anoxic zone designed to reduce only the nitrate nitrogen with anoxic recirculation in the return activated sludge. The second anoxic zone is designed for a higher nitrate nitrogen removal as mixed liquor is recycled from the aerobic zone. The significant advantage of the MUCT process is that it does not directly return nitrate nitrogen bearing mixed liquor to anaerobic zone. In this way, a low oxidation-reduction potential (ORP) remains to maximize phosphate release from PAOs. However, the particular type mixed liquor circulated to the anaerobic zone causes diluted MLSS in anaerobic zone. To compensate for MLSS dilution in anaerobic zone, size needs to be considered. A schematic diagram of this process is presented in Figure 3.1. Return activated sludge (RAS) is recycled to the first anoxic zone and internal recirculation returns nitrified mixed liquor from the aerobic zone to the second anoxic zone. The internal recirculation to the anaerobic zone comes from the first anoxic zone. The significance of the MUCT process is that it enables nitrate recycle to the anaerobic zone. The MUCT process treatment can enhance nitrogen removal by nitrification and denitrification combined with biological

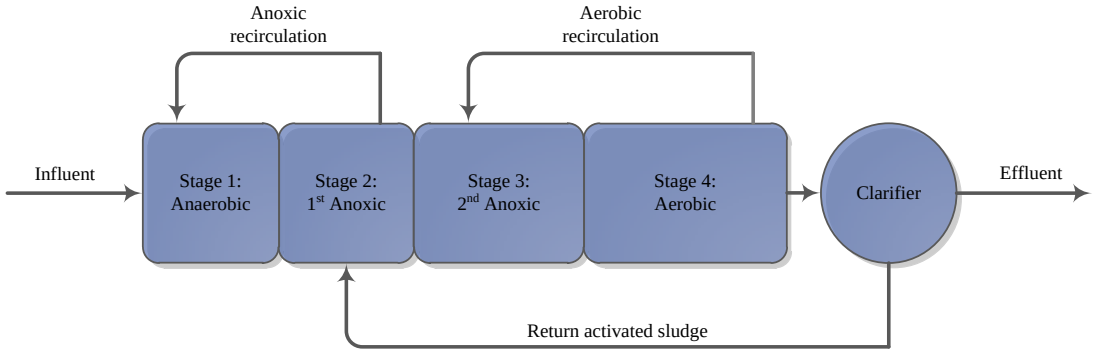

Figure 3.1 Modified University of Cape Town (MUCT) process schematic diagram

phosphorus (bio-P) removal. In the anaerobic zone, stimulation of PAOs takes place. In the 2nd anoxic compartment, pre-denitrification occurs. In this compartment the nitrate nitrogen is recirculated from the aerobic compartment. After nitrate nitrified the sludge in the 1st anoxic compartment, sludge is recirculated to the anaerobic compartment. In the aerobic compartment, nitrification takes place and the remaining COD is utilized by autotrophs. During internal aerobic recirculation, nitrate is recirculated from the aerobic compartment to the 2nd anoxic compartment. In the 2nd anoxic stage, denitrification takes place accomplishing both nitrogen and phosphorus removal. The MUCT process influent is mixed with phosphorus rich recycle from the anoxic stage. The PAOs release phosphorus in the process and utilize the volatile fatty acids (VFAs) produced as a by-product of soluble BOD conversion to poly-hydroxyalkanoates (PHA). These fermentation processes provide the necessary conditions that result in substantial polyphosphate degradation. Denitrification takes place in the two anoxic reactors resulting in enhanced phosphorus uptake by PAOs. Phosphorus uptake is rapid since the phosphorus rich mixed liquor is recirculated to the anaerobic compartment. The 2nd anoxic reactor receives nitrate rich mixed liquor from aerobic reactor. This results in nitrate reduction to gaseous nitrogen. The final reactor is the aerobic stage. It generates oxygen to oxidize the remaining BOD and ammonia. The mixed liquor from the aerobic reactor is recirculated to the 2nd anoxic reactor for denitrification. In the final clarifier, phosphorus is generated if this zone becomes septic. Subjecting the clarifier to re-aeration introduces oxygen to mixed liquor, ensuring that the final clarifier remains under aerobic conditions. The activated sludge from settling process is returned to the

1st anoxic reactor for regeneration of the entire process. Advantages and disadvantages of this process are presented below.

Advantages

- ✓ Enhanced phosphorus removal as a result of the reduced nitrate in anaerobic stage.
- ✓ Improved nitrogen removal through a nitrification/denitrification process, as well as aerobic and anoxic recirculation.
- ✓ 1st anoxic stage for recirculation of activated sludge denitrification. This stage protects the anaerobic stage for increased phosphorus release.

Disadvantages

- ✓ Complicated and intensive operation.
- ✓ More piping and pumping required as a result of additional recycle flow.
- ✓ High construction and operational costs.

3.7 THE AQUASIM PROGRAMME

The Aquasim programme is used to calculate mechanisms having the complexity of natural, laboratory or technical systems (Reichert, 1994). The mathematical models are tools to perform calculations and study evolution of a system. Basically, a set of non-linear ordinary or partial differential equations is used for mathematical models of environmental systems. A simplification of actual processes containing empirical model parameters is required for the mathematical models. ASM2d is one of the models which uses non-linear ordinary equations to describe the metabolism of microorganisms. Therefore, Aquasim can be used to simulate the metabolism of organisms for use in the ASM2d model.

Aquasim was used for implementing such models because it is able to simulate the kinetic equations that are necessary in this study. It can also identify model parameters, estimate parameter values and the uncertainty of calculated results (Reichert et al., 1995). Aquasim performs the simulation and identification of parameters of aquatic systems using three processes (Reichert, 1995):

1 Simulation: it compares calculated model values with experimental data to evaluate simulations. It determines whether certain model assumptions are compatible with experimental data. The user can change the model structure and parameter values as needed.

2 Parameter estimation: it estimates values automatically in a given model structure with respect to experimental data.

3 Sensitivity: the programme calculates linear sensitivity functions of particular variables with respect to each of the parameters included in the system. The yield of sensitivity analysis is a combination of identifiability and uncertainty. Both analyses use similarity in their mathematical techniques.

3.8 MODEL CALIBRATION WITH SYSTEMATIC APPROACH

This new method was developed using the identifiability approach and the experience-based approach. Parameter sensitivity was used to identify those parameters which most affect the model. The sensitivity method was used to reduce the number of model parameters. Additionally, the model was calibrated using an iterative process. High computational demand was avoided by reducing the size of ASM2d parameter subset. Four procedures were structured in this new approach. They can be divided into 4 main steps as shown in Figure 3.2.

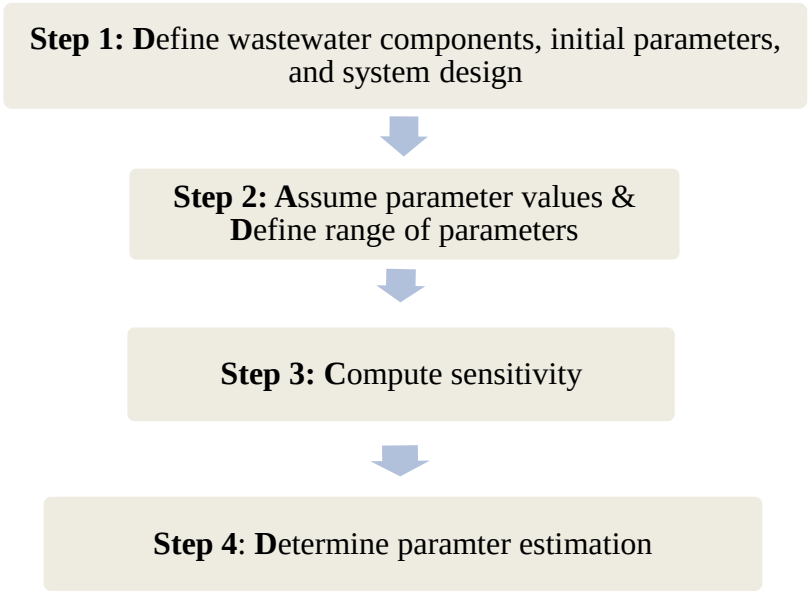

Figure 3.2 The procedures for schematic approach in studying the biological nutrient removal systems simulations.

Step 1: Calculate wastewater components, and initial parameters

The characterisation of wastewater components (influent parameters) and the calculation of initial parameters of wastewater treatment systems were based on author and previous work (Kampas, 2006). The wastewater composition, i.e. total chemical oxygen demand (TCOD), soluble chemical oxygen demand (SCOD), total Kjeldahl nitrogen (TKN) and phosphorus (P) were modeled using the calculational methods of ASM2 (Henze et al., 1995).

The system and the operating design for each condition of influent flow rate, reactor volumes, return sludge ratio, internal recirculation flow rate ratios, hydraulic retention time (HRT), solid retention time (SRT) and O_2 concentration were also obtained from reported results (Kampas, 2006). These are given in Table 3.7. In addition, the total HRT of anaerobic, anoxic and aerobic conditions, and SRT were 17 h and between 14-18 days, respectively. Reactor volumes for anaerobic, first anoxic, second anoxic and aerobic zones were 125, 120, 230 and 550 l, respectively. O_2 concentration was maintained between 2-4 mg l^{-1} in the aerobic zone and below 0.2 mg l^{-1} in anaerobic and anoxic zones. A return activated sludge ratio (R) of 0.85 (85% of the incoming flow) was used. An internal anoxic and aerobic recycle ratio was maintained at a value of 1 (100% of the incoming flow).

Results of the characterization of influent wastewater components are summarized in Table 3.8. They were investigated by taking one sample daily over a 70 day period by author. The concentrations of total chemical oxygen demand (TCOD), soluble COD (SCOD), biological oxygen demand (BOD), and volatile fatty acids (VFAs) were determined according to APHA Standard Methods (1998). The results showing influent wastewater characteristics, as well as P release in the anaerobic phase, and effluent conditions of the MUCT pilot scale biological phosphorus removal processes at steady state and operating at 17°C and at 23°C are shown in Table 3.9 and Table 3.10, respectively. The results conducted under condition having no disintegrated sludge (control) and with disintegrated sludge (test). The data in Table 3.9 and Table 3.10 were obtained from a previous Ph.D. study (Kampas, 2006). The experimental results at 17°C were used for calibration. Verification was based on the results at 23°C.

Table 3.7 The system design for pilot-scale biological nutrient removal (BNR) treatment plant (Kampas, 2006)

Flow rate	**Unit (l h^{-1})**	**Retention time**	**Unit (h)**
Influent	60	Anaerobic	2
Return activated sludge	51	First anoxic	2
Anoxic recycle	60	Second anoxic	3.8
Aerobic recycle	60	Aerobic	9.2

Table 3.8 Characterization of wastewater components obtained over a 70 day period

Date	**TCOD** (g COD/ m^3)	**SCOD** (g COD/ m^3)	**BOD_5** (g COD/ m^3)	**VFA** (g COD/ m^3)	**Date**	**TCOD** (g COD/ m^3)	**SCOD** (g COD/ m^3)	**BOD_5** (g COD/ m^3)
1	357.0	207.0	183.3	34.0	36	303.5	170.0	187.2
2	238.0	118.0	241.8	40.1	37	306.0	191.0	236.0
3	326.5	126.0	130.7	47.1	38	296.0	59.0	148.2
4	553.0	168.0	167.7	22.5	39	349.0	184.0	165.8
5	410.0	261.0	152.1	34.6	40	395.0	137.0	163.8
6	543.0	246.0	130.7	21.3	41		136.0	191.1
7	386.0	214.0	128.7	20.4	42	346.0	138.0	156.0
8	381.0	210.0	103.4	39.0	43	296.0	195.0	134.6
9	337.0	162.0	105.3	25.1	44	296.0	171.0	136.5
10	415.0	225.0	134.6	3.6	45	281.0	180.0	113.1
11	312.0	238.0	138.5	72.8	46	351.0	134.0	158.0
12	316.0	164.0	200.9	35.5	47	365.0	230.0	152.1
13	296.0	232.0	284.7	16.8	48	333.0		177.5
14	274.0	135.0	187.2	9.3	49	375.5		144.3
15	325.0	157.0	204.8	15.9	50	412.5		122.9
16	230.0	110.0	239.9	17.8	51	377.0		117.0
17	342.0	177.0	161.9	75.3	52	327.0		119.0
18	334.0	186.0	206.7	5.8	53	198.5		169.7
19	502.0	313.0	132.6	8.7	54	264.0		163.8
20	454.0	288.0	109.2	23.7	55	287.5		156.0
21	370.0	103.0	126.8	5.6	56	362.0		
22	314.0	109.0	138.5	48.2	57	285.0		
23	276.0	139.0	154.1	11.5	58	325.0		
24	197.0	62.0	195.0	53.1	59	300.5		
25		149.0	115.1	56.8	60	390.5		
26	249.0	205.0	169.7	37.7	61	281.5		
27	275.5	163.0	161.9	35.1	62	362.5		
28	380.0	180.0	122.9	36.1	63	301.0		
29	413.0	192.5	140.4	46.3	64	209.5		
30	348.0	186.0	208.7	38.1	65	182.0		
31	331.5	164.0	234.0	29.6	66	370.0		
32	430.0	162.0	202.8	29.2	67	391.0		
33	352.5	128.0	97.5		68	427.5		
34	386.0	159.0	136.5		69	194.0		
35	328.0	159.0	185.3		70	398.5		

T**able 3.9** Characterization of influent wastewater and experimental results under control (without DS) and test (with DS) conditions at 17°C

day[1]	Inf. TCOD g COD m^{-3}		Inf. SCOD g COD m^{-3}		Inf. TP g P m^{-3}		Inf. soluble P g P m^{-3}		Inf. TN[2] g N m^{-3}	Inf. NH_4[2] g N m^{-3}	Inf. TSS[2] g m^{-3}	P release g P m^{-3}		Eff. TP g P m^{-3}		Eff. NH_4 g N m^{-3}		Eff. NO_3 g N m^{-3}		MLSS g m^{-3}		Eff. COD g COD m^{-3}	
	Con	Test	Con.	Test	Con.	Test	Con.	Test				Con.	Test	Con.	Test	Con.	Test	Con.	Test	Con.	Test	Con	Test
1	282.67	315.09	124.09	138.22	7.09	8.56	5.29	6.51	58	36	89	12.3	14.5	4.2	4.9	0.05	0.05	14.1	13.7	2675	2860	58	50
2	381.67	414.09	157.83	171.96	7.29	8.66	5.49	6.63		33		14	15.4	4.9		0.07	0.06	13	12.6	2750	2810		
5	408.67	441.09	166.83	180.96	5.39	6.89	4.09	5.34	34	20.2	73	12	13.5	2.1			0.08	4	3.5	2705	2715	66	64
6	335.67	368.09	142.06	156.19	6.29	7.84	4.69	5.98		36.3		13.9	16.6	1.4	2.5	0.07	0.07	5.1	4.3	2705	2760		
7	395.67	428.09	162.55	176.68	7.59	9.19	5.69	7.02		40.2	104	13	14.2	1.9	2.6			9	8.2	2730	2930		
8	502.67	535.09	198.84	212.97	9.88	11.54	7.39	8.76		40.2				3	3.3	0.09	0.08	8.1	7.2	2790	3080		
9	376.67	409.09	155.97	170.1	8.39	10.08	6.29	7.69	61		102			2.9	2.9			7.6	5.9	2905	3110	48	70
12	386.67	419.09	159.37	173.5	5.49	7.31	4.09	5.6		29.7		13	13.6	2.3	2.2	0.07	0.05	5.9	5.5			70	66
13	326.67	359.09	138.9	153.03	6.09	7.96	4.59	6.14	62	41.3	91			3.1	4.2			10.3	9.3	2650	3010	70	46
14	336.67	369.09	142.41	156.54	7.59	9.5	5.69	7.28				13	15.3	3.1	4.2	0.09		15.6	14.4	2875	3170	74	66
15	392.67	425.09	161.4	175.53	7.09	9.05	5.29	6.92	59	37.8	101	12.5	12.4	3.2	3			15.1	14.2	2820	3090	66	70
16	416.67	449.09	169.54	183.67	7.49	9.49	5.59	7.25		29.2		12.7	12.9	4	4	0.09	0.1	7.7	9.4	2890	3180	78	72
19	358.67	391.09	149.87	164	7.89	10.03	5.89	7.67		36.1	102					0.09	0.09	8.3	9.2	2785	2895		
20	363.67	394.11	151.52	164.71	6.89	9.07	5.19	7				13.7	14.3	2.8	3.2	0.09	0.1	9.7	10.5	2775	3015		
21	342.67	376.71	144.44	159.33	6.29	8.52	4.69	6.54	50	29.3		15.3	15	3.1	3.3	0.09	0.09	10.4	11.1	2815	3105	52	60
22	420.67	453.09	170.9	185.03	7.29	9.56	5.49	7.38		33.1	108	13.2	13.4	3.2	3.4	0.1	0.08	9.6	10.5	2700	3025	68	66
23	356.67	389.09	149.19	163.32	6.89	9.21	5.19	7.11	56			13.9	15.4	2.7	2.8			10.8	9.4	2700	2760	74	66
25	326.67	359.09	138.9	153.03	6.09	8.5	4.59	6.59		24.8		13.7	13.2	2.8	2.9			11.8	10.1			72	76
26	386.67	419.09	159.4	173.53	7.39	9.84	5.59	7.63			124			2.7	2.3	0.09	0.07	10.7	7.2	2675	2930	58	50
27	363.67	396.09	151.52	165.65	6.89	9.39	5.19	7.26		37.6		13.8	14.9	2.8	3.1			12.9	9.9	2735	2885		
28	414.67	447.81	168.87	183.33	7.99	10.53	5.99	8.1	57	38.3		13.5	14.2	2.9	3.3	0.08	0.07	13.7	10.4	2660	2805	66	64
29	465.67	496.11	186.22	199.41	9.08	11.97	6.79	9.18				14.8	15.7	4.1		0.09	0.07	13.8	8.6	2685	2900		

[1] The sampling dates occurred after activated sludge wastewater systems reached steady state. [2]The experimental results under control and test conditions.

Table 3.10 Characterization of influent wastewater and experimental results under control (without DS) and test (with DS) conditions at 23°C

day[1]	Inf. TOD g COD m^{-3}		Inf. SCOD g COD m^{-3}		Inf. TP g P m^{-3}		Inf. soluble P g P m^{-3}		Inf. TN[2] g N m^{-3}	Inf. NH_4[2] g N m^{-3}	Inf. TSS[2] g m^{-3}	P release g P m^{-3}		MLSS g m^{-3}		Eff. TP g P m^{-3}		Eff. NH_4 g N m^{-3}		Eff. NO_3 g N m^{-3}		Eff. COD g COD m^{-3}	
	Con.	Test	Con.	Test	Con.	Test	Con.	Test				Con.	Test	Con.	Test	Con.	Test	Con.	Test	Con.	Test	Con.	Test
1	396.30	432.69	162.31	180.41	7.30	10.22	5.48	7.90		31.80	101	20.40	22.40	2750	2695	3.20	2.70	0.02	0.01	7.00	7.80	38	36
2	354.93	387.35	120.94	135.07	7.80	10.72	5.85	8.28	49.00	35.20													
3												17.20	19.20	2725	2590	2.00	1.90	0.01	0.01	8.10	7.40	40	50
4												17.50	22.60	2640	2725	2.30	2.50	0.04	0.03	8.50	8.70	38	40
5	396.30	452.56	162.31	200.27	8.20	10.92	6.15	8.41		40.50			20.00	2615	2850	3.40	4.20	0.03	0.04	10.90	11.60	38	48
6	451.93	468.45	217.94	216.17	8.00	10.99	6.00	8.48	60.00														
7	354.93	387.35	120.94	135.07	8.00	11.08	6.00	8.56															
8	354.93	387.35	120.94	135.07	7.50	10.68	5.63	8.26															
9	358.55	428.72	124.56	176.43	7.30	10.57	5.48	8.19		39.30	119	16.60	20.80	2540	2400	4.30	4.60	0.04	0.05	13.80	12.40	50	40
10	441.99	428.72	208.00	176.43	8.40	11.76	6.30	9.09	62.00	38.50	111	16.70	20.30	2540	2285	4.90	3.50	0.02	0.03	14.60	12.70	58	50
11												15.90	20.70	2405	2440								
13	356.57	484.35	122.58	232.06	6.60	10.22	4.95	7.95			117												
14	370.47	390.97	136.48	138.69	5.50	9.21	4.13	7.20															
15	372.46	474.41	138.47	222.13	6.70	10.51	5.03	8.18		29.50	100	16.90	23.00	2370	2640	4.30	3.50	0.03	0.04	12.70	12.60	40	60
16	475.77	388.99	241.78	136.70	7.20	11.09	5.40	8.63	49.00			17.40	20.90	2265	2770	4.20	4.50	0.02	0.03	7.20	5.40	64	62
19	354.93	387.35	120.94	135.07	7.20	11.19	5.40	8.71		30.90	103	15.50	19.60	2210	2760	2.80	2.90	0.03	0.03			56	60
20	354.93	385.37	120.94	134.13	7.60	11.86	5.70	9.23	53.00														
21	354.93	388.97	120.94	135.83	8.30	12.64	6.23	9.83															
22	398.29	402.89	164.30	150.61	7.90	12.33	5.93	9.60		29.80	107	14.80	23.00	2235	2655	0.90	1.50	0.04	0.04	8.30	7.10	58	60
23	346.63	404.88	112.64	152.59	7.40	11.92	5.55	9.31	50.00							0.70	1.30	0.04	0.03	4.80	4.20	56	66
24												17.10	22.70	2365	2760	0.90	2.60	0.02	0.01	6.40	5.80	64	62
25	372.46	508.19	138.47	255.90	7.20	11.81	5.40	9.23		33.70		19.20	22.70	2465	2965	0.80	3.10			6.60	6.00	52	62
26	398.29	430.71	164.30	178.42	7.50	12.29	5.63	9.60	56.00	33.30	86	17.70	22.60	2525	3025	0.90	2.20	0.01	0.01	6.60	5.70	62	64
27	354.93	387.35	120.94	135.07	8.20	13.08	6.15	10.20	58.00									0.04	0.03			38	36
28	354.93	388.07	120.94	135.40	8.30	13.27	6.23	10.35	58.00	30.60								0.03	0.04				
29	354.93	385.37	120.94	134.13	8.30	13.37	6.23	10.43	52.00	26.90	98	16.50	22.30	2625	2870	0.60	2.60			5.30	4.30	40	50
30	346.63	382.48	112.64	127.53	8.80	14.53	6.60	11.36	57.00	30.20	83					3.20	2.70			6.90	5.40	38	40

[1] The sampling dates occurred after activated sludge wastewater systems reached steady state. [2]The experimental results under control and test conditions.

Step 2: Assume the values of stoichiometric and kinetic parameters, and define the range of parameters.

A priori values of the stoichiometric and kinetic coefficients were found and set as default values. These parameter values were obtained from published literature (Henze et al., 1999). The range of parameters defined the minimum and maximum values of the stoichiometric and kinetic parameters. The minimum and maximum values for these parameters are given in Table 3.11.

Table 3.11 Default, minimum and maximum values for parameters used in ASM2d.

Symbol	Definition	Default	Min.	Max.	Units	Reference
Y_H	Yield coefficient	0.625			g COD/g COD	3
F_{XI}	Fraction of inert COD generated in biomass	0.10			g COD/g COD	3
Y_{PO4}	Poly-phosphate (PP) requirement (PO_4 per poly-hydroxy-alkanoates (PHA)	0.40	0.26	0.46	g P/g COD	3,4,5,7,8,10,11
Y_{PAO}	Yield coefficient (Biomass/PHA)	0.625	0.58	0.9	g COD/g COD	3,5,7
Y_{PHA}	PHA requirement for PP storage	0.20	0.20	0.32	g COD/g P	3
Y_A	Yield coefficient (Biomass/Nitrate)	0.24			g COD/g N	3
q_{PHA}	Rate constant for storage of X_{PHA}	3.00	0.36	9.03	g X_{PHA}/g	1,2,3,4,5,7,8,10,11
q_{PP}	Rate constant for storage of X_{PP}	1.50	1	10.88	g X_{PP}/g X_{PAO}/d	3,4,5,7,8,10,11
μ_{PAO}	Maximum growth rate of PAOs	1.00	0.67	2.97	d^{-1}	2,3,4,7,8,10,11
η_{NO3}	Reduction factor for anoxic activity	0.60	0.44	0.60		3,10
b_{PAO}	Rate for Lysis of X_{PAO}	0.20	0.04	0.27	d^{-1}	2,3,4,5,6,7,8,10
b_{PP}	Rate for Lysis of X_{PP}	0.20	0.03	0.20	d^{-1}	3,5,7,10
b_{PHA}	Rate for Lysis of X_{PHA}	0.20	0.08	0.20	d^{-1}	3,7
K_{O2}	Saturation/inhibition coefficient for	0.20	0.20	0.20	g O_2/m^3	3,7
K_{NO3}	Saturation coefficient for nitrate, S_{NO3}	0.50	0.50	0.50	g N/m^3	1,3,4,7,8,10
K_A	Saturation coefficient for acetate, S_A	4.00	1	32	g COD/m^3	3,5,7,10
K_{NH4}	Saturation coefficient for ammonium	0.05	0.01	0.05	g N/m^3	3,7,11
K_{PS}	Saturation coefficient for P in storage of	0.20	0.20	0.50	g P/m^3	3,5,7
K_P	Saturation coefficient for phosphate	0.01	0.01	3	g P/m^3	1,3,6,7
K_{ALK}	Saturation coefficient for alkalinity	0.10	0.02	0.10	mole	3,7,9
K_{MAX}	Maximum ratio of X_{PP}/X_{PAO}	0.34	0.152	0.37	g X_{PP}/g X_{PAO}	3,4,7,8,10
K_{PP}	Saturation coefficient for poly-	0.01	0.01	0.26	g X_{PP}/g X_{PAO}	1,3,7
K_{IPP}	Inhibition coefficient for PP storage	0.02	0.001	0.48	g X_{PP}/g X_{PAO}	3,4,7,8,10
K_{PHA}	Saturation coefficient for PHA	0.01	0.001	0.01	g X_{PHA}/g	2,3,4,7,8,10
$K_{O2\ AUT}$	Saturation coefficient for oxygen	0.5	0.1	1	g O_2/m^3	3,5
$K_{NH4\ AUT}$	Saturation coefficient for ammonium	1.00	0.3		g N/m^3	3,5

(1) Smolders et al. (1995), (2) Barker and Dold (1997), (3) Henze et al. (1999), (4) Penya-Roja et al. (2002), (5) Dudley et al. (2002), (6) Lopez and Morgenroth (2003), (7) Manga et al. (2003), (8) Ferrer et al. (2004), (9) Schuler (2005), (10) García-Usach et al. (2006), (11) Insel et al. (2006)

Step 3: Compute sensitivity

Sensitivity analysis is a technique for the selection of identifiable model parameter subsets and reducing the number of parameters to be used in modeling. The following sensitivity functions were used to compute the absolute, relative and mixed sensitivity in the Aquasim programme (Reichert, 1994).

$$\delta_{f,p}^{a,a} = \frac{\partial f}{\partial p} \tag{3.13}$$

$$\delta_{f,p}^{r,a} = \frac{1}{f}\frac{\partial f}{\partial p} \tag{3.14}$$

$$\delta_{f,p}^{a,r} = p\frac{\partial f}{\partial p} \tag{3.15}$$

$$\delta_{f,p}^{r,r} = \frac{p}{f}\frac{\partial f}{\partial p} \tag{3.16}$$

In the above functions, f refers to an arbitrary parameter value calculated by Aquasim. The variable, p, is a model parameter that is defined as having a constant value or is a real list variable. The absolute-absolute sensitivity function (3.13) is the absolute change in f per unit of change in p. The relative-absolute sensitivity function (3.14) is the relative change in f per unit of change in p. The absolute-relative sensitivity function (3.15) is the absolute change in f for a 100% change in p. The relative-relative sensitivity function (3.16) is the relative change in f for a 100% change in p. The absolute-relative sensitivity function (3.15) and the relative-relative sensitivity function (3.16) are the most useful because their units do not depend on parameter units. Sensitivity functions with larger values are more accurate identifiability parameters. The sensitivity helps in assessing the identifiability of model parameters. The identifiability analysis is used to check that model parameters can be uniquely determined with the aid of the available data and to calculate the uncertainty of the parameter estimates (Reichert, 1994).

Sensitivity analysis provides a ranking of the significant parameters that influence outputs. The relative sensitivity of an output i (y_i) as a function of an input parameter j (θ_j) is expressed as (Reichert and Vanrolleghem, 2001),

$$s_{i,j} = \frac{\theta_j}{y_i}\frac{\partial y_i}{\partial \theta_j} \tag{3.17}$$

The utilization of algebraic sensitivity analysis was used instead because its numerical value of sensitivity is valid only for a particular change in a specific value of θ_j (Norton, 2008). In contrast, the former produces algebraic relations. Numerical values of sensitivity provide much less information than algebraic relation. However, algebraic sensitivity is not as reliable if the model contains complicated equations such as the ASM2d model. As a result, a finite difference method was used to numerically determination the derivatives of Equation 3.17. A perturbation factor (the central difference approach) with a value of 10^{-4} (0.01%) was chosen for use in the sensitivity analysis of each parameter tested and set to the default ASM2d value. Using this perturbation factor value produced equal derivatives with forward and backward finite differences. Absolute values of individual sensitivities were present and contribute to the overall sensitivity of parameter.

Justifying prior uncertainty of model parameters is subject to critical judgment and experience using the simulation and its mathematical equations (Brun et al., 2002). Prior parameter uncertainty is a significant assessment for the calibration analysis. The modeling parameters were grouped into three classes of relative uncertainty. These are class 1 relative uncertainty 5% (accurately known parameter), class 2, relative uncertainty 20% (moderate accuracy of known parameters) and class 3, relative uncertainty 50% (very poorly known parameters) (Brun et al., 2002). Every modeling parameter was assigned to one of these classes. The prior uncertainty of kinetic parameters was classified into class 3 and a few parameters into class 2. The prior uncertainty of stoichiometric parameters was classified into class 1 except Y_{Hanox} and Y_{PAOanox}.

Step 4: Determine parameter estimation

The objective function of parameter estimation is based upon the predicted accuracy of measurements. The parameter estimation is calculated by minimizing the sum of squares of weighted deviations (SSWD) between measurement and calculation. Whereas $f_i(p)$ represents the variable obtained from the model calculation at a given time and location in a compartment of a parameter $p = (p_1,\ldots\ldots p_m)$ and $f_{meas,i}$ and $\boldsymbol{\sigma}_{meas,i}$ are values and standard deviation of real list variables.

$$x^2(p)=\sum_{i=1}^{n}\left(\frac{f_{meas,i}-f_i(p)}{\sigma_{meas,i}}\right)^2 \tag{3.18}$$

Additionally, Standard Error of Estimate (SEE) was also used to assess the accuracy of predictions (Equation 3.19). SEE is defined below (Irwin, 1949):

$$x(p) = \sqrt{\frac{\sum\left(f_{mea,i}-f_i(p)\right)^2}{N}} \tag{3.19}$$

Whereas $f_i(p)$ is the variable obtained from the model calculation at a given time and location of a parameter p, while $f_{meas,i}$ and N are values and degrees of freedom of real list variables.

This mathematical analysis is an optimization method because it can predict goodness of model fit to experiment data (Equation 3.18). It also determines error between prediction and model values (Equation 3.19).

Other researchers proposed minimization of the weighted residual sum of squares (WRSS) (Equation 3.20) to perform the parameter subset estimations (Brun et al., 2002).

$$WRSS = (Y - \eta(\theta))^T W(Y - \eta(\theta)) \tag{3.20}$$

Here, $\theta = [\theta_K, \theta_K]^T$ is the parameter vector with θ_K being a partition of θ consisting of all parameters included in K. W = diag$(1/sc_1^2, \ldots, 1/sc_n^2)$ is a diagonal matrix of weights with sc_i.

The termination criterion for calibration is to test model fit against experiment data as a measure of goodness of fit. This was done with a 95% confidence level. Model fitting was done by minimizing the sum of squares of weighted deviations (SSWD) between measured and calculated values (Equation 3.18).

Uncertainty of parameter estimations comes from range of applicability of the protocols, technical limitations of tools/sensors for data collection, design of data collection, and limited data versus complex model structure.

The proposed methodology of reducing parameter subsets in ASMs calibration involved the 2 significant methods: (1) sensitivity analysis, and (2) manual calibration. The sensitivity analysis identified the most influential parameters affecting model outputs, ranking their influence. Parameter sensitivity analysis is related to experiment data. The sensitivity analysis followed the method presented by Brun et al. (2001). An advantage of this sensitivity analysis is that it provides particular parameter significant rankings based upon specific information. Manual calibration is used for parameter selection using the available data. The iteration process in parameter selection does not require high computational demand, as did the identifiability approach proposed by Brun et al. (2002). It is a simplified method. This method applied an experience-based approach coupled with an identifiability approach. It avoids the requirement of prior knowledge on WWTPs and complex mathematical calculation necessitated by the experience-based approach and identifiability approach, respectively.

3.9 VERIFICATION

Verification is a method to determine whether the model is acceptable (Reckhow and Chapra, 1983). One indicator of verification is if the model can approach specified performance requirements (Rykiel, 1996). This method is based on the goodness-of-fit properties of models as a basis for judging the model suitability. This helps the user to gain confidence in using results of modeling (Power, 1993). By increasing the number of successful verification tests, one increases the degree of usefulness for the model (Omlin et al., 2001).

A predictive verification technique is a process of cross-verification, sometimes called confirmation or corroboration (Reckhow and Chapra, 1983). This is a useful method for verification models by using only subsets of all available data for calibration and testing with the rest of data (Omlin et al., 2001).

CHAPTER 4:

A CALIBRATION APPROACH TOWARDS REDUCING ASM2D PARAMETER SUBSETS IN THE PHOSPHORUS REMOVAL PROCESSES

CHAPTER 4. A CALIBRATION APPROACH TOWARDS REDUCING ASM2D PARAMETER SUBSETS IN THE PHOSPHORUS REMOVAL PROCESSES

ABSTRACT

A novel calibration approach that aims to reduce ASM2d parameter subsets and decrease the model complexity is presented. This approach does not require high computational demand and reduces the number of modeling parameters required to achieve the ASMs calibration by employing a sensitivity and iteration methodology. Parameter sensitivity is a crucial factor and the iteration methodology enables refinement of the simulation parameter values. When completing the iteration process, parameters values are determined in descending order of their sensitivities. The number of iterations required is equal to the number of model parameters of the parameter significance ranking. This approach was used for the ASM2d model to the evaluated EBPR phosphorus removal and it was successful. The results of the simulation provide calibration parameters. These included Y_{PAO}, Y_{PO4}, Y_{PHA}, q_{PHA}, q_{PP}, μ_{PAO}, b_{PAO}, b_{PP}, b_{PHA}, K_{PS}, Y_A, μ_{AUT}, b_{AUT}, $K_{O2\ AUT}$, and $K_{NH4\ AUT}$. Those parameters corresponded to the experimental data available.

Keywords: ASM2d, iteration methodology, calibration approach, sensitivity, phosphorous removal

4.1 INTRODUCTION

Activated sludge models (ASMs) have been used to understand microorganism mechanisms in activated sludge processes in order to design, upgrade or optimize various wastewater treatment plants (WWTPs) (Henze et al., 2000; Ruano et al., 2007). To study carbon, nitrogen and phosphorous removal, Activated Sludge Model No. 2d (ASM2d) is an essential model because it simulates the dynamics of biological mechanisms in enhanced biological phosphorus removal (EBPR) systems (Henze et al., 1999). ASM2d can explain phosphorus utilization by phosphorus accumulating organisms (PAOs) under aerobic conditions as well as denitrification mechanisms of PAOs. In contrast, Activated Sludge Model No. 2 (ASM2) can describe phosphorus uptake mechanisms under aerobic conditions only. However, the ASM2d model is complicated to calibrate. This is due to a requirement for a large number of model parameters. These are most often derived from the information content of particular wastewater treatment plants (WWTPs) (Brun et al., 2001; Brun et al., 2002; Machado et al., 2009).

The Modified University of Cape Town (MUCT) processes have been widely used in activated sludge WWTPs for prevention of eutrophication (Mino et al., 1998; Seviour et al., 2003; Soejima et al., 2008). Also, the MUCT processes are among the most effective for EBPR. This is due their design's capability to maintain truly anaerobic conditions for EBPR (Hamada et al., 2006; Vaiopoulou and Aivasidis, 2008). Other researchers (Ruano et al., 2007) reported that the model is over-parameterized due to the paucity of experimental observations. Therefore, reduction in the number of parameters that are required for calibration would make the model more user friendly, but doing so is challenging. Currently, there are two calibration approaches to reduce the number of required parameters. They are (1) the identifiability approach, and, (2) the experience-based approach. Mathematical analysis is used for identifiability determination. That is to say, there is an ordered determination of the magnitude of influence for each model parameter. It is based on sensitivity analysis as the priority step. The result is the parameter significance ranking, based upon local sensitivity analysis. It is followed by determination

of the identifiability parameter subsets. These results change from one modeling study to another. Thus, the identifiability approach generates the particular parameter subset specific for the information content of the data (Ruano et al., 2007). It is largely influenced by particular WWTPs configurations and their operation. It suffers from large computation demands during analysis. There are two techniques used in to do calculations in the identifiability method when using the activated sludge model. The first method is done by calculating the Fisher Information Matrix (FIM). FIM properties of D and mod-E criteria are used to find an identifiable parameter subset among numerous combinations when determining the identifiability of the ASM1 model (Weijers and Vanrolleghem, 1997). The D and Mod-E criteria are related to the parameter estimation accuracy and parameter correlation of a particular set of measurements (Dochain and Vanrolleghem, 2001). The D-criterion indicates the information content of the experiment. It is based on the determinant of the FIM. Conversely, the Mod-E criterion is based upon the ratio of the maximum to minimum eigenvalues of the FIM. It provides the parameter correlation. This approach was also successfully applied in other kinetic models (Reichert and Vanrolleghem, 2001; Checchi and Marsili-Libelli, 2005; Marsili-Libelli and Giusti, 2008). The identifiability approach is applied using diagnostic regression on the collinearity index (γ) and determinant measure (ρ). It calculates a parameter subset with negligible near-linear dependency. It was developed by Brun et al. (2002) for ASM2d calibration based on full-scale plant data by applying sensitivity analysis and subsequently iterating its parameter subset. The γ index is used to obtain the potential identifiability measure of a given parameter subset from all possible combinations, The parameter, ρ, is a relative measure suited for comparison of the parameter identifiability for different parameter subsets (Machado et al., 2009). Uncertainty analysis is included in the identifiability procedure. It is defined prior to making a selection of model parameters that will be used. The identifiability approach requires high levels of computer resources and performance. It relies on parameter significance values (Weijers and Vanrolleghem, 1997; Brun et al., 2001; Brun et al., 2002; Machado et al., 2009). Choices are made by the user including selection of simultaneous or sequential estimation when performing parameter estimation.

Parameter values obtained in this manner may be biased and depend upon the procedure used. Thus, they might not have the physical meaning originally thought. Additionally, errors may arise in the calibrated model if the resulting parameters are not carefully interpreted. Consequently, it is important to understand the identifiability properties of the model and to develop calibration procedures which consider with these properties (Weijers and Vanrolleghem, 1997). Its use is not practical. An application of process knowledge in combination with parameter significance ranking might be able to reduce parameter subset size. Alternatively, consideration of sensitivity analysis, identifying the most influential parameters in the model may be used to resolve this issue. Among researchers doing calibration using the identifiability approach, procedural differences exist. As a result, the experience-based approach is commonly used.

The experience-based approach requires process knowledge of particular activated sludge unit operations to derive model parameters (Melcer et al., 2003; Vanrolleghem et al., 2003; Sin et al., 2005; García-Usach et al. 2006). This approach makes use of the large amount of experience gained from studies of activated sludge wastewater treatment processes (Ruano et al., 2007). In using the experience-based approach for this study, values for process parameters were obtained from literature published by other researchers. The experience-based approach, employed by many protocols, proposes a fixed parameter set to be used for calibration. The analysis of these sets used in the Haaren model showed that this approach may have two consequences. The first problem with some protocols is that they considered optimistically large parameter sets that were poorly identifiable (García-Usach et al., 2006; Insel et al., 2006; Makinia et al., 2006). The second issue seen in other protocols is that were too conservative, calibrating fewer parameters than were identifiable (Melcer et al., 2003; Ruano et al., 2007). This causes waste of information. In practice, it is observed that the experience-based approaches were predominantly used, e.g., the HSG (Langergraber et al., 2004), WERF (Melcer et al., 2003), BIOMATH (Vanrolleghem et al., 2003), and STOWA (Hulsbeek et al., 2002) protocols. Experience-based methodology was applied to model calibration of nutrient-removing laboratory-scale SBRs under limited aeration (Insel

et al., 2006). The modified ASM2d was proposed by adding an organic nitrogen module incorporating a hydrolysis mechanism. The measurement of influent wastewater and other parameters, i.e., NH_4, O_2, MLVSS, NO_3, and PO_4 in each phase, were calibrated in order to observe simultaneous biological reactions. Model calibration performed to elucidate contributions of different processes to overall oxygen, nitrogen and phosphorus transformation. Other researchers calibrated the ASM2d model using the experience-based approach with parameters observed in biological nutrient removal pilot plants (García-Usach et al., 2006). The calibration methodology is given by Penya-Roja et al. (2002). They studied the influence of temperature on phosphorus accumulating organisms (PAOs). The parameters studied consisted of oxygen uptake rate (OUR), NH_4, BOD, COD, O_2, MLSS, MLVSS, NO_3, PO_4 concentrations as well as alkalinity in different reactors. Additionally, Ferrer et al. (2004) used the experience-based approach following the calibration methodology of Penya-Roja et al. (2002). The parameters required for application of the ASM2d model to full scale biological nitrogen and phosphorus removal plants were determined. They were TSS, VSS, NH_4, O_2, MLSS, MLVSS, NO_3, and PO_4 concentrations in influent and effluent of wastewater. Oxygen uptake rate (OUR) was continuously recorded for the calibration. The results obtained from plants' performance data enabled improvement in estimation of calibrated parameters thereby improving prediction of WWTP behavior.

The BIOMATH protocol is a methodology for calibration of the activated sludge plant models. It was proposed by Vanrolleghem et al. (2003). An application of this methodology was used measuring the following influent and effluent wastewater parameters in a nutrient removing oxidation ditch system: COD, TKN, NH_4, NO_3 and PO_4 concentrations. In addition the respirometric test was used to provide information about inert fractions. Furthermore, OUR profiles were examined in batch reactors to estimate Monod kinetics (Penya-Roja et al., 2002). Other protocols, HSG, WERF, and STOWA, also used similar parameters to calibrate ASMs models (Langergraber et al., 2004; Melcer et al., 2003; Hulsbeek et al., 2002). This experience-based approach used process

engineering knowledge in combination with cumulative experience in each of the particular studies. As a result, its application has so far been limited to general calibration. Both approaches are feasible methods to successfully attain modeling calibration. Each achieves values for the necessary stoichiometric and kinetic parameters and satisfies the simulation. The identifiability approach has the disadvantage of high computational demands for large data subset sizes (Ruano et al., 2007). The experience-based approach poses difficulty in choosing modeling parameters according to knowledge and experience with particular activated sludge WWTPs under study. This study is unique in that it employs both methods, rather than just one.

Regarding the limitations of the two calibration approaches discussed above, a new methodology is purposed in the current study. There are two important considerations needed to completely develop model calibration. These are (1) sensitivity analysis and (2) iteration in the calibration methodology. The sensitivity calculation produces a parameter significance ranking which is used to reduce the number of iterations required. It further represents the influence of model parameters on the simulation output (Weijers and Vanrolleghem, 1997; Brun et al., 2001; Brun et al., 2002; Machado et al., 2009). Then using the parameter significance ranking, the calibrated parameters are determined iteratively.

The purpose of this research is to present a methodology using the calibration approach. The goal was to avoid both high calculation demands and the requirement for a priori knowledge of all the parameters specific to the activated sludge treatment works. This new method was developed using the identifiability approach and the experience-based approach. The sensitivity method was used to reduce the number of model parameters. Parameter sensitivity was used to identify those parameters which most affect the model. Additionally, the model was calibrated using an iterative process. High computational demand was avoided by reducing the size of ASM2d parameter subset. Four procedures were structured in this new approach. First, the analysis of the wastewater characterization

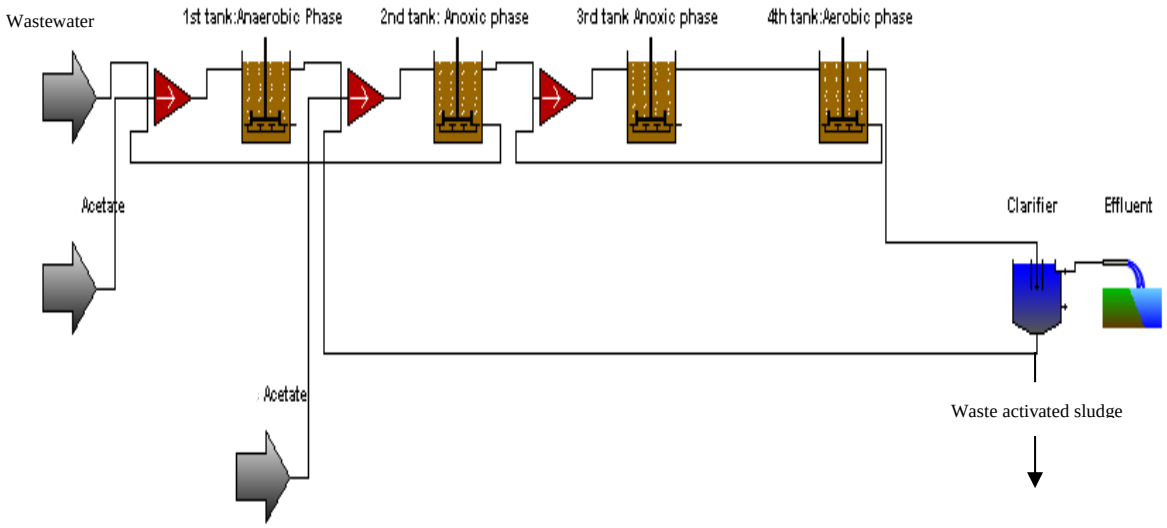

Figure 4.1 A schematic diagram of the activated sludge MUCT

and layout of the specific wastewater treatment plant were established. Second, initial default values of ASM2d parameters were defined. Demonstration of the range of values for stoichiometric and kinetic parameters was obtained from the literature. Third, analysis of the sensitivity of the ASM2d parameters was done using the experimental results of an activated sludge on a pilot-scale process to obtain the parameter significance ranking. Finally, model parameter values were refined by iteratively fitting them to the observed experimental results. This was done sequentially starting with the most significant parameter, continuing with subsequent parameters in order of decreasing impact upon the model.

4.2 MATERIALS AND METHODS

4.2.1 The MUCT pilot scale of EBPR processes

The results of the modeling calibration were determined experimentally using the MUCT pilot scale processes operated in the pilot hall facilities of the sewage treatment works of Cranfield University, UK. This pilot scale process (Figure 4.1) consisted of five reactors in

series. They included anaerobic, 1st anoxic, 2nd anoxic, aerobic phase and clarifier stages with effective volumes 0.125 m^3, 0.120 m^3, 0.230 m^3, 0.550 m^3 and 0.334 m^3, respectively. The solid retention time (SRT) was 15 days. The operating conditions of this system were: influent wastewater flow rate (Q_{IN} = 0.06 m^3 h^{-1}), return activated sludge flow rate (Q_R = 0.051 m^3 h^{-1}), anoxic recirculation flow rate (Q_1 = 0.06 m^3 h^{-1}) and aerobic recirculation flow rate (Q_2 = 0.06 m^3 h^{-1}). In order to develop EBPR processes, acetic acid was fed to influent. In order to develop EBPR, acetate was fed in the influent at an equivalent level (42.60 g COD m^{-3}) (acetate concentrations in municipal wastewater were not high enough to enable EBPR). In addition, acetate was added to anoxic phase in order to maintain it's influent concentration of anoxic reactor at 21.30 g COD m^{-3}. The ASM2d model fermentation, the fermentation products, and S_A, were modeled separately from other soluble organic materials (Henze et al., 1999). For all stoichiometric computations, it was assumed that S_A is equal to acetate as a simple carbon form. In reality a whole range of other fermentation products is possible (Henze et al., 1999). The two most common VFAs present in septic domestic wastewater are acetate and propionate (Pijuan et al., 2004). Calculations in most mechanistic models for EBPR represent VFAs as acetate. Acetate as a sole carbon sources is transformed primarily to poly-hydroxybutyrate (PHB). The majority of EBPR studies have been done using acetate as a carbon source or acetate in combination with other substrates (Pijuan et al., 2004). Other researchers reported that using acetate or ethanol as the sole carbon source resulted in PHB formation. These studies considered the effect of different carbon sources on aerobic storage in activated sludge (Beccari et al., 2002). Additionally, influent glutamic acid showed no appreciable formation of storage compounds using the ASM3 model. Lu et al. (2006) reported that alternating the sole carbon source in the feed between acetate and propionate was done to obtain highly enriched cultures of *Candidatus* Accumulibacter Phosphatis. These are considered to be PAOs of prime importance in EBPR systems. Tykesson et al. (2002) also used acetate as a sole carbon source for calibration of the ASM2d model to observe phosphorus release in batch tests for modeling an EBPR plant. Moreover, other researchers used acetate to prevent accumulation of phosphorus in EBPR systems. Using this approach, internal carbon

storage compounds, i.e., PHA, could be maintained at a high level (Krühne et al., 2003). The experimental samples were observed on a daily basis for the influent, anaerobic and aerobic stages as well as for the effluent. Average process temperature during steady state was maintained at 17°C. The sets of experiments, conducted at 17°C, were done over a one month period after operating AS systems at steady state for three months. The process was fed with municipal wastewater. The following influent parameters were determined: TCOD, SCOD, VFAs, S_F, TP, sol. P, TN, NH_4, and TSS concentrations. These parameters are required for application of ASM2d model to EBPR pilot scale wastewater treatment processes. Additionally, MLSS under aerobic conditions, P under anaerobic conditions, as well as effluent NH_4 and TP concentrations were determined.

4.2.2 Sensitivity analysis

The relative importance of parameters over the range of model inputs was calculated to evaluate the kinetic and stoichiometric parameters. This determined the parameters that most affected the effluent. Local sensitivity analysis was used to calculate the partial derivative of a specific set of parameter values. Finite difference approximation is the simplest way to calculate local sensitivities. The partial derivative can be mathematically formulated as follows:

$$\frac{\partial y_i}{\partial \theta_j} = \lim_{\Delta\theta_j \to 0} \frac{y_i(t, \theta_j + \Delta\theta_j) - y_i(t, \theta_j)}{\Delta\theta_j} \tag{4.1}$$

This equation is only valid if perturbation of the parameters is considered (De Pauw and Vanrolleghem, 2006). An application of the finite difference method uses the nominal value of the parameter $y_i(t, \theta_j)$ and p solutions of equations using perturbed parameters $y_i(t, \theta_j + \Delta\theta_j)$. Only one parameter is perturbed at a time while all others are kept at their nominal value. Sensitivity analysis results in an ordered ranking of parameters based upon

the magnitude of their influence on the model by using the absolute-relative sensitivity function (Soejima et al., 2008). The data used for the sensitivity analysis included values for total chemical oxygen demand (TCOD), total nitrogen (TN), total phosphorus (TP), phosphorus (P), total suspended solid (TS), mixed liquor suspended solid (MLSS), ammonium (NH_4), and nitrate (NO_3). The sensitivity calculations were implemented in relation to the following dimensional functions:

$$s_{i,j} = \frac{\Delta\theta_j}{sc_i}\frac{\partial y_i}{\partial\theta_j}, \quad \tilde{s}_{i,j} = \frac{s_{i,j}}{\sqrt{\sum_{k=1}^{n} s^2{}_{k,j}}} \tag{4.2}$$

The matrices $S = (s_{i,j})$ and $\tilde{S} = (\tilde{s}_{i,j})$, and the column vectors

$$s_j = (s_{i,j}, \dots, s_{n,j})^T \text{ and } \tilde{s}_j = (\tilde{s}_{i,j}, \dots, \tilde{s}_{n,j})^T$$

where $\partial y_i/\partial\theta_j$ is the absolute sensitivity of the model output y to the parameter θ_j at a particular time. The matrices, S and $\tilde{S}$, contain values of the various sensitive parameters. A finite difference method was used to approximate the absolute sensitivity value, in which the significant limitation of this method is that it is only valid for a small change in the parameter considered (Ruano et al., 2007). The vectors $\tilde{s}_j$ are defined as normalization: $\tilde{s}_j = s_j/\|\tilde{s}_j\|$. The $\Delta\theta_j$ value is the uncertainty range of the parameter θ_j according to prior knowledge which is classified into three uncertainty classes and sc_i is a characteristic scale of the variable y_i (Brun et al., 2002). Aquasim (Reichert, 1994) and interface UNSIM (Reichert, 2006), are computer programs designed for simulation and data analysis of aquatic systems. They were used to perform the sensitivity analysis. In the current study, sensitivity analysis followed the methodology of Brun et al. (2002). Reichert (1994) proposed using a difference methodology in calculating sensitivity. This sensitivity methodology can assess the identifiability of model parameters. The equations of the sensitivity analysis are presented as Equations 3.13 – 3.16. The uncertainty is estimated

using a linear estimation of the standard deviation, σ_f, of variables of interest, f. It is calculated using the following equation:

$$\sigma_f = \sqrt{\sum_i \left(\frac{\partial f}{\partial p_i}\right)^2 {\sigma_{pi}}^2} \tag{4.3}$$

$$\delta_{f,pi}^{err} = \frac{\partial f}{\partial p_i}\ \sigma_{pi}$$

Here p_i is the parameter and σ_{pi} its standard deviation. Hence, this uncertainty methodology is used to mathematically calculate the desired values. Uncertainty calculations were not done for the significant parameters. Sensitivity analysis was produced using the algebraic relations expressed as Equations 3.13 – 3.16. In contrast, Brun et al. (2002) identified the uncertainty of stoichiometric and kinetic parameters based on experience gained from experimental modeling. This was a difficult task. It requires much experience and deep knowledge of the mathematical models used. However, a proper assessment of prior parameter uncertainty is by far more delicate for the subsequent steps of the analysis. It is grouped into 3 classes based upon expert knowledge. In this method, class 3 consists of kinetic parameters which are very poorly known (class 3). Stoichiometric parameters are typically known (class 1), while conversion factors are placed into classes 2 and 3. Uncertainty values of 0.05, 0.2 and 0.5 are assigned to classes 1, 2 and 3, respectively. They are subsequently used in the sensitivity analysis (Equation 4.2). The resulting numerical sensitivity values were applied for particular changes in specific values (Norton, 2008).

4.2.3 Iteration methodology in the new calibration approach

Using all possible stoichiometric and kinetic parameters values in model would prevent calibration accuracy (Libelli et al., 2001). Such calculations would require a very long time, i.e., several days. Additionally, round off and truncation errors may be introduced and grow during the calculations. Our approach, therefore, employed the used of parameter subsets. Some parameters had to be categorized by the iteration tool into specific groups. These included nitrification, phosphorus removal and others, based on the available experimental data. Sensitivity parameter functions were used in the implementation iteration with GPS-X (Hydromantis, Inc., Hamilton, Canada). The procedures for that iteration calibration are shown in Figure 4.2. The number of stoichiometric and kinetic parameters used for ASMs' calibration was based on the sensitivity analyses. To demonstrate the significant parameters, ones with the root mean squared (RMS) values higher than 0 were considered.

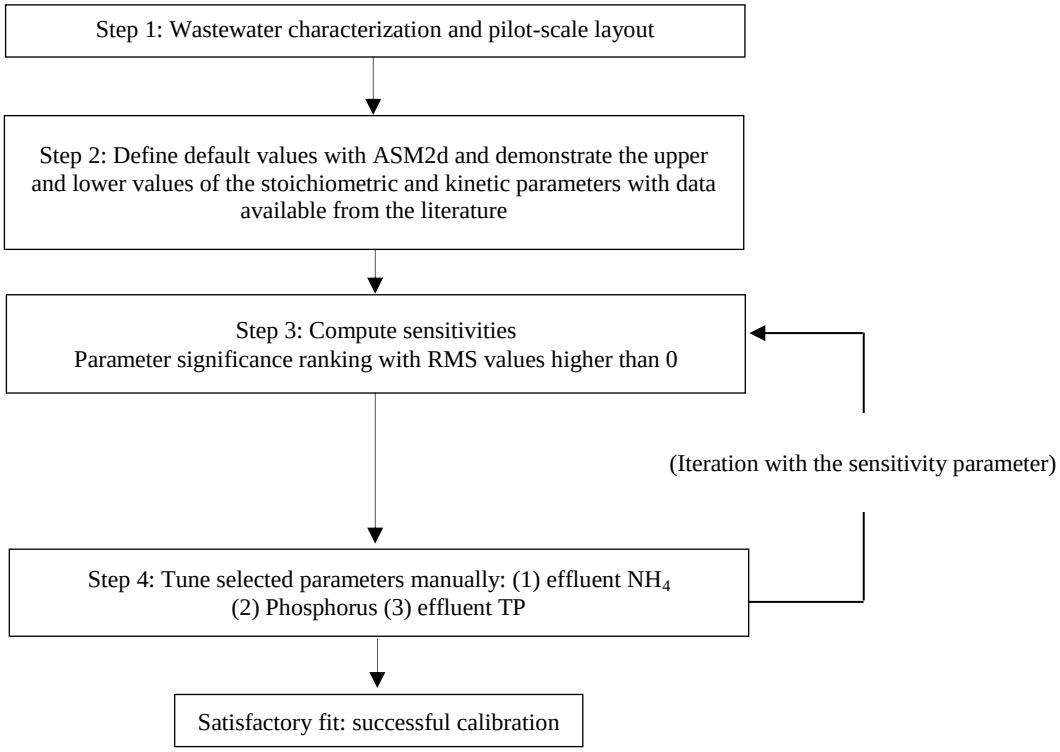

Figure 4.2 Procedure for selecting ASM2d parameter subsets

These parameters were used for model calibration. The parameters used to calibrate each experiment consisted of 30 important parameters. Manually, the parameters with the most significance were used first. Subsequent parameters were applied in the order of their parameter significance ranking. The first iteration for each sensitivity parameter calibration began with its ASM2d default value. New results were obtained if parameter values were significantly changed by iteration. Additionally, iteration of parameter values was done until small differences between actual and simulated results were obtained. This showed the influence of parameters upon experimental data. Parameter values were varied over their ranges, i.e., the upper and lower bounds of ASM2d parameters obtained from published studies of other researchers. These parameters were used for calibration as the simulation varied the values of the significant parameters. The number of iterations for each parameter was selected using minimization of results. These included the sum of squares of weighted deviations between measured and calculated values, as well as the standard error of estimate (SEE) calculated using Eq. 3.18 and 3.19. Calibrated values of these parameters comprised the parameter subset used to evaluate observed results according to goodness of fit. In manual calibration using GPS-X with a calibration function, the input values of parameters of interest were varied while other parameters were held fixed with specific values, i.e., default or calibrated values. Other parameters were applied in descending order of their significance using the same methodology. Results were obtained as the experimental data was fit to the calibrated model. Thus, the number of iterations of each experiment was determined by number parameters used multiplied the number of iterations of the calibration model. A stepwise manual iteration methodology was specifically adapted to EBPR in which the simulation results were calibrated using observed results with the parameter significance ranking in order to achieve a reasonable model fit. The iterative algorithm was reevaluated until refinement of the sensitivity parameters no longer affected the simulation output.

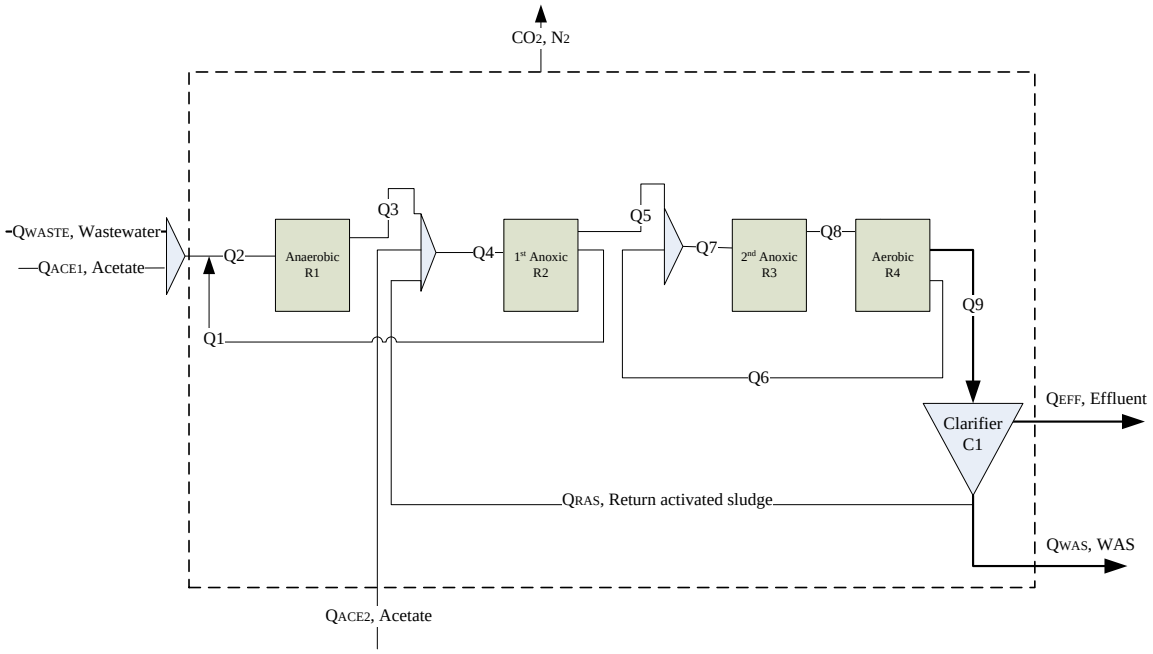

Figure 4.3 Figure demonstrating mass balance over the MUCT pilot-scale.

The precise measurement of data in wastewater treatment plants (WWTP) is important to their performance and the profit (Narasimhan and Jordache, 2000). A method of mass balance calculation proposed by Meijer et al. (2002) was used to improve the WWTP operation under study. It was modified based upon fermentation processes (Van der Heijden et al., 1994a). A WWTP mass balance obtained from practice can help to achieve reliable information of observed WWTP results. The mass balances over WWTPs can be used to estimate the fluxes of substances, compare operational conditions and draw conclusions of general validity (Nowak et al., 1999). Other researchers proposed a method to calculate the SRT from a total phosphorus (TP) balance (Brdjanovic et al., 2000). This approach is more accurate than calculating the SRT from sludge waste.

A basic overall WWTP mass balance of the solid, liquid and gas phases is presented in Figure 4.3. The significant conversions shown in Figure 4.3 are linked to COD conversion (CO_2 gas) and N conversion (N_2 gas). These mass balances can be expressed for the overall

WWTP as well as for individual reactors. This is because the significant conversions (CO_2 and N_2) are open balances. These balances cannot be closed. Their conversions can measure from flows. Equations (4.4) and (4.5) are used to calculate the closed water and TP balances. Evaluation of phosphorus mass balance is done directly (Figure 4.3). This can be done because TP does not leave the system via the gas phase. TP is measured in all in- and outgoing flows and determined by solving the TP balance. The internal conversions from the open COD and N balances can be determined by detecting the in- and outgoing COD and N in the desired process unit. The overall flow balance:

$$Q_{INF} - Q_{WAS} - Q_{EFF} = 0(Closed) \tag{4.4}$$

The overall TP balance (expressed as kg P d^{-1}):

$$TP_{INF} - TP_{WAS} - TP_{EFF} = 0\ (Closed) \tag{4.5}$$

The overall TN balance (expressed as kg N d^{-1}):

$$TN_{INF} - TN_{WAS} - TN_{EFF} = N_2 \tag{4.6}$$

The SRT affects treatment process performance, aeration tank volume, sludge production and oxygen requirements (Metcalf and Eddy, 2003). The SRT is the most crucial parameter for characterization of activated sludge. Therefore, a check on the SRT is a reliable modeling study. The classical SRT (Equation (4.7)) is based upon the sludge production. However, measuring the solids in the waste activated sludge (WAS) or return activated sludge (RAS) are inaccurate. This is due to large fluctuations of the settled solids in the final clarifier (Meijer et al., 2001). There are several ways to calculate the SRT. These are based on TP leaving the process (Equation 4.8)) and on TP entering the process, eliminating the need to know exactly the excess sludge wastage rate (Equation (4.9)), or via COD particulate (COD_{TSS}) leaving the process via the WAS (Equation (4.10)). To calculate the particulate phosphate in the sludge (TP_{TSS}), the difference between the total phosphorus

and the soluble phosphate is determined. The SRT calculation (Equation (4.7)–(4.10)) can be simplified if the stripper tank is not used or not available:

$$SRT_{classical} = \frac{V_{REACTOR} * TSS_{REACTOR}}{(Q_{WAS} * TSS_{WAS}) + (Q_{EFF} * TSS_{EFF})} \tag{4.7}$$

SRT calculated from the conserved TP balance based on TP leaving the process:

$$SRT_{TP_{TSS\_OUTPUTS}} = \frac{V_{REACTOR*} TP_{TSS\_REACTOR}}{(Q_{WAS} * TP_{TSS\_WAS}) + (Q_{EFF} * TP_{TSS\_EFF})} \tag{4.8}$$

$$SRT_{TP_{TSS\_INPUTS}} = \frac{V_{REACTOR} * TP_{TSS\_REACTOR}}{(Q_{INF} * TP_{INF}) - (Q_{WAS} * PO_{4\_WAS}) - (Q_{EFF} * PO_{4\_EFF})} \tag{4.9}$$

SRT calculated from the COD particulate leaving the process:

$$SRT_{COD_{TSS\_OUTPUTS}} = \frac{V_{REACTOR} * COD_{TSS\_REACTOR}}{(Q_{WAS} * COD_{TSS\_WAS}) + (Q_{EFF} * COD_{TSS\_EFF})} \tag{4.10}$$

4.3 RESULTS AND DISCUSSION

Step 1: Influent wastewater characteristics

Simulation of the operating period was completed for a steady state processes. The results of not using disintegrated sludge (DS, control) operated at 17°C were determined. Influent wastewater characteristics, as well as P release in an anaerobic phase, effluent NH_4 and TP of the MUCT pilot scale biological phosphorus removal processes at steady state are shown in Table 3.9. In addition, ASM2d model information of influent is summarized in Table 4.1.

Table 4.1 Characterization of influent components based upon ASM2d

Model Information		
Flow		
flow	2.88	[m^3/d]
Composite Variables		
Volatile Fraction		
VSS/TSS ratio	0.963	[gVSS/gTSS]
Composite Variables		
total suspended solids	1420	[g/m^3]
volatile suspended solids	1370	[g/m^3]
total inorganic suspended solids	52.4	[g/m^3]
total carbonaceous BOD5	343	[gO_2/m^3]
total COD	2210	[gCOD/m^3]
total TKN	101	[gN/m^3]
total phosphorus	52.3	[gP/m^3]
Additional Composite Variables		
filtered carbonaceous BOD5	45	[gO_2/m^3]
particulate carbonaceous BOD5	298	[gO_2/m^3]
filtered ultimate carbonaceous BOD	68.2	[gO_2/m^3]
particulate ultimate carbonaceous BOD	451	[gO_2/m^3]
total ultimate carbonaceous BOD	519	[gO_2/m^3]
filtered COD	135	[gCOD/m^3]
particulate COD	2080	[gCOD/m^3]
filtered TKN	33.1	[gN/m^3]
particulate TKN	67.9	[gN/m^3]
total nitrogen	101	[gN/m^3]
filtered phosphorus	10.5	[gP/m^3]
particulate phosphorus	41.8	[gP/m^3]
State Variables		
Inorganic Suspended Solids		
inert inorganic suspended solids	0.0085	[g/m^3]

Table 4.1 (cont.) Characterization of influent components based upon ASM2d

Model Information		
Organic Variables		
soluble inert organic material	66.3	[gCOD/m^3]
fermentable readily biodegradable substrate	18.7	[gCOD/m^3]
volatile fatty acids	49.4	[gCOD/m^3]
particulate inert organic material	1630	[gCOD/m^3]
slowly biodegradable substrate	44.2	[gCOD/m^3]
active heterotrophic biomass	247	[gCOD/m^3]
active autotrophic biomass	34.4	[gCOD/m^3]
active poly-P accumulating biomass	112	[gCOD/m^3]
poly-hydroxy-alkanoates (PHA)	13.7	[gCOD/m^3]
Dissolved Oxygen		
dissolved oxygen	0.00436	[gO_2/m^3]
Phosphorus Compounds		
soluble ortho-phosphate	10.4	[gP/m^3]
stored polyphosphate	17.5	[gP/m^3]
Nitrogen Compounds		
free and ionized ammonia	29.2	[gN/m^3]
nitrate and nitrite	0.315	[gN/m^3]
dinitrogen	8.04	[gN/m^3]
Alkalinity		
alkalinity	4.98	[mole/m^3]
Metal Precipitates		
metal-hydroxides	5.96E-05	[g/m^3]
metal-phosphates	0.000854	[g/m^3]
Model Stoichiometry		
Organic Fractions		
XCOD/VSS ratio	1.52	[gCOD/gVSS]
BOD5/BODultimate ratio	0.66	[-]
Nutrient Fractions		
N content of soluble inert organic material	0.0404	[gN/gCOD]
N content of fermentable readily biodegradable substrate	0.0661	[gN/gCOD]
N content of particulate inert organic material	0.0232	[gN/gCOD]
N content of slowly biodegradable substrate	0.0586	[gN/gCOD]
N content of active heterotrophic biomass	0.07	[gN/gCOD]
N content of active autotrophic biomass	0.07	[gN/gCOD]
N content of active poly-P accumulating biomass	0.07	[gN/gCOD]
P content of fermentable readily biodegradable substrate	0.00756	[gP/gCOD]
P content of particulate inert organic material	0.00987	[gP/gCOD]
P content of slowly biodegradable substrate	0.00876	[gP/gCOD]
P content of active heterotrophic biomass	0.02	[gP/gCOD]
P content of active autotrophic biomass	0.02	[gP/gCOD]
P content of active poly-P accumulating biomass	0.02	[gP/gCOD]

Step 2 Default values and a priori parameter set

In order to calibrate the ASM2d model, a number of default parameters were established. Their values were obtained from published literature. For the analysis, a priori assumption of parameter values had to be made. Such values were used as default values. These included stoichiometric and kinetics parameters of phosphorus accumulating organisms (PAOs). Maximum and minimum values for these parameters are given in Table 3.11.

Step 3: Parameter significance

The parameter significance ranking of the resulting sensitivity analysis was based on the total number of model outputs. The result showed which of these were the most significant of the data inputs, i.e., when the roots of mean squared (RMS) values of sensitivities were higher than 0. The RMS values indicate the mean sensitivity of the model output to a change in the parameter θ_j. A higher RMS value means that the value of the parameter θ_j has a stronger effect on the simulation model (Brun et al., 2002). A value of zero indicates that the simulation results do not depend on the parameter θ_j. Other researchers considered sensitivity parameters with RMS values that were greater than or equal to 0 (Machado et al., 2009). From the results, the first 40 ASM2d parameters were chosen in order of descending sensitivity. Sensitivity analysis was employed for 51 parameters in the initial classification. Other researchers reported that they used only the top 30 parameters. These were defined as those with RMS values greater than 0.07 and 0.10 in sensitivity analysis with default and optimized values, respectively (Brun et al., 2002). The derivatives of Eq. 4.2 were determined numerically by finite difference methodology since the ASM2d model analysis is too complicated to be done algebraically (Norton, 2008). The difference in calculation of sensitivity analysis is based upon the central difference approach. A perturbation factor of 10^{-4} was used for the sensitivity calculation of each test parameter around the default ASM2d values. De Pauw and Vanrolleghem (2006) reported that this perturbation factor was selected because it produced equal derivative values with forward and backward finite difference methods. The RMS values for wastewater processes under

study show the different values, i.e., low or high level of RMS values depending upon the WWTPs conditions. Other researchers found that selection of a reduced set of the most sensitive parameters with subsequent detailed analysis could be done. This reduced the parameter set from approximately 25 to a number between 10 and 15. This was done to reduce computation time in subsequent steps (Weijers and Vanrolleghem, 1997). Those parameters showed a scaled mean output sensitivity coefficient larger than 0.2 in at a least one of the outputs with the scale the sensitivity coefficient (Eq. 4.2). Reichert and Vanrolleghem (2001) proposed that the ranking should only used for a preliminary selection of a set of about 15 parameters, depending on the problem. Final subset selection from those parameters should be criteria based using the determinant or the condition number of the Fisher Information Matrix (FIM). Thus, choosing the number of significant parameter for the selection of subsets of identifiable model parameters for large environmental simulation models was related to experience. From this, the parameter subsets under these studies were reduced to the top 30 as shown in Table 4.2. Consequently, the resulting 30 parameters were used to for calibration in analyzing all experimental results. Other researchers (Weijers and Vanrolleghem, 1997) used sensitivity parameter rankings with roots of mean squared values larger than 0.2 and found 11 relevant parameters that were used to calibrate the Activated Sludge Model No. 1 (ASM1) applied to full-scale plant data. Differences in parameter significance rankings among studies of ASM2d are highly influenced by the data available for calibration. Important factors in this regard include consideration of particular WWTP configurations and operation, and some properties of collected data (Ruano et al., 2007). The parameter significance ranking showed that temperature correction coefficients and the parameters for PAOs were among the most influential parameters on the model outputs. In this study, ASM2d was calibrated using an identifiability method to describe nitrogen and phosphorus removal in the Haaren (The Netherlands) WWTP (Ruano et al., 2007). PAOs play an important role in the dynamics of the EBPR processes (Brun et al., 2002). In another application, this approach to ASM2d calibration used an identifiability analysis in a systematic manner. It was applied

Table 4.2 The ASM2d parameter significance ranking calculation with Aquasim and interface UNSIM

Ranking	Parameter	Roots of mean squared of sensitivities
1	Y_{PO4}	26.43
2	μ_{PAO}	23.45
3	Y_{PAO}	19.51
4	q_{PP}	18.35
5	$K_{O2\ AUT}$	18.01
6	$K_{NH4\ AUT}$	11.85
7	b_{PP}	8.93
8	μ_{AUT}	7.99
9	Y_{PHA}	4.76
10	b_{AUT}	2.76
11	b_{PHA}	2.16
12	Y_A	1.59
13	K_{IPP}	1.29
14	μ_H	1.11
15	η_{NO3}	1.01
16	q_{PHA}	0.94
17	K_{PS}	0.53
18	K_{PP}	0.47
19	K_{AUT}	0.23
20	$K_{ALK\ PAO}$	0.22
21	f_{XI}	0.07
22	K_{PHA}	0.04
23	K_{NO3}	0.03
24	K_F	0.02
25	K_h	0.02
26	K_X	0.01
27	K_P	0.01
28	q_{fe}	0.01
29	b_{PAO}	0.01
30	Y_H	0.01

to EBPR at a full scale WWTP in Switzerland (Brun et al., 2002). Additionally, to calibrate ASM2d for anaerobic/anoxic/oxic conditions (A2/O), a pilot WWTP used an identifiability approach (Machado et al., 2009). PAOs parameters were also among the most sensitive. Although other studies were in rough agreement, there were some differences. The parameter significance rankings of the current study are different from that of other researchers (Brun et al., 2002; Ruano et al., 2007; Machado et al., 2009). In the current study, the parameter with the highest sensitivity was Y_{PO4}.

However other researchers found this parameter's sensitivity to be ranked as 8th (Machado et al., 2009), 15th (Ruano et al., 2007), and it was excluded altogether in another study (Brun et al., 2002). Also researchers (Brun et al., 2002) found that parameter b_{PAO} had the highest sensitivity although it ranked 4th and 27th in other studies (Machado et al., 2009; Ruano et al., 2007). This parameter's sensitivity was ranked lower in the current study (29th). Considering the second most significant sensitivity ranking in this study, μ_{PAO}, it was of the same order as in one study (Brun et al., 2002), but it was at a lower position (17th) in other work (Ruano et al., 2007; Machado et al., 2009). Additionally, the current study found that μ_{AUT} had a higher sensitivity ranking than other studies (Brun et al., 2002; Ruano et al., 2007). However its ranking was lower than reported elsewhere (Machado et al., 2009). Furthermore the sensitivity analysis in other work (Soejima et al., 2008) used only two parameters, Y_{PAO} and Y_{PO4}. Here anaerobic/aerobic/anoxic processes for simultaneous nitrogen and phosphorus removal on NO_3 and PO_4 profiles were examined. One group of researchers (Yagci et al., 2006) used manually repeating simulation as a sensitivity approach to individual changes in the magnitude of related parameters for each model parameter. This was based on the steady state cyclic simulations of S_{PO4}, X_{PHA}, S_A and MLSS profiles containing the most sensitive parameters namely, Y_{PO4}, q_{PHA}, q_{PP}, K_{PHA} and lysis rates.

Step 4: The iteration processes with simulation of the ASM2d modeling

The calibration approach described here avoids the problem of needing extensive experience in activated sludge modeling and the difficulty of identifiability analysis. This approach iterates only based upon the parameter sensitivity. A stepwise methodology was used in the mathematical simulations in each of the iterations. The iteration number of each experimental data set was based on the number of parameters in the sensitivity analysis. Use of 30 iterative steps for each of the parameter data sets, i.e. the same number of parameters in the sensitivity ranking, was done to predict the output of NH_4 and TP in effluent and of PO_4 in anaerobic phase. Parameter significance ranking was used to perform

the calibration in order to fit the model's parameter values to the observed results. The most significant parameter was iterated first. This was followed by each of the other 29 parameters included in the parameter significance ranking in order of decreasing influence. Iterations begun with the initial default parameter value and were carried out under the steady state conditions. In the current study, 15 significant parameters were use of 30 sensitivity parameters (Table 4.2). This included 5 parameters of autotrophs and 10 parameters of PAOs, that influenced calibration of effluent NH_4, and PO_4 under anaerobic conditions and effluent TP, respectively. These parameters were used for the calibration. Simulation outcomes varied with the values of the different significant parameters. It was seen from the sum of squares of weighted deviations between measurement and calculation, and standard error of estimate (SEE) calculated, with Eq. 3.18 and 3.19, that these 15 parameters gave minimized results. Thus, these calibrated parameter values comprised working a parameter subset as is seen in the goodness of fit. Using the GPS-X manual function, input values of parameters under study were varied while other parameters were fixed with specific values, i.e., default or calibrated values. Simulation varied with input parameter values. For instance, the calibration of the effluent NH_4 with Y_{PO4}, had the highest sensitivity value. It was a first parameter changed, whist the other 29 parameters were set to their default values. As a result, Y_{PO4} did not influence effluent NH_4 concentration. It had no effect on the simulation model. Effluent NH_4 was the first experimental data set used to calibrate ASM2d parameters in order to observe the activity of autotrophs. The other parameter data sets, PO_4 in anaerobic phase and effluent TP, were not simultaneously calibrated. The next parameter for simulating effluent NH4 was μ_{PAO}. It also had no effect on the ASM2d calibration model as other parameter values were altered. Other parameters were used in similar fashion in descending order of sensitivity. Values of influential parameters were set to their default values for calibrations using other experimental data sets. For instance, the values of 5 important parameters for effluent NH_4 calibration were their defaults values in other calibrations. In the second set of experimental results, PO_4 in the anaerobic phase and effluent TP, were calibrated at the same time as the influence of parameters on PO_4 in anaerobic phase. They also changed the ASM2d

calibrated model of effluent TP. After calibration the values for each influence of parameter were found. As a result, only stoichiometric and kinetic parameters of PAOs, 10 parameters, were influential in these data sets. Particularly important parameters were used for observation of specific microorganisms, i.e., the ASM2d calibration with 10 significant parameters for PO_4 in an anaerobic phase and effluent TP was used to investigation PAOs behaviors. Additionally, the 5 calibrated parameters of effluent NH_4 described autotrophic mechanisms only. Thus, by following this calibration methodology the values of parameter subset were governed by the experimental data. The calibration results of the NH_4 experiments are shown in Table 4.3.

Table 4.3 The values of the calibrated ASM2d parameters

Symbol	ASM2d	Calibrated value	Units
Phosphorus Accumulating Organisms, PAOs			
Y_{PAO}	0.625	0.61	g COD/g COD
Y_{PO4}	0.4	0.40	g P/g COD
Y_{PHA}	0.20	0.24	g COD/g P
q_{PHA}	3.0	3.50	g X_{PHA}/g X_{PAO}/d
q_{PP}	1.5	1.50	g X_{PP}/g X_{PAO}/d
μ_{PAO}	1.0	1.00	d^{-1}
b_{PAO}	0.2	0.20	d^{-1}
b_{PP}	0.2	0.20	d^{-1}
b_{PHA}	0.2	0.20	d^{-1}
K_{PS}	0.2	0.35	g P/m^3
Autotrophs			
Y_A	0.24	0.24	g COD/g N
μ_{AUT}	1.0	1.20	d^{-1}
b_{AUT}	0.15	0.05	d^{-1}
$K_{O2\ AUT}$	0.5	0.50	g O_2/m^3
$K_{NH4\ AUT}$	1.00	0.15	g N/m^3

As a result of fitting the simulated data to the effluent NH_4 concentration, it was found that there were five significant parameters. They are: yield of autotrophic biomass per unit of NO_3^-N (Y_A), the maximum growth rate for autotrophs (μ_{AUT}), the decay rate of X_{AUT} (b_{AUT}), saturation coefficient for ammonium ($K_{NH4\ AUT}$), saturation coefficient for oxygen $K_{O2\ AUT}$. μ_{AUT} was increased to sustain autotrophic growth. Next b_{AUT} was decreased in relation to increasing autotrophic growth rate. Later $K_{NH4\ AUT}$ decreased because of low ammonium concentration in the aerobic phase. Both Y_A and $K_{O2\ AUT}$ were the same as their default values. Comparison of the parameter subsets to other experiments using different protocols is shown in Table 4.4. Significant parameters based upon NH_4 in effluent using the experienced-based approach for the experiments of sequencing batch reactors (SBRs) (Insel et al., 2006) were calibrated. To accomplish this, nutrients were removed under limited aeration conditions. The parameters examined included μ_{AUT} and K_{NH4}. In addition to calibration with an experienced-based approach to determine EBPR under different phosphorus/acetate (P/HAc) ratios with the ASM2d modeling in the SBR performance, it has been shown that only μ_{AUT} is necessary to calibrate NH_4 and NO_3 (Yagci et al., 2006). A practical identifiability approach for the ASM2d calibration is to select the parameter subset sizes for autotrophs with three calibrated parameters: b_{AUT}, K_{NH4} and μ_{AUT} (Brun et al., 2002).

Table 4.4 The parameter subsets in different studies

Parameter subsets	Reference
Y_{PAO}, Y_{PO4}, Y_{PHA}, q_{PHA}, q_{PP}, μ_{PAO}, b_{PAO}, b_{PP}, b_{PHA}, K_{PS}, Y_A, μ_{AUT}, b_{AUT}, $K_{O2\ AUT}$, $K_{NH4\ AUT}$	This study
b_{PAO}, μ_{PAO}, q_{PHA}, q_{PP}, b_{PP}, K_h, η_{fe}, b_{AUT}, K_{NH4}, μ_{AUT}	Brun et al. (2002)
b_{PAO}, Y_{PO4}, μ_{AUT}	Machado et al. (2009)
μ_{AUT}, α_{XI}, α_{SA}, α_{SF}, $\eta_{NO3\ HYD}$, K_{PHA}, μ_{PAO}	Melcer et al. (2003)
Y_H, μ_H, K_F, b_H, η_{NO3}, μ_A, K_{NH4}, b_A, Y_{PO4}, q_{PHA}, K_A, Y_{PAO}, μ_{PAO}, q_{PP}, b_{PAO}, K_{PHA}, K_{IPP}, K_{MAX},	García-Usach et al. (2006)
Y_{PAO}, Y_{PO4}	Soejima et al. (2008)
μ_{AUT}, K_{NH4}, K_X, K_N, K_O, K_{OA}, Y_{HNO3}, b_H, Y_{PO4}, q_{PHA}, μ_{PAO}, q_{PP}	Insel et al. (2006)
μ_{AUT}, b_{PAO}, b_{PP}, b_{PHA}, q_{PHA}, q_{PP}, K_{PHA}, Y_{PO4}	Yagci et al. (2006)
μ_{AUT}, $\eta_{NO3\ HYD}$, K_h, η_{fe}, μ_H, K_{O2}, η_{NO3}, $K_{NH4\ AUT}$, q_{PHA}, q_{PP}, Y_{PO4}	Makinia et al. (2006)
$K_{O2\ AUT}$, $K_{NH4\ AUT}$, b_{AUT}, η_{NO3}, b_H, K_{NO3}, K_{O2}	Hulsbeek et al. (2002)

Another study (Machado et al., 2009) on activated sludge anaerobic/anoxic/oxic (A^2/O) pilot WWTPs using an identifiability approach with the Fisher Information Matrix (FIM) tool to reduce ASM2d parameter subset sizes used only μ_{AUT}. This presents a calibrated autotroph parameter and the parameter subset size is b_{PAO}, Y_{PO4}, μ_{AUT}. The calibrated parameters included in the simulation of nitrogen removal at the Hanover-Gümmerwald pilot wastewater treatment plant were μ_{AUT}, $\eta_{NO3\ HYD}$, K_h, η_{fe}, μ_H, K_{O2}, η_{NO3}, $K_{NH4\ AUT}$, q_{PHA}, q_{PP}, and Y_{PO4}. This was based on ASM2d and ASM3P model concepts (Makinia et al., 2006). In the current study, several parameters govern the fitting of the simulation to model to PO_4 in anaerobic phase and effluent TP. Those parameters (Table 4.4) include: Y_{PAO}, Y_{PO4}, Y_{PHA}, q_{PHA}, q_{PP}, μ_{PAO}, b_{PAO}, b_{PP}, b_{PHA}, and K_{PS}. In another study (Soejima et al., 2008), Y_{PAO} and Y_{PO4} calibrated parameters were used to investigate the effect of extra acetate on the anaerobic/aerobic/anoxic (AOA) processes for simultaneous nitrogen and phosphorus removal based on the ASM2d modeling with the additional denitrifying PAOs (DNPAOs) kinetics. That modeling expressed the optimum concentration of supplementary COD and elucidated microorganism metabolism. Thus the application of that modeling to the different wastewater compositions, such as COD/N/P, can be conducive to predicting PAOs behavior (Soejima et al., 2008). To study phosphorus storage capacity-limiting and phosphorus loading-limiting conditions, there are 8 significant calibrated parameters. This includes μ_{AUT}, b_{PAO}, b_{PP}, b_{PHA}, q_{PHA}, q_{PP}, K_{PHA} and Y_{PO4}. It was used for the predicted simulations of S_{PO4}, X_{PHA}, S_A and MLSS profiles in the sequencing batch reactor (SBR) performance for EBPR fed with acetate as the carbon sole carbon source under different P/HAc ratios (Yagci et al., 2006). The calibration and simulation using the ASM2d model at different temperatures in a phosphorus removal pilot plant showed that the significant calibrated parameters include Y_H, μ_H, K_F, b_H, η_{NO3}, μ_A, K_{NH4}, b_A, Y_{PO4}, q_{PHA}, K_A, Y_{PAO}, μ_{PAO}, q_{PP}, b_{PAO}, K_{PHA}, K_{IPP}, and K_{MAX} (García-Usach et al., 2006). To simulate the O_2, COD, NH_4, and PO_4 data sets in an activated sludge system, a large parameter set (Hulsbeek et al., 2002) was included i_{NXS}, i_{NXI}, $K_{O2\ AUT}$, $K_{NH4\ AUT}$, b_{AUT}, η_{NO3}, b_H, K_{NO3}, and K_{O2}. In another study (Melcer et al., 2003) included μ_{AUT}, α_{XI}, α_{SA}, α_{SF}, $\eta_{NO3\ HYD}$, K_{PHA}, μ_{PAO}. This methodology was successful in calibrating pilot plant operation.

The expectation when using this in a full-scale site is that its use can reduce time required for calculation of parameter subset sizes. Subsequently, operation processes can be enhanced on basis of understanding organism behaviors. However, fluctuation of wastewater characteristics and complexity of operation systems may cause calculation errors.

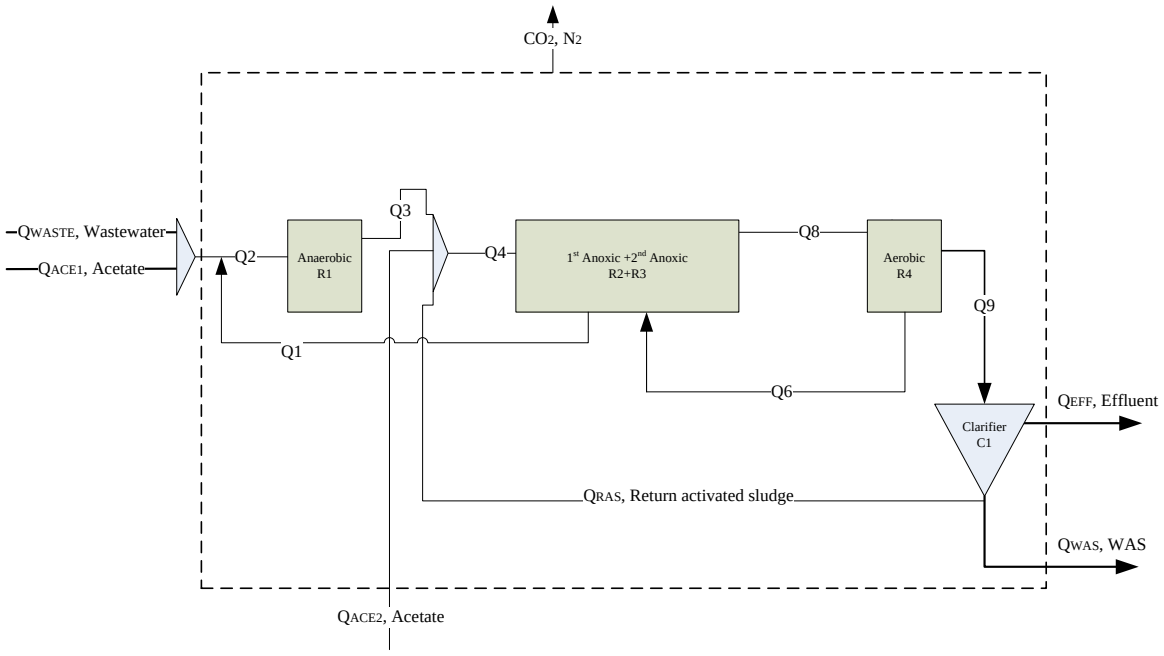

Figure 4.4 Schematic mass flow diagram of a MUCT pilot-scale.

To model a wastewater treatment plant (WWTP), dynamic models of activated sludge can be linked (Puig et al., 2008). In such models, the outputs of one unit operation become influents of the next down stream operation. The flow results of the mass balance are shown in Table 4.5. The flow rate of influent and outflow measurements was done to show the closed system of the overall flow balance (Figure 4.4). The measurements in the anaerobic and the 2nd anoxic phase were performed to check the recirculation flows (Q_1 and Q_6).

Table 4.5 Results of simulation used for mass balances

Parameters	Units	Influent (Q_{WASTE}+$Q_{ACE1\&2}$)	Effluent	Waste activated sludge (WAS)	Anaerobic phase	2nd anoxic phase
Flow, Q	[m^3/d]	1.4448	1.3700	0.0748	2.8824	4.1048
Total COD, TCOD	[gCOD/m^3]	472.4252	81.70	8050	2210	3960
Total Kjeldahl N, TKN	[gN/m^3]	63.7874	1.28	244	101	131
Nitrate, NO_3	[gN/m^3]	0	14.60	14.60	0.32	5.53
Total phosphorus, TP	[gP/m^3]	9.1495	2.63	194	52.30	95.50
Ortho-phosphate, PO_4	[gP/m^3]	6.7774	2.20	2.20	10.40	9.86

Table 4.6 Charaterisation mass balances of flow, TP, TKN, NO, COD and oxygen consumption (OC) in matrix format

Components		WWTP	R1	R2+R3	R4	C1	$WWTP_{TP}$	$R1_{TP}$	$(R2+R3)_{TP}$	$R4_{TP}$	$C1_{TP}$	$WWTP_{TKN}$	$WWTP_{NO}$	$WWTP_{COD}$	$WWTP_{OC}$
		1	2	3	4	5	6	7	8	9	10	11	12	13	14
Q_{INF}(Q_{WASTE}+$Q_{ACE1\&2}$)	1	1.4448					9.1495					63.7874		472.4252	
Q_{ACE1}	2	0.0024													
Q_1	3		1.4400	-1.4400				95.4							
Q_2	4		2.8824					52.3							
Q3	5		-2.8848	2.8848					53						
Q_{ACE2}	6			0.0024											
Q_{RAS}	7			1.2200		-1.2200			194						
Q_4	8			2.8872					15						
Q_6	9			1.4400	-1.4400				95.8						
Q_8	10			-4.1048	4.1048					96					
Q_9	11				-2.6648	2.6648					95.8				
Q_{EFF}	12	-1.3700				-1.3700	-2.63				-2.63	-1.28	-14.6	-81.7	-6.0
Q_{WAS}	13	-0.0748				-0.0748	-194				-194	-244	-14.6	-8050	-6.0
L_{NIT}	14											-1	1		-4.57
L_{DEN}	15												-1	-2.87	
OC_{COD}	16													-1	-1
OC_{NET}	17														

Each column represents a balance. Column 1-5 are flow balances. Columns 6-10 are P-balances, Columns 11-12 are N-balances, Column 13 is a C-balance. C1: balance over the clarifier, WWTP: balance over the total plant. The last 4 row "open" COD and N balances (L_{NIT}: nitrified load, L_{DEN}: denitrified load, OC_{COD}: oxygen consumption COD, OC_{NET}: net oxygen consumption). All empty spaces in the matrix represent zeros, elements with negative signs are outflows, and positive elements are inflows.

Overall the selected mass balances (done over the WWTP, anaerobic, anoxic and aerobic phases) are shown in a matrix format for the balancing calculation. The matrix format shown in Table 4.6, expresses flows and concentrations in different compartments at steady state. Table 4.7 shows the overall flow and total phosphorus (TP) balance. These are closed balances. From the flow balances it is seen that influent, effluent and WAS were maintainted at 1.4448, 1.37000 and 0.0748 m^3 d^{-1}, respectively. The COD, nitrogen and oxygen mass balances are opened represented in Table 4.8. The internal conversions and typical processes also are calculated. The net stoichiometric oxygen consumption based on simulations was used for the benchmarking the WWTP. According balanced data, the SRT can be calculated in different ways: (1) the solids balance (Equation (4.7)),

Table 4.7 Closed mass balance calculations of flow and total phosphorus (TP)

	Units	Balanced data
Flow balance		
Influent flow	[m^3/d]	1.4448
Effluent flow	[m^3/d]	1.3700
Waste activated sludge	[m^3/d]	0.0748
TP balance		
Influent flow	[gP/d]	9.15
Effluent flow	[gP/d]	2.63
Waste activated sludge (WAS)	[gP/d]	194.00

Table 4.8 Open mass balance calculations of COD, nitrogen and oxygen balances

	Units	Balanced data
COD balance		
COD uptake by PAOs (anaerobic conditions)	[gCOD/d]	30.00
COD denitrification (anoxic conditions)	[gCOD/m^3]	182.81
COD oxidation (aerobic conditions)	[gCOD/m^3]	82.10
Nitrogen balance		
Nitrification (aerobic conditions)	[gN/d]	51.31
Denitrification (anoxic conditions)	[gN/d]	29.14
Oxygen balance		
Total oxygen consumption	[gO_2/d]	135.46
Nitrogen oxidation (aerobic conditions)	[gO_2/d]	53.36
COD oxidation (aerobic conditions)	[gO_2/d]	82.10

Table 4.9 Calculation of the solids retention time

SRT calculation	Units	Balanced data
SRT based on MLSS	[Days]	6
SRT based on CODTSS	[Days]	5
SRT based on TPTSS outputs	[Days]	5
SRT based on TPTSS influent	[Days]	9

(2) the TP balance based on TP leaving the process (Equation (4.8)), (3) TP entering the process (Equation (4.9)) and (4) the COD particulate (CODTSS) leaving the process (Equation (4.10)). The SRT results are presented in Table 4.9. The SRT calculations base on RAS and waste activated sludge (WAS) flow can result in measurement error up to 40% (Meijer et al., 2002). The SRT results shown in Table 4.9 were calculated based on balanced data (Table 4.8). In this study, no gross measurements were observed and the results of the mass balancing evaluation underlines the accuracy of the WAS measurements. In balancing flow and TP for the WWTP, the error in the balancing process may occur due to variation of influent flow (Table 4.6). The varied influent flow is linked in calculation SRT (Table 4.9). Underestimation of the influent flow results in underestimation of the calculated internal conversions (Puig et al., 2008). The sensitivity between the internal conversions and the influent flow are specific for the operation of the WWTP. Therefore it is suitable for the benchmarking purposes (Puig et al., 2008). In this study, the variation in the SRT based on the simulation of TSS, COD and TP in the outflows was significantly different (Table 4.9). Calculated SRT varied between 5 and 9 days based upon the method of calculation. This shows how a design parameter, SRT, is influenced by errors. The chosen method of SRT calculation affects any mathematical model (Van Veldhuizen et al., 1999; Brdjanovic et al., 2000). It also influence the treatment process, sludge production and oxygen utilization (Metcalf and Eddy, 2003; Kreuzinger et al., 2004). The determination of SRT was based upon the output TP balances. TP was the smallest value of those among the overall SRT. Using P balances (closed) yields more information which can improve the data quality in the simulation. In the COD balance, oxygen consumption was not measured so it was impossible to detect measurement error in the CODTSS concentration.

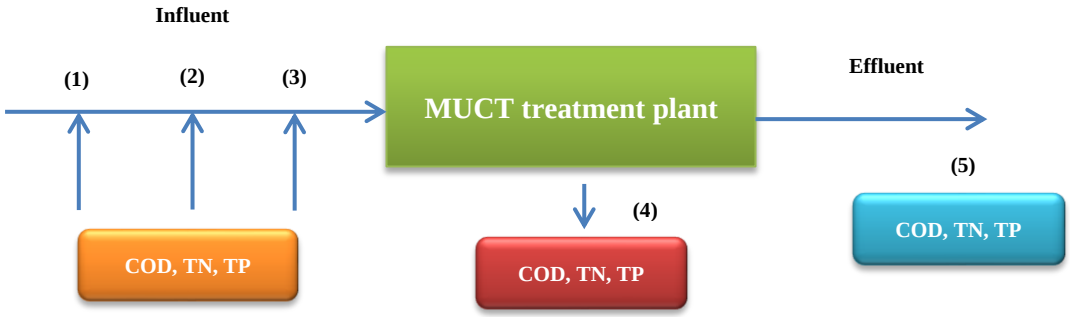

	Units	(1) Wastewater	(2) Acetate	(3) Acetate	(4) Waste activated sludge	(5) Effluent
flow	[m^3/d]	1.44	0.0024	0.0024	0.0748	1.37
Organic Variables						
soluble inert organic material	[gCOD/m^3]	67.4	0	0	63.7	63.7
fermentable readily biodegradable substrate	[gCOD/m^3]	33.9	0	0	0.382	0.382
volatile fatty acids	[gCOD/m^3]	42.3	25600	12800	0.0255	0.0255
particulate inert organic material	[gCOD/m^3]	212	0	0	6300	13.9
slowly biodegradable substrate	[gCOD/m^3]	55	0	0	25.4	0.0559
active heterotrophic biomass	[gCOD/m^3]	0	0	0	1030	2.26
active autotrophic biomass	[gCOD/m^3]	0	0	0	149	0.328
active poly-P accumulating biomass	[gCOD/m^3]	0	0	0	479	1.05
poly-hydroxy-alkanoates (PHA)	[gCOD/m^3]	0	0	0	0.832	0.00183
Phosphorus Compounds						
soluble ortho-phosphate	[gP/m^3]	6.8	0	0	2.2	2.2
stored polyphosphate	[gP/m^3]	0	0	0	95.7	0.21
Nitrogen Compounds						
free and ionized ammonia	[gN/m^3]	38.3	0	0	0.1	0.1

Figure 4.5 Characteristic of parameters based on the ASM2d model for influent, WAS and effluent in the pilot-scale MUCT.

A correct design of the measurement strategy is crucial for the evaluation of a full-scale WWTP (Puig et al., 2008). The average sludge composition, such as TP, TSS for balancing purposes, over a mixing period was used for a static evaluation. For every measurement point which 24-h composite samples were not available, 4 points (influent, anaerobic phase, aerobic phase and effluent) were chosen for grab samples. The errors in measured data in full-scale WWTPs may happen in practice. Neglecting statistical errors leads to erroneous calculations of operation and incorrect process design (Van Veldhuizen et al., 1999; Meijer et al., 2002). All balances (close and open balances) are shown the matrix format (Table 4.6). These clarifications of compositions calculated based on the simulation results are included in Table 4.10 and Table 4.11. In addition, the amouts of COD, nitrogen and phosphorus for influent and effluent are shown in Figure 4.5. The flow and TP balances (Table 4.7) were closed balances. The COD and nitrogen balances are open mass balances calculations (Table 4.8). In the nitrogen balances, the nitrogen load in nitrification was 51.31 g N d^{-1} and in denitrification it was 29.14 g N d^{-1}. The nitrified load and denitrified load were 80.44% and 45.79% of the nitrogen of 63.79 g N d^{-1}, respectively. The internal conversion errors could be related to underestimation of the influent flow. The total oxygen consumption (OC) mass balances were also considered as shown in Table 4.6 and Table 4.8. The evaluation of the OC was directly linked to the aeration input as well as the operational costs of the WWTPs. The OC used for nitrogen and carbon removal (Table 4.8) was 53.36 g O_2 $d^{-1}$and 82.10 g O_2 d^{-1}, respectively. They were 39.40% and 60.61% of oxygen amount used for nitrogen removal and carbon removal, respectively. The ratio of oxygen consumed over nitrogen removed was 1.5 kg O_2 kg N^{-1} versus 0.5 kg O_2 kg COD^{-1}. This oxygen requirement was used to account for each kg of influent nitrogen and influent organic matter.

Table 4.10 Characteristics of parameters based upon the ASM2d model in different compartments

	Influent Wastewater	Acetate to Anaerobic phase	Acetate to 1st Anoxic phase	Solid wastage	Effluent	Units
Flow						
flow	1.44	0.0024	0.0024	0.0748	1.37	[m^3/d]
Composite Variables						
Volatile Fraction						
VSS/TSS ratio	1	0	0	0.949	0.949	[gVSS/gTSS]
Composite Variables						
total suspended solids	114	0	0	5680	12.5	[g/m^3]
volatile suspended solids	114	0	0	5400	11.9	[g/m^3]
total inorganic suspended solids	0	0	0	287	0.631	[g/m^3]
total carbonaceous BOD5	86.6	16900	8450	1110	2.71	[gO_2/m^3]
total COD	410	25600	12800	8050	81.7	[gCOD/m3]
total TKN	64	0	0	244	1.28	[gN/m^3]
total phosphorus	9.18	0	0	194	2.63	[gP/m^3]
Additional Composite Variables						
filtered carbonaceous BOD5	50.3	16900	8450	0.269	0.269	[gO_2/m^3]
particulate carbonaceous BOD5	36.3	0	0	1110	2.44	[gO_2/m^3]
filtered ultimate carbonaceous BOD	76.2	25600	12800	0.408	0.408	[gO_2/m^3]
particulate ultimate carbonaceous BOD	55	0	0	1680	3.7	[gO_2/m^3]
total ultimate carbonaceous BOD	131	25600	12800	1690	4.11	[gO_2/m^3]
filtered COD	144	25600	12800	64.1	64.1	[gCOD/m3]
particulate COD	267	0	0	7990	17.6	[gCOD/m3]
filtered TKN	45.4	0	0	0.749	0.749	[gN/m^3]
particulate TKN	18.7	0	0	243	0.535	[gN/m^3]
total nitrogen	64	0	0	259	15.9	[gN/m^3]
filtered phosphorus	7.05	0	0	2.21	2.21	[gP/m^3]
particulate phosphorus	2.13	0	0	192	0.422	[gP/m^3]
State Variables						
Inorganic Suspended Solids						
inert inorganic suspended solids	0	0	0	0.0364	0.00008	[g/m^3]
Organic Variables						
soluble inert organic material	67.4	0	0	63.7	63.7	[gCOD/m^3]
fermentable readily biodegradable substrate	33.9	0	0	0.382	0.382	[gCOD/m^3]
volatile fatty acids	42.3	25600	12800	0.0255	0.0255	[gCOD/m^3]
particulate inert organic material	212	0	0	6300	13.9	[gCOD/m^3]
slowly biodegradable substrate	55	0	0	25.4	0.0559	[gCOD/m^3]
active heterotrophic biomass	0	0	0	1030	2.26	[gCOD/m^3]
active autotrophic biomass	0	0	0	149	0.328	[gCOD/m^3]
active poly-P accumulating biomass	0	0	0	479	1.05	[gCOD/m^3]
unbiodegradable particulates from cell decay	0	0	0	0	0	[gCOD/m^3]

Table 4.10 (cont.) Charaterise of parameters based upon the ASM2d model in different compartments

	Influent Wastewater	Acetate to Anaerobic phase	Acetate to 1st Anoxic	Solid wastage	Effluent	Units
internal cell storage product	0	0	0	0	0	[gCOD/m^3]
poly-hydroxy-alkanoates (PHA)	0	0	0	0.832	0.00183	[gCOD/m^3]
stored glycogen	0	0	0	0	0	[gCOD/m^3]
Dissolved Oxygen						
dissolved oxygen	0	0	0	6	6	[gO_2/m^3]
Phosphorus Compounds						
soluble ortho-phosphate	6.8	0	0	2.2	2.2	[gP/m^3]
stored polyphosphate	0	0	0	95.7	0.21	[gP/m^3]
stored polyphosphate (releasable)	0	0	0	0	0	[gP/m^3]
Nitrogen Compounds						
free and ionized ammonia	38.3	0	0	0.1	0.1	[gN/m^3]
soluble biodegradable organic nitrogen	0	0	0	0	0	[gN/m^3]
particulate biodegradable organic nitrogen	0	0	0	0	0	[gN/m^3]
nitrate and nitrite	0	0	0	14.6	14.6	[gN/m^3]
soluble unbiodegradable organic nitrogen	0	0	0	0	0	[gN/m^3]
dinitrogen	0	0	0	21.6	21.6	[gN/m^3]
alkalinity	5	0	0	2.95	2.95	[mole/m^3]
Model Stoichiometry						
Organic Fractions						
XCOD/VSS ratio	2.34	2.2	2.2	1.48	1.48	[gCOD/gVSS]
BOD5/BODultimate ratio	0.66	0.66	0.66	0.66	0.66	[-]
Nutrient Fractions						
N content of soluble inert organic material	0.07	0.01	0.01	0.01	0.01	[gN/gCOD]
N content of readily biodegradable substrate	0	0	0	0	0	[gN/gCOD]
N content of fermentable readily biodegradable substrate	0.07	0.03	0.03	0.03	0.03	[gN/gCOD]
N content of particulate inert organic material	0.07	0.02	0.02	0.02	0.02	[gN/gCOD]
N content of slowly biodegradable substrate	0.07	0.04	0.04	0.04	0.04	[gN/gCOD]
N content of active heterotrophic biomass	0.07	0.07	0.07	0.07	0.07	[gN/gCOD]
N content of active autotrophic biomass	0.07	0.07	0.07	0.07	0.07	[gN/gCOD]
N content of active poly-P accumulating biomass	0.07	0.07	0.07	0.07	0.07	[gN/gCOD]
P content of fermentable readily biodegradable substrate	0.0073	0.01	0.01	0.01	0.01	[gP/gCOD]
P content of particulate inert organic material	0.008	0.01	0.01	0.01	0.01	[gP/gCOD]
P content of slowly biodegradable substrate	0.008	0.01	0.01	0.01	0.01	[gP/gCOD]
P content of active heterotrophic biomass	0.02	0.02	0.02	0.02	0.02	[gP/gCOD]
P content of active autotrophic biomass	0.02	0.02	0.02	0.02	0.02	[gP/gCOD]
P content of active poly-P accumulating biomass	0.02	0.02	0.02	0.02	0.02	[gP/gCOD]

Table 4.11 Clarification of parameters based upon the ASM2d model in all compartments and in effleunt

Model information	Anaerobic phase, R1		1st Anoxic phase, R2		2nd Anoxic phase, R3		Aerobic phase, R4		Effluent	Units
	Input	Overflow	Input	Overflow	Input	Overflow	Input	Overflow		
Flow										
flow	2.8824	2.8824	4.1048	2.6648	4.1048	4.1048	4.1048	2.6648	1.3700	[m^3/d]
Composite Variables										
Volatile Fraction										
VSS/TSS ratio	0.963	0.974	0.959	0.962	0.957	0.953	0.953	0.949	0.949	[gVSS/gTSS]
Composite Variables										
total suspended solids	1420	1460	2710	2730	2740	2770	2770	2770	12.5	[g/m^3]
volatile suspended solids	1370	1420	2600	2630	2630	2640	2640	2630	11.9	[g/m^3]
total inorganic suspended solids	52.4	38	112	105	117	130	130	140	0.631	[g/m^3]
total carbonaceous BOD5	343	344	577	571	561	555	555	541	2.71	[gO_2/m^3]
total COD	2210	2230	3970	3970	3960	3970	3970	3950	81.7	[gCOD/m^3]
total TKN	101	92.7	138	138	131	132	132	119	1.28	[gN/m^3]
total phosphorus	52.3	53	95	95.4	95.5	96	96	95.8	2.63	[gP/m^3]
Additional Composite Variables										
filtered carbonaceous BOD5	45	40.2	33.2	11.6	7.65	1.08	1.08	0.269	0.269	[gO_2/m^3]
particulate carbonaceous BOD5	298	304	544	559	553	554	554	541	2.44	[gO_2/m^3]
filtered ultimate carbonaceous BOD	68.2	60.9	50.3	17.6	11.6	1.64	1.64	0.407	0.408	[gO_2/m^3]
particulate ultimate carbonaceous BOD	451	460	825	847	838	839	839	820	3.7	[gO_2/m^3]
total ultimate carbonaceous BOD	519	521	875	865	849	841	841	820	4.11	[gO_2/m^3]
filtered COD	135	127	116	83	76.6	66.5	66.5	64.7	64.1	[gCOD/m^3]
particulate COD	2080	2100	3850	3890	3890	3910	3910	3890	17.6	[gCOD/m^3]
filtered TKN	33.1	30.7	21.8	20.8	13.8	13.3	13.3	0.754	0.749	[gN/m^3]
particulate TKN	67.9	62	116	117	118	118	118	118	0.535	[gN/m^3]
total nitrogen	101	92.7	142	139	137	134	134	134	15.9	[gN/m^3]
filtered phosphorus	10.5	15.6	11.6	14	9.88	5.65	5.65	2.28	2.21	[gN/m^3]
particulate phosphorus	41.8	37.3	83.4	81.4	85.6	90.3	90.3	93.5	0.422	[gN/m^3]
State Variables										
Inorganic Suspended Solids										
inert inorganic suspended solids	0.0085	0.00862	0.0169	0.017	0.0173	0.0175	0.0175	0.0177	0.00008	[g/m^3]

Table 4.11 (cont.) Clarification of parameters based upon the ASM2d model in all compartments and in effleunt

Model information	Anaerobic phase, R1		1st Anoxic phase, R2		2nd Anoxic phase, R3		Aerobic phase, R4		Effluent	Units
	Input	Overflow	Input	Overflow	Input	Overflow	Input	Overflow		
Organic Variables										
soluble inert organic material	66.3	66.3	65.5	65.4	65	64.8	64.8	64.3	63.7	[gCOD/m^3]
fermentable readily biodegradable substrate	18.7	8.89	6.35	3.65	2.5	0.98	0.98	0.381	0.382	[gCOD/m^3]
volatile fatty acids	49.4	52	44	14	9.08	0.663	0.663	0.0256	0.0255	[gCOD/m^3]
particulate inert organic material	1630	1640	3030	3040	3050	3070	3070	3070	13.9	[gCOD/m^3]
slowly biodegradable substrate	44.2	41	36.3	33.5	26.1	22.9	22.9	12.4	0.0559	[gCOD/m^3]
active heterotrophic biomass	247	247	480	495	497	502	502	501	2.26	[gCOD/m^3]
active autotrophic biomass	34.4	34.5	68.7	68.7	70.1	70.1	70.1	72.7	0.328	[gCOD/m^3]
active poly-P accumulating biomass	112	112	221	223	227	231	231	233	1.05	[gCOD/m^3]
unbiodegradable particulates from cell decay	0	0	0	0	0	0	0	0	0	[gCOD/m^3]
internal cell storage product	0	0	0	0	0	0	0	0	0	[gCOD/m^3]
poly-hydroxy-alkanoates (PHA)	13.7	26	18.5	27.3	17.9	13.2	13.2	0.405	0.00183	[gCOD/m^3]
stored glycogen	0	0	0	0	0	0	0	0	0	[gCOD/m^3]
Dissolved Oxygen										
dissolved oxygen	0.00436	0.0000256	1.79	0.00871	2.11	0.0116	0.0116	6	6	[gO_2/m^3]
Phosphorus Compounds										
soluble ortho-phosphate	10.4	15.5	11.6	14	9.86	5.64	5.64	2.27	2.2	[gP/m^3]
stored polyphosphate	17.5	12.7	37.4	34.9	39	43.4	43.4	46.6	0.21	[gP/m^3]
stored polyphosphate (releasable)	0	0	0	0	0	0	0	0	0	[gP/m^3]
Nitrogen Compounds										
free and ionized ammonia	29.2	29.8	20.9	20.1	13.1	12.6	12.6	0.0996	0.1	[gN/m^3]
soluble biodegradable organic nitrogen	0	0	0	0	0	0	0	0	0	[gN/m^3]
particulate biodegradable organic nitrogen	0	0	0	0	0	0	0	0	0	[gN/m^3]
nitrate and nitrite	0.315	0.025	4.37	0.63	5.53	2.17	2.17	14.6	14.6	[gN/m^3]
soluble unbiodegradable organic nitrogen	0	0	0	0	0	0	0	0	0	[gN/m^3]
dinitrogen	8.04	8.33	12.3	16.1	18	21.6	21.6	21.7	21.6	[gN/m^3]
Alkalinity										
alkalinity	4.98	4.92	4.33	4.97	4.26	4.67	4.67	2.95	2.95	[mole/m^3]
Metal Precipitates										
metal-hydroxides	0.0000596	0.00004	0.000192	0.000119	0.000172	0.000168	0.000168	0.00027	1.21E-06	[g/m^3]
metal-phosphates	0.000854	0.000894	0.00159	0.00171	0.00166	0.00169	0.00169	0.00157	7.11E-06	[g/m^3]

Table 4.11 (cont.) Clarification of parameters based upon the ASM2d model in all compartments and in effleunt

Model information	Anaerobic phase, R1		1st Anoxic phase, R2		2nd Anoxic phase, R3		Aerobic phase, R4		Effluent	Units
	Input	Overflow	Input	Overflow	Input	Overflow	Input	Overflow		
Model Stoichiometry										
Organic Fractions										
XCOD/VSS ratio	1.52	1.48	1.48	1.48	1.48	1.48	1.48	1.48	1.48	[gCOD/gVSS]
BOD5/BODultimate ratio	0.66	0.66	0.66	0.66	0.66	0.66	0.66	0.66	0.66	[-]
Nutrient Fractions										
N content of soluble inert organic material	0.0404	0.01	0.01	0.01	0.01	0.01	0.01	0.01	0.01	[gN/gCOD]
N content of readily biodegradable substrate	0	0	0	0	0	0	0	0	0	[gN/gCOD]
N content of fermentable readily biodegradable substrate	0.0661	0.03	0.03	0.03	0.03	0.03	0.03	0.03	0.03	[gN/gCOD]
N content of particulate inert organic material	0.0232	0.02	0.02	0.02	0.02	0.02	0.02	0.02	0.02	[gN/gCOD]
N content of slowly biodegradable substrate	0.0586	0.04	0.04	0.04	0.04	0.04	0.04	0.04	0.04	[gN/gCOD]
N content of unbiodegradable particulates from cell decay	0	0	0	0	0	0	0	0	0	[gN/gCOD]
N content of active heterotrophic biomass	0.07	0.07	0.07	0.07	0.07	0.07	0.07	0.07	0.07	[gN/gCOD]
N content of active autotrophic biomass	0.07	0.07	0.07	0.07	0.07	0.07	0.07	0.07	0.07	[gN/gCOD]
N content of active poly-P accumulating biomass	0.07	0.07	0.07	0.07	0.07	0.07	0.07	0.07	0.07	[gN/gCOD]
P content of soluble inert organic material	0	0	0	0	0	0	0	0	0	[gP/gCOD]
P content of readily biodegradable substrate	0	0	0	0	0	0	0	0	0	[gP/gCOD]
P content of fermentable readily biodegradable substrate	0.00756	0.01	0.01	0.01	0.01	0.01	0.01	0.01	0.01	[gP/gCOD]
P content of particulate inert organic material	0.00987	0.01	0.01	0.01	0.01	0.01	0.01	0.01	0.01	[gP/gCOD]
P content of slowly biodegradable substrate	0.00876	0.01	0.01	0.01	0.01	0.01	0.01	0.01	0.01	[gP/gCOD]
P content of unbiodegradable particulates from cell decay	0	0	0	0	0	0	0	0	0	[gP/gCOD]
P content of active heterotrophic biomass	0.02	0.02	0.02	0.02	0.02	0.02	0.02	0.02	0.02	[gP/gCOD]
P content of active autotrophic biomass	0.02	0.02	0.02	0.02	0.02	0.02	0.02	0.02	0.02	[gP/gCOD]
P content of active poly-P accumulating biomass	0.02	0.02	0.02	0.02	0.02	0.02	0.02	0.02	0.02	[gP/gCOD]

4.4 CONCLUSIONS

Reducing parameter subset sizes in ASM2d calibration in EBPR treatment processes has been addressed by evaluating a novel calibration approach. The parameter significant ranking showed that the parameters for PAOs were among the most influential parameters on the model outputs. The parameter sensitivity analysis and the parameter subsets are related to data available for calibration. Sensitivity analysis, used to quantify the magnitude of the dependency of model prediction on particular parameters is similar to the method proposed by Brun et al. (2001). The sensitivity analysis is also applied to the experience-based approach; however, there is no detailed information on sensitivity analysis and parameter selection. Fixed subsets for parameter selection require a high degree of specialization without a mathematical/statistical approach. Fixed parameter subsets are the limiting factor in the experience-based approach. Parameter values of one WWTP may not be applicable to other WWTPs. The new calibration analysis uses experimental results to select parameters of a subset size with manual calibration. This is done while not using the identifiability approach. In contrast the other identifiability methodology to select parameter subset requires high computational demand to develop the collinearity index (γ) and the determinant measure (ρ) (Brun et al., 2001). The parameter values calculated for γ and ρ were based upon sensitivity analysis. This new approach can enable researchers to reduce heavy computation demand and avoids the need to choose the modeling parameters. This is a simplified approach for practical use.

CHAPTER 5:

EFFECT OF DISINTEGRATED SLUDGE IN ENHANCED BIOLOGICAL PHOSPHORUS REMOVAL (EBPR) IN ACTIVATED SLUDGE MUCT SYSTEMS

CHAPTER 5. EFFECT OF DISINTEGRATED SLUDGE IN ENHANCED BIOLOGICAL PHOSPHORUS REMOVAL (EBPR) IN ACTIVATED SLUDGE MUCT SYSTEMS

ABSTRACT

The evaluation of disintegrated sludge (DS) upon enhanced biological phosphorus removal (EBPR) processes was completed using Activated Sludge Model No. 2d (ASM2d) modeling. Successful calibration of phosphorus accumulating organisms (PAOs) and autotrophic mechanisms was achieved. Calibrated parameters included: Y_{PAO}, Y_{PO4}, Y_{PHA}, q_{PHA}, q_{PP}, μ_{PAO}, b_{PAO}, b_{PP}, b_{PHA}, K_{PS}, Y_A, μ_{AUT}, b_{AUT}, $K_{O2\ AUT}$, and $K_{NH4\ AUT}$. The first ten calibrated parameters were used to investigate PAOs. Inclusion of DS resulted in a higher influent phosphorus content (12.9 g P m^{-3}) than without DS (10.40 g P m^{-3}). Additionally, the influent phosphorus to acetate (S_A) ratio (0.26 g P g^{-1} COD) with influent DS was higher than without DS (0.21 g P g^{-1} COD). Influent phosphorus contents were 0.83% of TSS with DS and 0.73 % of TSS without DS. The influence of DS components upon phosphorus removal is not only based upon phosphorus and S_A, but also it is related to fermentable biodegradable products (S_F), and slowly biodegradable products (X_S). Furthermore, it is related to different phosphorus to COD (P/COD) ratios within influent DS. Varying carbon sources i.e., S_A, S_F, and X_S, resulted in P/COD ratios of 1.11 g P g^{-1} COD, 0.22 g P g^{-1} COD, 0.66 g P g^{-1} COD, respectively. Varying the carbon sources influenced to specific phosphorus release rates (SPRR) which were different depending upon the particular carbon source, i.e., S_A, S_F, and X_S. In each of these instances, SPRR for influent DS were 0.834 mg P g^{-1} VSS_{PAOs} h^{-1}, 3.9 mg P g^{-1} VSS_{PAOs} h^{-1}, and 0.31 mg P g^{-1} VSS_{PAOs} h^{-1}, respectively. In addition, paired-t test results demonstrated that DS components significantly enhanced biological phosphorus removal. Paired-t tests at 95% confident level to evaluate the significance of DS components to phosphorus release and effluent total phosphorus conditions showed significant differences. Four important DS components to EBPR are phosphorus, S_A, S_F, and X_S. This is reflected by p-value < 0.00001. In addition, the mean values of phosphorus release with and without DS showed a significant difference. Inclusion of

DS enhances phosphorus release. Higher carbon sources utilization and phosphorus release by PAOs was seen in the presence of DS than without. As a result, Y_{PAO} and Y_{PHA} values were different when utilizing DS and than without. Y_{PAO} (0.64 g COD g^{-1} COD), with DS was higher than without (0.61 g COD g^{-1} COD). Y_{PHA} (0.26 g COD g^{-1} P) with DS also was higher than without (0.24 g COD g^{-1} P). In addition those values change with temperature. Verification at 23°C was different than calibration (17°C). The last five calibrated parameters (Y_A, μ_{AUT}, b_{AUT}, $K_{O2\ AUT}$, and $K_{NH4\ AUT}$) used to calibrate autotrophs. Those calibrated parameter values under both conditions were similar. As a result, it is concluded that DS was not significant to autotrophic metabolism.

Keywords: ASM2d, calibration, disintegrated sludge, enhanced biological phosphorus removal (EBPR), PAOs, verification

5.1 INTRODUCTION

Eutrophication is a significant environmental problem which is due to the increase of nutrients in the aqueous environment. To prevent this problem, phosphorus levels need to be controlled as this is the crucial nutrient to be considered in relation to the algae blooms (Comeau et al., 1987). Generally phosphorus comes from various sources. Wastewater treatment plants (WWTPs) can act as a major contributor. In order to prevent phosphorus discharges at point sources into the environment, biological processes have been used in WWTPs (Henze et al., 2008). Enhanced biological phosphorus removal (EBPR) processes have been widely used in activated sludge WWTPs for the prevention of eutrophication (Mino et al., 1998; Seviour et al., 2003; Soejima et al., 2008). Modified University of Cape Town (MUCT) processes are some of the most effective EBPR processes. They are designed to maintain truly anaerobic conditions (Hamada et al., 2006; Vaiopoulou and Aivasidis, 2008). To study EBPR, Activated Sludge Model No. 2d (ASM2d) (Henze et al., 1999) is an important model to simulate the biological mechanisms in the EBPR systems. The ASM2d model can express the integrated mechanisms of phosphorus accumulating organisms (PAOs) under aerobic, anaerobic and anoxic conditions.

To facilitate and optimize phosphorus removal efficiency in EBPR, carbon sources are monitored and sometimes added to the biological WWTPs as they are most important to the performance of the systems (Kampas et al., 2009; Zheng et al., 2009). Disintegrated sludge (DS) can act as an EBPR carbon source to increase the efficiency of EBPR (Onyeche et al., 2002; Dewil et al., 2006). DS is comprised in part of soluble chemical oxygen demand (SCOD) such as: acetic acid and other volatile fatty acids (VFAs), total phosphate (TP), protein, DNA, polysaccharide and carbohydrate (Schmitz et al., 2000; Kampas et al., 2007). Protein is the predominant component among the various carbon compounds (Wang et al., 2006). In addition, carbon sources generated from mechanical disintegration can increase digestion efficiency in the wastewater pre-treatment processes (Tiehm et al., 2001). Also, an advantage of sludge disintegration in aerobic sequential batch reactors (SBR) is seen in improvement in chemical oxygen demand (COD) and total nitrogen (TN) removal. The magnitudes of increase in these values

were reported as 81% and 17-66%, respectively (Zhang et al., 2007). In biological nutrient removal (BNR) systems, increasing soluble chemical oxygen demand (SCOD) by adding disintegrated sludge has improved phosphorus release under anaerobic conditions. The observed increase was from 4.3 g m^{-3} PO_4–P to 14.9 g m^{-3} PO_4–P (Kampas et al., 2009). The increase in phosphorus release in anaerobic phase is due to utilization of VFAs and SCOD (Kampas et al., 2009). In addition, the study of Carucci et al. (1999) concluded that increasing phosphorus release is due to VFAs and fermentable organics (S_F). The result is that internal carbon sources from sludge disintegration are likely to be relevant substances for improvement of enhanced phosphorus removal efficiency. Therefore, understanding the microbiological mechanisms and identifying significant DS components is a feasible tool for investigating the effects of DS on the efficiency of phosphorus removal. These methods of investigation were implemented with mathematical modeling and statistical analysis (Deo et al., 2009; Chi et al., 2010).

The purpose of this research was to study the influence of DS upon phosphorus removal efficiency. This study investigated effects of DS on PAOs mechanisms. Four procedures were developed. First, ASM2d parameters which rely on wastewater influent characteristics and plant design as well as the parameters' ranges were calculated. Second, iteration procedures in the calibration methodology were used to fit the ASM2d modeling to the observed results. This procedure relied on sensitivity parameter ranking. Third, the means of the observed results were calculated and compared to simulated results. These comparisons were used to determine the essential components of DS to phosphorous removal. Finally, verification of the calibrated model was done in order to demonstrate that the experimental data agreed with observed results in the calibration.

5.2 MATERIALS AND METHODS

5.2.1 The MUCT pilot scale to EBPR processes

The experiments were done with the MUCT pilot scale activated sludge plant. The pilot scale consisted of two activated sludge plants in parallel, one using DS as carbon source in the influent (test) and no influent DS (control), respectively. A schematic of the reactor configuration in test is shown in Figure 5.1. The activated sludge process consisted of five reactors in series including anaerobic, 1st anoxic, 2nd anoxic, aerobic phases and a clarifier. They had effective volumes of 0.125 m^3, 0.120 m^3, 0.230 m^3, 0.550 m^3 and 0.334 m^3, respectively. The operating conditions included influent wastewater flow rate (Q_{IN} = 0.06 m^3 h^{-1}), return activated sludge flow rate (Q_R = 0.051 m^3 h^{-1}), anoxic recirculation flow rate (Q_1 = 0.06 m^3 h^{-1}) and aerobic recirculation flow rate (Q_2 = 0.06 m^3 h^{-1}). The sludge retention time (SRT) in test and control experiments was 15-days and 23-days, respectively. DS was fed to the test series only. In order to develop EBPR, acetic acid was fed in the influent at an equivalent level (42.60 g COD m^{-3}) in both the test and control (acetate concentrations in municipal wastewater were not high enough to enable EBPR). The amount of sludge that was disintegrated was equivalent to 5.88% of return activated sludge (RAS) flow increasing the volatile fatty acids (VFAs) in the influent by 2.0 g COD m^{-3}. Consequently, the acetate dose was reduced by 2.0 mg for every liter of wastewater in test. In addition, acetate was added to anoxic phase in order to maintain it's influent concentration of anoxic reactor at 21.30 g COD m^{-3}. Influent, anaerobic stage, aerobic stage and effluent were sampled on a daily basis. The characterization of influent and experimental results in control (without disintegrated sludge, DS) and test (with DS) at 17°C is shown in Table 3.9. Average temperature was maintained at 17°C.

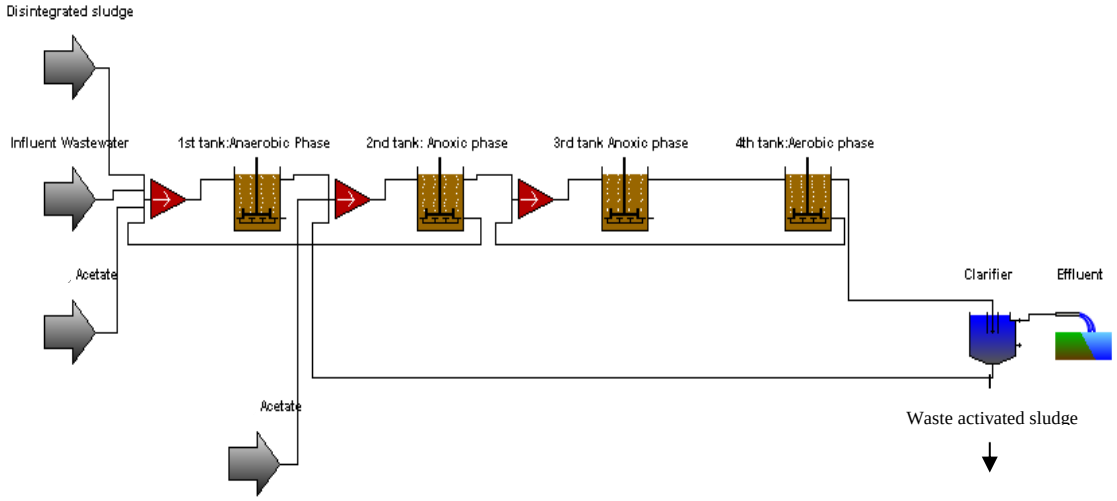

Figure 5.1 A schematic diagram of the activated sludge MUCT in test (DS)

5.2.2 Sensitivity analysis

Sensitivity analysis yields the relative importance of parameters over the range of model inputs calculated to evaluate parameters existing in ASM2d. It determines the most sensitive parameters impacting the performance of model output (Soejima et al., 2008). The data sets used in the calculation of the parameter significance ranking included the following concentrations: total chemical oxygen demand (TCOD), total nitrogen (TN), total phosphorus (TP), orthophosphate (PO_4), total suspended solid (TSS), mixed liquor suspended solid (MLSS), ammonium (NH_4), and nitrate (NO_3). The mathematical sensitivity calculations were shown in Equation (4.2). The implementation of sensitivity was described in section 4.2.2.

5.2.3 Iteration methodology

The large number of parameters in the ASM2d model requires high computational power. Also the calibration accuracy can be compromised if all parameters are used in simulation (Libelli et al., 2001). Accordingly, the parameters were categorized with the iteration method into specific groups such as nitrification, denitrification and phosphorus removal. This is an effective solution which avoids the aforementioned limitations. It is based on the experimental data available. GPS-X (Hydromantis, Inc., Hamilton, Canada) was used as the iteration tool. Mathematical iteration of the parameter significance ranking was conducted. The iteration steps included in the calibration methodology are shown in step 4 (Figure 4.2). A stepwise manual iteration methodology was specifically adapted for EBPR. The ASM2d modeling was calibrated with the parameter significance ranking to fit the observed results. The iterative algorithm was re-evaluated until the sensitivity parameter no longer affected the simulation output.

5.2.4 Statistical analysis

The difference in the means of two samples observed before and after treatment is an important statistic and can be used to produce a 95% confidence interval. A paired t-test was used to investigate the statistical significance of components of DS upon observed phosphorus removal (Deo and Halden, (2009); Viau E, Peccia J. (2009); Chi et al., (2010); Lai et al., (2010); Qi et al., (2010)). The assumptions are that the paired differences are independent and identically normally distributed (Goulden, 1956). The specific purpose was to determine if there was a difference between observed results and reported parameter values for experiments using and not using DS as an influent component. A pooled variance was generated. Application of this analysis was to identify the significant components in DS affecting EBPR. Also the mean differences between DS (test) and without DS (control) were observed.

5.3 RESULTS AND DISCUSSION

5.3.1 Wastewater characteristics

The ASM2d simulation was completed under steady state conditions. The values of the ASM2d parameters were defined in the first step of calibration (Figure 4.2). The influent characteristics measured in the test and control consisted of: dissolved oxygen (S_{O2in}), fermentation products (S_{Ain}), readily biodegradable substrate (S_{Fin}), inert soluble organic substrates (S_{Iin}), ammonium (S_{NH4in}), nitrate (S_{NO3in}), phosphate (S_{PO4in}), nitrogen (S_{N2in}), inert non-biodegradable organics (X_{Iin}), slowly biodegradable substrate (X_{Sin}), phosphorus-accumulating organisms (X_{PAOin}), stored polyphosphate of PAOs (X_{PPin}), and organic storage products of PAOs (X_{PHAin}). Acetic acid was fed to the anaerobic phase in both the test and control in order to develop EBPR. DS was fed only to the anaerobic phase of the test trial. The characterization of wastewater used is shown in Table 3.9. In addition, model information of influent components based upon ASM2d is summarized in Table 5.1.

Table 5.1 Model information of influent components of test (with DS) and control (without DS) experiments at 17°C with ASM2d calibration

Model Information	**Experimental results**			
	Test		**Control**	
Flow				
flow	2.88	[m^3/d]	2.88	[m^3/d]
Composite Variables				
Volatile Fraction				
VSS/TSS ratio	0.947	[gVSS/gTSS]	0.963	[gVSS/gTSS]
Composite Variables				
total suspended solids	1550	[g/m^3]	1420	[g/m^3]
volatile suspended solids	1470	[g/m^3]	1370	[g/m^3]
total inorganic suspended solids	81.8	[g/m^3]	52.4	[g/m^3]
total carbonaceous BOD5	370	[gO_2/m^3]	343	[gO_2/m^3]
total COD	2370	[gCOD/m^3]	2210	[gCOD/m^3]
total TKN	106	[gN/m^3]	101	[gN/m^3]
total phosphorus	64.8	[gP/m^3]	52.3	[gP/m^3]
Additional Composite Variables				
filtered carbonaceous BOD5	48.4	[gO_2/m^3]	45	[gO_2/m^3]
particulate carbonaceous BOD5	321	[gO_2/m^3]	298	[gO_2/m^3]
filtered ultimate carbonaceous BOD	73.4	[gO_2/m^3]	68.2	[gO_2/m^3]
particulate ultimate carbonaceous BOD	487	[gO_2/m^3]	451	[gO2/m3]
total ultimate carbonaceous BOD	561	[gO_2/m^3]	519	[gO_2/m^3]
filtered COD	143	[gCOD/m^3]	135	[gCOD/m^3]
particulate COD	2230	[gCOD/m^3]	2080	[gCOD/m^3]
filtered TKN	33.4	[gN/m^3]	33.1	[gN/m^3]
particulate TKN	72.4	[gN/m^3]	67.9	[gN/m^3]
total nitrogen	106	[gN/m^3]	101	[gN/m^3]
filtered phosphorus	13.1	[gP/m^3]	10.5	[gP/m^3]
particulate phosphorus	51.6	[gP/m^3]	41.8	[gP/m^3]
State Variables				
Inorganic Suspended Solids				
inert inorganic suspended solids	5.06	[g/m^3]	0.0085	[g/m^3]
Organic Variables				
soluble inert organic material	70.1	[gCOD/m^3]	66.3	[gCOD/m^3]
readily biodegradable substrate	0	[gCOD/m^3]	0	[gCOD/m^3]
fermentable readily biodegradable substrate	24	[gCOD/m^3]	18.7	[gCOD/m^3]
volatile fatty acids	49.4	[gCOD/m^3]	49.4	[gCOD/m^3]
particulate inert organic material	1740	[gCOD/m^3]	1630	[gCOD/m^3]
slowly biodegradable substrate	46.2	[gCOD/m^3]	44.2	[gCOD/m^3]
active heterotrophic biomass	258	[gCOD/m^3]	247	[gCOD/m^3]
active autotrophic biomass	35.6	[gCOD/m^3]	34.4	[gCOD/m^3]
active poly-P accumulating biomass	131	[gCOD/m^3]	112	[gCOD/m^3]
unbiodegradable particulates from cell decay	0	[gCOD/m^3]	0	[gCOD/m^3]
internal cell storage product	0	[gCOD/m^3]	0	[gCOD/m^3]
poly-hydroxy-alkanoates (PHA)	16.9	[gCOD/m^3]	13.7	[gCOD/m^3]
stored glycogen	0	[gCOD/m^3]	0	[gCOD/m^3]
Dissolved Oxygen				
dissolved oxygen	0.00406	[gO_2/m^3]	0.00436	[gO_2/m^3]
Phosphorus Compounds				
soluble ortho-phosphate	12.9	[gP/m^3]	10.4	[gP/m^3]
stored polyphosphate	25.6	[gP/m^3]	17.5	[gP/m^3]
stored polyphosphate (releasable)	0	[gP/m^3]	0	[gP/m^3]

Table 5.1 (cont.) Characterization of influent components of test (with DS) and control (without DS) experiments at 17°C with ASM2d calibration

Model Information	**Experimental conditions**			
	Test		**Control**	
Nitrogen Compounds				
free and ionized ammonia	29.3	[gN/m^3]	29.2	[gN/m^3]
soluble biodegradable organic nitrogen	0	[gN/m^3]	0	[gN/m^3]
particulate biodegradable organic nitrogen	0	[gN/m^3]	0	[gN/m^3]
nitrate and nitrite	0.179	[gN/m^3]	0.315	[gN/m^3]
soluble unbiodegradable organic nitrogen	0	[gN/m^3]	0	[gN/m^3]
dinitrogen	8.19	[gN/m^3]	8.04	[gN/m^3]
Alkalinity				
alkalinity	5	[mole/m^3]	4.98	[mole/m^3]
Metal Precipitates				
metal-hydroxides	5.96E-07	[g/m^3]	0.0000596	[g/m^3]
metal-phosphates	0.0000117	[g/m^3]	0.000854	[g/m^3]
Model Stoichiometry				
Organic Fractions				
XCOD/VSS ratio	1.52	[gCOD/gVSS]	1.52	[gCOD/gVSS]
BOD5/BODultimate ratio	0.659	[-]	0.66	[-]
Nutrient Fractions				
N content of soluble inert organic material	0.0388	[gN/gCOD]	0.0404	[gN/gCOD]
N content of readily biodegradable substrate	0	[gN/gCOD]	0	[gN/gCOD]
N content of fermentable readily biodegradable substrate	0.0581	[gN/gCOD]	0.0661	[gN/gCOD]
N content of particulate inert organic material	0.023	[gN/gCOD]	0.0232	[gN/gCOD]
N content of slowly biodegradable substrate	0.0587	[gN/gCOD]	0.0586	[gN/gCOD]
N content of unbiodegradable particulates from cell decay	0	[gN/gCOD]	0	[gN/gCOD]
N content of active heterotrophic biomass	0.07	[gN/gCOD]	0.07	[gN/gCOD]
N content of active autotrophic biomass	0.07	[gN/gCOD]	0.07	[gN/gCOD]
N content of active poly-P accumulating biomass	0.07	[gN/gCOD]	0.07	[gN/gCOD]
P content of soluble inert organic material	0	[gP/gCOD]	0	[gP/gCOD]
P content of readily biodegradable substrate	0	[gP/gCOD]	0	[gP/gCOD]
P content of fermentable readily biodegradable substrate	0.00859	[gP/gCOD]	0.00756	[gP/gCOD]
P content of particulate inert organic material	0.00988	[gP/gCOD]	0.00987	[gP/gCOD]
P content of slowly biodegradable substrate	0.00903	[gP/gCOD]	0.00876	[gP/gCOD]
P content of unbiodegradable particulates from cell decay	0	[gP/gCOD]	0	[gP/gCOD]
P content of active heterotrophic biomass	0.02	[gP/gCOD]	0.02	[gP/gCOD]
P content of active autotrophic biomass	0.02	[gP/gCOD]	0.02	[gP/gCOD]
P content of active poly-P accumulating biomass	0.02	[gP/gCOD]	0.02	[gP/gCOD]

5.3.2 Default values and ranges of parameters

The determination of model parameters is time consuming process. Henze et al (1999) suggested that the default values reported in a previous study should be assigned to the model parameters. Differences in the default values for the distribution of stoichiometric and kinetic parameters used in activated sludge models was varied from uncalibrated simulations (Sedran et al., 2006). The default values with the appropriate ranges based on published literature values are shown in Table 3.11. The values of the ASM2d parameters were used as the default values in the calibration. The specific range of the parameters was obtained from the values of ASM2d parameters gained from experience with WWTPs. In these studies, the ranges of values were used to limit the upper and lower bounds of parameter calibration with the assumption of uniform distribution of values. Other researchers proposed a method to define the ranges of values based on uncertainty classes (cl) and prior uncertainty ($\Delta\theta$) which were estimated from the data available (Brun, et al., 2002). The fundamental uniform distribution assumption is that none of the possible outcomes is more or less likely than any other (Helen, 1985). The uniform distribution assumption applies to continuous random variables, i.e., variables values obtained within a specified range. Constant values of the kinetic and stoichiometry parameters were obtained from specific experiments and literature (Smolders et al. (1995); Barker and Dold (1997); Henze et al. (1999); Dudley et al. (2002); Penya-Roja et al. (2002); Lopez and Morgenroth (2003); Manga et al. (2003); Ferrer et al. (2004); Schuler (2005); García-Usach et al. (2006); Insel et al. (2006); Sin et al. (2008)).

5.3.3 Sensitivity calculation

The parameter significance ranking of the resulting sensitivity analysis was based on the total number of model outputs. The values produced by the sensitivity analysis are produced in descending order of their effects in modeling observed results. Determination of significant parameters is based on those parameters having square roots of mean squared of sensitivities higher than 0. The parameter subset under these studies was reduced to the top 30 as shown in Table 4.2. These 30 parameters were used

to calibrate the ASM2d mode and to do verification of experimental results. Sensitivity parameter ranking was studied by Weijers and Vanrolleghem (1997). They introduced the concept of using scale sensitivity coefficients larger than 0.2. The study included 11 parameters for calibrating Activated Sludge Model No. 1 (ASM1) to full-scale plant data. In the study of Soejima et al. (2008), only Y_{PAO} and Y_{PO4} were significant parameters affecting simultaneous nitrogen and phosphorus removal. Their data sets measured NO_3 and PO_4 under anaerobic/aerobic/anoxic processes. An Aquarium programme was the experimental tool used. In agreement with Brun et al. (2002), PAOs played an important role in the dynamics of EBPR processes. Although there was rough agreement, the parameter significance ranking from Brun et al. (2002) is quite different from the current study and that of Ruano et al. (2007). Important factors in this regard include consideration of particular WWTP configurations and operation, and some properties of collected data (Brun et al., 2002). The parameter significance ranking showed that temperature correction coefficients and the parameters for PAOs were among the most influential parameters on the model outputs. In this study, ASM2d was calibrated using an identifiability method to describe nitrogen and phosphorus removal in the Haaren (The Netherlands) WWTP (Brun et al., 2002). PAOs play an important role in the dynamics of the EBPR processes (Ruano et al., 2007). In another application, this approach to ASM2d calibration used an identifiability analysis in a systematic manner. It was applied to EBPR at a full scale WWTP in Switzerland (Ruano et al., 2007). The most effective parameter was $b_{PAO,}$ as presented by Brun et al. (2002). It ranked (27^{th}) in the studies of Ruano et al. 2007, while it ranked (29^{th}) in the current study. Y_{PO4} was the most effective parameter in this study, but in the study of Ruano et al. 2007 it ranked (15^{th}). Brun et al. (2002) excluded it altogether in their study. The parameter, μ_{PAO} was found to be the second most significant parameter in this study. Its importance was equivalent to that found by Brun et al. (2002). The differences in parameter significance rankings among these studies are highly influenced by the information content of data available (Ruano et al., 2007).

5.3.4 Iteration in calibration methodology

A stepwise iteration process was employed in mathematical simulations. The number of iterative steps was 30, which is the same as number of parameters in the sensitivity ranking. It was used to evaluate the measured output. The experimental data set for calibration included NH_4 and TP in effluent and orthophosphate phosphorus release in the anaerobic phase. These values are shown in Table 3.9. The application of the sensitivity analysis was used for simulations in order to fit the observed results. The most effective parameter was found, followed by the subsequent 29 parameters included in the sensitivity parameter ranking. The iteration of experimental data set values was initiated with the default parameter values. The simulation was carried out under steady state conditions. The effluent NH_4 was the first experimental data set used to investigate autotrophic activity. Iterations through the sensitivity parameters were done in order to fit the results of simulation modeling to the observed values in data sets. The resulting calibrations with and without DS have the same calibrated parameters as shown in Table 5.2. The calibrated ASM2d parameters without DS in Table 5.2 are similar to values shown in Table 4.3, as the calibration was done under the same conditions.

Table 5.2 The values of the calibrated ASM2d parameters

Symbol	Default value (ASM2d)	DS	Without DS	Units
Phosphorus Accumulating Organisms: PAOs				
Y_{PAO}	0.625	0.64	0.61	g COD g^{-1} COD
Y_{PO4}	0.40	0.40	0.40	g P g^{-1} COD
Y_{PHA}	0.20	0.26	0.24	g COD g^{-1} P
q_{PHA}	3.00	3.50	3.50	g X_{PHA} g^{-1} X_{PAO} d^{-1}
q_{PP}	1.50	1.50	1.50	g X_{PP} g^{-1} X_{PAO} d^{-1}
μ_{PAO}	1.00	1.00	1.00	d^{-1}
b_{PAO}	0.20	0.20	0.20	d^{-1}
b_{PP}	0.20	0.20	0.20	d^{-1}
b_{PHA}	0.20	0.20	0.20	d^{-1}
K_{PS}	0.20	0.35	0.35	g P m^{-3}
Autotrophs:				
Y_A	0.24	0.24	0.24	g COD g^{-1} N
μ_{AUT}	1.00	1.20	1.20	d^{-1}
b_{AUT}	0.15	0.05	0.05	d^{-1}
$K_{O2\ AUT}$	0.50	0.50	0.50	g O_2 m^{-3}
$K_{NH4\ AUT}$	1.00	0.15	0.15	g N m^{-3}

To test model fit to experimental data, a Chi-Square test for goodness of fit was done. The null hypothesis (H_0) was that observed and predicted values are unequal. The alternate hypothesis (Ha) was that observed and predicted values have the same distribution. The null hypothesis (H_0) is rejected in favor of the alternate hypothesis (Ha). This is done with a 95% confidence level. Model fitting was done by minimizing the sum of squares of weighted deviations (SSWD) between measured and calculated values (Equation 3.17). The objective function of the sum of the squared weighted errors was constructed based upon weighted non-linear least-square analysis (Fang et al., 2009). In addition, standard error of estimate (SEE) was also observed to measure the accuracy of predictions (Equation 3.18). This is a regression model that minimizes the sum of squared deviation of prediction (Irwin, 1949). A variation of sum of squares arises from (1) range of applicability of the protocols, (2) technical limitations of tools/sensors for data collection, (3) limitations in transferring lab-scale data to full-scale models, (4) design of data collection (measurement campaigns, ad hoc versus versus mathematical approaches), and (5) complexity of model calibration (limited data versus complex model structure) (Sin et al., 2005). Effluent NH_4, phosphorus (P) release and effluent TP were modeled. Observed and predicted values under both test and control conditions were determined. Comparison showed that paired values were the same. This is shown by low p-values (p-values < 0.005) as shown in Table 5.3. The p-value for goodness of model fit for phosphorus release without DS was a bit higher (p-value = 0.02044). However this is still a strong fit. Furthermore, results of SEE are lower than SSWD results under both test and control conditions, i.e., with and without DS. Thus, it is important to determine the model's goodness of fit.

Table 5.3 Summary of statistical analysis of Chi-Square test for goodness of fit at a 95% confidence level in relation to SSWD, and SEE.

Parameters	**Chi-Square test**							
	DS			**WDS[1]**			**SEE**	
	p-value	*p-value* ≤ *α*	SSWD	*p-value*	*p-value* ≤ *α*	SSWD	**DS**	**WDS[1]**
Effluent NH_4	< 0.00001	ReH	12.86	< 0.00001	ReH	6.21	0.02	0.01
P release	< 0.00001	ReH	15.13	0.02044	ReH	24.95	0.92	0.92
Effluent TP	0.00033	ReH	19.52	0.00483	ReH	10.81	0.75	0.77

Note: ReH = Reject H_0 Hypothesis; *α* to all experiments = 0.05, WDS[1] is a without disintegrated sludge.

Five parameters were used to fit calibrated effluent NH_4 to observed values as shown in Figure 5.2. These parameters included: $K_{NH4\ AUT}$, μ_{AUT}, b_{AUT}, Y_A and $K_{O2\ AUT}$ as shown in Table 5.2. Another study to calibrate NH_4 was based on the removing nutrients under limited aeration conditions in sequencing batch reactors (SBRs) (Insel et al., 2006). $K_{NH4\ AUT}$ and μ_{AUT} were the calibrated parameters. A similar trend was observed in the study of Yagci et al. 2006. In this study, μ_{AUT} was the parameter used to calibrate NH_4 and NO_3 data sets. This study involved an SBR system to do EBPR under different phosphorus/acetate ratios. Also, in the study of Machado et al. (2009), μ_{AUT} is the only calibrated parameter used to represent autotrophic behavior ASM2d modeling and was used to investigate activated sludge anaerobic/anoxic/oxic (A^2/O) EBPR. In addition, autotrophic calibrated parameters (Brun et al., 2002) were b_{AUT}, $K_{NH4\ AUT}$ and μ_{AUT}. As a result (Table 5.2), Y_A values under both test and control conditions were similar to ASM2d (0.24 g COD g^{-1} N). The $K_{O2\ AUT}$ test and control values were also the same as that phosphorus/acetatef ASM2d (0.5 g O_2 m^{-3}). Another study (Dudley et al., 2002) found that the $K_{O2\ AUT}$ (0.4 g O_2 m^{-3}) concentration was lower than in the current study. The previous study was based on data collected from an activated sludge University of Cape Town (UCT) treatment plant at a Swedish sewage works. It was better able to explain heterotrophic usage of VFAs. However μ_{AUT} was set to 1.2 d^{-1} to obtain a reasonable model fit. This was higher than in ASM2d (1.0 d^{-1}) and done to sustain autotrophic growth. $K_{NH4\ AUT}$ (0.15 g N m^{-3}) in test and control experiments was less than that in ASM2d (1.00 g N m^{-3}). This occurred because of low ammonia concentration in the aerobic phase. In the study of Dudley et al. (2002), K_{NH4AUT} (0.3 g N m^{-3}) was lower than that found in ASM2d. $K_{NH4\ AUT}$ was changed to promote autotrophic growth. The observed b_{AUT} value (0.05 d^{-1}) was also lower than in ASM2d (0.15 d^{-1}). It decreased with increasing autotrophic growth. As with the results for NH_4 calibrated parameters, it was concluded that DS was not significant to autotrophic mechanisms. It can be concluded that carbon components in DS, including volatile fatty acids (S_A), fermentable biodegradable products (S_F) and slowly biodegradable products (X_S), do not affect autotrophic mechanisms.

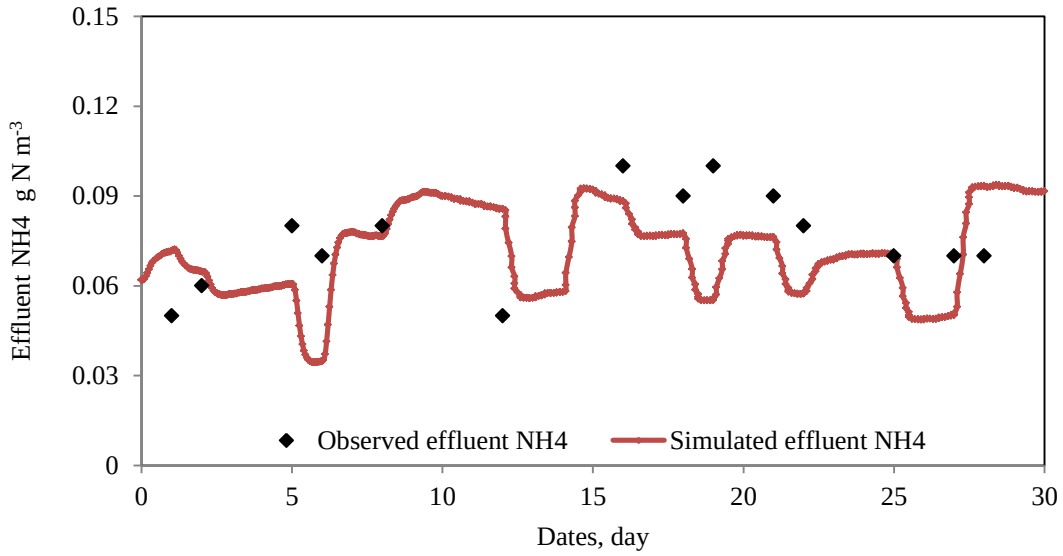

(a)

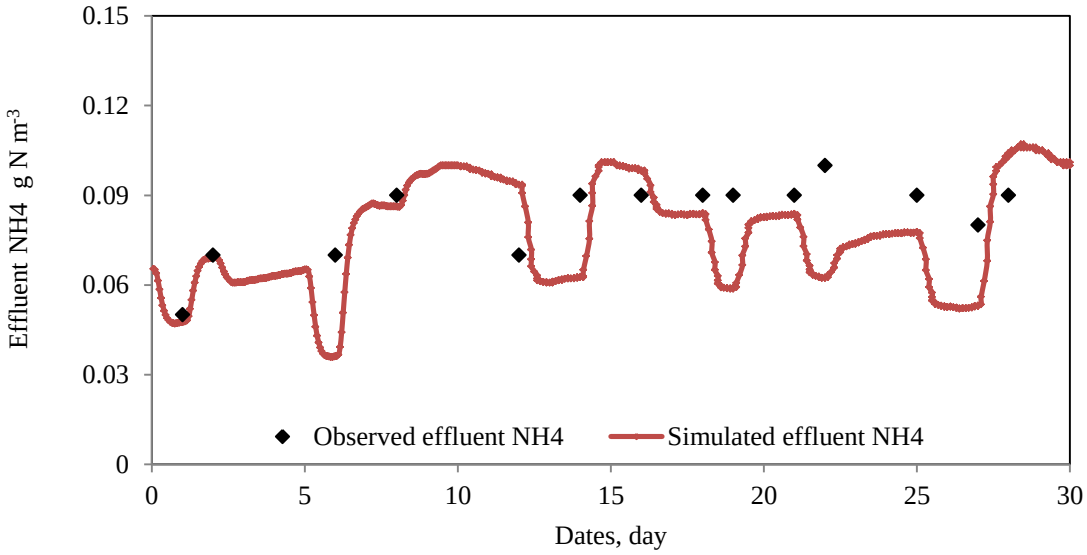

(b)

Figure 5.2 Calibration of effluent NH_4 at 17°C for (a) test and (b) control

The second data sets were used to observe PAOs mechanisms with phosphorus release in anaerobic phase and effluent TP shown in Table 3.9. These were relevant to the stoichiometric and kinetic parameters of PAOs only. These were no influence on heterotrophs and autotrophs. This is seen in the parameters subsets for PAOs calibration shown in Table 5.2. In contrast, the calibrated effluent NH_4, the first data sets were used to study the behaviors of autotrophs by employing the calibrated parameters shown in Table 5.2. Thus effluent NH_4 was affected only autotrophic mechanisms. Other researchers reported that $K_{NH4\ AUT}$ and μ_{AUT}, and other autotrophic parameters were obtained from calibration of NH_4 during nitrification (Insel et al., 2006). In addition, the calibrated NH_4 and NO_3 data sets used to describe the mechanisms of autotrophs with μ_{AUT} (Yagci et al., 2006). The simulation model fits for P release in anaerobic phase and effluent TP are shown in Figures 5.3 and 5.4, respectively. The following 10 parameters govern phosphorus release in anaerobic phase and effluent TP profiles: Y_{PAO}, Y_{PO4}, Y_{PHA}, q_{PHA}, q_{PP}, μ_{PAO}, b_{PAO}, b_{PP}, b_{PHA}, and K_{PS} (Table 5.2). To study the effects of extra acetate on simultaneous nitrogen and phosphorus removal based on the modified ASM2d, modeling of denitrifying PAOs (DNPAOs) kinetics was done (Soejima et al., 2008). It was concluded that Y_{PAO} and Y_{PO4} govern NO_3 and PO_4 concentrations. That modified modeling expressed the optimum concentration of supplementary COD and microbiological metabolism. Addition of supplementary COD to the different chemical oxygen demand/nitrogen/phosphorus (COD/N/P) compositions can enhance PAOs mechanisms. Yagci et al. (2006) studied phosphorus storage capacity-limiting and phosphorus loading-limiting conditions based on predicted simulations of S_{PO4}, X_{PHA}, S_A and MLSS profiles in the SBR performance to EBPR. Their calibrated parameters included Y_{PO4}, q_{PHA}, q_{PP}, K_{PHA}, b_{PAO}, b_{PP}, b_{PHA}, and μ_A. Empirical metabolic EBPR models (Comeau et al., 1986; Mino et al., 1987) directly relate production and utilization of intracellular polyphosphate (poly-P), and poly-hydroxy-alkanoates (PHA) or intracellular carbohydrates. Microorganisms employ EBPR to derive energy from poly-P degradation and utilize carbon under anaerobic conditions (Comeau et al., 1986; Mino et al., 1987). Stored carbon is used for growth and intracellular poly-P storage under aerobic conditions (Comeau et al., 1986; Mino et al., 1987). Selecting appropriate microorganisms is necessary to achieve EBPR (Jenkins & Tandoi, 1991; Mino et al., 1998). As a result, the ability to perform EBPR is related to the complexity of PAOs

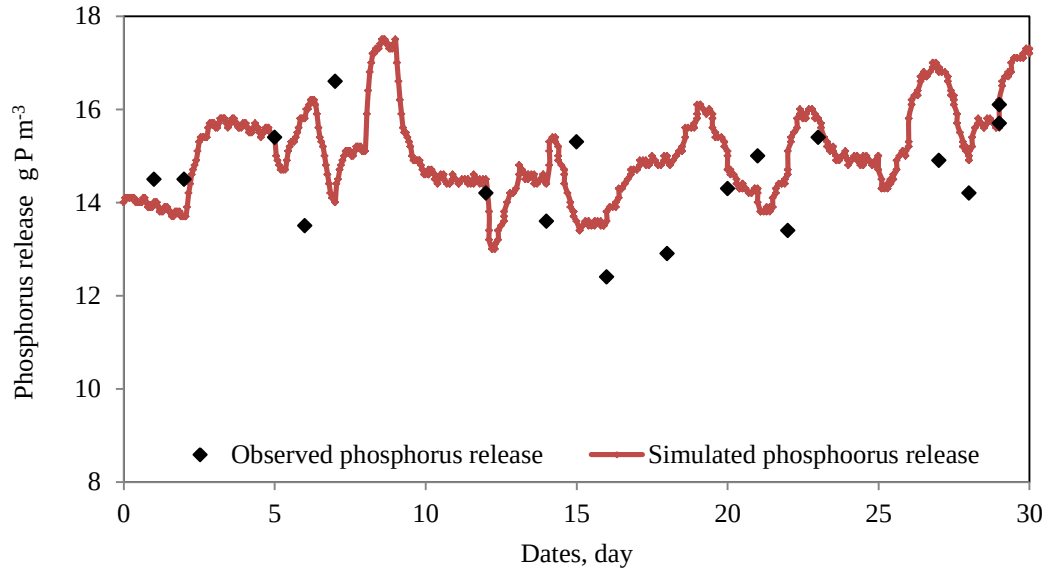

(a)

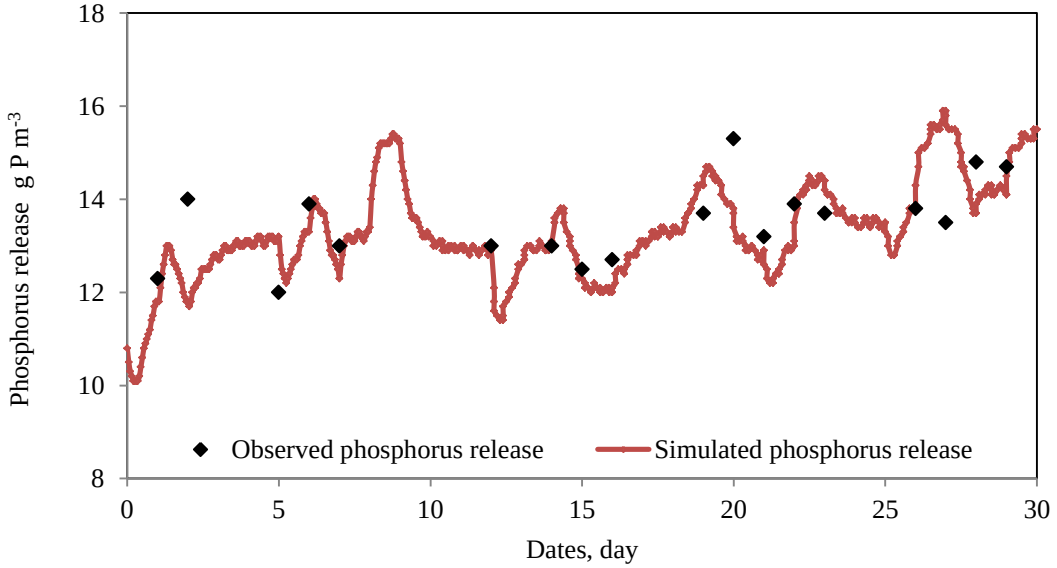

(b)

Figure 5.3 Calibration of phosphorus release in anaerobic phase at 17°C for (a) test and (b) control

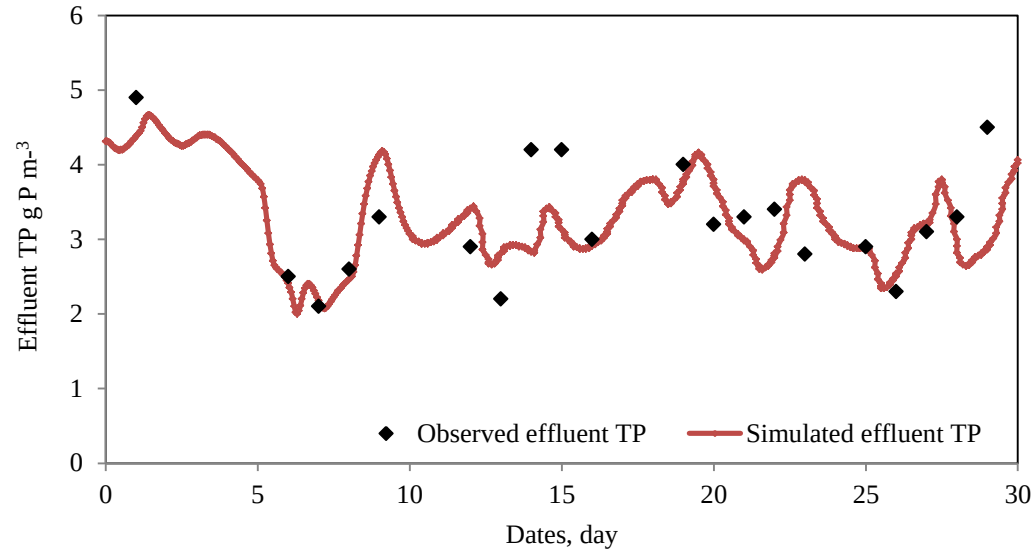

(a)

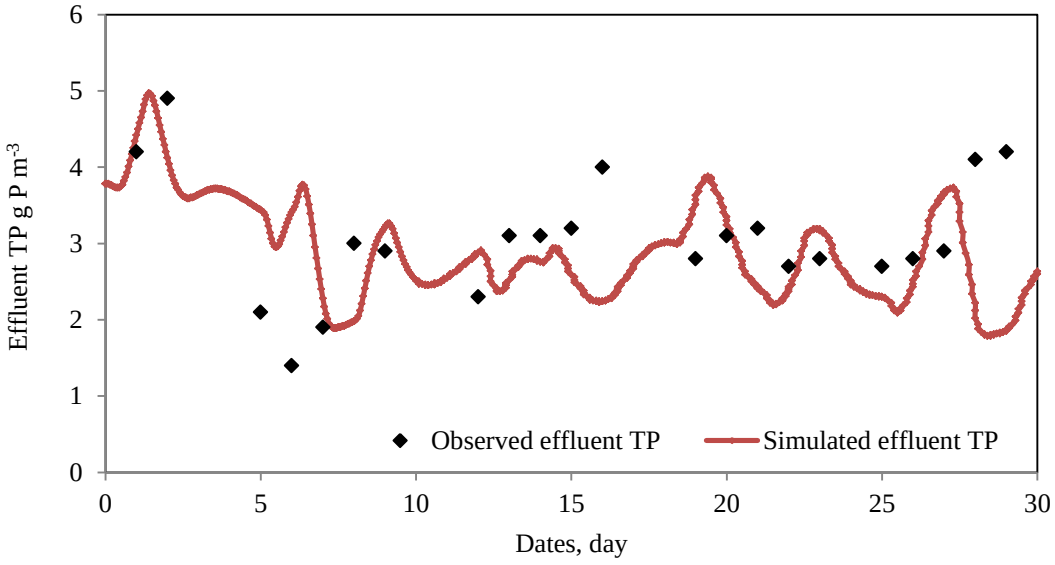

(b)

Figure 5.4 Calibration of effluent TP at 17°C for (a) test and (b) control

and glycogen accumulating organisms (GAOs). Both types of organisms use different energy sources (Cech and Hartman, 1993; Kuba et al., 1993; Liu et al., 1996). In addition, there is an internal energy-based competition between PAOs and GAOs for acetate utilization (Liu et al., 1997). PAOs and GAOs utilize energy from metabolism of intracellular poly-P and glycogen, respectively (Comeau et al., 1986; Mino et al., 1987; Liu et al., 1994). Carbon utilization by PAOs is based on poly-P degradation to generate energy in the anaerobic phase.

To study the effect of phosphorus to carbon (P/C) ratio upon favoring specific microorganisms, this ratio was decreased from 1:10 to 1:50 (Kong et al., 2002). ß-*Proteobacteria* decreased from approximately 77% of the total bacteria to 38%. This decrease the ß-*Proteobacteria* population coincided with a reduction in both the proportions of PAOs ß-proteobacterial *Rhodocyclus* and intracellular poly-P. As the P/C ratio in the feed stream (1/50) decreased there was a corresponding increase in proportion of GAOs (Kong et al., 2002). Comparison of the predominance of PAOs and GAOs as a function of P/C ratio is presented in Table 5.4. Another researcher (Liu, 1998) also reported that intracellular carbohydrate content at low levels was a prerequisite to achieving EBPR. Intracellular carbohydrate content is an internal energy source for GAOs (Matsuo et al., 1992; Satoh et al., 1992; Cech and Hartman, 1993). The energy sources used in anaerobic carbon utilization determined the dominant organisms. Other researchers (Liu et al., 1996) studied the conditions necessary to cause

Table 5.4 Comparison of the predominance of PAOs and GAOs as a function of P/C ratio

References	**P/C (wt/wt) ratios**	**Dominating microorganisms**
*This study	0.11	PAOs
**This study	0.09	PAOs
Kong et al. (2002)	Decrease from 0.1 to 0.02	GAOs
Liu et al. (1996)	0.02	GAOs
Liu et al. (1997)	decrease from 0.1 to 0.02	GAOs
Yagci et al. (2006)	0.07	GAOs

*DS; **Without DS

GAOs to predominate at a low P/C (2/100, wt/wt) ratio. They concluded that energy and reducing equivalents required for carbon uptake and storage are generated from the glycolysis of sugar. Also, their results suggest that microorganisms in sludge preferentially utilize glucose instead of cellular glycogen as an energy source during acid uptake. As a result, under low P/C conditions GAOs can utilize dissolved substrate and reduce biological phosphorus removal (Liu et al., 1996).

Regarding observation of the influence of DS upon phosphorus removal efficiency, characterization of DS was done. In the current study, acetic acid (HAc) was fed in same concentration to both test and control experiments. It was controlled to observe whether the PAOs mechanisms were affected by the DS components in relation to phosphorus. The components of DS contained not only HAc, which was in limited concentration under both two conditions, but also phosphorus. This resulted in a higher phosphorus/acetate ratio in the test influent (0.26 g P g^{-1} COD) than that in the control (0.21 g P g^{-1} COD). Also phosphorus contents of the feed stream in test and control experiments were0.83 % of TSS and 0.73 % of TSS respectively. As a result, PAOs at the higher phosphorus/acetate ratio take up more acetate and do so at a faster rate than those with a lower phosphorus/acetate ratio. PAOs in the current study tend to dominate at both P/C ratios (Table 5.4). This is because P/C ratios were greater than 0.1, a level above which PAOs predominant (Liu et al., 1996 & 1997; Kong et al., 2002; Yagi et al., 2006). Higher and faster carbon utilization rates of PAOs occurred at high P/C ratios (Fukase et al., 1984; Mino et al., 1987; Wentzel et al., 1988; Smolders et al., 1994; Liu et al., 1996; Liu et al., 1997). Liu et al. (1997) reported that decreasing P/C ratio from 20/100 to 2/100 did not affect carbon utilization and intracellular PHA storage under anaerobic conditions. However it caused internal poly-P storage content to decrease from 33% to 2%. As a result, EBPR was observed to decrease as GAOs predominated at lower the P/C ratio (2/100) (Liu et al., 1997). Furthermore, another study found that GAOs can utilize acetate under anaerobic conditions without using poly-P under lower phosphorus/acetate ratios (Yagci et al., 2006). Glycogen degradation produces energy for the utilization of acetic acid in GAOs. In addition the essential characteristics of PAOs and GAOs were studied under a low P/C ratio. PAOs

utilize carbon more slowly and GAOs consume the remaining acetate available (Manga et al., 2003). The process results from a direct relation between phosphorus release and X_{PHA} storage. It is represented by the rate constant for storage of PHA, q_{PHA} (Yagci et al., 2006). In the calibrated results of the current study, q_{PHA} in test and control experiments showed the same value (3.5 g X_{PHA} g^{-1} X_{PAO} d^{-1}). This was true even though the test condition demonstrated higher phosphorus release than did the control. However that value is higher than that observed in the ASM2d model (3.00 g X_{PHA} g^{-1} X_{PAO} d^{-1}). As a result, the q_{PHA} trend was in contrast to the above due to the higher phosphorus release under test conditions. It had a higher PHA storage due to uptake of more acetate. It is suggested that for further study, varying the concentration of carbon sources in DS be investigated with respect to q_{PHA}. The rate constant for storage of X_{PP}, q_{PP}, was also used to simulate phosphorus release in the anaerobic phase. In contrast to Yagci et al. (2006), q_{PP} was adjusted in the aerobic phase and effluent in order to observe phosphate uptake. That parameter, q_{PP}, showed the same value, 1.50 g X_{PP} g^{-1} X_{PAO} d^{-1}, in both test and control conditions. Its value was also found to the same as the default value (1.5 g X_{PP} g^{-1} X_{PAO} d^{-1}). Another kinetic parameter important to PAOs mechanisms, K_{PS} was increased to 0.35 g P m^{-3} in both test and control experiments. Other researchers reported that K_{PS} and q_{PP} were increased to 0.5 g P m^{-3} and 2.00 g X_{PP} g^{-1} X_{PAO} d^{-1}, respectively in the prediction capability of ASM2d for EBPR performance because of an expected correlation of these parameters (Yagci et al., 2006). Moreover, evaluation of ASM2 at high phosphorus concentrations found that K_{PS} and q_{PP} were 20 g P m^{-3} and 2.35 g X_{PP} g^{-1} X_{PAO} d^{-1}, respectively (Seco et al., 2001). The parameter, K_{PS}, was correlated to q_{PP} under both aerobic and anoxic conditions. Both parameters influenced the storage polyphosphate (PP) of PAOs processes. These controlled kinetic processes can be described by a Monod type expression as shown in Table 3.6. In the rate of PP storage (X_{PP}), the influence of K_{PS} depends on the phosphorus concentration. This is because phosphorus in PAOs was controlled with a phosphorus saturation limitation (Henze et al., 1999). In addition, storage PP in PAOs was related to the maximum capacity of storage PP as shown in 11st and 12nd processes in Table 3.6. Other studies reported that K_{PS} was increased to 0.5 g P m^{-3} without including q_{PP} as a calibrated parameter (Insel et al., 2006). Y_{PO4} was also taken in to account in the calibration as represented with an equivalent value (0.4 g P g^{-1} COD) for test and

control experiments. The default value was also equal to 0.4 g P g^{-1} COD. PHA is consumed by simultaneous utilization phosphate and the growth of PAOs. The parameter, b_{PP} was also involved in the endogenous metabolism of X_{PP} obtained after the poly-P transformation. That lysis of poly-P, b_{PP}, showed the same value (0.2 d^{-1}) in test, control and ASM2d modeling. The lysis rates defined by b_{PAO} and b_{PHA} showed constant values equal to 0.2 d^{-1} even though the phosphorus/acetate ratios between test and control experiments were different. In contrast to the studies of Yagci et al. (2006), bpp, b_{PAO} and b_{PHA} showed an ascending trend over these three kinetic parameters with increasing P/COD ratios. Y_{PAO}, in test experiments (0.64 g COD g^{-1} COD) was higher than in the controls (0.61 g COD g^{-1} COD) and ASM2d modeling (0.625 g COD g^{-1} COD). A higher value Y_{PAO} (0.9 g COD g^{-1} COD) was due to presence of GAOs (Ferrer et al., 2004). ASM2d does not differentiate between EBPR of PAOs and GAOs (Ferrer et al., 2004). The stoichiometric and kinetic equations in ASM2d were used in describing the processes of both types of bacteria. Additionally, glycogen is not considered an intracellular storage product in the ASM2d model. As a result, COD associated with GAOs and glycogen was expressed as X_{PAO}. In this case, Y_{PAO} was higher in a mixed population than in a pure culture of PAOs (Ferrer et al., 2004). Similarly, the higher value of Y_{PAO} (0.8 g COD g^{-1} COD) can be explained by the presence of GAOs (Penya-Roja et al., 2002). The value for Y_{PHA}, (0.26 g COD g^{-1} P) with influent DS was higher value than for the control (0.24 g COD g^{-1} P) and for ASM2d modeling (0.2 g COD g^{-1} P). The μ_{PAO} values under test and control conditions are equivalent to those of ASM2d modeling (1 d^{-1}).

5.3.5 The Significant Components to Phosphorus Removal

The paired t-test method was used to investigate the relationship between essential components of DS and phosphorus release under anaerobic phase. Also the relationships between DS components and effluent TP were investigated. The significant DS components are summarized in Table 5.5. The paired t-test to evaluate the effect of various DS components upon phosphorus release and effluent TP resulted in rejection of the null hypothesis (H_o) in all cases, in favor of the alternate of research (H_a) hypotheses. The four significant parameters in phosphorus removal efficiency are orthophosphate phosphorus (P), volatile fatty acids (S_A), fermentable biodegradable products (S_F) and slowly biodegradable products (X_S). This is seen in the magnitude of their p-values (p-value < 0.00001). Also the mean concentration of released phosphorus with and without influent DS is significantly different. As a result, it is shown with high confidence (p-value < 0.00001) that DS enhances phosphorus release.

Table 5.5 Summary of statistical analysis of the disintegrated sludge significant components at a 95% confidence level

Parameters	Comparison of two samples	Disintegrated sludge components	Paired t-test		
			Pearson correlation	***t-statistic***	***t-critical* ≤ *t-statistic***
P release		P	0.982	83.707	ReH
		S_A	0.998	48.809	ReH
		S_F	0.984	63.494	ReH
		X_S	1.000	33.035	ReH
	Test – Con.		0.906	12.081	ReH
Effluent TP		P	0.865	71.214	ReH
		S_A	0.997	51.469	ReH
		S_F	0.928	48.455	ReH
		X_S	1.000	32.984	ReH
	Test - Con.		0.762	22.710	ReH

Note: ReH = Reject H_o Hypothesis; *t-critical* to all experiments = 1.647; *p-value* to all experiments < 0.00001
Test-Con. = Test and Control

The influence of S_A, S_F and X_S DS components as carbon sources to EBPR systems was observed. It is related to PAOs. Phosphorus release in anaerobic conditions can demonstrate PAOs activity. Specific phosphorus release rate (SPRR) was used to observe the PAOs behavior. It is based upon PAOs biomass. The results show that SPRR of S_F DS component as carbon source was highest in comparison with other DS components (Table 5.6). The SPRR values were 0.834 mg P g^{-1} VSS_{PAOs} h^{-1}, 3.90 mg P g^{-1} VSS_{PAOs} h^{-1} and 0.31 mg P g^{-1} VSS_{PAOs} h^{-1} for S_A, S_F and X_S, respectively (Table 5.4). Additionally, the SPRR values with and without DS were 56.54 mg P g^{-1} VSS_{PAOs} h^{-1} and 52.88 mg P g^{-1} VSS_{PAOs} h^{-1}. The phosphorus and carbon feeding (P/C) ratios with and without were 0.11 and 0.09 (Table 5.4). The SPRR result with and without DS in this current study was lower than in the work of others (Panswad, et al. 2007). They were 106.2 - 156.9 mg P g^{-1} VSS_{PAOs} h^{-1}, 113.6 - 167.9 mg P g^{-1} VSS_{PAOs} h^{-1}, 84.7 - 127.9 mg P g^{-1} VSS_{PAOs} h^{-1} with P/C ratios of 0.02, 0.04 and 0.16 respectively. These values were obtained from EBPR systems. However, in the current research with and without DS was similar to results in SBR processes (52.0 – 76.9 mg P g^{-1} VSS_{PAOs} h^{-1}) of other researches (Panswad et al., 2003). Consequently, concentrations of effluent TP are significantly different with and without influent DS. High Pearson correlation coefficients (Table 5.5) suggest highly linear relationships between process parameters.

Table 5.6 Specific phosphorus release rates varying carbon sources and different phosphorus to COD (P/COD) ratios by adding DS (test)

Carbon source	**P/COD ratios**	**SPRR** **mg P g^{-1} VSS_{PAOs} h^{-1}**
Only S_A DS component	1.11	0.834
Only S_F DS component	0.22	3.9
Only X_S DS component	0.66	0.31

5.3.6 Verification of the Calibrated Model

Another set of experiments was conducted at a higher temperature (23°C) as shown in Table 3.10. It included the characterization of influent and experimental results in control (without DS) and test (with DS) conditions. In addition the characterization of influent carbon and influent phosphorus in control and test is shown in Table 3.10. Also, the model information of influent components based upon ASM2d was shown in Table 5.7. This was done to test whether experimental results agreed with experimental observations. In comparison both experiments to test the verification approach, they need to be controlled under the same conditions. In this study, the operating temperature conditions were different. This is because the experimental results were obtained in winter with average temperature of 17°C and the experimental observations were conducted in summer with average temperature of 23°C. Both experiments were conducted during different time periods. These observations could not have been made at the same time because there were limited in their number of activated sludge pilot-scale wastewater treatment reactors. Phosphorus release under test and control conditions showed close agreement (Figure 5.5**)**. Predicted values of phosphorus release obtained from model fitting were found to be the same as observed values under test and control conditions. The H_0 hypothesis was observed and predicted values are unequal. Ho was rejected at a 95% confidence level. This is shown by p-value of Chi-Square test for goodness having a value less than 0.05. The p-values under test and control conditions were < 0.00001 and 0.00005 respectively. As is seen from these p-values, confidence levels are 99.999% and 99.995% for test and control conditions, respectively. However, some calibrated parameters were different (Table 5.8). The Y_{PAO}, q_{PHA} and $K_{NH4\ AUT}$ values in verification were different from calibration. This may be due to the influence of temperature. Temperature can have an effect on biological reactions in two ways: (1) influencing the rates of enzymatically catalyzed reactions, and (2) affecting the rate of diffusion of the substrate into the cells. Neither way has been included in ASM2d. The Arrhenius equation is a method of expressing temperature effects using a temperature coefficient. This coefficient will be determined in Chapter 6. The other values were similar in verification and calibration (Table 5.8).

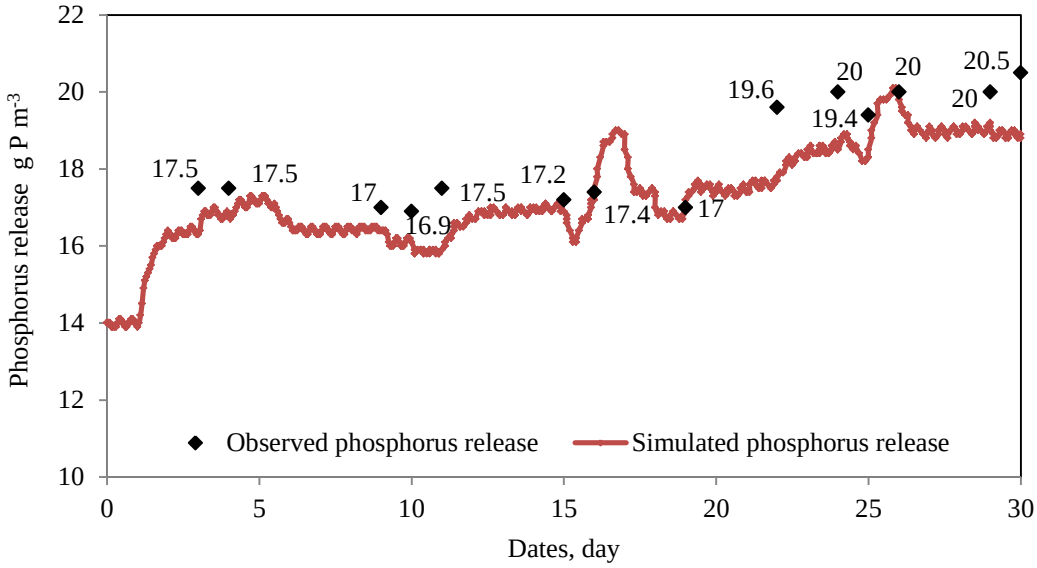

(a)

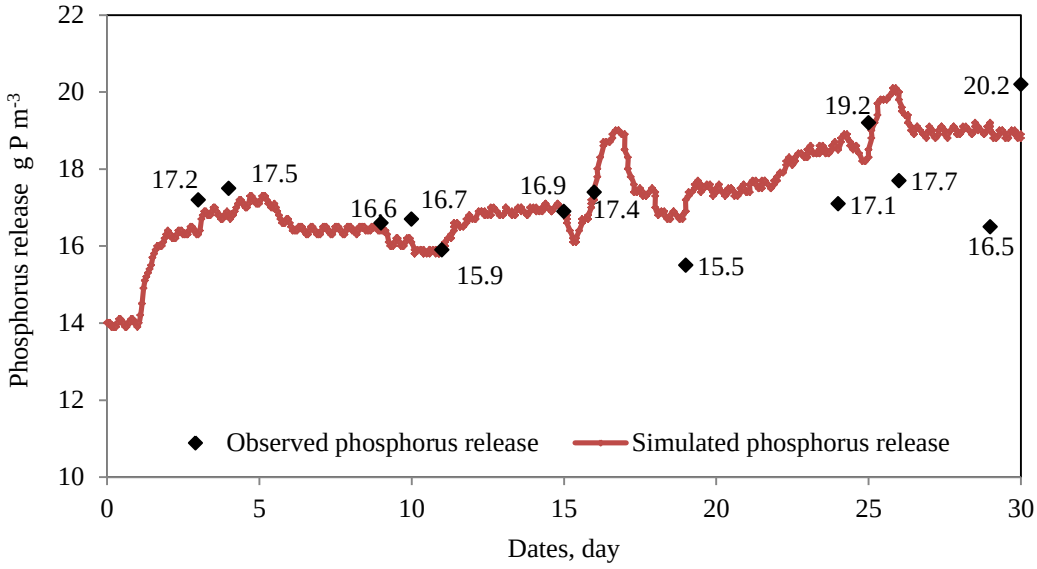

(b)

Figure 5.5 Verification of phosphorus release at 23°C (a) test (b) control.

Table 5.7 Model information of influent components of test (with DS) and control (without DS) experiments at 23°C with ASM2d calibration

Model Information				
	Experimental conditions			
	Test		**Control**	
Biological Model				
biological model	ASM2d		ASM2d	
Flow				
flow	2.88	[m^3/d]	2.88	[m^3/d]
Composite Variables				
Volatile Fraction				
VSS/TSS ratio	0.923	[gVSS/gTSS]	0.965	[gVSS/gTSS]
Composite Variables				
total suspended solids	1540	[g/m^3]	1280	[g/m^3]
volatile suspended solids	1420	[g/m^3]	1240	[g/m^3]
total inorganic suspended solids	119	[g/m^3]	44.6	[g/m^3]
total carbonaceous BOD5	355	[gO_2/m^3]	270	[gO_2/m^3]
total COD	2270	[gCOD/m3]	1990	[gCOD/m3]
total TKN	98.2	[gN/m3]	86.6	[gN/m3]
total phosphorus	75.7	[gP/m3]	46.8	[gP/m3]
Additional Composite Variables				
filtered carbonaceous BOD5	39.3	[gO_2/m^3]	37.8	[gO_2/m^3]
particulate carbonaceous BOD5	316	[gO_2/m^3]	232	[gO_2/m^3]
filtered ultimate carbonaceous BOD	59.1	[gO_2/m^3]	56.6	[gO_2/m^3]
particulate ultimate carbonaceous BOD	474	[gO_2/m^3]	348	[gO_2/m^3]
total ultimate carbonaceous BOD	534	[gO_2/m^3]	405	[gO_2/m^3]
filtered COD	117	[gCOD/m^3]	110	[gCOD/m^3]
particulate COD	2150	[gCOD/m^3]	1880	[gCOD/m^3]
filtered TKN	28.8	[gN/m^3]	28.5	[gN/m^3]
particulate TKN	69.5	[gN/m^3]	58.2	[gN/m^3]
total nitrogen	98.4	[gN/m^3]	86.8	[gN/m^3]
filtered phosphorus	12.4	[gP/m^3]	10.6	[gP/m^3]
particulate phosphorus	63.3	[gP/m^3]	36.2	[gP/m^3]
State Variables				
Inorganic Suspended Solids				
inert inorganic suspended solids	4.65	[g/m^3]	0.0281	[g/m^3]
Organic Variables				
soluble inert organic material	57.4	[gCOD/m^3]	53.7	[gCOD/m^3]
readily biodegradable substrate	0	[gCOD/m^3]	0	[gCOD/m^3]
fermentable readily biodegradable substrate	19.1	[gCOD/m^3]	13.4	[gCOD/m^3]
volatile fatty acids	43.2	[gCOD/m^3]	43.2	[gCOD/m^3]
particulate inert organic material	1680	[gCOD/m^3]	1530	[gCOD/m^3]
slowly biodegradable substrate	39.9	[gCOD/m^3]	38	[gCOD/m^3]
active heterotrophic biomass	229	[gCOD/m^3]	186	[gCOD/m^3]
active autotrophic biomass	32.5	[gCOD/m^3]	22.8	[gCOD/m^3]
active poly-P accumulating biomass	152	[gCOD/m^3]	86.7	[gCOD/m^3]
unbiodegradable particulates from cell decay	0	[gCOD/m^3]	0	[gCOD/m^3]
poly-hydroxy-alkanoates (PHA)	20.8	[gCOD/m^3]	14.6	[gCOD/m^3]
stored glycogen	0	[gCOD/m^3]	0	[gCOD/m^3]
Dissolved Oxygen				
dissolved oxygen	0.0051	[gO_2/m^3]	0.00383	[gO_2/m^3]

Table 5.7 (cont.) Model information of influent components of test (with DS) and control (without DS) experiments at 23°C with ASM2d calibration

Model information	**Experimental conditions**			
	Test		**Control**	
Phosphorus Compounds				
soluble ortho-phosphate	10.5	[gP/m^3]	12.6	[gP/m^3]
stored polyphosphate	14.9	[gP/m^3]	32.4	[gP/m^3]
stored polyphosphate (releasable)	0	[gP/m^3]	0	[gP/m^3]
Nitrogen Compounds				
free and ionized ammonia	25.4	[gN/m^3]	18.3	[gN/m^3]
soluble biodegradable organic nitrogen	0	[gN/m^3]	0	[gN/m^3]
particulate biodegradable organic nitrogen	0	[gN/m^3]	0	[gN/m^3]
nitrate and nitrite	0.199	[gN/m^3]	3.7	[gN/m^3]
soluble unbiodegradable organic nitrogen	0	[gN/m^3]	0	[gN/m^3]
dinitrogen	7.33	[gN/m^3]	11.3	[gN/m^3]
Alkalinity				
alkalinity	5.02	[mole/m^3]	4.46	[mole/m^3]
Metal Precipitates				
metal-hydroxides	7.98E-05	[g/m^3]	0.000266	[g/m^3]
metal-phosphates	0.00128	[g/m^3]	0.00239	[g/m^3]
Model Stoichiometry				
Organic Fractions				
XCOD/VSS ratio	1.51	[gCOD/gVSS]	1.48	[gCOD/gVSS]
BOD5/BODultimate ratio	0.668	[-]	0.66	[-]
Nutrient Fractions				
N content of soluble inert organic material	0.0377	[gN/gCOD]	0.01	[gN/gCOD]
N content of readily biodegradable substrate	0	[gN/gCOD]	0	[gN/gCOD]
N content of fermentable readily biodegradable substrate	0.0664	[gN/gCOD]	0.03	[gN/gCOD]
N content of particulate inert organic material	0.0224	[gN/gCOD]	0.02	[gN/gCOD]
N content of slowly biodegradable substrate	0.0521	[gN/gCOD]	0.04	[gN/gCOD]
N content of unbiodegradable particulates from cell decay	0	[gN/gCOD]	0	[gN/gCOD]
N content of active heterotrophic biomass	0.07	[gN/gCOD]	0.07	[gN/gCOD]
N content of active autotrophic biomass	0.07	[gN/gCOD]	0.07	[gN/gCOD]
N content of active poly-P accumulating biomass	0.07	[gN/gCOD]	0.07	[gN/gCOD]
P content of soluble inert organic material	0	[gP/gCOD]	0	[gP/gCOD]
P content of readily biodegradable substrate	0	[gP/gCOD]	0	[gP/gCOD]
P content of fermentable readily biodegradable substrate	0.00754	[gP/gCOD]	0.01	[gP/gCOD]
P content of particulate inert organic material	0.00981	[gP/gCOD]	0.01	[gP/gCOD]
P content of slowly biodegradable substrate	0.00807	[gP/gCOD]	0.01	[gP/gCOD]
P content of unbiodegradable particulates from cell decay	0	[gP/gCOD]	0	[gP/gCOD]
P content of active heterotrophic biomass	0.02	[gP/gCOD]	0.02	[gP/gCOD]
P content of active autotrophic biomass	0.02	[gP/gCOD]	0.02	[gP/gCOD]
P content of active poly-P accumulating biomass	0.02	[gP/gCOD]	0.02	[gP/gCOD]

Table 5.8 Parameter values of simulated modeling in verification and calibration

Symbol	ASM2d	Disintegrated sludge		Without disintegrated sludge		Units
		Verification	Calibration	Verification	Calibration	
Phosphorus Accumulating Organisms: PAOs						
Y_{PAO}	0.625	0.65	0.64	0.65	0.61	g COD g^{-1} COD
Y_{PO4}	0.40	0.40	0.40	0.40	0.40	g P g^{-1} COD
Y_{PHA}	0.20	0.26	0.26	0.24	0.24	g COD g^{-1} P
q_{PHA}	3.00	5.00	3.50	4.00	3.50	g X_{PHA} g^{-1} X_{PAO} d^{-1}
q_{PP}	1.50	1.50	1.50	1.50	1.50	g X_{PP} g^{-1} X_{PAO} d^{-1}
μ_{PAO}	1.00	1.00	1.00	1.00	1.00	d^{-1}
b_{PAO}	0.20	0.20	0.20	0.20	0.20	d^{-1}
b_{PP}	0.20	0.20	0.20	0.20	0.20	d^{-1}
b_{PHA}	0.20	0.20	0.20	0.20	0.20	d^{-1}
K_{PS}	0.20	0.35	0.35	0.35	0.35	g P m^{-3}
Autotrophs:						
Y_A	0.24	0.24	0.24	0.24	0.24	g COD g^{-1} N
μ_{AUT}	1.00	1.20	1.20	1.20	1.20	d^{-1}
b_{AUT}	0.15	0.05	0.05	0.05	0.05	d^{-1}
$K_{O2\ AUT}$	0.50	0.50	0.50	0.50	0.50	g O_2 m^{-3}
$K_{NH4\ AUT}$	1.00	0.05	0.15	0.05	0.15	g N m^{-3}

5.4 CONCLUSIONS

Including DS in the influent of WWTPs caused enhancement of PAOs in wastewater treatment. This is caused by a high phosphorus/acetate feed ratio resulting in higher utilization of carbon sources by PAOs. Those behaviors can be explained by Y_{PAO} and Y_{PHA}. Y_{PAO} (0.64 g COD g^{-1} COD), with influent DS was higher than without (0.61 g COD g^{-1} COD). Y_{PHA} (0.26 g COD g^{-1} P) with influent DS also was higher than without (0.24 g COD g^{-1} P). The value of both parameters varied due to orthophosphate, volatile fatty acids, fermentable biodegradable products and slowly biodegradable products components of DS. In addition, the values of calibrated parameters in relation to temperature show different verification and calibration result when conducted at 23°C and 17°C respectively.

CHAPTER 6:

ASM2D SIMULATION AT DIFFERENT TEMPERATURES AND DISINTEGRATED SLUDGE IN ENHANCED BIOLOGICAL PHOSPHORUS REMOVAL (EBPR) PROCESSES

CHAPTER 6. ASM2D SIMULATION AT DIFFERENT TEMPERATURES AND DISINTEGRATED SLUDGE IN ENHANCED BIOLOGICAL PHOSPHORUS REMOVAL (EBPR) PROCESSES

ABSTRACT

In this work, a biological phosphorus removal pilot plant was used to study the effects temperature and use of disintegrated sludge (DS) as a carbon source upon phosphorus accumulating organisms (PAOs). Experiments were carried out at 17 °C and 23 °C. The ASM2d model was calibrated at 17°C and 23°C under conditions with and without DS in the influent stream. Arrhenius equation constants were obtained for phosphorus removal processes influenced by temperature and DS. It was found that temperature and influent DS influences biological phosphorus removal. The Arrhenius equation constants (θ) of the yield coefficient (Y_{PAO}) with and without DS were 1.003 and 1.010, respectively. The Arrhenius equation constants for poly-hydroxy-alkanoates (PHA) storage (q_{PHA}) with and without DS were 1.061 and 1.023, respectively.

Keywords: Arrhenius equation; ASM2d; Biological Phosphorus Removal; Disintegrated Sludge; Phosphorus accumulating organisms (PAOs); Temperature

6.1 INTRODUCTION

Successful biological nutrient removal (BNR) wastewater treatment plants (WWTPs) are based upon a number of parameters. Carbon sources are essential factors for growth of microorganisms. Growth processes result in internal carbon storage (Thomas et al., 2003). Short-chain volatile fatty acids (VFAs) are suitable carbon sources for BNR (Elefsiniotis et al., 2004; Tong and Chen, 2007). Phosphorus accumulating organisms (PAOs) can utilize VFAs directly under anoxic condition without hydrolysis and fermentation processes (van Veldhuizen et al., 1999; Brdjanovic et al., 2000). In addition, VFAs can significantly enhance biological phosphorus removal (EBPR) processes (Llabres et al., 1999; Chen et al., 2004; Feng et al., 2009). VFAs are produced by different approaches. Disintegration sludge (DS) with mechanical deflaking can release soluble chemical oxygen demand (SCOD) as well as VFAs (Kampas et al., 2007). EBPR processes are successful using influent DS (Kampas et al., 2009; Soares et al., 2010).

Temperature is a fundamental factor that affects all living organisms (Erdal et al., 2003). It influences the rates of enzymatically catalysed reactions and the rate of diffusion of substrate into the cells (Grady et al., 1999). In EBPR processes, the diverse bacterial consortium consists of psychrophilic, pyschrotrophic and mesophilic heterophic bacteria (Grady et al., 1999). Temperature strongly influences the population composition of these groups due to their optimum growth temperatures (Grady et al., 1999). Temperature is one of the crucial factors to control microorganisms in EBPR processes (García-Usach et al., 2006). The influence of temperature on the kinetics of EBPR has also been investigated in numerous studies with contradictory conclusions. Higher phosphorus removal efficient was reported at high temperatures (20-37°C) (Brdjanovic et al., 1997). Another study of the impact of long term temperature changes on the stoichiometry and kinetics of different processes at 5, 10, 15, and 20°C was done (Baetens et al., 1999). At temperatures between 15 and 20°C, aerobic phosphorus uptake rate shows a maximum value (0.0532 g P g^{-1} active biomass h^{-1}). Other anaerobic and aerobic conversion rates increased with increasing temperature (5 to 20°C). Maximum specific phosphorus release rate increasing from 0.033 to 0.137 g Pg^{-1}

active biomass h^{-1} and maximum specific poly-hydroxy-butyrate (PHB) consumption rate increasing from 0.0089 to 0.0256 g PHB g^{-1} active biomass h^{-1}. At 5°C, acetate was utilized in the anaerobic stage. Unutilized acetate was then consumed in downstream aerobic stages. At low temperatures, the efficiency of EBPR improves in relation to Arrhenius constant (Erdal et al., 2003). García-Usach et al. (2006) reported that among process temperatures of 13, 20 and 24.5°C, that the highest efficiency was observed at 13°C. Additionally, temperature is influential in controlling competition between PAOs and glycogen accumulating organisms (GAOs). PAOs are the microorganisms responsible for the phosphorus removal processes (López-Vázquez et al., 2008). GAOs can take up organic substrate anaerobically without phosphorus release and are related to deterioration of EBPR processes (Mino et al., 1998). GAOs were a predominant microbial group when the temperature was gradually increased from 20°C to 35°C (Panswad et al., 2003). The PAOs was washed out from the systems when temperature was gradually increased. This is because the portion of energy required for maintenance increased substantially. Subsequently the energy availability for biomass growth rate was reduced (Panswad et al., 2003). Another study also reported that when temperature was increased from 22±1°C to 29±1°C and then was followed by a decrease to 14±1°C, the dominant cell group was changed from PAOs to GAOs (Ren et al., 2011). Lopez-Vazquez et al. (2009) reported that PAOs were the dominant microorganisms at low temperature (10°C) regardless of the influent carbon source or pH. PAOs become the dominant organisms under temperature conditions less than 20°C and the efficiency of EBPR processes is enhanced (Whang and Park, 2002 & 2006). López-Vázquez et al. (2007) also reported a similar phenomenon when temperature is lower than 20°C, the substrate uptake provided PAOs was with an advantage over GAOs. Additionally, López-Vázquez et al. (2008) found that temperature effects did not confer metabolic advantages to GAOs over PAOs when considering their aerobic metabolism. Competitive advantages were due to anaerobic processes. So far, even considering the work of other researchers, the effects of temperature on EBPR have not yet been completely elucidated.

Verification of mathematical models has been found to be a useful tool for the investigation of advanced control strategies for wastewater treatment plants (WWTPs).

(Ferrer et al., 2004). It assists in layout design, operation and controlling biological processes (Hu et al., 2003, Ferrer et al., 2004). In addition, verification of mathematical modelling can be used to optimise performance, or to predict the plant performance when influent conditions and temperature changes (García-Usach et al., 2006). Activated Sludge Model No. 2d (ASM2d) (Henze et al., 1999) is one of the most useful models. It can be used to describe the kinetics and behavior of autotrophs, heterotrophs, and PAOs involved in biological wastewater treatment. It predicts microorganism behaviors in carbon oxidation, nitrification, denitrification and phosphorus removal processes.

The strict standards for EBPR wastewater treatment plant effluents require better process control. Application of EBPR mathematical modeling to biological processes depends upon stoichiometric and kinetic coefficients which are only valid with small variations of temperatures or at a single temperature value (Brdjanovic et al., 1997). The role of temperature coefficients becomes more important. Use of ASM2d is one of the most promising approaches to elaborate optimising strategies. The influence of temperature and inclusion of DS as a carbon source on PAOs in EBPR has not been reported. This study aims to calibrate ASM2d for PAOs behavior in order to investigate combined effects of temperature and influent disintegrated sludge on EBPR. The pilot-scale MUCT processes were carried out at two different temperatures. The experimental results were calibrated using ASM2d. The Arrhenius equation was used to describe the effect of temperature on the rate of reactions in activated sludge systems. In this study, the Arrhenius equation was applied to investigate the influence of DS influent temperature on PAOs behavior. Effects were calculated after obtaining the calibrated parameters. The Arrhenius equation allows comparison of stoichiometric and kinetic results with the temperature coefficients of different processes considered in mathematical models (Henze et al., 2000). It defines the relationship between the value of the rate of the biological processes and temperatures at which they occur. In this study, process coefficients were categorized by two different temperatures (17 and 23 C).

6.2 MATERIALS AND METHODS

6.2.1 The MUCT pilot scale

Experimental data shown in Table 3.9 and Table 3.10 were used to predict the metabolic mechanisms of PAOs and autotrophs in WWTPs using ASM2d modelling (Panswad et al., 2003). The experiments were done with a MUCT pilot scale process. It was operated in the pilot hall facilities of the Sewage Treatment Works of Cranfield University, UK. The pilot scale consisted of two series of reactors using influent DS (test) and influent with no DS (control), respectively. A schematic of reactor configuration of test and control is shown in Figure 5.1 and Figure 4.1, respectively. The process consisted of five reactors in series. These included anaerobic, 1st anoxic, 2nd anoxic, aerobic phases and clarifier stages. They had effective volumes of 0.125 m^3, 0.120 m^3, 0.230 m^3, 0.550 m^3 and 0.334 m^3, respectively. The operating conditions included influent wastewater flow rate (Q_{IN} = 0.060 m^3 h^{-1}), return activated sludge flow rate (Q_R = 0.051 m^3 h^{-1}), anoxic recirculation flow rate (Q_1 = 0.060 m^3 h^{-1}) and aerobic recirculation flow rate (Q_2 = 0.060 m^3 h^{-1}). An equivalent mixed liquor suspended solid (MLSS) in both test and control was maintained. The solid retention time (SRT) in test and control experiments was 15-days and 23-days, respectively. The first data set average temperature during steady state was maintained at 17°C. Another set of experiments was conducted at a higher constant temperature (23°C). Both sets of experiments, i.e., those conducted at 17°C and at 23°C, were done over a one month period after operating AS systems at steady state for three months. Both values were average temperatures. The pilot-scale WWTP was operated without controlling temperature. Thus, the temperature varied which included ±1.0 standard deviation. The solid retention time (SRT) in test and control experiments was 45-days and 16-days, respectively. This was done to maintain appropriate MLSS levels. Both series of experiments were conducted under the same conditions. DS was fed to the test series only. In order to develop EBPR, acetic acid was fed to the influent at an equivalent level in both the test and control. Acetate concentrations in municipal wastewater were not high enough to enable EBPR. The control was fed with acetic acid only added to the influent. For the test, acetic acid and DS were added to the influent. DS contained acetic

acid as one if its components. Influent, anaerobic stage, aerobic stage and effluent were sampled on a daily basis.

6.2.2 Simulation methodology

This methodology is presented in Chapter 4. Aquasim (Reichert, 1994) and interface UNSIM (Reichert, 2003 & 2006) programs were used to calculate the sensitivity analysis. GPS-X (Hydromantis, Inc., Hamilton, Canada) was used as the simulation tool. The ASM2d model was calibrated with the parameter significance ranking resulting from Aquasim and interface UNSIM calculations. The iterative algorithm using GPS-X was re-evaluated until the sensitivity parameter no longer affected the simulation output.

6.2.3 Temperature coefficient

The effect of temperature on biomass reaction rates for small temperature differences can be expressed by the modified Arrhenius equation:

$$k_1 = k_2 * \theta^{(T_1 - T_2)} \qquad (6.1)$$

where k_1 is the stoichiometric and kinetic coefficient in ASM2d at temperature T_1. k_2 is the stoichiometric and kinetic coefficient in ASM2d at temperature T_2. In this study, the values of k_1 and k_2 were obtained at 17 and 23°C, respectively. θ is a temperature coefficient. The θ values were calculated by fitting equation (6.1) to the stoichiometric and kinetic values at specific temperatures. The equation has proved well suited for fitting these types of data (López-Vázquez et al., 2007). This allowed comparison of temperature coefficients for different processes considered in mathematical models (Henze et al., 1995). In this study, θ of different processes at 17 and 23°C were presented. The influence of temperature on stoichiometric and kinetic coefficients was determined by calculation of ASM2d calibration parameters after obtaining the Arrhenius equation constant. This was done to enable use of data generated at separate temperatures during two different investigation periods.

6.3 RESULTS AND DISCUSSION

6.3.1 Wastewater characteristics

Simulation of operating periods was completed for steady state processes. The influent wastewater characteristics at 17 and 23°C are summarized in Table 3.9 and 3.10, respectively. In addition, the model information of influent components at 17 and 23°C are shown in Table 5.1 and Table 5.7, respectively.

6.3.2 ASM2d calibration

Kinetic and stoichiometric ASM2d parameters having high influence on process outputs were determined and considered as sensitivity parameters. Parameter sensitivity ranking was obtained from sensitivity analysis. Resulting sensitivity parameters were used for ASM2d calibration. Sensitivity analysis and calibration followed an approach discussed previously in Chapter 4. The values of k_1 and k_2 obtained for PAOs and autotrophs are shown in Table 6.1. ASM2d calibration for the experiments done at 17 and 23°C with and without influent DS was performed once steady state was achieved. There are no calibration results for heterotrophic organisms at 17 and 23°C conditions. This is because heterotrophic activity is not significantly different at these two temperatures.

Table 6.1 Values of k_1 and k_2 coefficients of the calibrated ASM2d model at 17 and 23°C, respectively

Parameters	Definition	ASM2d	k_1		k_2		Units
			DS	Without DS	DS	Without DS	
Y_{PAO}	Yield coefficient (Biomass/ poly-hydroxy-alkanoates (PHA))	0.625	0.64	0.61	0.65	0.65	g COD g^{-1} COD
Y_{PO4}	polyphosphate (PP) requirement (PO_4 release) per PHA stored	0.4	0.4	0.4	0.4	0.4	g P g^{-1} COD
Y_{PHA}	PHA requirement for PP storage	0.20	0.26	0.24	0.26	0.24	g COD g^{-1} P
q_{PHA}	Rate constant for storage of X_{PHA} (base X_{PP})	3.0	3.5	3.5	5.0	4.0	g X_{PHA} g^{-1} X_{PAO} d^{-1}
q_{PP}	Rate constant for storage of X_{PP}	1.5	1.5	1.5	1.5	1.5	g X_{PP} g^{-1} X_{PAO} d^{-1}
μ_{PAO}	Maximum growth rate of PAOs	1.0	1.0	1.0	1.0	1.0	d^{-1}
b_{PAO}	Rate for Lysis of X_{PAO}	0.2	0.2	0.2	0.2	0.2	d^{-1}
b_{PP}	Rate for Lysis of X_{PP}	0.2	0.2	0.2	0.2	0.2	d^{-1}
b_{PHA}	Rate for Lysis of X_{PHA}	0.2	0.2	0.2	0.2	0.2	d^{-1}
K_{PS}	Saturation coefficient for phosphorus in storage of PP	0.2	0.35	0.35	0.35	0.35	g P m^{-3}
Y_A	Yield coefficient (Biomass/Nitrate)	0.24	0.24	0.24	0.24	0.24	g COD g^{-1} N
μ_{AUT}	Maximum growth rate of X_{AUT}	1.0	1.2	1.2	1.2	1.2	d^{-1}
b_{AUT}	Decay rate of X_{AUT}	0.15	0.05	0.05	0.05	0.05	d^{-1}
$K_{O2\ AUT}$	Saturation coefficient for oxygen	0.5	0.5	0.5	0.5	0.5	g O_2 m^{-3}
$K_{NH4\ AUT}$	Saturation coefficient for ammonium (substrate)	1.00	0.15	0.15	0.05	0.05	g N m^{-3}

PAOs kinetic parameters obtained at 17°C indicate that the yield coefficient (Y_{PAO}) and poly-hydroxy-alkanoates (PHA) storage (q_{PHA}) decreased. In contrast, a saturation coefficient for ammonium (substrate), $K_{NH4\ AUT}$, in autotrophs was lower at 23°C than at 17^{o}C. Values of Y_{PAO}, Y_{PO4}, and K_{MAX} in PAOs are different in ASM2d because of the presence of GAOs (Penya-Roja et al., 2002; Ferrer et al., 2004). K_{MAX} refers to the maximum ratio X_{PP}/X_{PAO}. GAOs are treated in the same manner as PAOs in ASM2d in that they cannot store polyphosphate. On the basis of this ASM2d assumption, PAOs and GAOs are not different (Ferrer et al., 2004). Glycogen is not represented as an intracellular storage product in ASM2d. Thus, GAOs and glycogen were presented in PAOs (Penya-Roja et al., 2002; Ferrer et al., 2004). Observed Y_{PAO} values at 17 and 23°C with and without influent DS are higher than predicted by ASM2d (Table 6.1). One exception is that Y_{PAO} without influent DS at 17°C is lower than predicted by ASM2d. GAOs are present in pilot-scale WWTPs. Under anaerobic conditions, both PAOs and GAOs can store VFAs internally in the form of PHA. PAOs utilize energy from polyphosphate and glycogen degradation. In contrast, GAOs utilize energy from glycogen degradation only. When increasing GAO population, Y_{PO4} values are decreased (Henze et al., 1995, Ferrer et al., 2004). In this study Y_{PO4} (0.4) was found to have a similar value to that predicted by ASM2d. The behavior of Y_{PO4} with respect to ASM2d is different from that seen for Y_{PAO}. Y_{PO4} values in other studies were reported to be 0.42 and 0.46 g P g^{-1} COD in Elche B and Elda WWTPs, respectively (Ferrer et al., 2004). It was concluded that GAOs were absent in Elche B WWTPs since the value of Y_{PO4} was close to the predicted ASM2d value (0.4). Additionally, Elda WWTPs contained GAOs, even though Y_{PO4} was much higher than the expected value for a mixed population of PAOs and GAOs. This caused a higher pH (7.95). Y_{PAO} at 17°C was lower than at 23°C. This result suggests that even though the values of kinetic parameters decrease as temperature is reduced, the efficiency of EBPR processes is higher at lower temperatures. PAOs occur at 10°C or less because they are psychrotrophic. Under these conditions, PAOs growth rate is higher than non-PAOs in EBPR systems (Erdal et al., 2003). This results in an increased PAOs population at lower temperatures (Erdal et al., 2003). The EBPR performance at 20°C was lower than at 10°C even though the kinetic parameter values increased when temperature was increased from 10 to 20°C (Erdal et al., 2003). The reason for higher efficiency of

EBPR performance at lower temperature was related to reduce competition for substrate by non-PAOs under anaerobic conditions.

The Arrhenius relationship (Equation 6.1) was employed using the ASM2d parameters. A set of calibrated parameters is required in order to use this equation. The θ constant values of the Arrhenius equation were calibrated parameter resulting from experiments conducted at 17 and 23°C (Table 6.2). The Arrhenius constant values of PAOs expressed in Table 6.2 can be categorized into two groups. The first group, consists of temperature independent parameters ($\theta = 1$) where stoichiometric, saturation, lysis rate coefficients are included. Stoichiometric and kinetic parameters, with the exception of Y_{PAO}, are included. The second group consisted of temperature dependent parameters ($\theta \neq 1$) where the kinetic parameters Y_{PAO} and q_{PHA} are included. These Arrhenius constant values for the PAOs reflected the temperature influences ($\theta \neq 1$) on the biological phosphorus removal processes. The rate constant for storage of X_{PHA} (Y_{PHA}) is more affected by temperature than the yield coefficient (Y_{PAO}). Additionally, θ of q_{PHA} with DS is higher than θ of q_{PHA} without DS. In contrast, θ of Y_{PAO} without DS is higher than θ of Y_{PAO} with DS. From the experimental results, it is clear that P removal is negatively affected by high temperature (23°C). Previous researchers observed that at 20 and 30°C the accumulation of storage polymers is strongly dependent upon temperature (Viconneau et al. 1985; Florentz et al., 1987). They reported less PHB formation at higher temperatures. In addition better P removal efficiency was found at lower temperatures (5-15°C). Other researchers reported that at 5 and 10°C, incomplete P uptake was observed in the aerobic phase as a result of the influence of temperature on the oxygen consumption rate in BPR systems (Brdjanovic et al., 1997). In the investigation of Panswad et al. (2003), the PAOs were predominantly lower-range mesophiles or perhaps psychrophiles. In contrast, GAOs were found to be mid-range mesophilic organisms with their optimum growth temperatures between 25.0 and 32.5°C. There are conflicting reports concerning the effects of temperature on BPR. For example, BPR efficiency was reported to be improved at higher temperatures (20-37°C) (McClintock et al., 1993; Converti et al., 1995). Temperature not only influences metabolic activities of PAOs, but also affects $K_{NH4\ AUT}$ (0.832), the autotrophic reaction rate. Its rate is increased at lower temperatures.

Table 6.2 Arrhenius constant value (θ) for PAOs

Symbol	θ	
	DS	**Without DS**
Y_{PAO}	1.003	1.010
Y_{PO4}	1	1
Y_{PHA}	1	1
q_{PHA}	1.061	1.023
q_{PP}	1	1
μ_{PAO}	1	1
b_{PAO}	1	1
b_{PP}	1	1
b_{PHA}	1	1
K_{PS}	1	1
Y_A	1	1
μ_{AUT}	1	1
b_{AUT}	1	1
$K_{O2\ AUT}$	1	1
$K_{NH4\ AUT}$	0.832	0.832

PAOs processes in ASM2d, the mean value of the Arrhenius constant obtained for q_{PHA} and Y_{PAO} (θ = 1.032 and 1.017 with and without influent DS, respectively) are closer to the ASM2d values. The literature values for q_{PHA} and Y_{PAO} Arrhenius constants are given in Table 6.3.

Under anaerobic conditions, θ values obtained for the rate constant for storage of PHA (q_{PHA}) and the maximum rate for phosphorus release (estimated as the product Y_{PO4}*q_{PHA}) were the same values with and without influent DS. They were 1.061 and 1.023, respectively. It was observed, that the temperature influence on the maximum rate for PHA storage is similar to influence of temperature on the maximum rate of phosphorus release. This result is different from that of other researchers (Table 6.3).

Under aerobic conditions, θ values obtained for the rate constant for storage of polyphosphate (q_{pp}) was equal to 1. This value is different from that reported in other studies (Table 6.3).

Table 6.3 Comparison of Arrhenius constant value (θ) for PAOs

Temperature, °C	q_{PHA}	Phosphorus release	Y_{PAO}	Poly-P storage	Reference
17 & 23	*1.061	*1.061	*1.003	*1.000	This study
17 & 23	**1.023	**1.023	**1.010	**1.000	This study
13 & 20	1.035	1.022	0.996	1.053	García-Usach et al. (2006)
10 & 20	1.041	1.041	-	1.041	ASM2d (Henze et al., 1999)
15 & 20	1.079 ±0.024	1.071±0.032	-	1.067±0.006	Baetens et al. (1999)
15 - 20	1.095±0.013	1.075±0.012	-	1.031±0.017	Brdjanovic et al. (1998)
15 & 20	-	1.018	-	1.025	Helmer and Kunst (1998)
5 - 20	1.080±0.011	1.055±0.019	-	1.048±0.012	Brdjanovic et al. (1997)
10 - 30	1.048	1.043	-	1.055	Mamais and Jenkins (1992)

*DS, **Without DS

6.4 CONCLUSIONS

The values of calibrated stoichiometric and kinetic parameters showed an important dependence on additional carbon sources from influent DS and temperature. The phosphorus removal process was efficiently performed in the two experiments carried out showing a maximum value for Y_{PAO} and q_{PHA} at 23°C. The PAOs calibrated parameters indicated the presence of GAOs in the process. This is because the Y_{PAO} values at 17 and 23°C with and without influent DS were higher than values predicted by ASM2d. At 17°C the biological phosphorus removal efficiency was more effective than at 23°C.

The Arrhenius constant values obtained for the PAOs represented the temperature influences on biological phosphorus removal processes. The rate constant for storage of poly-hydroxy-alkanoates storage (q_{PHA}) is more influence by the temperature than the maximum rate for phosphorus release. θ values for q_{PHA} were 1.061 and 1.023 with and without influent DS, respectively.

CHAPTER 7:

GENERAL DISCUSSION

CHAPTER 7. GENERAL DISCUSSION

The work outlined in this research identified a number of key features that can potentially be used in understanding the influence of disintegrated sludge (DS) on enhanced biological phosphorus removal (EBPR). In keeping with the overall aim of the project, these findings include the following:

Reducing parameter subset sizes in ASM2d calibration in EBPR treatment processes was addressed by evaluating a novel calibration approach. The parameter sensitivity analysis and the parameter subsets are related to data available for calibration. Sensitivity analysis, used to quantify the magnitude of the dependency of model prediction upon particular parameters is similar to the methodology proposed by Brun et al. (2001). Sensitivity analysis is also applied to the experience-based approach; however, there is no detailed information on sensitivity analysis and parameter selection. In this method, fixed subsets for parameter selection require a high degree of specialization without a mathematical/statistical approach. Fixed parameter subsets are the limiting factor in the experience-based approach. Parameter values of one WWTP may not be applicable to other WWTPs. The new calibration analysis uses experimental results to select parameters of a subset size with manual calibration. This is done while not using the identifiability approach, In contrast the other identifiability methodology to select parameter subset requires high computational demand to develop the collinearity index (γ) and the determinant measure (ρ) (Brun et al., 2001). The parameter values calculated for γ and ρ were based upon sensitivity analysis. This new approach can enable researchers to reduce heavy computation demand and avoid the need to choose the modeling parameters. This is a simplified approach for practical use.

There were four structured procedures in this new approach. First, analysis of the wastewater characterization and layout of the specific wastewater treatment plant were established. Second, initial default values of ASM2d parameters were defined. The range of values for stoichiometric and kinetic parameters was obtained from the literature. Third, analysis of the sensitivity of the ASM2d parameters was done using the experimental results of an activated sludge on a pilot-scale process to obtain the

parameter significance ranking. Finally, model parameter values were refined by iteratively fitting them to the observed experimental results. This was done sequentially starting with the most significant parameter, continuing with subsequent parameters in order of decreasing impact upon the model. An application of this approach was applied to study EBPR using pilot scale a MUCT activated sludge process.

Step 1: Influent wastewater characteristics

Simulation of an operating period was completed for a steady state processes. The results predicted influent wastewater characteristics, as well as P release in anaerobic phase, effluent NH_4 and TP of the MUCT pilot scale biological phosphorus removal processes at steady state. Addition results of the characterization of influent wastewater components were also clarified.

Step 2: Default values and a priori parameter set

In order to calibrate the ASM2d model, a number of default parameters were established. Their values were obtained from published literature. For the analysis, an a priori assumption of parameter values had to be made. These were used as default values. They included stoichiometric and kinetics parameters of phosphorus accumulating organisms (PAOs).

Step 3: Parameter significance

The parameter significance ranking of the resulting sensitivity analysis was based on the total number of model outputs. The results showed which of these were the most significant of the data inputs, i.e., when their roots of mean squared (RMS) values of sensitivities were higher than 0. The RMS values indicate the mean sensitivity of the model output to a change in a parameter, θ_j. A higher RMS value means that the value of the parameter θ_j has a stronger effect on the simulation model (Brun et al., 2002). A value of zero indicates that the simulation results do not depend on the parameter, θ_j. Some researchers considered sensitivity parameters with RMS values that were greater

than or equal to 0 (Machado et al., 2009). From the results, the first 40 ASM2d parameters were chosen in order of descending sensitivity. Sensitivity analysis was employed for 51 these parameters in the initial classification. Other researchers reported that they used only the top 30 parameters. These were defined as those with RMS values greater than 0.07 and 0.10 in sensitivity analysis with default and optimized values, respectively (Brun et al., 2002).

The derivatives of Eq. 4.2 were determined numerically by finite difference methodology since the ASM2d model analysis is too complicated to be done algebraically (Norton, 2008). The difference in calculation of sensitivity analysis is based upon the central difference approach. A perturbation factor of 10^{-4} was used for the sensitivity calculation of each test parameter around the default ASM2d values. De Pauw and Vanrolleghem (2006) reported that this perturbation factor was selected because it produced equal derivative values with forward and backward finite difference methods.

The RMS values for wastewater processes in the current study show different values, i.e., either low or high level of RMS values depending upon the WWTPs conditions. Other researchers found that selection of a reduced set of the most sensitive parameters with subsequent detailed analysis could be done. The parameter set was reduced from approximately 25 to a number between 10 and 15. Computation time was reduced in subsequent steps (Weijers and Vanrolleghem, 1997). Those parameters showed a scaled mean output sensitivity coefficient larger than 0.2 in at a least one of the outputs. Reichert and Vanrolleghem (2001) proposed that ranking should only use for a preliminary selection of a set of about 15 parameters, depending on the problem. Final subset selection from those parameters should be criteria based using the determinant or the condition number of the Fisher Information Matrix (FIM). Thus, choosing the number of significant parameter for the selection of subsets of identifiable model parameters for large environmental simulation models was related to experience. From this, the parameter subsets under these studies were reduced. Consequently, the resulting 30 parameters were used for calibration in analyzing all experimental results.

Other researchers (Weijers and Vanrolleghem, 1997) used sensitivity parameter rankings with roots of mean squared values larger than 0.2 and found 11 relevant parameters that were used to calibrate Activated Sludge Model No. 1 (ASM1) applied to full-scale plant data. Differences in parameter significance rankings among studies of ASM2d are highly influenced by the data available for calibration. Important factors in this regard include consideration of particular WWTP configurations and operation, and some properties of collected data (Ruano et al., 2007). The parameter significance ranking showed that temperature correction coefficients and the parameters for PAOs were among the most influential parameters on the model outputs. In this study, ASM2d was calibrated using an identifiability method to describe nitrogen and phosphorus removal in the Haaren (the Netherlands) WWTP (Ruano et al., 2007). PAOs play an important role in the dynamics of the EBPR processes (Brun et al., 2002).

In another application, this approach to ASM2d calibration used an identifiability analysis in a systematic manner. It was applied to EBPR at a full scale WWTP in Switzerland (Brun et al., 2002). Additionally, to calibrate ASM2d for anaerobic/anoxic/oxic conditions (A2/O), a pilot WWTP used an identifiability approach (Machado et al., 2009). PAOs parameters were also among the most sensitive. Although other studies were in rough agreement, there were some differences.

The parameter significance rankings of the current study are different from that of other researchers (Brun et al., 2002; Ruano et al., 2007; Machado et al., 2009). In the current study, the parameter with the highest sensitivity was Y_{PO4}. However other researchers ranked this parameter's sensitivity as 8^{th} (Machado et al., 2009), 15^{th} (Ruano et al., 2007), and it was excluded altogether in another study (Brun et al., 2002). Also researchers (Brun et al., 2002) found that parameter, b_{PAO}, had the highest sensitivity although it ranked 4^{th} and 27^{th} in other studies (Machado et al., 2009; Ruano et al., 2007). This parameter's sensitivity was ranked lower in the current study (29^{th}).

Considering the second most significant sensitivity ranking in this study, μ_{PAO} was of the same order as in one study (Brun et al., 2002), but it was at a lower position (17th) in other work (Ruano et al., 2007), (Machado et al., 2009). Additionally, the current

study found that μ_{AUT} had a higher sensitivity ranking than other studies (Brun et al., 2002; Ruano et al., 2007). However its ranking was lower than reported elsewhere (Machado et al., 2009). Furthermore the sensitivity analysis in other work (Soejima et al., 2008) used only two parameters, Y_{PAO} and Y_{PO4}. Here anaerobic/aerobic/anoxic processes for simultaneous nitrogen and phosphorus removal on NO_3 and PO_4 profiles were examined. One group of researchers (Yagci et al., 2006) used manually repeating simulation as a sensitivity approach to individual changes in the magnitude of related parameters for each model parameter. This was based on steady state cyclic simulations of S_{PO4}, X_{PHA}, S_A and MLSS profiles using the most sensitive parameters namely, Y_{PO4}, q_{PHA}, q_{PP}, K_{PHA} and lysis rates.

Step 4: The iteration processes with simulation of the ASM2d modeling

The calibration approach described here avoids the problem of needing extensive experience in activated sludge modeling and the difficulty of identifiability analysis. This approach iterates only based upon the parameter sensitivity. A stepwise methodology was used in the mathematical simulations in each of the iterations. The number of iterations of each experimental data set was based on the number of parameters in the sensitivity analysis. Use of 30 iterative steps for each of the parameter data sets, i.e. the same number of parameters in the sensitivity ranking, was done to predict the output of NH_4 and TP in effluent and of PO_4 in anaerobic phase. Parameter significance ranking was used to perform the calibration in order to fit the model's parameter values to the observed results. The most significant parameter was iterated first. This was followed by each of the other 29 parameters included in the parameter significance ranking in order of decreasing influence. Iterations begun with the initial default parameter value and were carried out under the steady state conditions.

In the current study, 15 significant parameters were use of 30 sensitivity parameters. This included 5 parameters of autotrophs and 10 parameters of PAOs, that influenced calibration of effluent NH_4, and PO_4 under anaerobic conditions and effluent TP, respectively. These parameters were used for the calibration. Simulation outcomes varied with the values of the different significant parameters. It was seen from the sum

of squares of weighted deviations between measurement and calculation, and standard error of estimate (SEE) calculated, that these 15 parameters gave minimized results. Thus, these calibrated parameter values comprised a working parameter subset as is seen in the goodness of fit. Using the GPS-X manual function, input values of parameters under study were varied while other parameters were fixed with specific values, i.e., default or calibrated values. Simulation varied with input parameter values.

For example, the calibration of the effluent NH_4 with Y_{PO4} had the highest sensitivity value. It was a first parameter changed, whist the other 29 parameters were set to their default values. As a result, Y_{PO4} was not seen to influence effluent NH_4 concentration. It had no effect on the simulation model. Effluent NH_4 was the first experimental data set used to calibrate ASM2d parameters in order to observe the activity of autotrophs. The other parameter data sets, PO_4 in anaerobic phase and effluent TP, were not simultaneously calibrated.

The next parameter for simulating effluent NH_4 was μ_{PAO}. It also had no effect on the ASM2d calibration model as other parameter values were altered. Other parameters were used in similar fashion in descending order of sensitivity. Values of influential parameters were set to their default values for calibrations using other experimental data sets. For instance, the values of 5 important parameters for effluent NH_4 calibration were set to their defaults values in other calibrations.

In the second set of experimental results, PO_4 in the anaerobic phase and effluent TP, were calibrated at the same time as the influential parameters of PO_4 metabolism in an anaerobic phase. ASM2d calibrated model of effluent TP was also changed. After calibration, the values for each influential parameter were found. As a result, the only stoichiometric and kinetic parameters of PAOs were 10 influential parameters in these data sets. Particularly important parameters were used for observation of specific microorganisms, i.e., ASM2d calibration using 10 significant parameters for PO_4 metabolism in an anaerobic phase and effluent TP was used to investigation PAOs behaviors. Additionally, the 5 calibrated parameters for effluent NH_4 described

autotrophic mechanisms only. Thus, by following this calibration methodology, the values of parameter subset were governed by the experimental data.

As a result of fitting the simulated data to the effluent NH_4 concentration, it was found that there were five significant parameters. They are: yield of autotrophic biomass per unit of NO_3^-N (Y_A), the maximum growth rate for autotrophs (μ_{AUT}), the decay rate of X_{AUT} (b_{AUT}), the saturation coefficient for ammonium ($K_{NH4\ AUT}$), and the saturation coefficient for oxygen $K_{O2\ AUT}$.

The value of μ_{AUT} was increased to sustain autotrophic growth. Next b_{AUT} was decreased in relation to increasing autotrophic growth rate. Later, $K_{NH4\ AUT}$ was decreased because of low ammonium concentration in the aerobic phase. Both Y_A and $K_{O2\ AUT}$ remained relatively unchanged from their default values. Significant parameters were calibrated based upon NH_4 concentrations in effluent using the experienced-based approach for experiments in sequencing batch reactors (SBRs) (Insel et al., 2006). To accomplish this, nutrients were removed under limited aeration conditions. The parameters examined included μ_{AUT} and K_{NH4}. In addition to calibration with an experienced-based approach to determine EBPR under different phosphorus/acetate ratios with the ASM2d modeling in the SBR performance, it has been shown that only μ_{AUT} is necessary to calibrate NH_4 and NO_3 (Yagci et al., 2006). A practical identifiability approach for the ASM2d calibration is to select the parameter subset sizes for autotrophs with three calibrated parameters: b_{AUT}, K_{NH4} and μ_{AUT} (Brun et al., 2002).

In a further study (Machado et al., 2009) examined an activated sludge anaerobic/anoxic/oxic (A^2/O) pilot WWTPs using an identifiability approach with the Fisher Information Matrix (FIM) tool. Their purpose was to reduce ASM2d parameter subset sizes using only μ_{AUT}. This presents a calibrated autotroph parameter and the parameter subset size of b_{PAO}, Y_{PO4}, μ_{AUT}. The calibrated parameters included in the simulation of nitrogen removal at the Hanover-Gümmerwald pilot wastewater treatment plant were μ_{AUT}, $\eta_{NO3\ HYD}$, K_h, η_{fe}, μ_H, K_{O2}, η_{NO3}, $K_{NH4\ AUT}$, q_{PHA}, q_{PP}, and Y_{PO4}. This was based on ASM2d and ASM3P model concepts (Makinia et al., 2006).

In the current study, several parameters govern the fitting of the simulation to model to PO_4 in anaerobic phase and effluent TP. These parameters include: Y_{PAO}, Y_{PO4}, Y_{PHA}, q_{PHA}, q_{PP}, μ_{PAO}, b_{PAO}, b_{PP}, b_{PHA}, and K_{PS}. In another study (Soejima et al., 2008), Y_{PAO} and Y_{PO4} calibrated parameters were used to investigate the effects of extra acetate on the anaerobic/aerobic/anoxic (AOA) processes for simultaneous nitrogen and phosphorus removal based on the ASM2d modeling with the additional denitrifying PAOs (DNPAOs) kinetics. That modeling determined the optimal concentration of supplementary COD and elucidated microorganism metabolism. Thus the application of this modeling to different wastewater compositions varying COD/N/P, can be conducive to predicting PAOs behavior (Soejima et al., 2008).

To study phosphorus storage capacity-limiting and phosphorus loading-limiting conditions, there are 8 significant calibrated parameters. These include μ_{AUT}, b_{PAO}, b_{PP}, b_{PHA}, q_{PHA}, q_{PP}, K_{PHA} and Y_{PO4}. They were used for simulations of S_{PO4}, X_{PHA}, S_A and MLSS profiles in sequencing batch reactor (SBR) performance for EBPR when fed with acetate as the carbon sole carbon source under different phosphorus/acetate ratios (Yagci et al., 2006). Calibration and simulation using the ASM2d model at different temperatures in a phosphorus removal pilot plant showed that the significant calibrated parameters included Y_H, $\mu_{H,}$ K_F, $b_{H,}$ η_{NO3}, μ_A, K_{NH4}, b_A, Y_{PO4}, q_{PHA}, K_A, Y_{PAO}, μ_{PAO}, q_{PP}, b_{PAO}, K_{PHA}, K_{IPP}, and K_{MAX} (García-Usach et al., 2006). To simulate the O_2, COD, NH_4, and PO_4 data sets in an activated sludge system, a large parameter set (Hulsbeek et al., 2002) was used that included i_{NXS}, i_{NXI}, $K_{O2\ AUT}$, $K_{NH4\ AUT}$, $b_{AUT,}$ η_{NO3}, b_H, K_{NO3}, and K_{O2}. In another study (Melcer et al., 2003) included $\mu_{AUT,}$ $\alpha_{XI,}$ $\alpha_{SA,}$ $\alpha_{SF,}$ $\eta_{NO3\ HYD}$, K_{PHA}, and μ_{PAO} in their simulation. This methodology was successful in calibrating pilot plant operations. The expectation when using this in a full-scale site is that its use can reduce time required for calculation of parameter subset sizes. Subsequently, operational processes can be enhanced on basis of understanding organism behaviors. However, fluctuation of wastewater characteristics and complexity of operation systems may cause calculation errors.

Evaluation of the effect of influent disintegrated sludge (DS) upon enhanced biological phosphorus removal (EBPR) processes was simulated using Activated Sludge Model No. 2d (ASM2d). ASM2d calibration of the experimental results with and without influent DS was done using the new calibration approach. It was found that the resulting calibrations with and without influent DS have the same calibrated parameters. Including DS in the influent of WWTPs caused enhancement of PAOs in wastewater treatment. It resulted in a higher influent phosphorus content (12.9 g P m^{-3}) than without DS (10.40 g P m^{-3}). Influent phosphorus contents were 0.83% of TSS with DS and 0.73 % of TSS without DS. Additionally, the influent phosphorus to acetate ratio (0.26 g P g^{-1} COD) with influent DS was higher than without DS (0.21 g P g^{-1} COD). This caused a higher utilization of carbon sources by PAOs. Those behaviors can be explained by examining Y_{PAO} and Y_{PHA}. Y_{PAO} (0.64 g COD g^{-1} COD), with influent DS was higher than without (0.61 g COD g^{-1} COD). Y_{PHA} (0.26 g COD g^{-1} P) with influent DS also was higher than without (0.24 g COD g^{-1} P). The influence of DS components upon phosphorus removal is not only based upon phosphorus and acetate (S_A), but also it is related to fermentable biodegradable products (S_F), and slowly biodegradable products (X_S). Furthermore, it is related to different phosphorus to COD (P/COD) ratios within influent DS.

Varying carbon sources i.e., S_A, S_F, and X_S, resulted in P/COD ratios of 1.11 g P g^{-1} COD, 0.22 g P g^{-1} COD, 0.66 g P g^{-1} COD, respectively. Varying the carbon sources influenced specific phosphorus release rates (SPRR) which were different depending upon the particular carbon source, i.e., S_A, S_F, or X_S. In each of these instances, SPRR for influent DS were 0.834 mg P g^{-1} VSS_{PAOs} h^{-1}, 3.9 mg P g^{-1} VSS_{PAOs} h^{-1}, and 0.31 mg P g^{-1} VSS_{PAOs} h^{-1}, respectively.

To test model fit to experimental data, a Chi-Square test for goodness of fit was done. The null hypothesis (H_0) was that observed and predicted values are unequal, i.e., the model was unsuccessful in predicting experimental results. The alternate hypothesis (H_a) was that observed and predicted values have the same distribution. The null hypothesis (H_0) was rejected in favor of the alternate hypothesis (H_a). This is done at a 95% confidence level. Model fitting was done by minimizing the sum of squares of

weighted deviations (SSWD) between measured and calculated values. The objective function of the sum of the squared weighted errors was constructed based upon weighted non-linear least-square analysis (Fang et al., 2009). In addition, standard error of estimate (SEE) was also calculated to measure the accuracy of predictions. This is a regression model that minimizes the sum of squared deviation of prediction (Irwin, 1949). A variation of sum of squares arises from (1) range of applicability of the protocols, (2) technical limitations of tools/sensors for data collection, (3) limitations in transferring lab-scale data to full-scale models, (4) design of data collection (measurement campaigns, ad hoc versus mathematical approaches), and (5) complexity of model calibration (limited data versus complex model structure) (Sin et al., 2005). Effluent NH_4, phosphorus (P) release and effluent TP were modeled. Observed and predicted values under both test and control conditions were determined. Comparison showed that paired values were the same. This is shown by low p-values (p-values < 0.005). The p-value for goodness of model fit for phosphorus release without DS was a bit higher (p-value = 0.02044). However this is still a strong fit (p-value < 0.05). Furthermore, results of SEE are lower than SSWD results under both test and control conditions, i.e., with and without DS. Thus, it supports the model's goodness of fit.

Five parameters were used to fit calibrated effluent NH_4 to observed values. These parameters included: $K_{NH4\ AUT}$, μ_{AUT}, b_{AUT}, Y_A and $K_{O2\ AUT}$. Another study to calibrate NH_4 was based on the removal of nutrients under limited aeration conditions in sequencing batch reactors (SBRs) (Insel et al., 2006). $K_{NH4\ AUT}$ and μ_{AUT} were the calibrated parameters. A similar trend was observed in the study of Yagci et al. 2006. In this study, μ_{AUT} was the parameter used to calibrate NH_4 and NO_3 data sets. This study used an SBR system to do EBPR under different phosphorus/acetate ratios. Furthermore, in the study of Machado et al. (2009), μ_{AUT} was the only calibrated parameter used to represent autotrophic behavior ASM2d modeling and was used to investigate activated sludge anaerobic/anoxic/oxic (A2/O) EBPR. In addition, autotrophic calibrated parameters (Brun et al., 2002) were found as b_{AUT}, $K_{NH4\ AUT}$ and μ_{AUT}. As a result, Y_A values under both test and control conditions were similar to those of ASM2d (0.24 g COD g^{-1} N). The $K_{O2\ AUT}$ test and control values were also the same

as that of ASM2d (0.5 g O_2 m^{-3}). In another study Dudley et al. (2002) found that the $K_{O2\ AUT}$ concentration (0.4 g O_2 m^{-3}) was lower than observed in the current study. The previous study was based on data collected from an activated sludge University of Cape Town (UCT) treatment plant at a Swedish sewage works. It was better able to explain heterotrophic usage of VFAs. However μ_{AUT} was set to 1.2 d^{-1} to obtain a reasonable model fit. This was higher than in ASM2d (1.0 d^{-1}) and done to sustain autotrophic growth. $K_{NH4\ AUT}$ (0.15 g N m^{-3}) in test and control experiments was less than that in ASM2d (1.00 g N m^{-3}). This occurred because of low ammonia concentration in the aerobic phase. In the study of Dudley et al. (2002), K_{NH4AUT} (0.3 g N m^{-3}) was lower than that found in ASM2d. $K_{NH4\ AUT}$ was changed to promote autotrophic growth. The observed b_{AUT} value (0.05 d^{-1}) was also lower than in ASM2d (0.15 d^{-1}). It decreased with increasing autotrophic growth. As with the results for NH_4 calibrated parameters, it was concluded that DS did not significantly affect autotrophic mechanisms. It can be concluded that carbon components in DS, including volatile fatty acids as acetate (S_A), fermentable biodegradable products (S_F) and slowly biodegradable products (X_S), do not affect autotrophic mechanisms.

A second series of data sets were used to elucidate PAOs mechanisms of phosphorus release in anaerobic phase and effluent TP. These data sets were relevant only to investigation of the stoichiometric and kinetic parameters of PAOs. They had no influence upon heterotrophs and autotrophs. This is seen in the parameters subsets for calibration. In contrast to calibrated effluent NH_4, the first data sets were used to study the behaviors of autotrophs by employing the calibrated parameters. Thus effluent NH_4 affected only autotrophic mechanisms. Other researchers reported $K_{NH4\ AUT}$ and μ_{AUT}, and other autotrophic parameters obtained from calibration of NH_4 during nitrification (Insel et al., 2006). In addition, the calibrated NH_4 and NO_3 data sets were used to describe the mechanisms of autotrophs with μ_{AUT} (Yagci et al., 2006). The simulation model fits P release in anaerobic phase and effluent TP well.

The following 10 parameters govern phosphorus release in anaerobic phase and effluent TP profiles: Y_{PAO}, Y_{PO4}, Y_{PHA}, q_{PHA}, q_{PP}, μ_{PAO}, b_{PAO}, b_{PP}, b_{PHA}, and K_{PS}. To study the effects of extra acetate on simultaneous nitrogen and phosphorus removal based on the

modified ASM2d, modeling of denitrifying PAOs (DNPAOs) kinetics was done (Soejima et al., 2008). It was concluded that Y_{PAO} and Y_{PO4} govern NO_3 and PO_4 concentrations. That modified modeling expressed the optimum concentration of supplementary COD and microbiological metabolism. Addition of supplementary COD to the different chemical oxygen demand/nitrogen/phosphorus (COD/N/P) compositions enhanced PAOs mechanisms. Yagci et al. (2006) studied phosphorus storage capacity-limiting and phosphorus loading-limiting conditions based on predicted simulations of S_{PO4}, X_{PHA}, S_A and MLSS profiles in the SBR performance to EBPR. Their calibrated parameters included Y_{PO4}, q_{PHA}, q_{PP}, K_{PHA}, b_{PAO}, b_{PP}, b_{PHA}, and μ_A. Empirical metabolic EBPR models (Comeau et al., 1986; Mino et al., 1987) directly relate production and utilization of intracellular polyphosphate (poly-P), and poly-hydroxy-alkanoates (PHA) or intracellular carbohydrates. Microorganisms employ EBPR to derive energy from poly-P degradation and utilize carbon under anaerobic conditions (Comeau et al., 1986; Mino et al., 1987). Stored carbon is used for growth and intracellular poly-P storage under aerobic conditions (Comeau et al., 1986; Mino et al., 1987). Selecting appropriate microorganisms is necessary to achieve EBPR (Jenkins & Tandoi, 1991; Mino et al., 1998). As a result, the ability to perform EBPR is related to the complexity of PAOs and glycogen accumulating organisms (GAOs). Both types of organisms use different energy sources (Cech and Hartman, 1993; Kuba et al., 1993; Liu et al., 1996). In addition, there is an internal energy-based competition between PAOs and GAOs for acetate utilization (Liu et al., 1997). PAOs and GAOs utilize energy from metabolism of intracellular poly-P and glycogen, respectively (Comeau et al., 1986; Mino et al., 1987; Liu et al., 1994). Carbon utilization by PAOs is based on poly-P degradation to generate energy in the anaerobic phase.

To study the effect of phosphorus to carbon (P/C) ratio upon favoring specific microorganisms, this ratio was decreased from 1:10 to 1:50 (Kong et al., 2002). Population of ß-*Proteobacteria* decreased from approximately 77% of the total bacteria to 38%. This decrease in the ß-*Proteobacteria* population coincided with a reduction in both the proportions of PAOs, ß-proteobacterial, *Rhodocyclus* and intracellular poly-P. As the P/C ratio in the feed stream (1/50) decreased there was a corresponding increase

in proportion of GAOs (Kong et al., 2002). Another researcher (Liu, 1998) reported that intracellular carbohydrate content at low levels was a prerequisite for achieving EBPR.

Intracellular carbohydrate content is an internal energy source for GAOs (Matsuo et al., 1992; Satoh et al., 1992; Cech and Hartman, 1993). The energy sources used in anaerobic carbon utilization determined the dominant organisms. Other researchers (Liu et al., 1996) studied the conditions necessary to cause GAOs to predominate at a low P/C (1/50, wt/wt) ratio. They concluded that energy and reducing equivalents required for carbon uptake and storage are generated from the glycolysis of sugar. Also, their results suggest that microorganisms in sludge preferentially utilize glucose over cellular glycogen as an energy source during acid uptake. As a result, under low P/C conditions GAOs can utilize dissolved substrate and reduce biological phosphorus removal (Liu et al., 1996).

When making observations of the influence of DS upon phosphorus removal efficiency, characterization of DS was done. In the current study, acetic acid was fed in same concentration to both test and control experiments. Acetic acid concentration was controlled to determine if the PAOs mechanisms were affected by the DS components in relation to phosphorus concentration. The components of DS contained not only acetic acid, which was in limited concentration under both two conditions, but also phosphorus. This resulted in a higher phosphorus/acetate ratio in the test influent (0.26 g P g^{-1} COD) than that in the control (0.21 g P g^{-1} COD). Also phosphorus contents of the feed stream in test and control experiments were 0.83 % of TSS and 0.73 % of TSS respectively. As a result, PAOs at the higher phosphorus/acetate ratio take up more acetate and do so at a faster rate than those with a lower phosphorus/acetate ratio. PAOs in the current study tend to dominate at both P/C ratios. This is because P/C ratios were greater than 0.1, a level above which PAOs predominant (Liu et al., 1996 & 1997; Kong et al., 2002; Yagi et al., 2006). Higher and faster carbon utilization rates of PAOs occurred at high P/C ratios (Fukase et al., 1984; Mino et al., 1987; Wentzel et al., 1988; Smolders et al., 1994; Liu et al., 1996; Liu et al., 1997). Liu et al. (1997) reported that decreasing P/C ratio from 20/100 to 2/100 did not affect carbon utilization and intracellular PHA storage under anaerobic conditions. However it caused internal

poly-P storage content to decrease from 33% to 2%. As a result, EBPR was observed to decrease as GAOs predominated at lower the P/C ratio (2/100) (Liu et al., 1997). Furthermore, a further study found that GAOs can utilize acetate under anaerobic conditions without using poly-P at lower phosphorus/acetate ratios (Yagci et al., 2006). Glycogen degradation produces energy for utilization of acetic acid in GAOs. Additionally, the essential characteristics of PAOs and GAOs were studied under a low P/C ratio.

PAOs utilize carbon more slowly and GAOs consume the remaining available acetate (Manga et al., 2003). The process results from a direct relation between phosphorus release and X_{PHA} storage. It is represented by the rate constant for storage of PHA, q_{PHA} (Yagci et al., 2006). In the calibrated results of the current study, q_{PHA} in test and control experiments showed the same value (3.5 g X_{PHA} g^{-1} X_{PAO} d^{-1}). This was true even though the test conditions showed higher phosphorus release than did the control. However that value is higher than that predicted by the ASM2d model (3.00 g X_{PHA} g^{-1} X_{PAO} d^{-1}). As a result, the q_{PHA} trend was in different than the above due to the higher phosphorus release under test conditions. PHA storage was greater due to uptake of more acetate. It is suggested that for further study, varying the concentration of carbon sources in DS be investigated with respect to q_{PHA}.

The rate constant for storage of X_{PP}, q_{PP}, was also used to simulate phosphorus release in the anaerobic phase. In contrast to Yagci et al. (2006), q_{PP} was adjusted in the aerobic phase and effluent in order to observe phosphate uptake. That parameter, q_{PP}, showed the same value, 1.50 g X_{PP} g^{-1} X_{PAO} d^{-1}, under both test and control conditions. Its value was also found to the same as the default value (1.5 g X_{PP} g^{-1} X_{PAO} d^{-1}). Another kinetic parameter important to PAOs mechanisms, saturation coefficient for P in storage of poly-P, $K_{PS,}$ was increased to 0.35 g P m^{-3} in both test and control experiments. Other researchers reported that K_{PS} and q_{PP} were increased to 0.5 g P m^{-3} and 2.00 g X_{PP} g^{-1} X_{PAO} d^{-1}, respectively by using ASM2d to predict these two parameters. (Yagci et al., 2006). Moreover, evaluation of ASM2 at high phosphorus concentrations found that K_{PS} and q_{PP} were 20 g P m^{-3} and 2.35 g X_{PP} g^{-1} X_{PAO} d^{-1}, respectively (Seco et al., 2001). The parameter, K_{PS}, was related to to q_{PP} under both aerobic and anoxic conditions, but

at different values under each of these conditions. Both parameters influenced storage polyphosphate (PP) of PAOs processes. These controlled kinetic processes can be described by a Monod type expression. In the rate of PP storage (X_{PP}), the influence of K_{PS} depends upon phosphorus concentration. This is because phosphorus in PAOs was controlled by a phosphorus saturation limitation (Henze et al., 1999). In addition, storage PP in PAOs was related to the maximum capacity of storage PP as shown in 11st and 12nd processes. Other studies reported that K_{PS} was increased to 0.5 g P m^{-3} without including q_{PP} as a calibrated parameter (Insel et al., 2006). Y_{PO4} was also taken in to account in the calibration and represented with an equivalent value (0.4 g P g^{-1} COD) for test and control experiments. The default value was also equal to 0.4 g P g^{-1} COD. PHA is consumed by simultaneous utilization phosphate and the growth of PAOs.

The parameter, b_{PP} was also involved in the endogenous metabolism of X_{PP} obtained after the poly-P transformation. Lysis of poly-P, b_{PP}, showed the same value (0.2 d^{-1}) under test and control as well as ASM2d modeling. The lysis rates defined by b_{PAO} and b_{PHA} showed constant values equal to 0.2 d^{-1} even though the phosphorus/acetate ratios between test and control experiments were different. In contrast to the studies of Yagci et al. (2006), bpp, b_{PAO} and b_{PHA} showed an ascending trend with increasing P/COD ratios. Y_{PAO} in test experiments (0.64 g COD g^{-1} COD) was higher than in the controls (0.61 g COD g^{-1} COD) and ASM2d modeling (0.625 g COD g^{-1} COD). A higher value Y_{PAO} (0.9 g COD g^{-1} COD) was due to presence of GAOs (Ferrer et al., 2004). ASM2d does not differentiate between EBPR of PAOs and GAOs (Ferrer et al., 2004). The stoichiometric and kinetic equations in ASM2d were used in describing the processes of both types of bacteria. Additionally, glycogen is not considered an intracellular storage product in the ASM2d model. As a result, COD associated with GAOs and glycogen was expressed as X_{PAO}. In this case, Y_{PAO} was higher in a mixed population than in a pure culture of PAOs (Ferrer et al., 2004). Similarly, the higher value of Y_{PAO} (0.8 g COD g^{-1} COD) can be explained by the presence of GAOs (Penya-Roja et al., 2002). The value for Y_{PHA}, (0.26 g COD g^{-1} P) with influent DS was higher value than for the control (0.24 g COD g^{-1} P) and for ASM2d modeling (0.2 g COD g^{-1} P). The μ_{PAO} values under test and control conditions are equivalent to those of ASM2d modeling (1 d^{-1}).

Inclusion of DS components in the influent feed stream of our experiments promoted enhanced phosphorous removal. The significant DS sludge components that have impact upon phosphorus removal efficiency can be investigated using statistical analysis. The paired t-test method was used to investigate the relationship between essential components of DS and phosphorus release under anaerobic phase. Also the relationships between DS components and effluent TP were investigated. The paired t-test to evaluate the effects of various DS components upon phosphorus release and effluent TP resulted in rejection of the null hypothesis (H_o) in all cases, in favor of the alternate of research (H_a) hypotheses. The null hypothesis (H_0) was that the prediction of phosphorous release with influent DS and without influent DS was equal when considering several parameters. Theses parameters include P, S_A, S_F and X_S. The alternate hypothesis (Ha) was that prediction of phosphorous release with influent DS and without influent DS with the same parameters had different distributions. The four significant parameters in phosphorus removal efficiency are orthophosphate phosphorus (P), volatile fatty acids (S_A), fermentable biodegradable products (S_F) and slowly biodegradable products (X_S). This is seen in the magnitude of their p-values (p-value < 0.00001). Also the mean concentration of released phosphorus with and without influent DS is significantly different. As a result, it is shown with high confidence (p-value < 0.00001) that DS enhances phosphorus release. The influence of S_A, S_F and X_S DS components as carbon sources to EBPR systems was observed. It is related to PAOs. Phosphorus release under anaerobic conditions can show PAOs activity. Specific phosphorus release rate (SPRR) was used to indicate the PAOs behavior. It is proportional to PAOs biomass. The results show that SPRR of S_F DS component as carbon source was highest in comparison with other DS components. The SPRR values were 0.834 mg P g^{-1} VSS_{PAOs} h^{-1}, 3.90 mg P g^{-1} VSS_{PAOs} h^{-1} and 0.31 mg P g^{-1} VSS_{PAOs} h^{-1} for S_A, S_F and X_S, respectively. Additionally, the SPRR values with and without DS were 56.54 mg P g^{-1} VSS_{PAOs} h^{-1} and 52.88 mg P g^{-1} VSS_{PAOs} h^{-1}, respectively. The phosphorus and carbon feeding (P/C) ratios with and without were 0.11 and 0.09. The SPRR result with and without DS in this current study was lower than in the work of others (Panswad, et al. 2007). They were 106.2-156.9 mg P g^{-1} VSS_{PAOs} h^{-1}, 113.6 - 167.9 mg P g^{-1} VSS_{PAOs} h^{-1}, 84.7-127.9 mg P g^{-1} VSS_{PAOs} h^{-1} with P/C ratios of 0.02, 0.04 and 0.16 respectively.

These values were obtained from EBPR systems. However, in the current research with and without DS, results were similar to those of SBR processes (52.0 – 76.9 mg P g^{-1} VSS_{PAOs} h^{-1}) reported by other researchers (Panswad et al., 2003). Consequently, concentrations of effluent TP are significantly different with and without influent DS. High Pearson correlation coefficients suggest highly linear relationships between process parameters.

Verification was used to determine if the model could achieve specified performance requirements. This was done to test whether different data sets agreed with each other. In this study, the operating temperature conditions (17°C and 23°C) were different. This is because the experimental results were obtained in winter with an average temperature of 17°C and the experimental observations were conducted in summer with an average temperature of 23°C. The experiments were conducted during different time periods. In comparison, since both experiments were to test the verification approach, they needed to be controlled under the same conditions. These observations could not have been made at the same time because there were limited in their number of activated sludge pilot-scale wastewater treatment reactors.

Predicted values of phosphorus release obtained from model fitting were found to be the same as observed values under test and control conditions. The H_o hypothesis was that observed and predicted values are unequal. H_o was rejected at a 95% confidence level. This is shown by p-value of Chi-Square test for goodness having a value less than 0.05. The p-values under test and control conditions were < 0.00001 and 0.00005, respectively. As is seen from these p-values, confidence levels are 99.999% and 99.995% were obtained for test and control conditions, respectively. However, some calibrated parameters were different. The Y_{PAO}, q_{PHA} and $K_{NH4\ AUT}$ values in verification (23°C) were different from those of calibration (17°C). This may be due to the influence of temperature.

Additionally, the effects temperature and inclusion of influent disintegrated sludge (DS) as a carbon source upon PAOs in a biological phosphorus removal pilot plant were found. Experiments were carried out at 17°C and 23°C. PAOs kinetic parameters

obtained at 17°C indicate that the yield coefficient (Y_{PAO}) and poly-hydroxy-alkanoates (PHA) storage (q_{PHA}) decreased. In contrast, a saturation coefficient for ammonium (substrate), $K_{NH4\ AUT}$, in autotrophs was lower at 23°C than at 17°C. Values of Y_{PAO}, Y_{PO4}, and K_{MAX} in PAOs are different in ASM2d because of the presence of GAOs (Penya-Roja et al., 2002; Ferrer et al., 2004).

K_{MAX} refers to the maximum ratio X_{PP}/X_{PAO}. GAOs are treated in the same manner as PAOs in ASM2d in that they cannot store polyphosphate. On the basis of this ASM2d assumption, PAOs and GAOs are not different (Ferrer et al., 2004). Glycogen is not represented as an intracellular storage product in ASM2d. Thus, GAOs and glycogen were presented in PAOs (Penya-Roja et al., 2002; Ferrer et al., 2004). Observed Y_{PAO} values at 17 and 23°C with and without influent DS are higher than predicted by ASM2d. One exception is that Y_{PAO} without influent DS at 17°C is lower than predicted by ASM2d. GAOs are present in pilot-scale WWTPs. Under anaerobic conditions, both PAOs and GAOs can store VFAs internally in the form of PHA. PAOs utilize energy from polyphosphate and glycogen degradation. In contrast, GAOs utilize energy from glycogen degradation only. As GAO population increases as Y_{PO4} values are decreased (Henze et al., 1995, Ferrer et al., 2004). In this study Y_{PO4} (0.4) was found to have a similar value to that predicted by ASM2d. The behavior of Y_{PO4} with respect to ASM2d is different from that seen for Y_{PAO}.

Y_{PO4} values in other studies were reported to be 0.42 and 0.46 g P g^{-1} COD in Elche B and Elda WWTPs, respectively (Ferrer et al., 2004). It was concluded that GAOs were absent in Elche B WWTPs since the value of Y_{PO4} was close to the predicted ASM2d value (0.4). Additionally, Elda WWTPs contained GAOs, even though Y_{PO4} was much higher than the expected value for a mixed population of PAOs and GAOs. This caused a higher pH (7.95). Y_{PAO} at 17°C was lower than at 23°C. This result suggests that even though the values of kinetic parameters decrease as temperature is reduced, the efficiency of EBPR processes is higher at lower temperatures. PAOs occur at 10°C or less because they are psychrotrophic. Under these conditions, PAOs growth rate is higher than non-PAOs in EBPR systems (Erdal et al., 2003). This results in an increased PAO population at lower temperatures (Erdal et al., 2003). The EBPR performance at

20°C was lower than at 10°C even though the kinetic parameter values increased when temperature was increased from 10 to 20°C (Erdal et al., 2003). The reason for higher efficiency of EBPR performance at lower temperature was related to reduce competition for substrate by non-PAOs under anaerobic conditions.

The Arrhenius relationship was employed using ASM2d parameters. A set of calibrated parameters is required in order to use this equation. The θ constant values of the Arrhenius equation were determined from experiments conducted at 17 and 23°C. The Arrhenius constant values of PAOs can be categorized into two groups. The first group, consists of temperature independent parameters ($\theta = 1$) where stoichiometric, saturation, lysis rate coefficients are included. Stoichiometric and kinetic parameters, with the exception of Y_{PAO}, are included. The second group consisted of temperature dependent parameters ($\theta \neq 1$) where the kinetic parameters Y_{PAO} and q_{PHA} are included. These Arrhenius constant values for the PAOs reflected the temperature influences ($\theta \neq 1$) on the biological phosphorus removal processes. The rate constant for storage of X_{PHA} (Y_{PAO}) is more affected by temperature than the yield coefficient (Y_{PAO}). Additionally, θ of q_{PHA} with DS is higher than θ of q_{PHA} without DS. In contrast, θ of Y_{PAO} without DS is higher than θ of Y_{PAO} with DS. From the experimental results, it is clear that P removal is negatively affected by higher temperature (23°C). Previous researchers observed that at 20 and 30°C the accumulation of storage polymers is strongly dependent upon temperature (Viconneau et al. 1985; Florentz et al., 1987). They reported less PHB formation at higher temperatures. In addition better P removal efficiency was found at lower temperatures (5-15°C). Other researchers reported that at 5 and 10°C, incomplete P uptake was observed in the aerobic phase as a result of the influence of temperature on the oxygen consumption rate in BPR systems (Brdjanovic et al., 1997). In the investigation of Panswad et al. (2003), PAOs were predominantly lower-range mesophiles or perhaps psychrotrophs. In contrast, GAOs were found to be mid-range mesophilic organisms with their optimum growth temperatures between 25.0 and 32.5°C. There are conflicting reports concerning the effects of temperature on BPR. For example, BPR efficiency was reported to be improved at higher temperatures (20-37°C) (McClintock et al., 1993; Converti et al., 1995). Temperature not only influences metabolic activities of PAOs, but also affects $K_{NH4\ AUT}$ (0.832), the autotrophic reaction

rate. Its rate is increased at lower temperatures. For PAOs processes in ASM2d, the mean value of the Arrhenius constant obtained for q_{PHA} and Y_{PAO} (θ = 1.032 and 1.017 with and without influent DS, respectively) are closer to the ASM2d values. Under anaerobic conditions, θ values obtained for the rate constant for storage of PHA (q_{PHA}) and the maximum rate for phosphorus release (estimated as the product Y_{PO4}*q_{PHA}) were the same values with and without influent DS. They were 1.061 and 1.023, respectively. It was observed that the temperature influence on the maximum rate of PHA storage is similar to influence of temperature on the maximum rate of phosphorus release. This result is different from that of other researchers. Under aerobic conditions, θ values obtained for the rate constant for storage of polyphosphate (q_{pp}) were equal to 1. This value is different from that reported in other studies (García-Usach et al., 2006; Baetens et al. 1999; Henze et al., 1999; Brdjanovic et al., 1998; Helmer and Kunst, 1998; Brdjanovic et al., 1997; Mamais and Jenkins, 1992).

CHAPTER 8:

CONCLUSIONS AND FUTURE WORK

CHAPTER 8. CONCLUSIONS AND FUTURE WORK

8.1 CONCLUSIONS

This project investigated the influence of disintegrated sludge (DS) on enhanced biological phosphorus removal (EBPR). The main aspects studied were related to phosphorus removal efficiency in relation to phosphorus accumulating organisms (PAOs) kinetics in the Modified University of Cape Town (MUCT) systems. With regard to the objective of this study, a series of conclusions can be drawn from Activated Sludge Model No. 2d (ASM2d) modeling calibration carried out through this research.

1. Reducing parameter subset sizes in the ASM2d modeling calibration in EBPR treatment processes has been addressed by evaluating a novel calibration approach. The parameter sensitivity analysis and the parameter subsets are related to data available for calibration. Sensitivity analysis, used to quantify the magnitude of the dependency of model prediction on particular parameters is similar to the method proposed by Brun et al. (2001). The sensitivity analysis is also applied to the experience-based approach; however, there is no detailed information on sensitivity analysis and parameter selection. Fixed subsets for parameter selection require a high degree of specialization without a mathematical/statistical approach. Fixed parameter subsets are the limiting factor in the experience-based approach.

   The new calibration analysis uses experimental results to select parameters of a subset size with manual calibration. This is done while not using the identifiability approach. In contrast the other identifiability methodology to select parameter subset requires high computational demand to develop the collinearity index (γ) and the determinant measure (ρ) (Brun et al., 2001). This new approach can enable researchers to reduce heavy computation demand and avoids the need to choose the modeling parameters. This is a simplified approach for practical use.

2. The evaluation of DS upon EBPR processes was completed using the ASM2d. The influence of DS upon phosphorus removal efficiency, was investigated by feeding the same concentration of acetate to both test and control experiments. It was controlled to observe whether the PAOs mechanisms were affected by the DS components in relation to phosphorus. The components of DS contained not only acetate, which was in limited concentration under both two conditions, but also phosphorus. Including DS in the influent of WWTPs resulted in a higher influent phosphorus content (12.90 g P m^{-3}) than without DS (10.40 g P m^{-3}). Also phosphorus contents of the feed stream in test and control experiments were 0.83 % of TSS and 0.73 % of TSS respectively. In addition, the influent phosphorus to acetate ratio (0.26 g P g^{-1} COD) with influent DS was higher than without DS (0.21 g P g^{-1} COD).

   Successful calibration of PAOs and autotrophic mechanisms was achieved. It was found that the resulting calibrations with and without DS have the same calibrated parameters. Calibrated parameters included: Y_{PAO}, Y_{PO4}, Y_{PHA}, q_{PHA}, q_{PP}, μ_{PAO}, b_{PAO}, b_{PP}, b_{PHA}, K_{PS}, Y_A, μ_{AUT}, b_{AUT}, $K_{O2\ AUT}$, and $K_{NH4\ AUT}$. The first ten calibrated parameters were used to investigate PAOs. There are only two parameters, yield coefficient (Biomass/PHA) (Y_{PAO}) and PHA requirement for PP storage (Y_{PHA}) from those ten calibrated parameters of PAOs, shown the difference of values. Different values were used to clarify the increase of EBPR during using DS as external carbon sources. PAOs behaviors can be explained by Y_{PAO} and Y_{PHA}. Y_{PAO} (0.64 g COD g^{-1} COD), with influent DS was higher than without (0.61 g COD g^{-1} COD). Y_{PHA} (0.26 g COD g^{-1} P) with influent DS also was higher than without (0.24 g COD g^{-1} P).

   In addition, PAOs behaviours at the higher phosphorus/carbon ratio (0.11 g P g^{-1} COD) would take up more acetate than those with a lower phosphorus/carbon ratio (0.09 g P g^{-1} COD). This was supported by other researchers proposed that PAOs could utililize higher and faster carbon at higher phosphorus/carbon ratio (Fukase et al., 1984; Mino et al., 1987; Wentzel et al., 1988; Smolders et al., 1994; Liu et al., 1996; Liu et al., 1997; Kong et al., 2002; Yagi et al., 2006).

3. Inclusion of DS components in the influent feed stream of our experiments promoted enhanced phosphorous removal. The paired t-test method was used to investigate the relationship between essential components of DS and phosphorus release under anaerobic phase. Also the relationships between DS components and effluent TP were investigated. The four significant parameters in phosphorus removal efficiency are orthophosphate phosphorus (P), volatile fatty acids (S_A), fermentable biodegradable products (S_F) and slowly biodegradable products (X_S). This is seen in the magnitude of their p-values (p-value < 0.00001). Also the mean concentration of released phosphorus with and without influent DS is significantly different (p-value < 0.00001).

   In addition, specific phosphorus release rate (SPRR) was also used to investigate the influence of S_A, S_F and X_S DS components on phosphorus release under anaerobic conditions. The results show that SPRR of S_F DS component as carbon source was highest in comparison with other DS components. The SPRR values were 0.834 mg P g^{-1} VSS_{PAOs} h^{-1}, 3.90 mg P g^{-1} VSS_{PAOs} h^{-1} and 0.31 mg P g^{-1} VSS_{PAOs} h^{-1} for S_A, S_F and X_S, respectively. Additionally, the SPRR values with and without DS were 56.54 mg P g^{-1} VSS_{PAOs} h^{-1} and 52.88 mg P g^{-1} VSS_{PAOs} h^{-1}.

4. Verification was used to determine if the model can achieve specified performance requirement. This was done to test whether different data agreed with other. In comparison both experiments to test the verification approach, they need to be controlled under the same conditions. In this study, the operating temperature conditions (17°C and 23°C) were different. These observations could not have been made at the same time because there were limited in their number of activated sludge pilot-scale wastewater treatment reactors. There are three parameters in verification, the yield coefficient (Y_{PAO}), poly-hydroxy-alkanoates (PHA) storage (q_{PHA}) and saturation coefficient for ammonium ($K_{NH4\ AUT}$), that have different values from those in calibration.

The Arrhenius equation was used to describe the effect of temperature on the rate of reactions in activated sludge systems. The temperature coefficient (θ) is a result of the Arrhenius equation. The temperature dependent parameters ($\theta \neq 1$) where the kinetic parameters Y_{PAO} and q_{PHA} are included. These Arrhenius constant values for the PAOs reflected the temperature influences ($\theta \neq 1$) on the biological phosphorus removal processes. It is clear that P removal is negatively affected by high temperature (23°C). Under anaerobic conditions, θ values obtained for the rate constant for storage of PHA (q_{PHA}) and the maximum rate for phosphorus release (Y_{PO4}*q_{PHA}) were the same values with (1.061) and without (1.023) influent DS. As a result, the temperature influence on the maximum rate for PHA storage is similar to influence of temperature on the maximum rate of phosphorus release.

8.2 FUTURE WORK AND RECOMMENDATIONS

The research conducted in this project has shown that disintegrated sludge (DS) can enhance biological phosphorus removal (EBPR). It is because Y_{PAO} and Y_{PHA} coefficients in PAOs mechanisms increased. EBPR was affected by the presence of phosphorus, volatile fatty acids, fermentable biodegradable products and slowly biodegradable products in DS. The influence of temperature using influent DS was significant. Higher phosphorus removal efficiency occurred at a lower temperature (17°C). This was true even though Arrhenius equation constants (θ) of Y_{PAO} and q_{PHA} at a higher temperature (23°C) were greater than at a lower temperature (17°C). Therefore further study to follow this research should focus on PAOs mechanism at temperatures other than 17°C and 23°C as well as further modification of mathematical modelling. This will further clarify the variety of PAOs behaviors in different temperatures. In addition, heterotrophic kinetics upon transformation of slowly biodegradable products and fermentable biodegradable products in DS are observed. These organisms can hydrolyse and utilise slowly biodegradable products and fermentable biodegradable products, respectively. These results are related to PAOs using VFAs as carbon sources.

In summary, the following work will serve well as a continuation of the current study:

1. The activated sludge EBPR systems should be operated over different temperature ranges. Observation of the stoichiometric and kinetic coefficients of PAOs and other organisms should be done to understand the influences of temperature and DS on EBPR processes.

2. Concentrations of fermentable biodegradable product and slowly biodegradable fractions in DS can be varied in EBPR systems to investigate their effects on organisms' behaviour. This is important for achievement of EBPR in wastewater treatment plants using suitable influent DS characteristics.

REFERENCES

Ahn JH, Shin SG, Hwang S. (2009), "Effect of microwave irradiation on the disintegration and acidogenesis of municipal secondary sludge", *Chemical Engineering Journal*, vol. 153, pp. 145-150.

Akin B, (2008). "Waste activated sludge disintegration in an ultrasonic batch reactor", *Clean*, vol. 36, no. 4, pp. 360-365.

Akin B, Khanal SK, Sung S, Grewell D, Van-Leeuwen J. (2006), "Ultrasoundpre-treatment of waste activated sludge, "*Water Science and Technology*, vol. 6 pp. 35–42.

Artan N, Tasli, R, Ozgur, N, Ohron, D. (1997), "The fate of phosphorus under anoxic conditions in biological nutrient removal activated sludge systems", *Proceedings of the Second International Specialists Conference on Microorganisms in Activated Sludge and Biofilm Processes*, pp. 319-326.

Baetens D, Vanrolleghem PA, Van Loosdrecht MCM, Hosten LH. (1999), "Temperature effects in Bio-P removal", *Water Science and Technology*, vol. 39, pp. 215-225.

Barat, R., Montoya, T., Seco, A. & Ferrer, J. 2011, "Modelling biological and chemically induced precipitation of calcium phosphate in enhanced biological phosphorus removal systems", *Water research*, vol. 45, no. 12, pp. 3744-3752.

Barber WP (2005). The effects of ultrasound on sludge digestion. *Journal of the Chartered Institution of Water and Environmental Management*, vol. 19, no.(11, pp. 2-7.

Barker PS, Dold PL. (1996), "Sludge production and oxygen demand in nutrient removal activated sludge systems", *Water Science and Technology*, vol.34 no. 5-6, pp. 43-50.

Barker PS, Dold, PL. (1997), "General model for biological nutrient removal activated-sludge systems: Model presentation", *Water Environment Research*, vol. 69, no. 5, pp. 969-984.

Beccari M, Dionisi D, Giuliani A, Majon A, Ramadori R, (2002), "Effect of different carbon sources on aerobic storage by activated sludge", *Water Science and Technology*, vol. 45, no. 6, pp. 157-168.

Bixio, D., Van Hauwermeiren, P., Thoeye, C. & Ockier, P. (2001), *Impact of cold and dilute sewage on pre-fermentation - A case study*.

Boltz, J.P., Johnson, B.R., Daigger, G.T. & Sandino, J. (2009), "Modeling integrated fixed-film activated sludge and moving-bed biofilm reactor systems I: Mathematical treatment and model development", *Water Environment Research*, vol. 81, no. 6, pp. 555-575.

Bougrier C, Carre`re H, Delgene`s JP. (2005), "Solubilisation of waste-activated sludge by ultrasonic treatment", *Chemical Engineering Journal*, vol. 106, no. 2, pp. 163-169.

Bougrier C, Battimelli A, Delgenes JP, Carrere H. (2007), "Combined ozone pretreatment and anaerobic digestion for the reduction of biological sludge production in wastewater treatment", *Ozone Science and Engineering*, vol. 29, pp. 201–206.

Bowes MJ, Smithb JT, Jarviea HP, Neal C, Bardenc R. (2009), "Changes in point and diffuse source phosphorus inputs to the River Frome (Dorset, UK) from 1966 to 2006", *Science of the Total Environment*, vol. 407, pp. 1954-1966.

Brdjanovic D, Van Loosdrecht MCM, Hooijmans CM, Alaerts GJ, Heijnen JJ. (1997), "Temperature effects on physiology of biological phosphorus removal", *J Environ Eng*, vol. 123, pp. 144-152.

Brdjanovic D, van Loosdrecht MCM, Hooijmans CM, Mino T, Alaerts GJ, Heijnen JJ. (1998), "Effect of polyphosphate limitation on the anaerobic metabolism of phosphorus-accumulating microorganisms", *Applied Microbiology and Biotechnology*, vol.50, pp. 273–276.

Brdjanovic D, Logemann S, Van Loosdrecht MCM, Hooijmans CM, Alaerts GJ, Heijnen JJ. (1998), "Influence of temperature on biological phosphorus removal: Process and molecular ecological studies", *Water Research*, no. 32, pp. 1035-1048.

Brdjanovic D, Slamet A, van Loosedrecht MCM, Hooijmans CJ, Alaerats GJ, Hejinen JJ (2000), "Modeling COD, N and P Removal in a Full-Scale WWTP Haarlem Waaderpolder", *Water Res*earch, vol. 34, n. 3, pp. 846-858.

Brun R, Kühni M, Siegrist H, Gujer W, Reichert P. (2002), "Practical identifiability of ASM2d parameters - Systematic selection and tuning of parameter subsets", *Water Research*, vol. 36, pp. 4113-4127.

Brun R, Reichert P, Künsch HR. (2001), "Practical identifiability analysis of large environmental simulation models", *Water Resour Research*, vol. 37, pp. 1015-1030.

Cao YS, Ang CM, Raajeevan KS, Kiran AK, Lai KC, Ng SW, Zulkifli I and Wah YL, (2006), "Analysis of phosphorus removal and anaerobic selector performance in a full-scale activated sludge process in Singapore", *Water Science and Technology*, vol. 54, no. 8, pp. 237-246.

Caravelli A, Giannuzzi L, Zaritzky N. (2006), "Effect of ozone on filamentous bulking in a laboratory scale activatedsludge reactor using respirometry and INT-dehydrogenase activity", *Journal of Environmental Engineering*, vol. 132, pp. 1001–1010

Carballa M, Manterola G, Larrea L, Ternes T, Omil F, Lema JM, (2007), "Influence of ozone pre-treatment on sludgeanaerobic digestion: Removal of pharmaceutical and personalcareproducts", *Chemosphere*, vol. 67, no. 7, pp. 1444-1452.

Carrette, R., Bixio, D., Thoeye, C. & Ockier, P. 2001, *Full-scale application of the IAWQ ASM no. 2d model*.

Carucci A, Kühni M, Brun R, Carucci G., Koch G, Majone M, Siegrist H. (1999), "Microbial competition for the organic substrates and its impact on EBPR systems under conditions of changing carbon feed", *Water Science and Technology*, vol. 39, no. 1, pp. 75–85.

Cech JS and Hartman P. (1993), "Competition between polyphosphate and polysaccharide accumulating bacteria in biological phosphorus removal system", *Water Research*, vol. 27, pp. 1219-1225.

Cha Z, Lin CF, Cheng CJ, Hong PKA. (2010), "Removal of oil and oil Sheen from produced water by pressure-assisted ozonation and sand filtration", *Chemosphere*, vol. 78, pp. 583–590.

Chadwick, D.R., Chen, S., 2002. Manures. In: Haygarth, P.M., Jarvis, S.C. (Eds.), Agriculture, Hydrology and Water Quality. CAB International, Wallingford.

Chai, Q., Amrani, S.H. & Lie, B. (2006), "Parameter identifiability analysis and model fitting of a biological wastewater model", *Computer Aided Chemical Engineering*, vol. 21, no. C, pp. 409-414.

Checchi N, Marsili-Libelli S. (2005), "Reliability of parameter estimation in respirometric models", *Water Research*, vol. 39, no. 15, pp. 3686-96.

Chen Y, Randall AA, McCue T. (2004), "The efficiency of enhanced biological phosphorus removal from real wastewater affected by different ratios of acetic to propionic acid", *Water Research*, vol. 38, no. 1, pp. 27-36.

Cheng C, Hong PKD, Lin CF. (2012), "Improvedsolubilization of activatedsludge by ozonation in pressurecycles", Chemosphere, vol. 87, no. 6, pp. 637–643.

Chi Y, Li Y, Ji M, Qiang H, Deng H, Wu Y. (2010), "Mesophilic and thermophilic digestion of thickened waste activated sludge: A comparative study", *Advanced Materials Research*, vol. 113-116, pp. 450-458.

Chu LB, Yan ST, Xing XH, Yu AF, Sun SL, Jurcik B. (2008), "Enhanced sludgesolubilization by microbubble ozonation", *Chemosphere*, no. 72, pp. 205–212.

Chu L, Wang J, Wang B, Xing XH, Yan S, Sun X, Jurcik B. (2009), "Changes in biomassactivity and characteristics of activatedsludgeexposed to lowozonedose", *Chemosphere*, vol. 77, no. 2, pp 269-272.

Clayton AJ, Wentzel MC, Ekama GA, Marais GVR. (1991), "Denitrification kinetics in biological nitrogen and phosphorus removal systems treating municipal wastewaters", *Water Science and Technology*, vol. 23, no. 4/6, pp. 1025-1035.

Converti A, Rovatti M, Borghi MD, (1995), "Biological removal of phosphorus from wastewaters by alternating aerobic and anaerobic conditions", *Water Research*, vol. 29 no. 1, pp. 263–269

Comeau Y, Hall KJ, Hancock REW and Oldham WK. (1986), "Biochemical model for enhanced biological phosphorus removal", *Water Research* vol. 20, pp. 1511-1521.

Comeau Y, Rabionwitz B, Hall KJ, Oldham WK. (1987), "Phosphate release and uptake in enhanced biological phosphorus removal from wastewater", *Journal of the Water Pollution Control Federation*, vol. 59, pp. 707-715.

Cumby TR, Brewer AJ, Dimmock SJ. (1999). "Dirty water from dairy farms, I: biochemical characteristics", *Bioresource Technology*, vol. 67, pp. 155–160.

Daigger GT, Crawford GV & Johnson BR. (2010), "Full-scale assessment of the nutrient removal capabilities of membrane bioreactors", *Water Environment Research*, vol. 82, no. 9, pp. 806-818.

Dawes EA and Senior PJ. (1973), "The role and regulation of energy reserve polymers in microorganisms", *Advances in Microbial Physiology*, pp. 136.

De Pauw DJW and Vanrolleghem PA. (2006), "Practical aspects of sensitivity function approximation for dynamic models", *Mathematical and Computer Modelling of Dynamical Systems*, vol. 12, no. 5, pp. 395-414.

Deo RP, Halden RU. (2009), "Empirical model for predicting concentrations of refractory hydrophobic organic compounds in digested sludge from municipal wastewater treatment plants", *Environmental Chemistry*, vol. 6, pp. 544-550.

Dewil R, Baeyens J, Goutvrind R. (2006), "Ultrasonic treatment of waste activated sludge", *Environmental Program*, vol. 25, pp. 121-128.

Dewil R, Baeyens J, Goutvrind R. (2006), "Ultrasonic treatment of waste activated sludge", *Environ Prog*, vol. 25, pp. 121-128.

Dold, PL, Wentzel MC, Billing AE, Ekama GA, Marais GVR. (1991), Activated Sludge Simulation Program Water Research Commission, South Africa: P/Bag X03, Gezina 0031, South Africa.

Dochain D, and Vanrolleghem PA. (2001). Dynamical modelling and estimation in wastewater treatment processes. *IWA Publishing*, London, UK.

Doğan I, Sanin FD. (2009), "SaninAlkaline solubilization and microwaveirradiation as a combined sludge disintegration and minimization method", *Water Research*, vol. 43, no. 8, pp. 2139–2148

Dudley J, Buck G, Ashley R, Jack A. (2002), "Experience and extensions to the ASM2 family of models", *Water Science and Technology*, vol. 45, pp. 177-186.

Dunne E, Culleton N, O'Donovan G, Harrington R. (2005), A farm-scale integrated constructed wetland to treat farmyard dirty water. Final Report RMIS 3649. Teagasc,Carlow.http://ww.teagasc.ie/research/reports/environment/4649/eopr4649.htm>.

Dymaczewski, Z. 2007, "The activated sludge process simulation - A preparation stage for Poznan WWTP", *Environmental Engineering - Proceedings of the 2nd National Congress of Environmental Engineering*, pp. 281.

Dytczak MA, Oleszkiewicz JA. (2008), "Performancechange during long-term ozonation aimed at augmenting denitrification and decreasing waste activatedsludge", *Chemosphere*, vol. 73, pp. 1529-1532.

Dziurla MA, Salhi M, Leroy P, Paul E, Ginestet P, Block JC. (2005), "Variations of respiratory activity and glutathione in activatedsludgesexposed to low ozone doses",*Water Research*, vol. 39, pp. 2591–2598.

Edwards AC and Withers PJA. (2008), "Transport and delivery of suspended solids, nitrogen and phosphorus from various sources to freshwaters in the UK", *Journal of Hydrology*, vol. 350, pp. 144– 153

EEA. Source apportionment of nitrogen and phosphorus inputs into the aquatic environment. European Environment Agency, Copenhagen, Denmark; 2005. p. 48.

Eikelboom DH and Van Buijsen H JJ. (1983), "Microscopic sludge investigation manual", *TNO Research Institute. Delft, 2nd Ed.,*.

Ekama GA, Wentzel MC. (1999), "Denitrification kinetics in biological N and P removal activated sludge systems treating municipal wastewaters", *Water Science and Technology*, vol. 39, no. 6, pp. 69-77.

Elefsiniotis P; Wareham DG; Smith MO. (2004), "Use of volatile fatty acids from an acid-phase digester for denitrification", *Journal of biotechnology*, vol. 36, no. 114, pp. 289–297.

El-Hadj TB, Dosta J, Marquez-Serrano R, Mata-Alvarez J. (2007), "Effect of ultrasound pretreatment in mesophilic and thermophilic anaerobic digestion with emphasis on naphthalene and pyrene removal", Water Research, vol 41, no. 1, pp 87-94

Erdal UG, Erdal ZK, Randall CW. (2003), "The competition between PAOs (phosphorus accumulating organisms) and GAOs (glycogen accumulating organisms) in EBPR (enhanced biological phosphorus removal) systems at different temperatures and the effects on system performance", *Water Science and Technology*, vol. 47, pp. 1-8.

Erden G, Demir O, Filibeli A. (2010), "Disintegration of biologicalsludge: Effect of ozoneoxidation and ultrasonictreatment on aerobic digestibility", *Bioresource Technology*, vol. 101, no. 21, pp. 8093-8098.

Eskicioglu C, Kennedy KJ, Droste RL. (2006), "Characterization of soluble organic matter of wasteactivatedsludge before and after thermal pretreatment", *Water Rearch*, vol. 40, pp. 3725–3736.

Fang F, Ni BJ, Yu HQ. (2009), "Estimating the kinetic parameters of activated sludge storage using weighted non-linear least-squares and accelerating genetic algorithm", *Water Research*, vol. 43, no.10, pp. 2595–2604.

Feng L, Chen Y, Zheng X. (2009), "Enhancement of waste activated sludge protein conversion and volatile fatty acids accumulation during waste activated sludge anaerobic fermentation by carbohydrate substrate addition: the effect of pH", *Environmental Science and Technology*, vol. 43, no. 12, pp. 4373-4380.

Feng X, Lei HY, Deng JC, Yu Q, Li HL. (2009), "Physical and chemical characteristics of waste activated sludge treated ultrasonically", *Chemical Engineering and Processing*, vol. 48, no. 1, pp. 187–194

Ferrer J, Morenilla JJ, Bouzas A, García-Usach F. (2004), "Calibration and simulation of two large wastewater treatment plants operated for nutrient removal", *Water Science and Technology*, vol. 50, pp. 87-94.

Fleischer, E.J., Broderick, T.A., Daigger, G.T., Fonseca, A.D., Holbrook, R.D. & Murthy, S.N. (2005), "Evaluation of membrane bioreactor process capabilities to meet stringent effluent nutrient discharge requirements", *Water Environment Research*, vol. 77, no. 2, pp. 162-178.

Florentz M, Caille D, Bourdon F, Sibony J. (1987), "Biological nutrient removal in. France", *Water Science and Technology*, vol. 19, no. 4, pp. 1171-1173.

Flores-Alsina, X., Gernaey, K.V. & Jeppsson, U. 2012, "Benchmarking biological nutrient removal in wastewater treatment plants: Influence of mathematical model assumptions", *Water Science and Technology*, vol. 65, no. 8, pp. 1496-1505.

Filali-Meknassi, Y., Auriol, M., Tyagi, R.D., Comeau, Y. & Surampalli, R.Y. 2005, "Design strategy for a simultaneous nitrification/denitrification of a slaughterhouse wastewater in a sequencing batch reactor: ASM2d modeling and verification", *Environmental technology*, vol. 26, no. 10, pp. 1081-1100.

Fukase T, Shibata M and Miyaji Y. (1984), "The role of an anaerobic stage on biological phosphorus removal", *Water Science and Technology*, vol. 17, pp. 69-80.

Gao, P., Liu, Z.-., Xue, G., Zhou, M.-., Liu, L., Zhao, Y.-. & Han, D. (2009), "Modeling dissolved oxygen effects on biological nutrient removal in a sequencing batch reactor with activated sludge model 2d", *3rd International Conference on Bioinformatics and Biomedical Engineering, iCBBE 2009*.

Gao Y, Peng Y, Zhang J, Wang S, Guo J, Ye L. (2011), "Biological sludge reduction and enhanced nutrient removal in a pilot-scale system with 2-step sludge alkaline fermentation and A_2O process", *Bioresource Technology*, vol. 102, pp. 4091-4097.

García-Usach F, Ferrer J, Bouzas A, Seco A. (2006), "Calibration and simulation of ASM2d at different temperatures in a phosphorus removal pilot plant", *Water Science and Technology*, vol. 53, pp. 199-206.

Gernaey KV, Van Loosdrecht MCM, Henze M, Lind M. and Jorgensen SB. (2004), "Activated sludge wastewater treatment plant modelling and simulation: State of the art", *Environmental Modelling & Software*, vol. 19, pp.763-783.

Gommers PJF, van Schie BJ, van Dijken JP. and Kuenen JG. (1988), "Biochemical limits to microbial growth yields: an analysis of mixed substrate utilization", *Biotechnology and Bioengineering*, vol. 32, no. 1, pp. 86-94.

Gottschalk G. (1979), "Metabolic diversity of aerobic heterotrophs: Biosynthesis of monomers and polymers", *Bacterial Metabolism, 1st Ed.,* , pp. 110-111.

Goulden CH. 1956. Methods of Statistical Analysis, 2nd ed. New York: Wiley. 50-55.

Grady CPL Jr, Daigger GT, Lim HC. 1999. Biological Wastewater Treatment 2nd edition. Marcel Deker, Inc. New York.

Greenway M, Woolley A. (1999), "Constructed wetlands in Queensland: Performance efficiency and nutrient bioaccumulation", *Ecological Engineering*, vol. 12, pp. 30–55.

Gschloss T, Steinmann C, Schleypen P, Melzer A. (1998), "Constructed wetlands for effluent polishing of lagoons", *Water Research*, vol. 32, pp. 2639–2649.

Guangming Z, Panyue Z, Yanming C, (2006), "Ultrasonicenhancement of industrialsludgesettingability and dewateringability", *Tsinghua Science & Technology*, vol. 11, pp. 373–378.

Guisasola, A., Pijuan, M., Baeza, J.A., Carrera, J. & Lafuente, J. (2006), "Improving the start-up of an EBPR system using OUR to control the aerobic phase length: A simulation study", *Water Science and Technology*, vol. 53, no. 4-5, pp. 253-262.

Gujer W, Henze M, Mino T., Matsuo T, Wentzel M. C. and Marais GVR. (1995), "The activated sludge model No. 2: Biological phosphorus removal", *Water Science and Technology*, vol. 31, no. 2, pp. 1-11.

Hao, X., Wang, Q., Cao, Y. & van Loosdrecht, M.C.M. (2011), "Evaluating sludge minimization caused by predation and viral infection based on the extended activated sludge model No. 2d", *Water research*, vol. 45, no. 16, pp. 5130-5140.

Hamada K, Kuba T, Torrico V, Okazaki M, Kusuda T. (2006). "Comparison of nutrient removal efficiency between pre- and post-denitrification wastewater treatments", *Water Science and Technology*, vol. 53, pp. 169-175.

Harold EM., *The vital force: a study of bioenergetics*, W.H. Freeman and Co., New York, 1986.

Hauduc H, Rieger L, Takács I, Héduit A, Vanrolleghem PA and Gillot S. (2010), "A systematic approach for model verification: Application on seven published activated sludge models", *Water Science and Technology*, vol. 61, no. 4, pp. 825-838.

Helen MW. (1985). "De Moivre on the law of normal probability". In Smith, David Eugene. *A source book in mathematics*. Dover. p. 78.

Helmer C, Kunst S. (1998), "Low temperature effects on phosphorus release and uptake by microorganisms in EBPR plants", Water Science and Technology, vol. 37, pp. 531-539.

Henze M, Grady CPL, Jr, Gujer, W, Marais, GVR and Matsuo T. (1987), "Activated Sludge Model No. 1", IAWPRC Task Group on Mathematical Modelling Design and Operation of Biological Wastewater Treatment, Scientific and Technical Report No. 1, IAWPRC, London.

Henze M, Gujer W, Mino T, Matsuo T, Wentzel MC, Marais GVR. (1995), "Wastewater and biomass characterization for the activated sludge model No. 2:

Biological phosphorus removal", *Water Science and Technology*, vol. 31, no. 2, pp. 13-23.

Henze M, Gujer W, Mino T, Matsuo T, Wentzel MC, Marais, GVR. (1995), "Activated Sludge Model No. 2", IAWQ Scientific and Technical Report No. 3, IAWQ, London U.K. 32 pp.

Henze M, Gujer W, Mino T, Matsuo T, Wentzel MC, Marais GVR, Van Loosdrecht MCM. (1999), "Activated Sludge Model No.2d, ASM2d", *Water Science and Technology*, vol. 39, no. 1, pp. 165-182.

Henze M, Gujer W, Mino T, van Loosdrecht MCM. 2000. Activated Sludge Models ASM1, ASM2, ASM2d and ASM3. IWA Scientific and Technical Report No. 9. IWA Publishing. London, UK.

Henze M, van Loosdrecht MCM, Ekama GA and Brdjanovic D. 2008. Biological Wastewater Treatment Principle, Modelling and Design. IWA publishing, London, UK.

Hong PKA, Nakra S. (2009), "Rapid extraction of sediment contaminants by pressurecycles", *Chemosphere*, vol. 74, pp. 1360–1366.

Hong JK Park, N, Teeradej YO, Lee YK, Cho CH. (2006), "ParkPretreatment of sludge with microwaves for pathogen destruction and improved anaerobic digestion performance", *Water Environment Research*, vol. 78, no. 1 , pp. 76–83.

Hong PKA, Cai X, Cha Z. (2008a), "Pressure-assisted chelation extraction of lead from contaminated soilEnviron", *Pollution*, vol. 153 , pp. 14–21.

Hong KA, Nakra s, Kao CMJ, Hayes DF. (2008b), "Pressure-assisted ozonation of PCB and PAH contaminated sediments", *Chemosphere*, vol. 72 , pp. 1757–1764.

Hu Z, Wentzel MC, Ekama GA. (2003), "Modelling biological nutrient removal activated sludge systems - A review", *Water Research*, vol. 37, no. 14, pp. 3430-3444.

Hu ZR, Wentzel MC, Ekama GA. (2007), "A general kinetic model for biological nutrient removal activated sludge systems: Model development", *Biotechnology and Bioengineering*, vol. 98, no. 6, pp. 1242-1258.

Hulsbeek JJW, Kruit J, Roeleveld PJ, Van Loosdrecht MCM. (2002), "A practical protocol for dynamic modelling of activated sludge systems", *Water Science and Technology*, vol. 45, no. 6, pp. 127-36.

Iacopozzi I, Innocenti V, Marsili-Libelli S, Giusti E. (2007), "A modified activated sludge model no. 3 (ASM3) with two-step nitrificationedenitrification", *Environmental Modelling & Software*, vol. 22, no. 6, pp. 847-861.

Insel G, Sin G, Lee DS, Nopens I, Vanrolleghem PA. (2006), "A calibration methodology and model-based systems analysis for SBRs removing nutrients under limited aeration conditions", *Journal of Chemical Technology and Biotechnology*, vol. 81, pp. 679-687.

Irwin JO. (1949). "The standard error of an estimate of expectation of life, with special reference to expectation of tumourless life in experiments with mice", *The Journal of Hygiene*, vol. 47, no. 2, pp. 188–189.

Jenkins D, Tandoi V. (1991), "The applied microbiology of enhanced biological phosphate removal – accomplishments and needs", *Water Research*, vol. 25, pp. 1471-1478.

Jeppsson U, Rosen C, Alex J, Copp J, Gernaey KV, Pons MN, Vanrolleghem A. (2006). "Towards a benchmark simulation model for plant-wide control strategy performance evaluation of WWTPs". *Water Science and Technology*, vol. 53, no. 1, pp. 287–295.

Jiang T, Myngheer S, De Pauw DJW, Spanjers H, Nopens I, Kennedy MD, Amy G & Vanrolleghem PA. (2008), "Modelling the production and degradation of soluble microbial products (SMP) in membrane bioreactors (MBR)", *Water research*, vol. 42, no. 20, pp. 4955-4964.

Ji Z, Chen Y. (2010), "Using sludge fermentation liquid to improve wastewater short-cut nitrification-denitrification and denitrifying phosphorus removal via nitrite", *Environmental Science and Technology*, vol. 44, pp. 8957-8963.

Kampas, P. 2006, *Sidestream treatment for improved BNR process performance* School of Applied Sciences Department of Sustainable Systems Centre for Water science, PhD Thesis Cranfield University.

Kampas P, Parsons SA, Pearce P, Ledoux S, Vale P, Churchley J, Cartmell E. (2007), "Mechanical sludge disintegration for the production of carbon source for biological nutrient removal", *Water Research,* vol. 41, pp. 1734-1742.

Kampas P, Parsons SA, Pearce P, Ledoux S, Vale P, Cartmell E, Soares A. (2009), "An internal carbon source for improving biological nutrient removal", *Bioresource Technology*, vol. 100, pp. 149-154.

Kauder, J., Boes, N., Pasel, C. & Herbell, J.-. (2007), "Combining models ADM1 and ASM2d in a sequencing batch reactor simulation", *Chemical Engineering and Technology,* vol. 30, no. 8, pp. 1100-1112.

Kennedy, K.J. & McHarg, A.M. (2007), "Optimization of municipal wastewater biological nutrient removal using ASM2d", *Journal of Environmental Engineering and Science,* vol. 6, no. 1, pp. 31-43.

Kern J, Idler C. (1999), "Treatment of domestic and agricultural wastewater by reed bed systems", *Ecological Engineering*, vol. 12, pp. 13–25.

Kerrn-Jespersen, J.P. & Henze, M.(1993), "Biological phosphorus uptake under anoxic and aerobic conditions", *Water research,* vol. 27, no. 4, pp. 617-624.

Khanal SK, Grewell D, Sung S. and Van Leeuwen J. (2007). Ultrasound applications in wastewater sludge pretreatment: A review. *Critical Reviews in Environmental Science and Technology*, 37 (4), 277-313.

Kishida N, Kim J, Tsuneda S, Sudo R. (2006), "Anaerobic/oxic/anoxic granular sludge process as an effective nutrient removal process utilizing denitrifying polyphosphate-accumulating organisms", *Water Research,* vol. 40, no. 12, pp. 2303-2310.

Kong YH, Beer M, Rees GN, Seviour RJ. (2002), "Functional analysis of microbial communities in aerobic-anaerobic sequencing batch reactor fed with different phosphorus/carbon (P/C) ratios", *Microbiology*, vol. 148, pp. 2299-2307.

Kreuzinger N, Clara M, Strenn B, Kroiss H. (2004). "Relevance of the sludge retention time (SRT) as design criteria for wastewater treatment plants for the removal of endocrine disruptors and pharmaceuticals from wastewater", *Water Science and Technology*, vol. 50, no. 5, pp. 149–156.

Krühne U, Henze M, Larose A, Kolte-Olsen A, Bay Jørgensen S. (2003), "Experimental and model assisted investigation of an operational strategy for the BPR under low influent concentrations", *Water Research*, vol. 37, no. 8, pp. 1953-1971.

Kuba T, Smolders G, van Loosdrecht MCM, Heijnen JJ. (1993), "Biological phosphorus removal from wastewater by anaerobic-anoxic sequencing batch reactor", *Water Science and Technology*, vol. 27 pp. 241-252.

Kuba T, Wachtmeiste A, Van Loosdrecht MCC, Heijnen JJ. (1994), "Effect of nitrate on phosphorus release in biological phosphorus removal systems", *Water Science and Technology*, vol. 30, no. 6 pt 6, pp. 263-269.

Kuba, T., Murnleitner, E., Van Loosdrecht, M. C. M. and Heijnen, J. J. (1996), "A metabolic model for biological phosphorus removal by denitrifying organisms", *Biotechnology and Bioengineering*, vol. 52, no. 6, pp. 685-695.

Kuba T, Van Loosdrecht MCM, Brandse FA, Heijnen JJ. (1997), "Occurrence of denitrifying phosphorus removing bacteria in modified UCT-type wastewater treatment plants", *Water Research*, vol. 31, no. 4, pp. 777-786.

Kulaev IS, The biochemistry of inorganic polyphosphates, Wiley, New York, 1979.

Lai C-, Tan H, Luo G, Ruan Y, Zhou W, Sun D. (2010), "Denitrification and kinetic characteristics using biodegradable polymers as carbon source and biofilm carrier", *Huanjing Kexue/Environmental Science*, vol. 31, pp.:1839-1845.

Langergraber G, Rieger L, Winkler S, Alex J, Wiese J, Owerdieck C, Ahnert M, Simon J, Maurer M. (2004), Water Science and Technology A guideline for simulation studies of wastewater treatment plants", *Water Science and Technology*, vol. 50, pp. 131-138.

Laurent J, Casellas M, Pons MN, Dagot C. (2009), "Flocs surface functionality assessment of sonicated activated sludge in relation with physico-chemical properties", *Ultrasonics Sonochemistry*, vol. 16, pp. 488–494.

Lee CY, Lee CC, Lee FY, Tseng SK, Liao CJ. (2004), "Performance of subsurface flow constructed wetland taking pretreated swine effluent under heavy loads", *Bioresource Technology*, vol. 92, pp. 173–179.

Lee, S.H., Ko, J.H., Park, J.B., Im, J.H., Kim, J.R., Lee, J.J., Kim, C.W. (2006), "Use of activate sludge model No. 3 and Bio-P module for simulating five-stage step-feed enhanced biological phosphorous removal process", *Korean Journal of Chemical Engineering*, vol. 23, no. 2, pp. 203–208.

Li X, Chen H, Hu L, Yu L, Chen Y, Gu G. (2011), "Pilot-scale waste activated sludge alkaline fermentation, fermentation liquid separation, and application of fermentation liquid to improve biological nutrient removal", *Environmental Science and Technology*, vol. 45, pp. 1834-1839.

Libelli SM, Ratini P, Spagni A, Bortone G. (2001), "Implementation, study and calibration of a modified ASM2d for the simulation of SBR processes", *Water Science and Technology*, vol. 43, pp. 69-76.

Liu WT, Mino T, Nakamura K, Matsuo T. (1994), "Role of glycogen in acetate uptake and polyhydroxyalkanoate synthesis in anaerobic–aerobic activated sludge with a minimized polyphosphate content", *Journal of Fermentation and Bioengineering*, vol. 77, no. 5, pp. 535–540.

Liu WT, Mino T, Nakamura K, Matsuo T. (1996), "Glycogen accumulating population and its anaerobic substrate uptake in anaerobic-aerobic activated sludge without biological phosphorus removal", *Water Research*, Vol.30, pp. 75-82.

Liu WT, Nakamura K, Matsuo T, Mino T. (1997), "Internal energy-based competition between polyphosphate and glycogen-accumulating bacteria in biological phosphorus removal reactors—effect of P/C feeding ratio". *Water Research*, Vol.31, no. 6, pp. 1430–1438.

Liu YH. (1998), "Relation between sludge carbohydrate content and biological phosphate removal", *Water Research*, vol. 32, pp. 1635-1641.

Liu XL, Liu H, Chen JH, Dua JG, Chen C. (2008), "Enhancement of solubilization and acidification of wasteactivatedsludge by pretreatment", Waste Management, vol. 28, pp. 2614–2622.

Llabres P, Pavan P, Battistioni P, Cecchi F, Mata-Alvarez J. (1999), "The use of organic fraction of municipal solid waste hydrolysis products for biological nutrient removal in wastewater treatment plants", *Water Research*, vol. 33, no. 1, pp. 214-222.

Lopez C, Morgenroth E. 2003. Modeling the performance of enhanced biological phosphorus removal systems under dynamic loading conditions using different mathematical models. WEFTEC 2003, 76th Annual Conference of the Water Environment Federation, Los Angeles.

Lopez-Vazquez CM, Song Y-, Hooijmans CM, Brdjanovic D, Moussa MS, Gijzen HJ, Van Loosdrecht MMC. (2007), "Short-term temperature effects on the anaerobic

metabolism of glycogen accumulating organisms", *Biotechnology and Bioengineering*, vol. 97, pp. 483-495.

López-Vázquez CM, Hooijmans CM, Brdjanovic D, Gijzen HJ, Van Loosdrecht MCM. (2007), "A practical method for quantification of phosphorus- and glycogen-accumulating organism populations in activated sludge systems", *Water Environment Research*, vol. 79, no. 13, pp. 2487-2498.

López-Vázquez CM, Hooijmans CM, Brdjanovic D, Gijzen HJ, van Loosdrecht MCM. (2008), "Factors affecting the microbial populations at full-scale enhanced biological phosphorus removal (EBPR) wastewater treatment plants in The Netherlands", *Water Research*, no. 42, pp. 2349-2360.

Lopez-Vazquez CM, Oehmen A, Hooijmans CM, Brdjanovic D, Gijzen HJ, Yuan Z, van Loosdrecht MCM. (2009), "Modeling the PAO-GAO competition: Effects of carbon source, pH and temperature", *Water Research*, vol. 43, pp. 450-462.

Lu H, Oehmen A, Virdis B, Keller J, Yuan Z. (2006), "Obtaining highly enriched cultures of *Candidatus* Accumulibacter phosphates through alternating carbon sources", *Water Research*, vol. 40, no. 20, pp. 3838–3848.

Luederitz V, Eckert E, Lange-Weber M, Lange A, Gersberg RM. (2001), "Nutrient removal efficiency and resource economics of vertical flow and horizontal flow constructed wetlands", *Ecological Engineering*, vol. 18, pp. 157–171.

Machado VC, Tapia G, Gabriel D, Lafuente J, Baeza JA. (2009), "Systematic identifiability study based on the Fisher Information Matrix for reducing the number of parameters calibration of an activated sludge model", *Environmental Modelling and Software*, vol. 24, pp. 1274-1284.

Makinia J, Rosenwinkel KH, and Spering V. (2005), "Long-term simulation of the activated sludge process at the Hanover-Gümmerwald pilot WWTP", *Water Research*, vol. 39, no. 8, pp. 1489–1502.

Makinia J, Rosenwinkel K, Spering V (2006), "Comparison of two model concepts for simulation of nitrogen removal at a full-scale biological nutrient removal pilot plant", *Journal of Environmental Engineering*, vol. 132, no. 4, pp. 476-87.

Makinia, J., Pagilla, K., Czerwionka, K. & Stensel, H.D. (2011), "Modeling organic nitrogen conversions in activated sludge bioreactors", *Water Science and Technology*, vol. 63, no. 7, pp. 1418-1426.

Makinia, J., Drewnowski, J., Swinarski, M., Czerwionka, K., Kaszubowska, M. & Majtacz, J. (2012), "The impact of precipitation and external carbon source addition on biological nutrient removal in activated sludge systems - experimental investigation and mathematical modeling", *Water Practice and Technology*, vol. 7, no. 1.

Mamais D, Jenkins D. (1992), "The effects of MCRT and temperature on enhanced biological phosphorus removal", *Water Science and Technology*, no. 26, pp. 955-965.

Manga J, Ferrer J, Garcia-Usach F, Seco A. (2001), "A modification to the activated sludge model no. 2 based on the competition between phosphorus-accumulating organisms and glycogen accumulating organisms", *Water Science and Technology*, vol. 43, pp. 161-171.

Manga J, Ferrer J, Seco A, Garcia-Usach F. (2003), "Design of nutrient removal activated sludge systems", *Water Science and Technology*, vol. 47, pp. 115-122.

Mantovi P, Marmiroli M, Maestri E, Tagliavini S, Piccinini S, Marmiroli N. (2003), "Application of a horizontal subsurface flow constructed wetland on treatment of dairy parlor wastewater", *Bioresource Technology*, vol. 88, pp. 85–94.

Mao T, Show K, (2007), "Show Influence of ultrasonication on anaerobic bioconversion of sludge" Water Environment Research, vol. 79, pp. 436–441.

Mao T, Show KY. (2006), "Show Performance of high-rate sludge digesters fed with sonicated sludge", *Water Science and Technology*, vol. 54, pp. 27–33.

Marsili Libelli, S., Ratini, P., Spagni, A. & Bortone, G. 2001, *Implementation, study and calibration of a modified ASM2d for the simulation of SBR processes*.

Marsili-Libelli F, Giusti E. (2008), "Water quality modelling for small river basins". *Environmental Modelling & Software*, vol. 23, pp. 451-463.

Matsuo T, Mino T, Satoh H. (1992), "Metabolism of organic substrate in anaerobic phase of biological phosphate uptake process", *Water Science and Technology*, vol. 25, no. 6, pp. 83-92.

Maurer M, Abramovich D, Siegrist, H, Gujer, W. (1999), "Kinetics of biologically induced phosphorus precipitation in waste-water treatment", *Water Research*, vol. 33, no. 2, pp. 484–493.

McClintock SA; Randall CW; Pattarkine VM. (1993), "Effects of temperature and mean cell residence time on biological nutrient removal processes", *Water Environment Research*, vol. 65, no. 5, pp. 110-118.

Meijer SCF, van Loosdrecht MCM, Heijnen JJ. (2001). "Metabolic modelling of full-scale biological nitrogen and phosphorus removing WWTP's". *Water Research*, vol. 35, no. 11, pp. 2711–2723.

Meijer SCF, van der Spoel H, Susanti S, Heijnen JJ, van Loosdrecht MCM, (2002). "Error diagnostics and data reconciliation for activated sludge modelling using mass balances". *Water Science Technology*, vol. 45, no. 6, pp. 145–156.

Meinhold J, Filipe CDM, Daigger GT, Isaacs S. (1999), "Characterization of the denitrifying fraction of phosphate accumulating organisms in biological phosphate removal". *Water Science and Technology,* vol. 39, no. 1, pp. 31-42.

Melcer H, Dold PL, Jones RM, Bye CM, Takacs I, Stensel HD, Wilson AW, Sun P, and Bury S. (2003), "Methods for wastewater characterization in activated sludge modelling" Water Environ. Res. Found (WERF). Alexandria, VA, USA.

Metcalf Eddy, (2003). Wastewater engineering: treatment and reuse, fourth ed. McGraw-Hill Higher Education, New York, ISBN 0-07-112250-8.

Minervini D. (2008), "The Potential of Ultrasound Treatment for Sludge Reduction." School of Applied Sciences Department of Sustainable Systems Centre for Water Science, PhD Thesis, Cranfield University.

Mino T, Arun V, Tsuzuki Y and Matsuo T. (1987), "Effect of phosphorus accumulation on acetate metabolism in the biological phosphorus removal process", pp. 27-38. In Advances in Water Pollution Control: Biological Phosphate Removal from Wastewaters (Edited by Ramadori R.). Pergamon Press, Oxford.

Mino T, Van Loosdrecht MCM, Heijnen JJ. (1998), "Microbiology and biochemistry of the enhanced biological phosphate removal process". *Water research,* vol. 32, no. 4, pp. 3193-3207.

Mitchell, G., 2001. The quality of urban stormwater in Britain and Europe: Database and recommended values for strategic planning models. Technical Report, School of Geography, Universityof Leeds.

Mitchell P, Chemiosmotic coupling and energy transduction, Glynn Research, Bodmin, Cornwall, UK, 1986.

Moodley R, Wentzel MC, Ekama GA. (2000), "External nitrification in BNR activated sludge systems with varying aerobic mass fractions", Proceedings of the Sixth Biennial WISA Conference and Exhibition.

Munz G, Lubello C, Oleszkiewicz Jan A. (2011), "Modeling The Decay Of Ammonium Oxidizing Bacteria", *Water Research*, vol. 45, pp. 557-564.

Murnleitner E, Kuba T, Van Loosdrecht MCM, Heijnen JJ. (1997), "An integrated metabolic model for the aerobic and denitrifying biological phosphorus removal", *Biotechnology and Bioengineering*, vol. 54, no. 5, pp. 434-450.

Na S, Kim YU, Khim J. (2007), "Physiochemical properties of digested sewage sludge with ultrasonic treatment", *Ultrasonics Sonochemistry*., vol. 14, pp. 281–285.

Narasimhan, S, Jordache, C. (2000), Data Reconciliation and Gross Error Detection: an Intelligent Use of Process Data. Gulft Publishing Company, Houston, ISBN 0-88415-255-3.

Neal C, Jarvie HP, Neal M, Love AJ, Hill L, Wickham H. (2005), "Water quality of treated sewage effluent in a rural area of the upper Thames Basin, southern England, and the impacts of such effluents on riverine phosphorus concentrations", *Journal of Hydrology*, vol. 304, pp. 103–117.

Newman JM, Clausen JC, Neafsey JA. (2000), "Seasonal performance of a wetland constructed to process dairy milkhouse wastewater in connecticut", *Ecological Engineering*, vol. 14, pp. 181–198.

Ni B, Xie W, Liu S, Yu H, Gan Y, Zhou J, Hao E. (2010), "Development of a mechanistic model for biological nutrient removal activated sludge systems and application to a full-scale WWTP", *AICHE Journal*, vol. 56, no. 6, pp. 1626-1638.

Norton JP. (2008), "Algebraic sensitivity analysis of environmental models", *Environmental Modelling & Software*, vol. 23, pp. 963-972.

Nowak O, Franz A, Svardal K., Muller V, Kuhn V. (1999). "Parameter estimation for activated sludge models with the help of mass balances". *Water Science Technology*, vol. 39, no. 4, pp. 113–120.

Oehmen A, Zeng, RJ, Keller JR, Yuan Z. (2007), "Modeling the aerobic metabolism of polyphosphate-accumulating organisms enriched with propionate as a carbon source", *Water Environment Research*, vol. 79, no. 13, pp. 2477-2486.

Omlin M, Brun R, Reichert P. (2001), "Biogeochemical model of Lake Zürich: Sensitivity, identifiability and uncertainty analysis", *Ecological Modelling*, vol. 141, no. 1-3, pp. 105-123.

Onyeche TI, Schläfer O, Bormann H, Schröder C, Sievers M. (2002), "Ultrasonic cell disruption of stabilised sludge with subsequent anaerobic digestion" *Ultrasonics*, vol. 40, pp. 31-35.

Pai, T.-., Ouyang, C.-., Su, J.-. & Leu, H.-. 2001, "Modelling the stable effluent qualities of the A2O: Process with activated sludge model 2d under different return supernatant", *Journal of the Chinese Institute of Engineers, Transactions of the Chinese Institute of Engineers,Series A/Chung-kuo Kung Ch'eng Hsuch K'an*, vol. 24, no. 1, pp. 75-84.

Pai, T.Y., Ouyang, C.F., Su, J.L. & Leu, H.G. 2001, "Modelling the steady-state effluent characteristics of the TNCU process under different return mixed liquid", *Applied Mathematical Modelling*, vol. 25, no. 12, pp. 1025-1038.

Pai, T.Y., Tsai, Y.P., Chou, Y.J., Chang, H.Y., Leu, H.G. & Ouyang, C.F. (2004), "Microbial kinetic analysis of three different types of EBNR process", *Chemosphere*, vol. 55, no. 1, pp. 109-118.

Panswad T, Doungchai A, Anotai J. (2003), "Temperature effect on microbial community of enhanced biological phosphorus removal system", *Water Research*, vol. 37, pp. 409-415.

Panswad T, Tongkhammak N, Anotai J. (2007), "Estimation of intracellular phosphorus content of phosphorus-accumulating organisms at different P:COD feeding ratios", *J Environ Manage*, vol. 84, pp. 141-145.

Park WJ, Ahn JH, Hwang S, Lee CK, (2009), "Effect of output power, target temperature, and solid concentration on the solubilization of wasteactivatedsludge using microwave irradiation", *Bioresource Technology*, vol. 101, no. 1, pp. S13–S16

Penya-Roja JM, Seco A, Ferrer J, Serralta J. (2002), "Calibration and validation of activated sludge model no.2d for Spanish municipal wastewater", *Environmental Technology*, vol. 23, pp. 849-862.

Pieterse NM, Bleuten W, Jorgensen SE. (2003). "Contribution of point sources and diffuse to nitrogen and phosphorus loads in lowland river tributaries", *Journal of Hydrology*, vol. 271, no. 1–4, pp. 213–225.

Pijuan, M, Oehmen A, Baeza JA, Casas C, Yuan Z. (2008), "Characterizing the biochemical activity of full-scale enhanced biological phosphorus removal systems: A comparison with metabolic models", *Biotechnology & Bioengineering*, vol. 99, no. 1, pp. 170-179.

Pijuan M, Saunders AM, Guisasola A, Baeza JA, Casas C, Blackall LL. (2004), "Enhanced biological phosphorus removal in a sequencing batch reactor using propionate as the sole carbon source", *Biotechnology and Bioengineering*, vol. 85, no. 1, pp. 56-67.

Pilli S, Bhunia P, Yan S, LeBlanc RJ, Tyagi RD, Surampalli RY. (2011), "Ultrasonic pretreatment of sludge: a review", *Ultrasonics sonochemistry*, 18, no. 1, pp. 1-18.

Power M. (1993), "The predictive validation of ecological and environmental models", Ecological Modelling, vol. 68, no. 1-2, pp. 33-50.

Puig S, van Loosdrecht MCM, Colprim J, Meijer SCF. (2008), Data evaluation of full-scale wastewater treatment plants by mass balance, *Water Research*, vol. 42, no. 18, pp. 4645-4655,

Qi W, Liu H, Qu J, Hu C, Lan H, Berg M, Ren H, Xu W. (2010), "Polycyclic aromatic hydrocarbons in effluents from wastewater treatment plants and receiving streams in Tianjin, China. Environ Monit Assess, pp. 1-14.

Reckhow KH, Chapra SC. (1983), "Confirmation of water quality models", *Ecological Modelling*, vol. 20, no. 2-3, pp. 113-133.

Reichert P. (1994), "Aquasim - A tool for simulation and data analysis of aquatic systems", *Water Science and Technology*, vol. 30, no. 2, pp. 21-30.

Reichert P. (1995), "Design techniques of a computer program for the identification of processes and the stimulation of water quality in aquatic systems", *Environmental Software*, vol. 10, no. 3, pp. 199-210.

Reichert P, Von Schulthess R, Wild D. (1995), "The use of aquasim for estimating parameters of activated sludge models", *Water Science and Technology*, vol. 31, no. 2, pp. 135-147.

Reichert P, Vanrolleghem P. (2001), "Identifiability and uncertainty analysis of the River Water Quality Model No. 1 (RWQM1)", *Water Science and Technology*, vol. 43, pp. 329-338.

Reichert P. 2003. UNCSIM – A program package for statistical inference and sensitivity, identifiability, and uncertainty analysis, Dubendorf, CH: Swiss Federal Institute for Environmental Science and Technology (EAWAG).

Reichert P. (2006), "A standard interface between simulation programs and systems analysis software", *Water Science Technology*, vol. 53, pp. 267-275.

Ren N, Kang H, Wang X, Li N. (2011), "Short-term effect of temperature variation on the competition between PAOs and GAOs during acclimation period of an EBPR system", *Frontiers of Environmental Science and Engineering in China*, vol. 5, pp. 277-282.

Rieger L, Koch G, Kühni M, GujeR W, Siegrist H. (2001), "The eawag bio-p module for activated sludge model no. 3", *Water Research*, vol. 35, no. 16, pp. 3887-3903.

Roels JA, Energetics and kinetics in biotechnology, Elsevier, Amsterdam., 1983.

Ruano MV, Ribes J, De Pauw DJW, Sin G. (2007), "Parameter subset selection for the dynamic calibration of activated sludge models (ASMs): Experience versus systems analysis", *Water Science and Technology*, vol. 56, pp. 107-115.

Rykiel EJ. (1996), "Testing ecological models: The meaning of validation", *Ecological Modelling*, vol. 90, no. 3, pp. 229-244.

Salsabil MR, Prorot , Casellas M, Dagot C. (2009) "Pre-treatment of activated sludge: effect of sonication on aerobic and anaerobic digestibility", *Chemical Engineering Journal*, vol. 148, pp. 327–335.

Satoh H, Mino T, Matsuo T. (1992), "Uptake of organic substrates and accumulation of polyhydroxyalkanoates linked with glycolysis of intracellular carbohydrates under anaerobic condition in the biological excess phosphate removal process", *Water Science and Technology*, vol. 26, no. 5-6, pp. 933-942.

Satoh H, Ramey WD, Koch FA, Oldham WK, Mino T, Matsuo T. (1996), "Anaerobic substrate uptake by the enhanced biological phosphorus removal activated sludge treating real sewage", *Water Science and Technology*, vol. 34, no. 1-2, pp. 9-16.

Schmitz U, Berger CR, Orth H. (2000), "Protein analysis as a simple method for the quantitative assessment of sewage sludge disintegration", *Water Research, vol.* 34, pp. 3682-3685.

Schuler AJ. (2005), "Diversity matters: Dynamic simulation of distributed bacterial states in suspended growth biological wastewater treatment systems", *Biotechnology & Bioengineering*, vol. 91, pp. 62-74.

Seco A, Ferrer J, Serralta J, Manga J, Muñoz M. (2001), "Evaluation of Activated Sludge Model No. 2 at high phosphorus concentrations", *Environmental Technology*, vol. 22, no.5, pp. 497-507.

Sedran SA, Mehrotra AS, Pincince AB. (2006), "The dangers of uncalibratged activated sludge simulation packages", *Water Environment Federation*, pp. 3290-3303.

Seggelke, K. & Rosenwinkel, K.-.(2002), "Online-simulation of the WWTP to minimise the total emission of WWTP and sewer system", *Water Science and Technology*, vol. 45, no. 3, pp. 101-108.

Serralta, J., Ferrer, J., Borrás, L. & Seco, A. (2004), "An extension of ASM2d including pH calculation", *Water research,* vol. 38, no. 19, pp. 4029-4038.

Serralta, J., Ferrer, J., Borrás, L. & Seco, A. (2006), "Effect of pH on biological phosphorus uptake", *Biotechnology and bioengineering,* vol. 95, no. 5, pp. 875-882.

Seviour RJ, Mino T, Onuki M. (2003), "The microbiology of biological phosphorus removal in activated sludge systems", *FEMS Microbiol Rev*, vol. 27, pp. 99-127.

Show KY, Mao T, Lee DJ. (2007). "Optimisation of sludge disruption by sonication", *Water Research*, vol. 41, no. 20, pp. 4741-4747.

Siegrist H, Rieger L, Koch G, Kühni M, Gujer W. (2002), "The EAWAG Bio-P module for activated sludge model No. 3", *Water Science and Technology*, vol. 45, no.6, pp. 61-76.

Sin G, Guisasola A, De Pauw DJW, Baeza JA, Carrera J, Vanrolleghem PA. (2005), "A new approach for modelling simultaneous storage and growth processes for activated sludge systems under aerobic conditions", *Biotechnology & Bioengineering*, vol. 92, pp. 600-613.

Sin G, Van Hulle SWH, De Pauw DJW, Griensven AV, Vanrolleghem PA. (2005), "A critical comparison of systematic calibration protocols for activated sludge models: A SWOT analysis", Water Research, vol. 39, pp. 2459-2474.

Sin G, De Pauw DJW, Weijers S, Vanrolleghem PA. (2008), "An efficient approach to automate the manual trial and error calibration of activated sludge models" *Biotechnology & Bioengineering*, vol. 100, no. 3, pp. 516-528.

Smolders GJF, Van der Meij J, Van Loosdrecht MCM, Heijnen JJ. (1994a), "Model of the anaerobic metabolism of the biological phosphorus removal process: Stoichiometry and pH influence", *Biotechnology & Bioengineering,* vol. 43, no. 6, pp. 461-470.

Smolders GJF, Van Der Meij J, Van Loosdrecht MC, Heijen JJ. (1994b), "Stoichiometric model of the aerobic metabolism of the biological phosphorus removal process", *Biotechnology & Bioengineering*, vol. 44, no. 7, pp. 837-848.

Smolders GJF, Van der Meij J, Van Loosdrecht MCM, Heijnen JJ. (1995a), "A structured metabolic model for anaerobic and aerobic stoichiometry and kinetics of the biological phosphorus removal process", *Biotechnology & Bioengineering*, vol. 47, no. 3, pp. 277-287.

Smolders GJF, Van Loosdrecht MCM, Heijnen JJ. (1995b), "A metabolic model for the biological phosphorus removal process", *Water Science and Technology*, vol. 31, no. 2, pp. 79-93.

Soares A, Kampas P, Maillard S, Wood E, Brigg J, Tillotson M, Parsons SA, Cartmell E. (2010), "Comparison between disintegrated and fermented sewage sludge for production of a carbon source suitable for biological nutrient removal", *Journal of Hazardous Materials*, vol. 175, pp. 733-739.

Soejima K, Matsumoto S, Ohgushi S, Naraki K, Terada A, Tsuneda S, Hirata A. (2008), "Modeling and experimental study on the anaerobic/aerobic/anoxic process for simultaneous nitrogen and phosphorus removal: The effect of acetate addition", *Process Biochemistry*, vol. 43, pp. 605-614.

Šorm R, Bortone G, Saltarelli R, Jeníček P, Wanner J, Tilche A. (1996), "Phosphate uptake under anoxic conditions and fixed-film nitrification in nutrient removal activated sludge system", *Water Research*, vol. 30, no. 7, pp. 1573-1584.

Stouthamer AH. (1979), "The search for correlation between theoretical and experimental growth yields", *International Review of Biochemistry.*, vol. 21, pp. 1-47.

Stryer L, Biochemistry, W.H. Freeman and Co., San Francisco, CA., 1979.

Swinarski, M., Makinia, J., Stensel, H.D., Czerwionka, K. & Drewnowski, J. 2012, "Modeling external carbon addition in biological nutrient removal processes with an extension of the international water association activated sludge model", *Water Environment Research,* vol. 84, no. 8, pp. 646-655.

Tang B, Yu L, Huang S, Luo J, Zhuo Y. (2010), "Energyefficiency of pre-treatingexcesssewagesludge with microwaveirradiation", *Bioresource Technology,* vol. 101, no. 1, pp. 5092-5097.

Tanner CC, Clayton JS, Upsdell MP. (1995). "Effect of loading rate and planting on treatment of dairy farm wastewaters in constructed wetlands. 2. Removal of nitrogen and phosphorus", *Water Research,* vol. 29, pp. 27–34.

Thomas, M.; Wright, P.; Blackall, L. L.; Urbain, V.; Keller, J. (2003), "Optimisation of Noosa BNR plant to improve performance and reduce operating costs", *Water Science and Technology*, vol. 47, pp. 141–148.

Tiehm A, Nickel K, Zellhorn M, Neis U. (2001). "Ultrasonic waste activated sludge disintegration for improving anaerobic stabilization ", *Water Res*earch, vol. 35, pp. 2003-2009.

Tong J, Chen Y. (2007), "Enhanced biological phosphorus removal driven by short-chain fatty acids produced from waste activated sludge alkaline fermentation", *Environmental Science and Technology*, vol. 41, pp. 7126–7130.

Trutnau M, Petzold M, Mehlig L, Eschenhagen M, Geipel K, Müller S, Bley T, Röske I. (2010), "Using a carbon-based ASM3 EAWAG Bio-P for modelling the enhanced biological phosphorus removal in anaerobic/aerobic activated sludge systems", *Bioprocess and Biosystems Engineering,* vol. 34, pp. 287-295.

Tykesson E, Aspegren H, Henze M, Nielsen PH, Jansen JC. (2002), "Use of phosphorus release batch tests for modelling an EBPR pilot plant", *Water Science and Technology*, vol. 45, no. 6, pp. 99-106.

Vaiopoulou E, Aivasidis A. (2008), "A modified UCT method for biological nutrient removal: Configuration and performance", *Chemosphere*, vol. 72, pp. 1062-1068.

Vallet B, Labelle M, Rieger L, Bigra S, Parent S, Juteau P, Villemur R, Comeau Y. (2009), "Inhibition of biological phosphorus removal in a sequencing moving bed biofilm reactor in seawater", *Water Science and Technology*, vol. 59, no. 6, pp. 1101-1110.

Van der Heijden RTJM, Heijnen JJ, Hellinga C, Romein B, Luyben KChAM. (1994). "Linear constraint relations in biochemical reaction systems: I. Classification of the calculability and the balance ability of conversion rates". *Biotechnology and Bioengineering*, no. 43, no. 1, pp. 3–10.

van Groenestijn JW, Deinema MH, Zehnder AJB. (1987), "ATP production from polyphosphate in Acinetobacter strain 210A", *Archives of Microbiology*, vol. 148, no. 1, pp. 14-19.

van Veldhuizen HM, van Loosdrecht MCM, Heijnen JJ. (1999), "Modelling biological phosphorus and nitrogen removal in a full scale activated sludge process", *Water Research*, vol. 33, no. 16, pp. 3459-3468.

Vanrolleghem PA, Insel G, Petersen B, Sin G, De Pauw D, Nopens I, Weijers S and Gernaey KI, 2003 A comprehensive model calibration procedure for activated sludge model. In Proceedings: of the 76th Annual WEF Technical Exhibition and Conference (WEFTEC2003). Los Angeles, CA, USA, October 11-15, 2003, (on CD-ROM)

Viau E, Peccia J. (2009), "Evaluation of the enterococci indicator in biosolids using culture-based and quantitative PCR assays", *Water Research*, vol. 43, pp. 4878-4887.

Viconneau JC, Hascoet MC, Florentz M., The first application of biological phosphorus removal in France. In Proc. Int. Conf. Management Strategies for Phosphorus in the Environment, Selper, UK; 1985.

Vlekke GJFM, Comeau Y, Oldham WK. (1988), "Biological phosphate removal from wastewater with oxygen or nitrate in sequencing batch reactors", *Environmental Technology Letters*, vol. 9, no. 8, pp. 791-796.

Wang, L., Zhang, D., Lu, P. & Li, Z. 2010, "Calibration and verification of biological phosphorus metabolism ASM2D for a bench-scale MSBR system", *Disaster Advances*, vol. 3, no. 4, pp. 334-339.

Wang F, Lu S, Ji M. (2006), "Components of released liquid from ultrasonic waste activated sludge disintegration", *Ultrason Sonochem*, vol. 13, pp. 334-338.

Wang F, Wang Y, Ji M. (2005), "Mechanisms and kinetics models for ultrasonic waste activated sludge disintegration", *Journal of Hazardous Materials*, vol. 123 no. 1–3, pp. 145–150.

Weijers SR, Vanrolleghem PA. (1997), "A procedure for selecting best identifiable parameters in calibrating Activated Sludge Model No. 1 to full-scale plant data", *Water Science and Technology*, vol. 36, pp. 69-79.

Wentzel MC, Loewenthal RE, Ekama GA and Marais GVR. (1988), "Enhanced polyphosphate organism cultures in activated sludge systems--Part 1: enhanced culture development", *Water SA*, vol. 14, pp. 81-92.

Wentzel MC, Lotter LH, Loewenthal RE, Marais GVR. (1986), "Metabolic behavior of *Acinetobacter* spp. in enhanced biological phosphorus removal - a biochemical model", *Water SA*, vol. 12, no. 4, pp. 209-224.

Wentzel MC, Loewenthal RE, Ekama GA, Marais GVR. (1988), "Enhanced polyphosphate organism cultures in activated sludge systems - Part 1: Enhanced culture development", *Water SA*, vol. 14, no. 2, pp. 81-92.

Wentzel MC, Ekama GA, Loewenthal RE, Dold PL, Marais GRV. (1989a), "Enhanced polyphosphate organism cultures in activated sludge systems. Part II: Experimental behavior", *Water SA*, vol. 15, no. 2, pp. 71-88.

Wentzel MC, Dold, PL, Ekama, GA, Marais GVR. (1989b), "Enhanced polyphosphate organism cultures in activated sludge systems. Part III: Kinetic model", *Water SA*, vol. 15, no. 2, pp. 89-102.

Wentzel MC, Lotter LH, Ekama GA, Loewenthal RE, Marais, GVR. (1991), "Evaluation of biochemical models for biological excess phosphorus removal", *Water Science and Technology*, vol. 23, no. 4-6, pp. 567-576.

Wentzel MC, Ekama GA, Marai GVR. (1992), "Processes and modelling of nitrification denitrification biological excess phosphorus removal systems - A review", *Water Science and Technology*, vol. 25, no. 6, pp. 59-82.

Whang L, Park J.K. (2002), "Competition between polyphosphate- and glycogen-accumulating organisms in biological phosphorus removal systems - Effect of temperature", *Water Science and Technology*, vol. 46, pp. 191-194.

Whang L, Park JK. (2006), "Competition between polyphosphate- and glycogen-accumulating organisms in enhanced-biological-phosphorus-removal systems: Effect of temperature and sludge age", *Water Environment Research,* vol. 78, no. 1, pp. 4-11.

Wilson GL, Matijasevich AS, Mitchell DRG, Schulz JC, Will GD. (2006), "Modification of TiO_2 for enhanced surface properties: finite ostwald ripening by a microwave hydrothermal processLangmuir", *Water Research*, vol. 22, no.5, pp. 2016–2027.

Withers PJA, Sharpley AN. (2008), "Characterization and apportionment of nutrient and sediment sources in catchments", *Journal of Hydrology*, vol. 350, pp. 127–30.

Xiao Ma , Ye Li , Meng Zhang, Fangzhao Zheng, Shuang Du. (2011), "Assessment and analysis of non-point source nitrogen and phosphorus loads in the Three Gorges Reservoir Area of Hubei Province, China", *Science of the Total Environment*, vol. 412-413, pp. 154-161.

Xie, W.-., Zhang, R., Li, W.-., Ni, B.-., Fang, F., Sheng, G.-., Yu, H.-., Song, J., Le, D.-., Bi, X.-., Liu, C.-. & Yang, M. 2011, "Simulation and optimization of a full-scale Carrousel oxidation ditch plant for municipal wastewater treatment", *Biochemical engineering journal*, vol. 56, no. 1-2, pp. 9-16.

Yagci N, Artan N, Cokgor EU, Randall CW, Orhon D. (2003), "Metabolic model for acetate uptake by a mixed culture of phosphate- and glycogen-accumulating organisms under anaerobic conditions", *Biotechnology and Bioengineering*, vol. 84, no. 3, pp. 359-373.

Yagci N, Insel G, Tasli R, Artan N, Randall CW, Orhon D. (2006), "A new interpretation of ASM2d for modeling of SBR performance for enhanced biological phosphorus removal under different P/HAc ratios", *Biotechnology and Bioengineering*, vol. 93, pp. 258-270.

Yasui H, Komatsu K, Goel R, Li YY, Noike T.(2005), "Full-scale application of anaerobic digestion process with partial ozonation of digested sludge", *Water Science and Technology*, vol. 52, no. 1-2, pp. 245–252.

Yoshida, Y., Kim, Y., Saito, T. & Tanaka, K. (2009), "Development of the modified activated sludge model describing nitrite inhibition of aerobic phosphate uptake", *Water Science and Technology*, vol. 59, no. 4, pp. 621-630.

Yu Q, Lei HY, Li Z, Li HL, Chen K, Zhang XH, Liang RL. (2010), "Physical and chemical properties of waste-activated sludge after microwave treatment", *Water Research*, vol. 44, no. 9, pp. 2841–2849.

Zhang P, Zhang G, Wang W. (2007a), "Ultrasonic treatment of biological sludge: floc disintegration, cell lysis and inactivation", *Bioresource Technology*, vol. 98, no. 1, pp. 207-210.

Zhang G, Zhang P, Yang J, Chen Y. (2007b), "Ultrasonic reduction of excess sludge from the activated sludge system", *Journal of Hazardous Material, vol.* 145, pp. 515-519.

Zhang, B., Zhou, X.-. & Ren, N.-. (2008), "Novel phosphorus and nitrogen removal process for municipal sewage treatment: Performance evaluation and design optimization", *Huanjing Kexue/Environmental Science,* vol. 29, no. 6, pp. 1518-1525.

Zhang G, Yang J, Liu H, Zhang J. (2009), "Sludge ozonation: Disintegration, supernatant changes and mechanisms", *Bioresource Technology*, vol. 100, no. 3, pp. 1505-1509.

Zhang P, Chen Y, Zhou Q, Zheng X, Zhu X, Zhao Y. (2010), "Understanding short-chain fatty acids accumulation enhanced in waste activated sludge alkaline fermentation: Kinetics and microbiology", *Environmental Science and Technology*, vol. 44, pp. 9343-9348.

Zheng X, Tong J, Li H, Chen Y. (2009), "The investigation of effect of organic carbon sources addition in anaerobic-aerobic (low dissolved oxygen) sequencing batch reactor for nutrients removal from wastewaters" *Bioresource Technol*ogy, vol. 100, pp. 2515-2520.

Zheng X, Chen Y, Liu C. (2010), "Waste activated sludge alkaline fermentation liquid as carbon source for biological nutrients removal in anaerobic followed by alternating aerobic-anoxic sequencing batch reactors", *Chinese Journal of Chemical Engineering*, vol. 18, pp. 478-485.

Zhou Y, Pijuan M, Zeng RJ, Yuan Z. (2009a), "Involvement of the TCA cycle in the anaerobic metabolism of polyphosphate accumulating organisms (PAOs)", *Water Research*, vol. 43, pp. 1330-1340.

Zhou X, Zhang Y, Hu M. & Shi W. (2009b), "Optimization design for nutrients removal process with activated sludge 2D model", *Huagong Xuebao/CIESC Journal,* vol. 60, no. 12, pp. 3122-3129.

Zhou X, Zhang Y, Hu M & Jiang M. (2010), "Nitrogen and phosphorus removal of AmOn integrative process: Effect and design optimization", *Tongji Daxue Xuebao/Journal of Tongji University,* vol. 38, no. 10, pp. 1468-1472.

Zhou Z, Wu Z, Wang Z, Tang S, Gu G, Wang L, Wang Y. & Xin, Z. (2011), "Simulation and performance evaluation of the anoxic/anaerobic/aerobic process for biological nutrient removal", *Korean Journal of Chemical Engineering,* vol. 28, no. 5, pp. 1233-1240.